UNIVERSITY OF CALIFORNIA SAN DIEGO

Fish otoliths and fisher knowledge as mobile monitors of environmental conditions: an integrated approach

A dissertation submitted in partial satisfaction of the requirements for the degree Doctor of Philosophy

in

Marine Biology

by

Leticia Maria Cavole

Committee in charge:

Professor Octavio Aburto Oropeza, Chair
Professor Andrew Frederick Johnson, Co-Chair
Professor Carolyn Kurle
Professor Lisa Levin
Professor Karin Limburg
Professor Richard Norris
Professor Stuart Sandin

2021

The dissertation of Leticia Maria Cavole is approved, and it is acceptable in quality and form for publication on microfilm and electronically.

University of California San Diego

2021

DEDICATION

Para minha família, especialmente aos meus avós maternos e paternos

EPIGRAPH

"Sometimes it's better to be kind than to be right. We do not need an intelligent mind that speaks, but a patient heart that listens"

Gautama Buddha

"Valeu a pena? Tudo vale a pena
Se a alma não é pequena.
Quem quer passar além do Bojador
Tem que passar além da dor.
Deus ao mar o perigo e o abismo deu,
Mas nele é que espelhou o céu."

Fernando Pessoa

TABLE OF CONTENTS

LIST OF TABLES

LIST OF FIGURES

ACKNOWLEDGMENTS

I believe that humans have a responsibility to restore earth's ecosystems. We will only be able to do so if we understand the importance of its most delicate components and if we include natural resource users as well as the public in the process of conservation. Soon after beginning my doctorate, I realized that there is no way to elucidate the secrets of nature, and no way to change our reality, without collaborative work and a shared passion for the natural world. As such, I am grateful to many people that have contributed to my personal growth as a scientist and as a human being in the past five years I have been at Scripps.

I am grateful to my main advisor, Octavio Aburto Oropeza, for giving me the opportunity to join his lab and for providing me with the right tools and independence to conduct my field work and posterior analyses. Octavio has always believed in me and has taught me to think critically about the scientific process and the importance of science communication.

I am thankful to each member of my doctoral committee. Lisa Levin, thank you for your enthusiasm towards my questions and the insights you've made possible. It is very genuine and as profound as the ecosystems you have dedicated your life to. I am grateful for your feedback on each of my chapters and for the opportunity you gave me to see deep ecosystems "alive" using the ROV SuBastian while on the Falkor cruise. This experience has opened my eyes to the sophisticated beauty of these ecosystems. Karin Limburg, thank you for sharing your time and otolithic expertise with me. I will never forget the two weeks we spent underground at the Synchrotron, all your patience, and your willingness to teach me about the basics of microchemistry. Richard Norris, thank you for offering me your constructive views during my path at Scripps. I appreciate all the hours that we have spent discussing the marvelous aspects of science. Stuart Sandin, thank you for all constructive feedback, and for helping me to think

critically at my main questions and hypotheses. It has been an honor to be your student, and I have learnt so much. Carolyn Kurle, I have so enjoyed all our conversations, and the advice you have provided me throughout my PhD. Thank you for teaching me that simplicity is a better approach for conveying our research to the public and policymakers. Last, but not least, thank you Andrew Frederick Johnson for motivating me to apply for the doctorate program at Scripps, all those years ago, and for being a support to me ever since. I appreciate all the rapid responses you have provided for each and all of my chapters. Your versatility is truly a source of inspiration!

During my PhD, numerous collaborations have been able to thrive, adding profoundly to the science in my thesis. I am particularly grateful to Jessica Miller, who has been so present and attentive to all the inquiries I've had. Thank you for your time and for all effective advice. Kevin McKeegan, I am so happy a simple email has allowed such a wonderful collaboration to grow. I am grateful to you, a planetary science expert, for being so interested in learning more about fish and offering me your incredible instrument (SIMS) to analyze them. It is absolutely fantastic how distinct fields of knowledge could converge and meteorites and fish can use similar techniques to unravel patterns of their environment of formation! I would like to thank Anne Gro Vea Salvanes for introducing me to the special bearded gobies from Namibia and for being so generous in her support for part of my LA-ICPMS analyses. Thank you also for providing such interesting insights on my results. A special thanks to Adrian Munguia Vega, for helping me to integrate distinct techniques (genetics and otoliths) into my dissertation. I really enjoyed all our meetings and your points of view, and I have learned so much with you.

Thanks to Jose Marin Jarrin, Maria José Barrágan, and Solange Andrade from the Charles Darwin Foundation. All of you have helped and supported the socio-ecological context

of my science. Thank you, José, for also giving me a lot of good advice regarding the microchemistry analysis of the Galápagos fishes. Thank you, Natalya Gallo, for introducing me to deep sea fish and for sharing your expertise and fish samples with me. I have enjoyed so much our conversations and shared passion for the deep-sea fishes.

A singular thanks to Paul Dayton. The shine in your eyes when you talk about nature is a true inspiration to continue my academic journey and constant learning process. Perhaps, the love for nature cannot be taught, but can definitely be shared.

Thank you, all members of the Scripps Department, especially Gilbert, Shelley and Maureen McGreevy for all time you have allocated to all students at SIO, including myself, and for always providing accurate and helpful feedback. Thank you, Rob Monroe, for the opportunity you gave me to attend COP25 and for helping me to convey my science to a broader audience.

Thanks to my 2015 cohort, my lab mates and to my closest friends here. Erica Ferrer, thank you so much for being such an honest and kind person, and for sharing a state of "soliphilia" with me. Daniela Faggiani, Nathali-Cordero, Alfredo Girón and Tiago Leão, thank you for being my Brazilian-Mexican family here.

Gabriel Castro, thank you for supporting me with care, love and respect during all these years. It would be quite impossible to imagine my years at SIO without your continuous support and grace. I am so glad we have been sharing so many experiences!

This dissertation would not be possible without several funding sources. I would like to particularly thanks CNPQ for giving a full fellowship (#213540/2014-2) that supported 4 years of my doctorate at Scripps. Thanks to the Tegner 2016 Fellowship, the 2018 Tinker Field Research Grant and the Helmsley Charitable Trust for supporting my field campaigns and chemical analysis. Thank you to the Herrider Family Foundation and H. William Menard

Memorial Fund for supporting the last years of my doctorate research. These were essential years to conclude the main findings of this dissertation.

Special thanks to my family. To my mother for always supporting my education and for giving me a sense of direction. To my father for making me a dreamer. To my maternal grandparents, for loving me so genuinely during their lives. To my siblings, Pedro and Mariana, for being my friends and for caring about my well-being. To my niece Alice and Catarina, for their smiles that continue to inspire me.

MATERIAL PUBLISHED IN THE DISSERTATION

Chapter 1, in part, is being prepared for submission of the material. Cavole L.M., Zwolinski J., Castro-Falcón G., Johnson A.F., Hertwig A., Ming-Chang L., McKeegan K.D., Aburto-Oropeza O. The dissertation author was the primary investigator and author of this material.

Chapter 2, in full, is a reprint of the material as it appears in Marine Ecology Progress Series. Cavole L.M., Miller J.A., Salinas-de-Léon P., Aburto-Oropeza O., Jarrin J.R.M., Johnson A.F. The dissertation author was the primary investigator and author of this material.

Chapter 3, in part, is being prepared for submission of the material. Cavole L.M., Munguia-Vega A., Miller J.A., Salinas-de-Léon P., Jarrin J.R.M., Johnson A.F., Rastoin-Laplane E., Girón-Nava A., Aburto-Oropeza O. The dissertation author was the primary investigator and author of this material.

Chapter 4, in part, is being prepared for submission of the material. Cavole L.M., Limburg K., Gallo N., Salvanes A.G.V., Ramírez-Valdez A., Levin L.A, Aburto-Oropeza O., Hertwig A., Ming-Chang L., McKeegan K.D. The dissertation author was the primary investigator and author of this material.

Chapter 5 in full, is a reprint of the material as it appears in Marine Policy. Cavole L.M., Andrade-Vera S., Jarrin J.R.M., Dias D.F., Aburto-Oropeza O., Barrágan-Paladines M.J. The dissertation author was the primary investigator and author of this material.

VITA

2012	Bachelor of Oceanography, Universidade Federal do Rio Grande, Brazil
2014	Master of Science in Biological Oceanography, Universidade Federal do Rio Grande, Brazil
2021	Doctor of Philosophy in Marine Biology, University of California San Diego

PUBLICATIONS

Cavole L.M., Miller J., Salinas-de-Léon P., Aburto-Oropeza O., Marin-Jarrin J, Johnson A.F. 2020. The role of extrinsic variation – cohabiting juvenile fish species exhibit similar otolith elemental signatures. *Marine Ecology Progress Series*. 646, 109-125. https://doi.org/10.3354/meps13394

Cavole L.M and DeCarlo, T. 2020. Early observations of heat-induced coral bleaching in the Galápagos Islands. *Reef Encounter* 35, 68-72.

Cavole, L.M., Andrade-Vera S., Marin-Jarrin J, Dias D.F., Aburto-Oropeza O., Barragán-Paladines M.J. 2020: Using local ecological knowledge of fishers to infer the impact of climate variability in Galapagos small-scale fisheries, *Marine Policy*. 121:104195 https://doi.org/10.1016/j.marpol.2020.104195

Cavole L.M., Cardoso L.G., Almeida M.S., Haimovici M. 2018 Unravelling growth trajectories from complicated otoliths - the case of brazilian codling *Urophycis brasiliensis*. *Journal of Fish Biology* 92(5), 1290-1311. https://doi.org/10.1111/jfb.13586

Cavole L.M. et al. 2016. Biological Impacts of the 2013–2015 Warm-Water Anomaly in the Northeast Pacific: Winners, Losers, and the Future. *Oceanography* 29 (2), 273-285. https://doi.org/10.5670/oceanog.2016.32

Cavole L.M., Haimovici M. 2015. The use of otolith microstructure in resolving issues of ageing and growth of young *Micropogonias furnieri* from southern Brazil. *Marine Biology Research* 11 (9), 933-943. https://doi.org/10.1080/17451000.2015.1031799

Cavole L.M., Arantes C.C., Castello L. 2015. How illegal are tropical small-scale fisheries? An estimate for arapaima in the Amazon. *Fisheries Research* 168, 1-5. http://dx.doi.org/10.1016/j.fishres.2015.03.012

ABSTRACT OF THE DISSERTATION

Fish otoliths and fisher knowledge as mobile monitors of environmental conditions: an integrated approach

by

Leticia Maria Cavole

Doctor of Philosophy in Marine Biology

University of California San Diego, 2021

Professor Octavio Aburto Oropeza, Chair

Professor Andrew Frederick Johnson, Co-Chair

Fish and fishers are affected by the environmental conditions they experience throughout their lives, from daily, annual to decadal time scales. Currently, the oceans are changing fast, as global warming increases the temperature of the water and reduces oxygen levels within it. However, there is still an important knowledge gap about how these shifting conditions influence wild populations of fish, especially in the early life stages of tropical species inhabiting mangrove lagoons or for adult fishes dwelling in the deep ocean. In this dissertation, we use the chronological and chemical properties of otoliths – calcified structures within the inner ear of fish – to investigate how temperature correlates with fish growth, to improve our understanding of their populations, and to develop proxies for hypoxia exposure in deep-sea fishes. Chapter 1

asks how the water temperature inside mangrove lagoons regulates the first year of growth for yellow snappers in the Gulf of California. We found that these animals grow faster in warmer waters until they experience a thermal threshold (~ 32° C) beyond which their growth rate is reduced. Chapter 2 tests the effects of extrinsic (water chemistry and temperature) and intrinsic (growth rate and taxonomy) factors on otolith chemistry. Using distinct species from Galápagos (yellow snapper and sailfin grouper) and the same species (yellow snapper) between Galápagos and the Gulf of California, we observed that extrinsic factors seem to be more important than intrinsic factors as influences on otolith microchemistry. Chapter 3 examines the population structure of yellow snappers in the Gulf of California and Galápagos mangroves by using otolith microchemistry and genetic analyses in tandem. These methodologies were complementary and helped to elucidate a source-sink metapopulation structure for Galápagos snappers, and a self-recruitment scenario for the Gulf snappers, with important implications for the mangrove management at these ecosystems. Chapter 4 explores the use of fish as mobile monitors of hypoxic conditions in Oxygen Minimum Zones (OMZs). Surprisingly, fishes with distinct life-history traits (longevity and thermal history) and from different OMZs (NE Pacific and SE Atlantic), but exposed to comparable low oxygen conditions, exhibited high similarity in their otolith chemistry. These findings may provide a baseline for tracking the ongoing expansion of OMZs. Lastly, Chapter 5 inquires how fishers' local ecological knowledge (LEK) in the Galápagos Archipelago can help to elucidate the effects of climate variability on fish. We observed that LEK is in line with the scientific literature regarding distributional shifts in marine species and anomalous weather conditions during strong El Niño years.

CHAPTER 1:

The role of temperature on fish growth: insights from mangrove microcosms

LETICIA MARIA CAVOLE, JUAN ZWOLINSKI, GABRIEL CASTRO FALCÓN, ANDREW FREDERICK JONHSON, ANDREAS HERTWIG, MING-CHANG LIU, HAYLE SUE, KEVIN D. MCKEEGAN, OCTAVIO ABURTO-OROPEZA

Abstract

Ocean warming is changing the normal range of distribution for marine organisms, emphasizing the need to understand how habitat-specific temperature influences growth of fish. We examined the relationship between water temperatures and growth of the juvenile yellow snapper, *Lutjanus argentiventris,* which dwell in mangroves of the Gulf of California. *In situ* daily temperatures were recorded for one year and aligned to otolith oxygen isotope values ($\delta^{18}O$) and daily growth increments. The thermal history reconstruction using otolith $\delta^{18}O$ values captured the immense water seasonality ($\Delta T \sim 20$ °C) observed in our mangrove sites, validating this technique for fish inhabiting mangrove ecosystems for the first time. Using a GAM model, we observed that *in situ* water temperature and age of individuals were significant drivers of daily growth increment width, with increasing water temperature and fish age resulting in increasing and decreasing daily growth increment width, respectively. However, beyond a temperature threshold (28 - 32°C), juvenile daily growth increment width is reduced, potentially linked to metabolic stress. On a larger spatial scale, the effect of temperature variability was assessed using satellite sea surface temperature and calculated growth rates for yellow snappers from eight mangroves in the Gulf of California. Juveniles grew faster in the warmer and less variable waters of the southern region of the Gulf relative to juveniles in the central and northern regions. The waters adjacent to all mangroves in the Gulf of California are warming faster than global average (0.04 °C $year^{-1}$ vs. 0.01 °C $year^{-1}$). This poses a risk to the essential nursery role of mangrove waters and indicates that these ecosystems and the marine biota within them might face detrimental conditions of growth with ongoing climate change.

Introduction

Climate change is a major threat to global biodiversity and ecosystem functioning (Thomas et al., 2004; IPCC 2013, 2019) and its effects are evident across a range of environments and biota (Parmesan & Yohe, 2003; Parmesan, 2006). In the marine realm, the increase in ocean temperature has changed several population parameters in fishes, such as the normal distributional range (Perry et al., 2005; Cheung et al., 2010), population structure and composition (Drinkwater et al., 2005; Cheung et al., 2013), growth and reproductive rates (Righton et al., 2010; Pankhurst & Munday, 2011), and mean body sizes (Rijn et al., 2017).

Understanding how the increase of water temperature can impact reproduction, growth, survival, susceptibility to disease and migration pathways of wild populations is increasingly important (Planque et al., 2010). Within this context, looking at early life-stages of fish can be particularly relevant, as they are more sensitive to environmental fluctuations than adults (Munday et al., 2008; Righton et al., 2010; Pankhurst & Munday, 2011). Until now, most studies evaluating the impact of water temperature in the early life stages on fish growth have focused on species from temperate ecosystems (Houde, 1989; Handeland et al., 2008; Jørgensen et al., 2020) or coral reefs (Munday et al., 2008; Wenger et al., 2016), usually under short-duration and unrealistic laboratory conditions (Przeslawski et al., 2015), and/or restricted to the analysis of few days of growth (Pepin, 1991; Wenger et al., 2016). As a consequence, most studies today have not been able to replicate the wide array of conditions experienced by a fish in its natural environment throughout an entire life stage (e.g., embryo, larvae, juveniles), nor do they consider the seasonality of environmental conditions, which might create site-specific variability in the growth responses observed. In the present study, we describe the growth of juvenile *Lutjanus argentiventris* (yellow snappers) and the temperature variability of their mangrove habitats in

order to understand how water temperature can influence juvenile fish growth in these "natural laboratory" microcosms.

Mangroves are important refuge habitats, especially under current climate change, acting as a buffer against storms, hurricanes, tsunamis and sea level rise. Therefore, mangrove systems offer essential coast protection services (Alongi, 2008) and their specialized root system – called pneumatophores – provides complex, three-dimensional substrates (Walden et al., 2019). These ecosystems are also used by an extensive range of aquatic species for shelter and food and play a major role as nursery habitats enhancing the growth and survival of juvenile fish (Beck et al., 2001; Nagelkerken et al., 2008). In the Gulf of California, mangrove trees constitute key foundation species in desertic coasts, and its fringe length is believed to be proportional to fisheries yields for important economic marine species offshore (Aburto-Oropeza et al., 2008). The microhabitat formed by the roots of mangrove trees is used especially for shelter and foraging by juveniles of the yellow snapper *Lutjanus argentiventris* during their first year of growth, before they leave these habitats to integrate the adult stock in the rocky reefs offshore (Aburto-Oropeza et al., 2009). This species has a wide distributional range, occurring in the Eastern Pacific Ocean from southern California to Peru, and represents an important component of artisanal fisheries in the Gulf of California (Allen, 1985; Erisman et al., 2010).

In this study, we investigated how the growth of juveniles of yellow snappers is influenced by the temperature variability inside mangrove lagoon waters and among mangroves in the Gulf of California. Our specific hypotheses were: 1) the $\delta^{18}O$ profiles in otoliths can reconstruct the thermal history of juvenile fish, thus confirming their residence in those waters, 2) juvenile fish will increase their daily somatic growth with the increase of *in situ* daily water temperature, until a thermal threshold is reached, 3) growth rates (mm day^{-1}) of juvenile

populations will vary along a sea surface temperature (SST) latitudinal gradient in the Gulf of California.

Material and Methods

In order to understand how juveniles of yellow snapper *Lutjanus argentiventris* grew inside each mangrove lagoon and between distant mangroves, we: (1) compared the thermal histories of yellow snapper juveniles (obtained from $\delta^{18}O$ profiles in otoliths, n=4) with *in situ* water temperature (**Figure 1.1**; white stars), (2) measured the width of daily growth increments in 53 juvenile otoliths and analyzed its relationship with *in situ* water temperature and the fish's estimated total age (**Figure 1.1**; white stars), and (3) estimated the growth rates (mm day^{-1}) of 173 yellow snapper juveniles from eight mangrove sites spanning a marked latitudinal SST gradient in the Gulf of California (**Figure 1.1**; colorful dots). We first test if the temperatures reconstructed from otolith $\delta^{18}O$ profiles follow the *in-situ* intra-annual variability in water temperature (up to ~ 20 °C inside the mangrove lagoons). Then, assuming that these juveniles spend their first year of growth inside these lagoons, we compared their growth at local and latitudinal spatial scales.

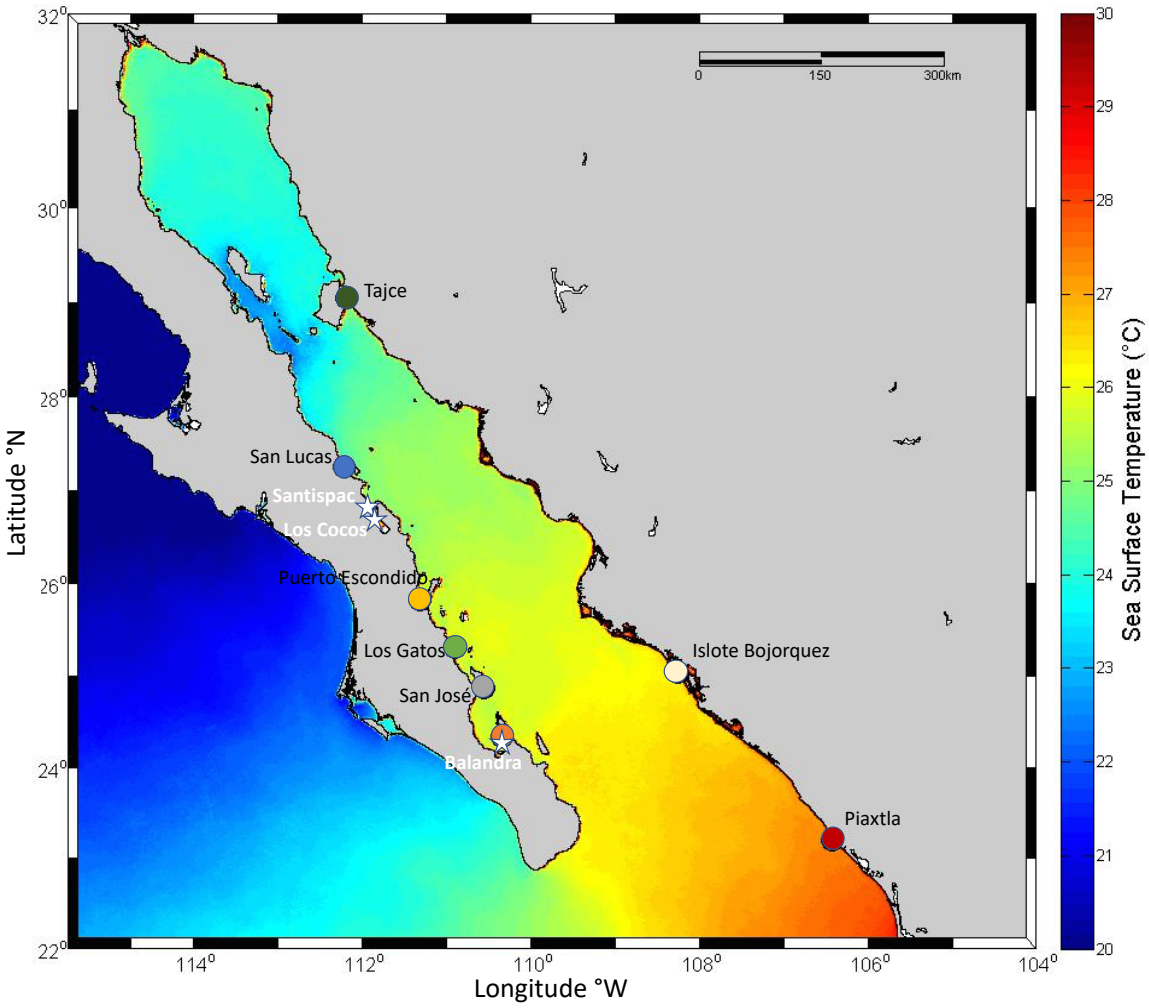

Figure 1.1. Fish collection area for the yellow snapper *Lutjanus argentiventris*. White stars correspond to mangrove sites where juveniles were collected in 2018 and 2019 for thermal history reconstruction (n=4) and daily-growth increment profiles (n=53). Colorful dots correspond to mangrove sites where juveniles were collected in 2003 and 2004 for the estimate of population growth rates (n=173) along a sea surface temperature (SST) latitudinal gradient.

Thermal history reconstruction using otolith oxygen isotopes ($\delta^{18}O$)

We constructed $\delta^{18}O$ profiles for four otoliths of yellow snappers collected in three mangrove lagoons (Santispac, Los Cocos and Balandra) along the eastern side of Baja California peninsula (**Table 1.1)**. These juveniles were collected in January of 2018 and January and February of 2019 (**Figure 1.1**; white stars).

In situ $\delta^{18}O$ values were measured from the core of the otolith to the edge using secondary ion mass spectrometry (SIMS) to reconstruct temporally resolved thermal histories (**Figure 1.S1**). Otoliths were cleaned in methanol and mounted in epoxy resin in aluminum rings together with reference materials for isotope measurements. Samples were polished progressively to reveal microincrements (i.e., daily increments) using silicon carbide grinding papers of different grit sizes (600, 800, 1200) and to flatten the otolith surface to the μm scale. Polished sections were sonicated in methanol, dried, and gold coated. Otolith sections were examined visually with optical microscopy (Olympus BX51, USA). Pictures were taken at 100, 200 and 400x total magnification using transmitted and reflected light to assist in location of analytical spots for the isotope measurements at the otolith's surface.

Oxygen isotope compositions across the otolith sections were measured using the Cameca IMS-1290-HR ion microprobe at the W.M. Keck Foundation Center for Isotope Geochemistry, UCLA, during two analytical sessions (May-2019, Nov-2019). A Cs^+ primary ion beam of ~2 nA (Nov-2019) or ~3 nA (May-2019) was rastered (5×5 μm^2) over the sample surface (Gaussian beam, ion probe pits of ~10 μm). A normal-incidence electron flood gun was used for charge compensation. Following 30 s (May-2019) or 45 s (Nov-2019) of pre-sputtering and subsequent beam centering routines, measurements were done by simultaneously collecting $^{16}O^-$ and $^{18}O^-$ using two Faraday cups in the multicollection detector array. Data were acquired in 6 (Nov-2019) or 10 (May-2019) cycles; counting time for each of the cycles was 10 s. Mass resolving power was set to 2500 for both sessions.

To correct for instrumental mass fractionation (IMF) and to monitor instrumental drift, in-house reference materials (Joplin calcite, $\delta^{18}O$ = 5.8 ‰ [only May-2019]; Optical calcite $\delta^{18}O$ = 11.1 ‰, Jellynose otolith $\delta^{18}O$ = 30 - 34‰ (Shiao et al., 2017); relative to Vienna Standard

Mean Ocean Water (VSMOW)) were measured throughout the analytical sessions. The average isotope ratio of the reference material measured throughout that day was used to correct for IMF when no instrumental drift was detected over the course of 24 hrs. However, in the case where instrumental drift was observed, a standard-unknown-standard bracketing approach was applied. The reproducibility (2 standard deviations) of $\delta^{18}O$ values of reference materials was: Joplin calcite, 0.4 ‰, over two days; Optical calcite, 0.3 - 2.0 ‰, range of values for several brackets.

Measurement errors are given as 2σ and reflect both the measurement precision (2 standard error) for each analysis and the reproducibility (2 standard deviation) of standard measurements on the analysis day. Data are reported as δ values in parts per thousand (permil; ‰) relative to VSMOW, (**Eq. (1)**).

Eq. 1
$$\delta^{18}O = 1000 * \left(\frac{\frac{^{18}O}{^{16}O}_{sample}}{\frac{^{18}O}{^{16}O}_{VSMOW}} - 1 \right)$$

We also converted our VSMOW values relative to Vienna Pee Dee Belemnite (VPDB) following Coplen et al. (1983) to make comparison easier across the literature (**Eq. (2)**).

Eq. 2 $\delta^{18}O_{VSMOW} = 1.03091 \cdot \delta^{18}O_{VPDB} + 30.91‰$ (Coplen et al., 1983)

Habitat temperatures were estimated from $\delta^{18}O$ values according to the equations presented by Høie et al. (2004) (**Eq. (3) and (4)**), based on otolith carbonate chemistry. Temperature (*T*) was calculated in Kelvin and was converted to Celsius (°C.) Since there were no $\delta^{18}O$ values recorded for seawater **(**$\delta^{18}O_{sw}$**)** inside the mangrove lagoons of Baja California, we

calculated it based on the outermost $\delta^{18}O$ value of each otolith, which were presumed to reflect the known temperature at the time of fish capture.

Eq. 3 $$\alpha = \frac{\delta^{18}O_{otolith}+1000}{\delta^{18}O_{seawater}+1000}$$

Eq. 4 $$1000 \ln \alpha = 16.75 \left(\frac{1000}{T}\right) - 27.09$$ (Høie et al., 2004)

For three individuals, we replicated $\delta^{18}O$ values at points at similar distances from the core (trying to follow the curvature of the same calendar rings in each side of the otolith) and the general trend of increasing $\delta^{18}O$ values was consistent for both growth axes. We aligned each otolith $\delta^{18}O$ value with a calendar date based on the counting of daily growth increments from the otolith core to the edge of each $\delta^{18}O$ point, which are gold in color using transmitted light microscopy (**Figure 1.S1a**).

We correlated the fish reconstructed temperature using otolith $\delta^{18}O$ values and the *in situ* water temperature recorded by HOBO data loggers for each specimen using the *Pearson* correlation coefficient (R) and significance levels (*p*), after meeting assumptions of normality (Shapiro-Wilk). The data analyses for thermal history reconstruction were performed using the statistical programming platform R (R Core Team, 2015) and figures were generated using the package *ggplot2* (Wickham, 2016) and *ggpubr* (Kassambara, 2020).

Daily otolith growth and in situ HOBO temperature at finer spatial scale

Study area and sample collection

We measured the width of 4,229 daily growth increments across the otoliths of 53 yellow snapper juveniles. The size of these juveniles ranged from 24 to 114 mm in Standard Length (SL), and they were collected at the same sites and times as those used for thermal reconstruction from otolith $\delta^{18}O$ values (e.g., Santispac, Los Cocos and Balandra), (**Figure 1**; white stars).

Daily growth width (µm)

Daily increment-width profiles were determined for each individual using the IMAGEPRO PLUS v.6.0 image processing software (Media Cybernetics, Rockville, MD, USA). Increment widths (µm) were measured along the longest axis on the ventral side of the otolith.

Modelling in situ temperature (HOBO) and daily growth width (µm)

HOBO temperature data loggers recorded the water temperature inside each of the three mangrove sites at every 10 minutes, for 360 days. For Santispac, the temperature was recorded between December 22nd, 2016 and December 18th, 2017. For Los Cocos, the temperature was recorded between January 21st, 2018 and January 15th, 2019. For Balandra, the temperature was recorded between January 21st, 2018 and January 18th, 2019. Temperature records were averaged for each day and were then aligned with the corresponding daily increment width (using the same calendar date) for each juvenile throughout their lifetime.

We used Generalized Additive Models (GAM) to determine the relationship between *in situ* temperature (°C), age (days) and the growth (i.e., daily increment width) of yellow snapper juveniles inside each mangrove site. GAMs are better suitable for modelling non-linear relationships than traditional regression analysis due to the use of non-parametric smoothers. We

used individual fish (fish_uo) as the random effect term and a single common (global) smoother for all observations (Pedersen et al., 2019). The global model was:

```
Global_model <- gam (growth ~ s(temperature, k=10, bs="tp") + s(age) + s(fish_uo, k=14,
bs="re"),  data=growth_data, method="REML", family=Gamma(link=log))
```

where bs="re" denotes a random effect for each individual fish, and k=14 was chosen because there were 14 juvenile fish inside this mangrove example. We evaluated the model fit using the percent deviance explained and the visualization of diagnostic plots. We also constructed individual models where growth was a function of temperature or age in order to assess the percentage of deviance explained for each of these factors separately.

```
Temperature_model <- gam (growth ~ s(temperature, k=10, bs="tp"),
                    data=growth_data, method="REML", family=Gamma(link=log))
```

```
Age_model <- gam (growth ~ s(age),
                data=growth_data, method="REML", family=Gamma(link=log))
```

The relationship between growth width (hereafter referred to as “effect”) and water temperature allowed us to identify temperature thresholds beyond which juvenile growth is reduced at each site. Threshold responses were identified when an abrupt change in growth was observed corresponding to a small change in *in situ* temperature. The R package “mgcv” (Wood, 2017) was used to run the GAM analyses.

Juvenile growth rates (mm day^{-1}) and sea surface temperature (SST) on a latitudinal spatial scale

Study area and sample collection

Juvenile young-of-the-year *L. argentiventris* from 17.9 to 136.2 mm in Standard Length (SL) were collected at eight mangroves sites during June and October of 2003 and 2004 in both sides of the Gulf of California (e.g., Baja California Peninsula and the Mainland), (n=173). The five mangrove sites located along the Peninsula, from north to south, were: San Lucas, Puerto Escondido, Los Gatos, San Jose and Balandra. The mangrove sites on the Mexican mainland were: Tajce, Islote Bojorquez and Barra de Piaxtla (**Figure 1.1**; colorful dots). Upon collection, fish samples were preserved in 100% ethanol for laboratory post-processing. Each specimen was weighed (g), and standard length (SL) was measured (mm).

Otolith processing

The sagittal otoliths were removed, cleaned and stored dry in Eppendorf vials. We processed otoliths adapting the methodology developed by Zgliczynski (2015). In summary, we attached the sagittal otolith to the edge of a microscope slide using thermoplastic cement (Crystalbond™) to expose the region of the otolith rostrum and to keep the nucleus region protected on the microscope slide. We used successively finer alumina polishing papers (30µm – 3µm) and a wet grinding-polishing wheel (South Bay Technology INC. Model 900) to polish the exposed region of the otolith to the edge of the microscope slide. The otolith portion attached to the edge of microscope slide was then reheated using a digital hotplate and relocated to the central area of the slide. The otolith was then upturned, so that its flat (previously polished) side was glued to the microscope slide (avoiding any bubbles underneath) and its post-rostrum was

oriented vertically. The remained section was then manually polished to the nucleus of the otolith (until the core was visible) by using successively finer sandpapers (Micro-Mesh® of grits 400, 600, 800 and 1200). As soon as the transverse section was polished sufficiently to expose daily increments, a thin layer of rapid mounting media (Entellan®) was applied above the otolith section to improve the clarity and contrast of the daily growth increments. The entire process for obtaining otoliths with readable daily growth increments can take between 60-75 minutes for each otolith. Sagittal thin sections were examined under a compound microscope at 400-1000x magnification using transmitted light. Daily growth rings were counted and interpreted using standard techniques applicable for the early life stages of tropical fish (Green et al., 2009).

Age determination and juvenile growth comparison among mangroves

A total of 173 juveniles of *Lutjanus argentiventris* were aged at the daily level. The relationship between the standard length of the fish (SL) and its age (days) was linear for most juveniles. Thus, the growth rate (mm day^{-1}) of juveniles at each specific mangrove site was calculated as the slope coefficient of the linear regression between SL (mm) and Age (days):

$$\text{Standard Length of the fish (mm)} = a * \text{Age (days)} + b,$$

where "a" is the instantaneous growth rate. By using site-specific linear equations, we were able to estimate the growth rate for each individual. We then performed a one-way analysis of variance (ANOVA) to test if there is any statistically significant difference in the mean growth rates (mm day^{-1}) of juveniles among mangrove sites.

Because we do not have the *in-situ* temperature data for these samples collected ~ 17-18 years ago, we used the sea surface temperature (SST) adjacent to each mangrove site to estimate the influence of the water temperature on juvenile growth rates. First, we constrained the available SST values during the lifetime of each individual, since we have their birth and capture date estimates. Second, the average temperature experienced throughout the lifetime of each individual was calculated. Thirdly, we calculated the average temperature experienced by juveniles in each mangrove lagoon and compared it with the respective growth rates of these populations (based on 10-30 individuals) in those sites.

Sea surface temperature (SST) adjacent to mangrove sites in the Gulf of California

We tested if the SST adjacent to mangrove sites inside the Gulf of California has changed in the past 20 years. First, we overlapped polygons of 25 km^2 with the most updated (2015) distribution map of mangroves for this region (obtained from CONABIO geoinformation portal website; http://www.conabio.gob.mx/informacion/gis/). This approach generated 624 polygons, mostly concentrated along the mainland states of Sinaloa, Sonora, and Nayarit, with some small mangrove patches located in the eastern side of Baja California (**Figure 1.S2**). Second, we downloaded the available daily SST within each of these polygons. The full-resolution data products are merged from data from multiple sensors: SeaWiFS (1997 to 2010), MODIS-Terra (MODIST, 2000 to present), MODIS-Aqua (MODISA, 2002 to present), MERIS (2003 to 7 April 2012). For the overlapping periods, datasets from all available sensors are merged. Corresponding sea-surface temperature (SST) products are created from MODIST (2000 to present) and MODISA (2002 to present). Lastly, we calculated the SST anomaly for the period 2000 to 2019.

Results

Thermal history reconstruction of four juveniles (SIMS)

We measured $\delta^{18}O$ values from the otolith core to its edge in order to reconstruct the thermal histories of four yellow snapper juveniles inhabiting Santispac, Los Cocos and Balandra mangrove habitats (**Table 1.1**). The changes in oxygen isotopic ratios were very pronounced and ranged from 25.04 to 29.83 ‰ relative to VSMOW and the standard errors (2σ) of individual measurements ranged from ± 0.37 to ± 0.87 ‰ (mean 0.61‰) (**Figure 1.S3**). The estimated habitat temperature for all snappers varied from 13.71 ± 2.87 to 34.63 ± 2.61 °C. The correlation between *in situ* temperature and temperature reconstructed using otolith $\delta^{18}O$ ratios were significant for samples # 104, # 47 and # 141, but not for # 103 (**Figure 1.2**). If we remove six outliers, supposedly corresponding to anomalous weather events experienced by specimens #103 and #104 (see below in discussion), the correlation and significance increase considerably for these individuals (**Figure 1.S4**).

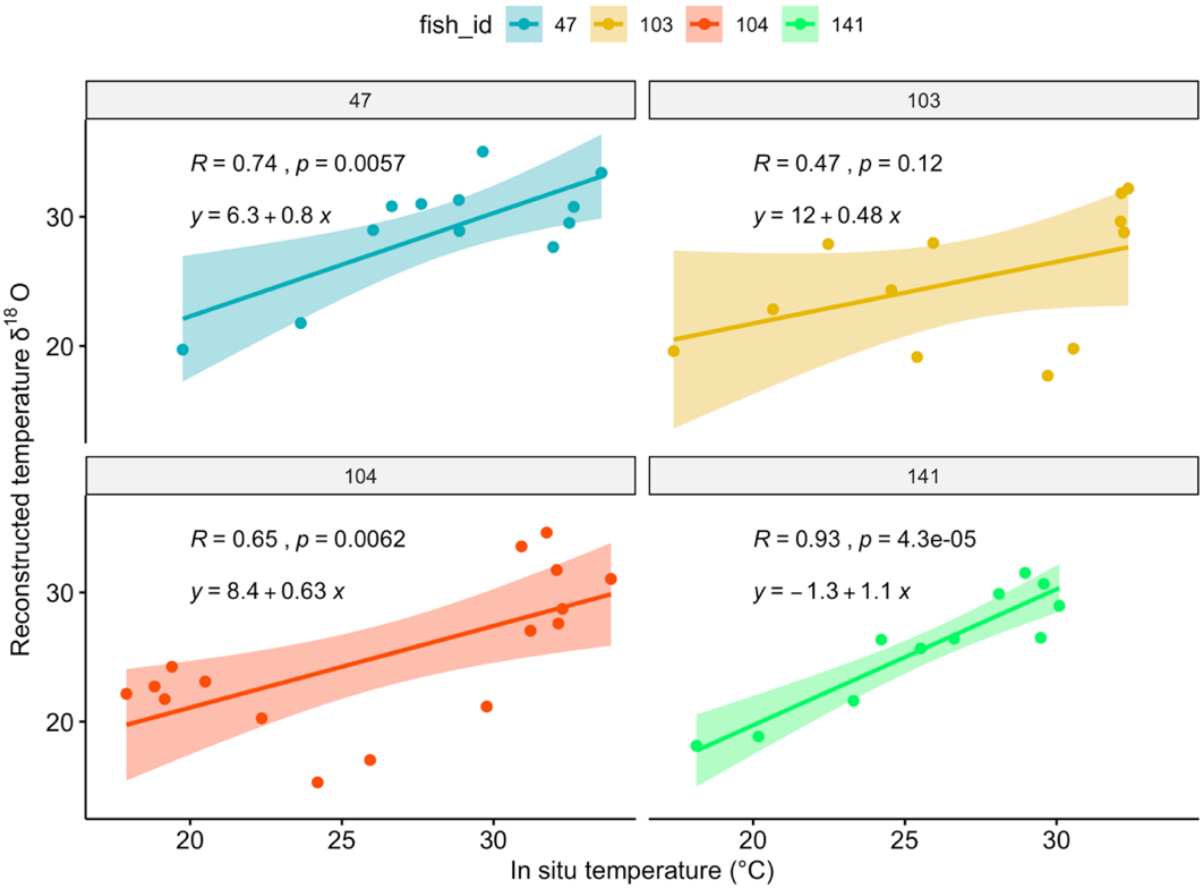

Figure 1.2. Relationship between the reconstructed habitat temperature (using fish otolith $\delta^{18}O$ profiles) and the *in-situ* water temperature recorded by HOBO data loggers. Pearson correlation coefficient (R) and significance level (*p*) are displayed for four juveniles of yellow snapper.

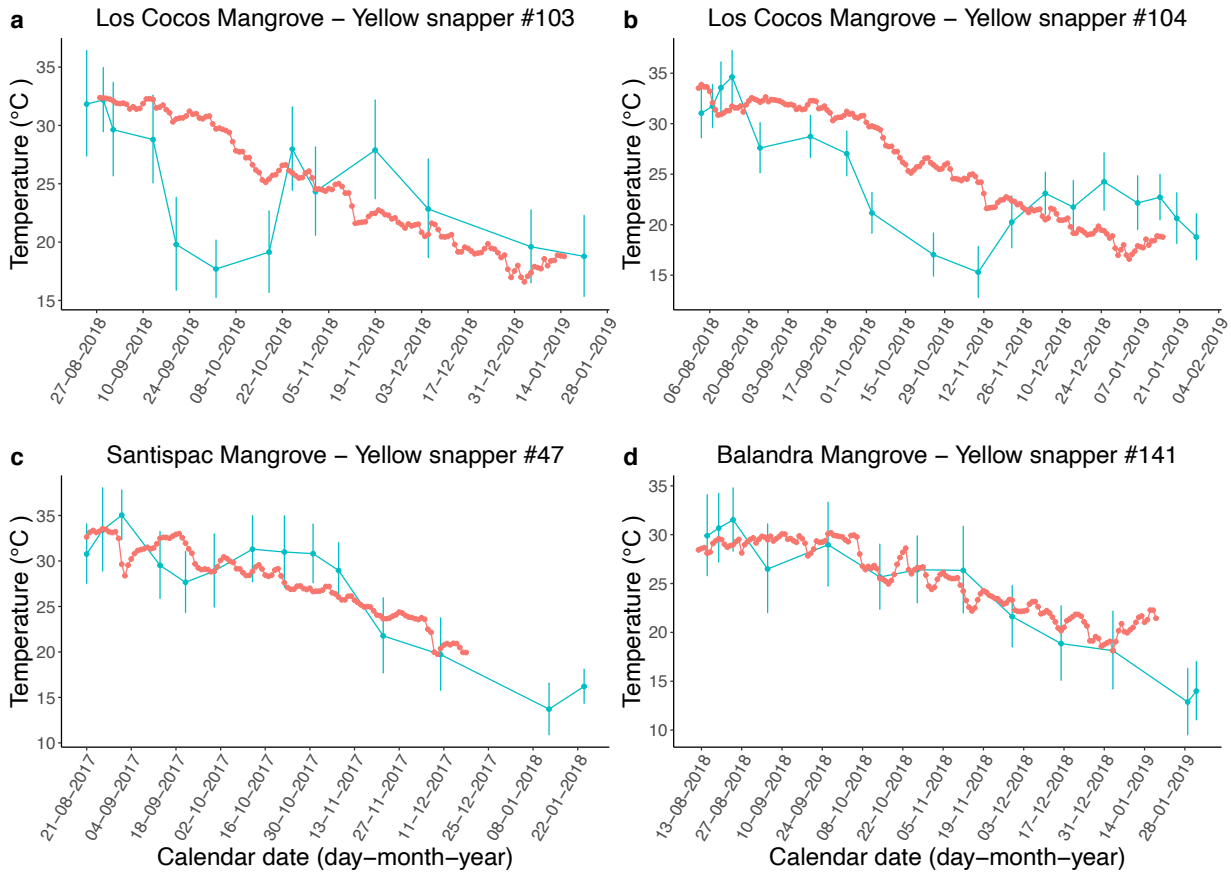

Figure 1.3. Thermal history reconstruction for four yellow snapper juveniles based on otolith $\delta^{18}O$ ratios (blue line) and *in situ* mangrove water temperature recorded by HOBO data loggers (red line). Calendar dates for $\delta^{18}O$ ratios were estimated based on the age of fish (days) at each $\delta^{18}O$ measurement spot.

The lowest values for $\delta^{18}O$ were observed close to the otolith core (indicating higher temperatures at the end of larval stage) whilst the highest values for $\delta^{18}O$ were observed at the otolith edge (indicating lower temperatures at the late juvenile stage), (**Figure 1.3**).

For the specimen # 104 (Los Cocos mangrove), the mean temperature of 18.77 °C at the time of collection, and the outer edge $\delta^{18}O$ values of 28.07 ‰, resulted in a calculated -2.59 ‰ $\delta^{18}O$ for seawater (**Table 1.1**). Using this $\delta^{18}O$ value for seawater, we were able to calculate the temperatures in which this juvenile lived. Otolith $\delta^{18}O$ values varied from 25.04 to 28.07 ‰ for this specimen (**Figure 1.S3**), resulting in reconstructed temperatures from 15.29 to 34.63 °C.

This range of values is similar to the range of *in situ* temperature recorded from the HOBO logger (daily averages from 16.59 to 33.86 °C). However, a mismatch between the reconstructed temperature and *in situ* temperature was detected when the juvenile was between 60 and 100 days old, from late September 2018 to late October 2018 (**Figure 1.3a**).

For specimen # 103 (Los Cocos mangrove), the mean temperature of 18.77 °C at the time of fish collection, and the outer edge $\delta^{18}O$ values of 28.11 ‰, resulted in a calculated -2.55 ‰ $\delta^{18}O$ for seawater (**Table 1.1**). Otolith $\delta^{18}O$ values varied from 25.52 to 28.33 ‰ for this individual (**Figure 1.S3**), resulting in reconstructed temperatures from 17.69 to 32.18 °C. This range of values is similar to the range of *in situ* temperature recorded from the HOBO logger (daily averages from 16.59 to 33.86 °C). Similar to juvenile # 104, the juvenile # 103 exhibited a mismatch between the reconstructed temperature and *in situ* water temperature, when this specimen was between 20 and 60 days old, mainly for the month of October 2018 (**Figure 1.3b**).

Individual # 47 (Santispac mangrove) was collected about one month after the HOBO logger stopped recording the ambient temperature. We estimated its $\delta^{18}O$ seawater based on the temperature at the formation of the spot closest to the temperature data available. Using the mean temperature of 19.75 °C and the $\delta^{18}O$ values of 28.60 ‰, the estimated value for $\delta^{18}O$ seawater was -1.89 ‰ (**Table 1.1**). Otolith $\delta^{18}O$ values varied from 25.68 to 29.83 ‰ for this juvenile (**Figure 1.S3**), resulting in reconstructed temperatures from 13.71 to 35.03 °C. This range of values is similar to the range of *in situ* temperature recorded from the HOBO data logger (daily averages from 15.84 to 33.55 °C) and both time series followed a similar negative trend across time (**Figure 1.3c**).

Individual # 141(Balandra mangrove) was collected two weeks after the HOBO logger stopped recording the ambient temperature. Thus, we estimated its $\delta^{18}O$ seawater based on the

temperature at the formation of the spot closest to the temperature data available. Using the mean temperature of 18.13 °C and the $\delta^{18}O$ values of 28.45 ‰, resulted in a value of -2.35 ‰ for $\delta^{18}O$ seawater (**Table 1.1**). Otolith $\delta^{18}O$ values varied from 25.86 to 29.54 ‰ for this individual, resulting in reconstructed temperatures from 12.87 to 31.51 °C. Most values are similar to the range of *in situ* temperature recorded from the HOBO (18.13 to 30.32 °C), except by the last two spots closest to the edge of the otolith (12.87 and 13.99 °C) (**Figure 1.3d**).

Overall, the seasonal change in mangrove water temperature was sufficiently pronounced to result in markedly distinct otolith $\delta^{18}O$ signatures. All juvenile experienced ~ 4 ‰ of variation for $\delta^{18}O$ values, which is equivalent to approximately 20 °C of habitat temperature variation.

Individual growth (μm) and in situ temperature

We measured the width of daily otolith increments (μm) as a proxy for individual somatic growth in 53 young-of-the-year yellow snappers. The juveniles measured between 24 to 103 mm of standard length (SL) and were between 46 to 157 days old. They were sampled at the three mangrove sites located on the eastern side of Baja California peninsula (**Figure 1.1**; white stars, **Table 1.2**).

For all sites, the smoothed functions of temperature (°C) and age (days) were significant (GAM model), and we examined the assumptions of normality and constant variance for scaled residuals through diagnostic plots (**Figures 1.S5 – 1.S7**). The relationship between the daily growth increment width in μm (juvenile growth) and *in situ* water temperature (°C) was mostly nonlinear. Using generalized additive models (GAMs) we found that both temperature and the age of individuals explained a high amount of variance for daily growth width across the fish lifetime. In all locations, we observed a positive effect of water temperature on growth

(increment width) (**Figures 1.4a - 1.6a**) and an age-dependent negative effect on growth (i.e., the increment width decreases as fish gets older) (**Figures 1.4b - 1.6b**).

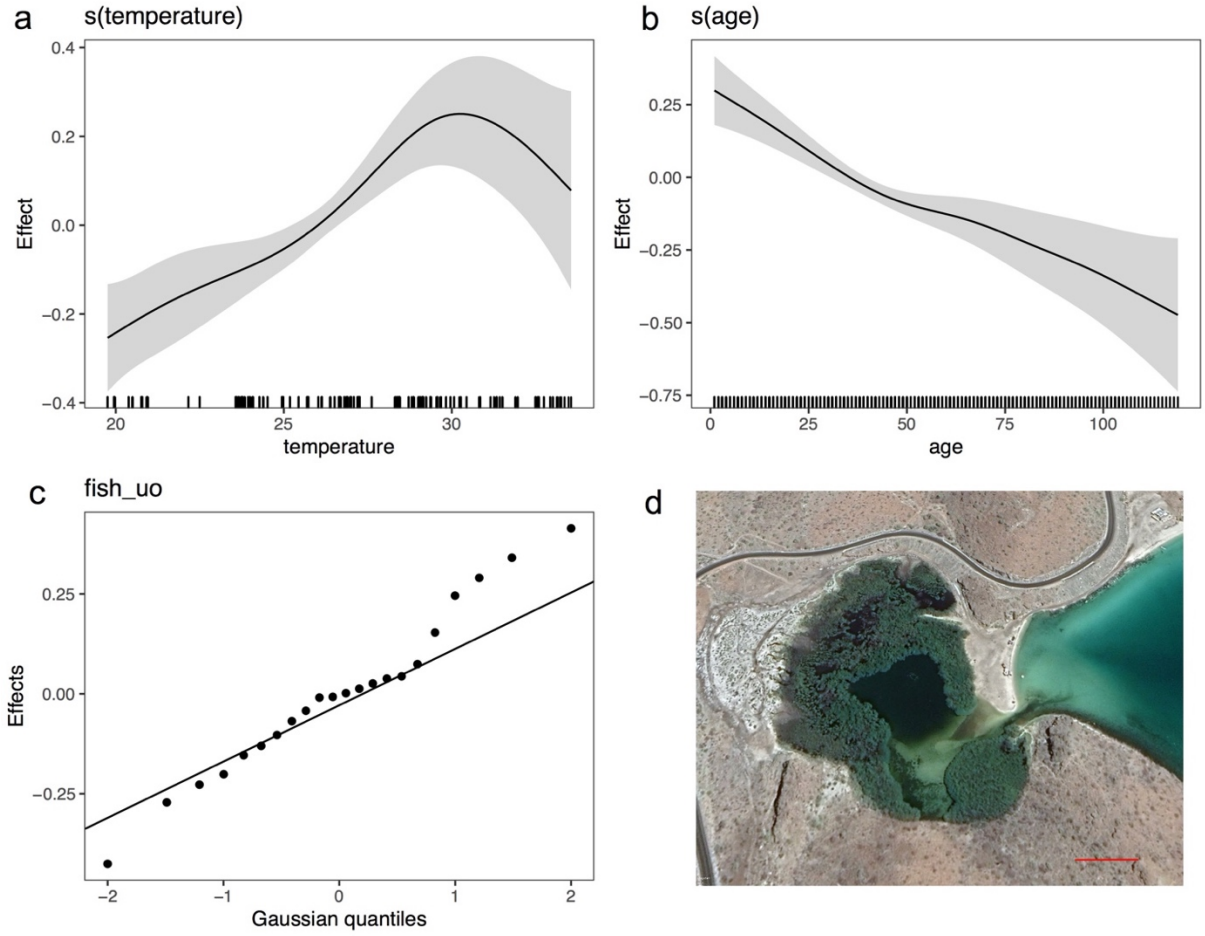

Figure 1.4. Width of daily growth increment (Effect) of yellow snapper juveniles in Santispac mangrove as a function of (a) temperature (°C) and (b) age (days). Black line represents the expected value with a confidence interval shown in gray. (c) Quantile-quantile plot of the random effects against Gaussian quantiles, used to check the appropriateness of the normal random effect assumption. (d) aerial view of Santispac mangrove, showing a rounded lagoon. Inserted map scale (red line) corresponds to 50 meters.

For fish at the Santispac mangrove site (northernmost site, $n = 22$), all explanatory variables were significant ($p < 0.001$) and were able to explain 46.8 % of the model variance. Temperature alone, explained 23.1 % of the variance in daily increment widths (**Figure 1.4**).

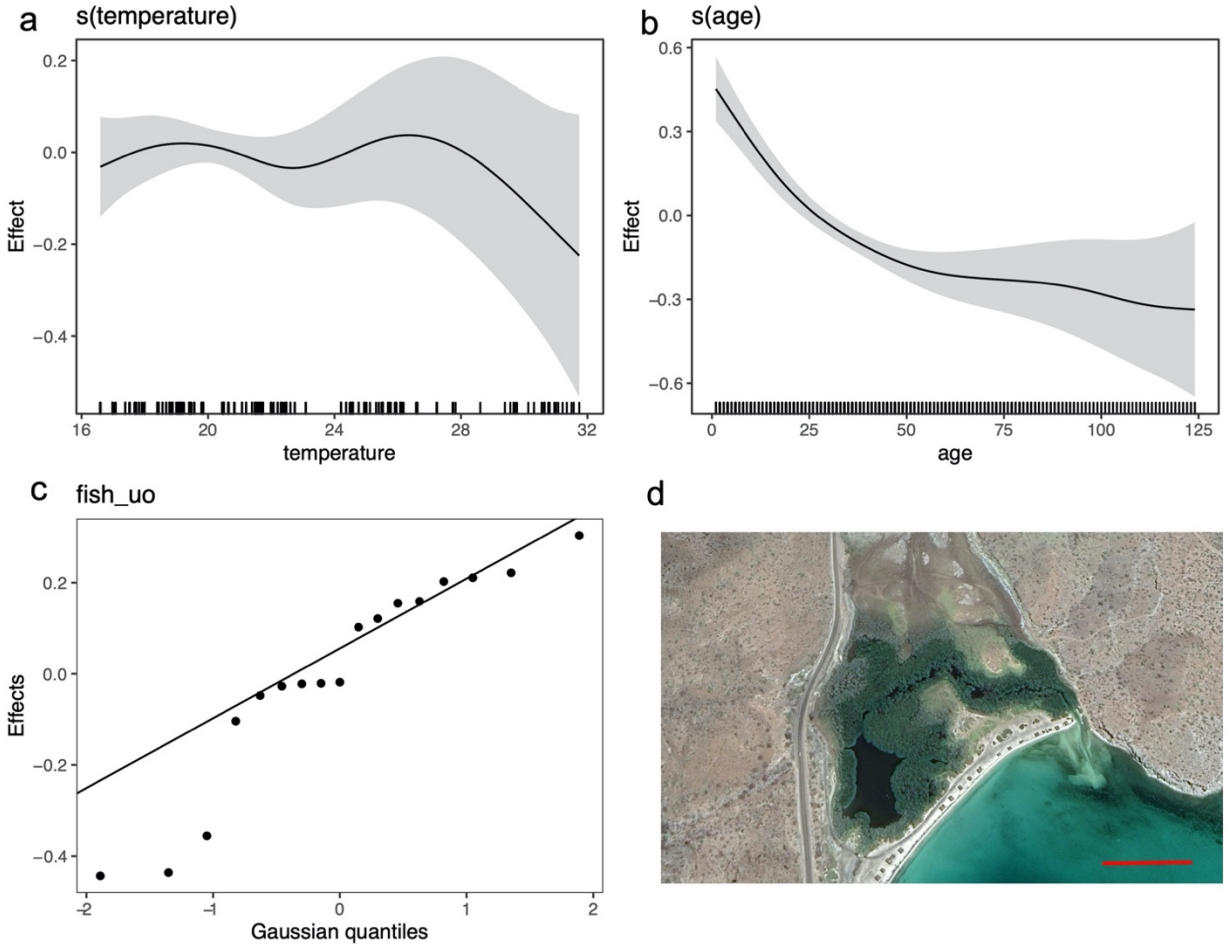

Figure 1.5. Width of daily growth increment (Effect) of yellow snapper juveniles in Los Cocos mangrove as a function of (a) temperature (°C) and (b) age (days). Black line represents the expected value with a confidence interval shown in gray. (c) Quantile-quantile plot of the random effects against Gaussian quantiles, used to check the appropriateness of the normal random effect assumption. (d) aerial view of Los Cocos mangrove, showing a long tidal channel that connects the bay area with an inland lagoon. Inserted map scale (red line) corresponds to 100 meters.

For fish at the Los Cocos mangrove site (n = 17), age and temperature explained 48.1 % of the variance on daily growth width, but only age was significant ($p < 0.001$). Temperature played a minor role, explaining ~5 % of the model variance. The juveniles in the Los Cocos

mangrove behaved differently from other sites. In this mangrove, juvenile growth oscillates up to around 28 °C, decreasing abruptly thereafter (**Figure 1.5**).

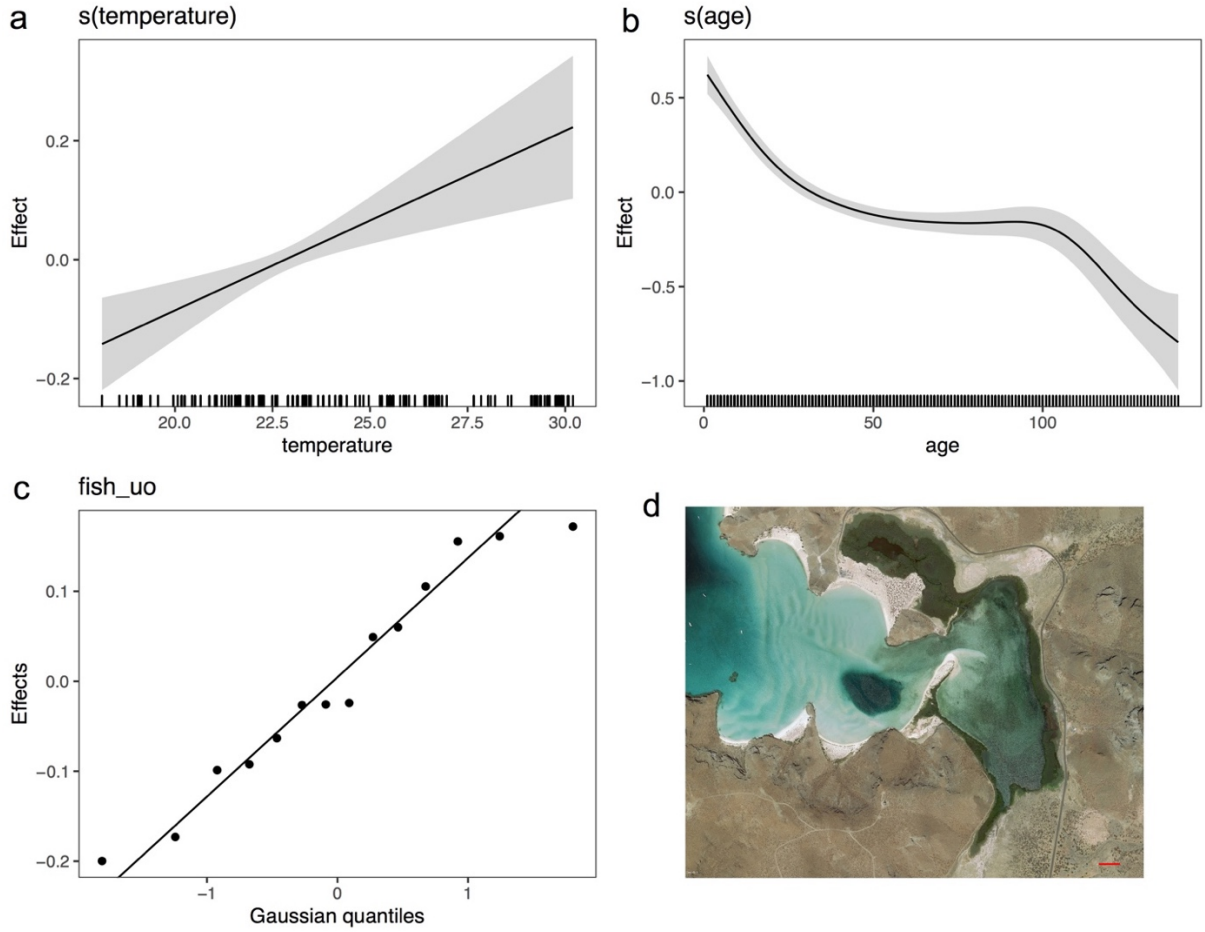

Figure 1.6. Width of daily growth increment (Effect) of yellow snapper juveniles in Balandra mangrove as a function of (a) temperature (°C) and (b) age (days). Black line represents the expected value with a confidence interval shown in gray. (c) Quantile-quantile plot of the random effects against Gaussian quantiles, used to check the appropriateness of the normal random effect assumption. (d) aerial view of Balandra mangrove, showing a long tidal channel that connects the bay area with an inland lagoon. Inserted map scale (red line) corresponds to 100 meters.

For fish at the Balandra mangrove site (southernmost site, $n = 14$), temperature and age were significant explanatory variables ($p < 0.001$) and were able to explain 50.2 % of the variance on daily growth width. Age had the highest explanatory power, and explained 41.5 % of

the variance on fish growth, followed by temperature, which explained 31 % of the variance (**Figure1. 6**).

For fish at the Santispac and Los Cocos sites (northern mangroves), juveniles grew with the increase of temperature until reaching a thermal threshold. For Santispac, the threshold seems to be approximately 30 °C, whereas for Los Cocos it seems to be approximately 28 °C.

Population growth (mm day^{-1}) and SST across a large spatial scale

We aged 173 yellow snapper juveniles of 17.9 to 136.2 mm standard length (SL) and from 16 to 294 days of age along mangroves distributed over a latitudinal range in which temperature varies (**Table 1.3, Figure 1.S8**). The growth rates of snapper juveniles (mm day^{-1}) within each mangrove site differed at ~ 800 km apart on the mainland side and ~ 380 km apart on the peninsula side. There was a positive correlation between juvenile growth rates within each mangrove site and the average SST adjacent to these mangroves (**Figure 1.S8a**). Growth rates followed a latitudinal gradient, with fish growing relatively faster in consistently warmer waters (ANOVA $p < 0.05$) or during the warmer seasons (e.g., Los Gatos juveniles lived mainly the summer months, with average temperatures of 29.27± 0.95) (**Figure 1.7**). The correlation between growth and temperature is more pronounced in the mangroves located on the Peninsula side ($R^2 = 0.86$) (**Figure 1.S8b**) than in the Mainland side ($R^2 = 0.02$) (**Figure 1.S8c**). Along the Baja California peninsula, juveniles at the southernmost mangrove site (Balandra, growth rate = 0.41 mm day^{-1}) grew almost twice as fast as juveniles from the northernmost mangrove site (San Lucas, growth rate = 0.25 mm day^{-1}), whereas such a latitudinal pattern was not evident along the mainland side.

Figure 1.7. Juvenile growth rates (mm/day) for yellow snappers (*n*=173) from eight mangrove sites in the Gulf of California.

SST trends around mangroves in the Gulf of California

Although there is large intra-annual variation in SST, we observed a positive linear trend of sea surface temperatures (SST) adjacent to all mangrove sites inside the Gulf of California for the past 20 years. This trend corresponds to an increase of approximately 0.04 °C year^{-1} (**Figure 1.8**). The number of days that are above three chosen temperature thresholds (28, 30 and 32°C) is higher for the period 2010-2019, compared with the period 2000-2009 (**Figure 1.S9**). For example, between 2000-2009, there were 19 days above 32 °C, while between 2010-2019, there were 30 days.

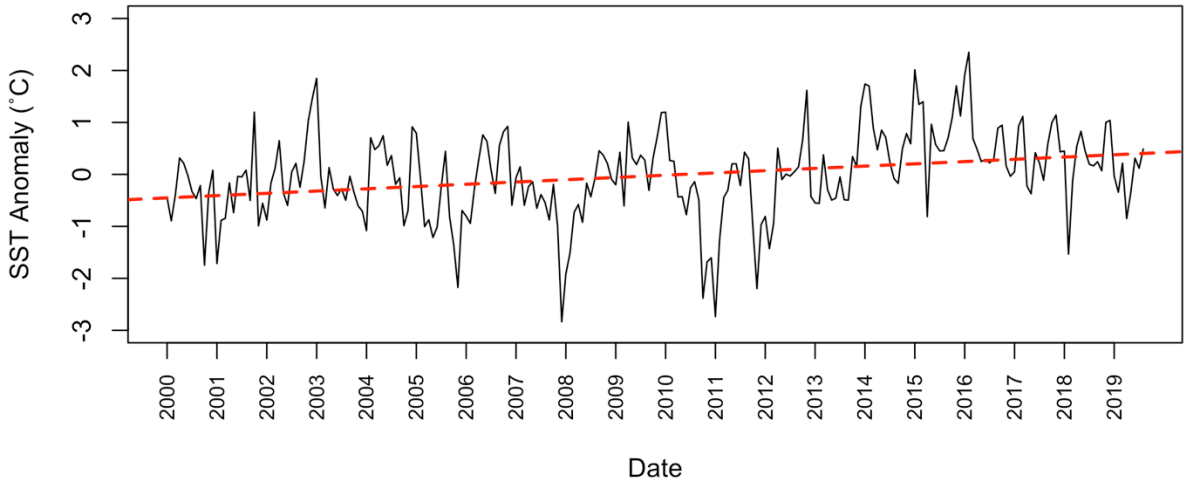

Figure 1.8. Sea surface temperature (SST) anomaly trend adjacent to all mangrove sites inside the Gulf of California, calculated for the period 2000-2019.

Discussion

The mangrove lagoons in the Gulf of California – especially those located along the semi-arid desertic coast of eastern Baja California peninsula – are enigmatic ecosystems that have triggered paradigm shifts on the understanding of carbon sequestration potential (Ezcurra et al., 2016), ecosystem service valuation (Aburto-Oropeza et al., 2008) and ecological importance (Whitmore et al., 2005). These systems are essential nurseries and/or temporary habitats for at least one hundred and sixty fish species in the Gulf of California (Whitmore et al., 2005), and the immense temperature variation in its waters - both intra-annual and latitudinal - have allowed us to estimate the role of water temperature on juvenile fish growth. We used oxygen isotope values and daily resolved increments on otoliths as "flight recorders" of the environmental conditions experienced during the juvenile's lifetime within these habitats.

Thermal reconstruction inside mangrove microcosms

The oxygen isotope ratio $\delta^{18}O$ of otoliths is primarily controlled by the temperature and the oxygen isotope ratio of the water in which the fish resided (Kalish, 1991a, Kalish, 1991b, Weidman & Miller, 2000). Therefore, for fully marine species, the $\delta^{18}O$ values in the otolith are dictated by the intra-annual temperature seasonality of the environment. The fractionation of ^{18}O when deposited into otolith aragonite increases in relation to ^{16}O, as the temperature of the environment decreases. This leads to a change in ^{18}O of otolith aragonite, such that $\delta^{18}O$ in per mils [‰] is negatively related to the water temperature (Kim & O'Neil, 1997). Commonly, the $\delta^{18}O$ of carbonate organisms decreases at around 1 ‰ with the concomitant increase of 5 °C of ambient temperature (Weidman & Millner 2000).

Our results showed a variation from -1.03 ‰ to -5.69 ‰ VPDB, which is similar to the observed values between +0.99 ‰ to -4.09 ‰ VPDB for *Cynoscion othonopterus* (Gulf corvina) in the upper Gulf of California (Rowell et al., 2005; Rowell, 2006). This is encouraging as the present study is, to the best of our knowledge, the first attempt in using $\delta^{18}O$ values on carbonate structures to reconstruct temperatures inside a mangrove lagoon. Typically, mangrove lagoons would not be the ideal ecosystems for thermal history reconstruction because these systems experience a large fluctuation on salinity due to the inflow of freshwater sources, which are known to temporally shift the $\delta^{18}O$ values in seawater towards more negative values. However, the semi-arid mangroves along the peninsula of Baja California lack river inflow contributions, making them appropriate ecosystems to test for thermal reconstruction based on otolith $\delta^{18}O$ values. Here, we assumed that the water salinity did not vary much or at least not enough to overwhelm the seasonal temperature effect on the otolith's isotopic composition. Indeed, we observed that the temperature reconstructed using otolith $\delta^{18}O$ approach tracked the range of *in situ* temperature the snapper juveniles experienced on these lagoons. This correspondence was

coherent for juveniles from Balandra (# 141) and Santispac (# 47) sites, and less consistent for juveniles from Los Cocos (# 103 and # 104) mangrove site. The mismatch between *in situ* temperature and temperature-reconstructed from otolith δ^{18} values in fish from Los Cocos mangrove coincides with calendar times of September - October 2018 for juvenile # 103, and October 2018 for juvenile # 104 (**Figure 1.3)**. This corresponds to the 2018 hurricane season in Baja California peninsula (e.g., Tropical Depression Nineteen-E, Hurricane Rosa and Hurricane Sergio), which led to high precipitation levels, locally known as "chubascos", that ran down the adjacent mountains to the small mangrove lagoons along the coast. It is possible that during these events, (1) juveniles from Los Cocos sought refuge in colder waters of the deeper inland pond at this mangrove (**Figure 1.5d**), and/or (2) juveniles experienced stressful events that decreased their metabolism, resulting in higher otolith δ^{18} values and, consequently, lower estimated temperatures compared to those measured *in situ* (Gabitov, 2013). In agreement with the hypothesis stated in (1), Jones & Campana (2009) observed that the ambient temperature reconstructed from otolith δ^{18} values in cod species *Gadus morhua* revealed small-scale thermoregulatory movements as a response to unusual cooling and warming conditions. Unusual environmental conditions are accentuated during strong hurricane events and could lead to those few positive excursions observed in our juvenile otolith δ^{18} values.

For Santispac (juvenile # 47), the inconsistencies in otolith $\delta^{18}O$ values observed were not as abrupt as those observed in Los Cocos juveniles, and followed an opposite pattern; negative excursions in otolith $\delta^{18}O$ values led to higher reconstructed temperatures. Juveniles at this site were possibly exposed to more negative $\delta^{18}O$ waters from the 2017 hurricane season rain (e.g., Tropical Storm Lidia) and, in agreement with this explanation, the small size of this lagoon (**Figure 1.4d**) would favor water dilution from precipitation events. For Santispac mangrove, we

observed that its frontal fringe was destroyed after this hurricane season (L. Cavole, personal observation, Jan 2018).

Regardless of the mechanisms behind these relatively short temporal (~ 30 days) inconsistencies, the range of expected values derived from temperature-reconstructed otolith $\delta^{18}O$ values were consistent with *in situ* temperature data, demonstrating that these juveniles are exposed to ~ 18-20 °C of variation and that they likely remain inside these sites during their first year of growth (Aburto-Oropeza et al., 2009). Stephenson et al. (2001) observed otoliths of similar species – the red emperor *Lutjanus sebae* and the Rankin cod *Epinephelus multinotatus* – in the north of Western Australia, and found that the values of stable oxygen isotopes were also strongly related to sea surface temperature (SST); the $\delta^{18}O$ values decreased with increasing SST, although the average temperature variation for their sites were less than 5 °C. The present study validates the use of otolith $\delta^{18}O$ to detect the extensive temperature variability in mangrove waters along the Baja California Peninsula. The application of this technique is promising at the desertic coasts of Baja California and can improve the understanding of how temperature controls the distribution, abundance, movement and ecology of marine fish at critical early life stages.

Daily growth widths (µm) and in situ HOBO temperature

Although there may be individual variations in growth, the global growth pattern of various fish within a population and region is expected to reflect any shared environmental signal (Black et al., 2013). For the Gulf of California mangrove lagoons, we hypothesized that the water temperature might play a key role on modulating the growth patterns of yellow snapper juveniles. Yellow snapper *Lutjanus argentiventris* grew in a nonlinear way accordingly with the

in-situ temperature, and in two mangrove lagoons, they seem to exhibit a temperature threshold beyond which their growth is reduced. For coral fishes, growth declines above an optimal temperature, or in low food conditions with high temperature (Munday et al., 2008), and when temperature interacts with other abiotic factors, such as tides (Wenger et al., 2016). Thus, we believe that the highest temperatures that these juveniles experience during the peak of the summer season might help to explain the thermal limits observed. There is a wide array of experimental studies that support this assumption. Pörtner & Knust (2007) and Pörtner & Peck (2010) observed thermally limited oxygen delivery on fishes, such that at higher temperatures, the increase of fish metabolism causes higher demands of oxygen at the same time that this gas is being reduced in the water due to its decrease in solubility. The reduction of growth observed here followed site-specific thresholds and it is apparent only in the juveniles from our northernmost sites (Los Cocos and Santispac). As we move towards northern areas inside the Gulf of California, the intra-annual temperature variability is increased (Galland et al., 2019), and our HOBO data confirm this trend inside mangrove lagoons that are under the influence of strong tidal variability (Santispac and Los Cocos juveniles inhabited waters from 15 °C to 34 °C whereas Balandra juveniles inhabited less temperature variable waters from 18 °C to 30 °C). Individuals from Santispac seemed to exhibit a higher temperature threshold (~ 32 °C) than those from Los Cocos (~28 °C). Also, Santispac mangrove geomorphology lacks a long channel and an inland lagoon (**Figure 1.4d**), which could potentially serve as a cold thermal refuge during extreme high temperature conditions. This suggests that the juveniles within this site might be exposed to very warm days without the option to seek refuge, likely forcing them to increase their thermal resilience, although future studies focusing on genetic analysis would be necessary to test this hypothesis.

Juvenile growth rates (mm day^{-1}) and SST

In order to assess how juveniles might grow across larger spatial scales (100s km), we analyzed juveniles from mangroves that differ in minimum, maximum and average water temperatures. Mangrove lagoons are key nursery habitats, enabling juveniles to attain sizes offering refuge from predators at a faster rate, which is a crucial process and allows for an attenuation of mortality pressure (Houde, 2002). Individuals that grow quickly may migrate to the sea after less than a year in the mangroves, while slow-growing fish may delay migration, remaining in the mangroves until they would attain a larger size (> 10 cm of SL). Thus, larger and faster-growing members of the cohort may be the first ones to occupy the most profitable territories offshore, while the smaller, slower-growing fish, may fail to find remaining suitable adult habitats.

The growth patterns of yellow snapper juveniles showed a consistent latitudinal pattern. The slope of the regression line relating the standard length (SL) of *Lutjanus argentiventris* to age (days) described an average growth rate for all juveniles of 0.35 mm/day (± 0.05 se), (R^2 = 0.66). The growth rates estimated at the present study was similar to the previously estimated by Aburto-Oropeza et al. (2009), although the last author used a different otolith pair (i.e., lapillus). Based on daily growth readings from several juveniles at each site, it was possible to identify some large spatial growth patterns for juvenile *L. argentiventris*. Along the Baja Peninsula side, the juveniles showed a progressive increase in their growth rates with decreasing latitude, with our southernmost site (Balandra, 0.41 mm/day) presenting a higher growth rate than our northernmost site (San Lucas, 0.25 mm/day). We believe this pattern is mainly driven by the typical SST gradient observed inside the Gulf of California, which would imply higher metabolic rates and consequently a faster growth in the south, warmer waters. At the Mainland side

mangroves, we observed a distinct pattern, less consistent with the temperature gradient. For example, the high growth rate observed at the high-latitude, mainland site of Tajce (0.40 mm/day), may be due to the high productivity of this mangrove system itself. Tajce is a region that encompasses nine mangrove patches where the diversity of habitats may enable a high and wide array of prey species. The mainland has large coastal lagoons with extensive mangrove forests (Contreras-Espinosa and Warner, 2004; Aburto-Oropeza et al., 2009) and its oceanographic conditions differ from those in the peninsula and enhance habitat suitability for snapper prey. In the Peninsula, many mangroves (e.g., San Jose, San Lucas and Puerto Escondido) are small forest patches in which the lagoons can remain closed for several months, creating hypoxic conditions, and consequently suboptimal conditions of growth (Aburto-Oropeza et al., 2009).

Whereas faster juvenile growth rate seems to follow a general temperature-latitudinal gradient, or inhabitance during the summer months of the year (e.g., Los Gatos mangrove), these juveniles seem to be already experiencing a thermal maximum beyond which their growth is reduced (based on the GAM analysis of daily increment width and *in-situ* water temperature). This finding is troublesome, considering that semi-enclosed seas like the Sea of Cortéz (inside the Gulf of California) show a warming trend since the 1950s (Lluch-Cota et al., 2010) and several impacts on the marine community are frequently documented (Páez-Osuna et al., 2016). Our analysis of water temperature adjacent to these mangrove sites confirmed this prediction. The warming of the water temperature around all mangrove sites inside the Gulf (0.0432 °C $year^{-1}$) is much higher than the global land and ocean average (0.014 °C $year^{-1}$) since 1981 (NOAA, 2019) and the global sea surface temperature (0.013 °C $year^{-1}$) over the past 100 years (NOAA,

2020), emphasizing the urgency of unravelling the effects of climate change in coastal environments, such as mangrove lagoons, and its associated and biodiverse marine biota.

Conclusions

We demonstrate that juveniles of yellow snappers experience up to 20 °C of temperature variability in mangrove waters, with otolith $\delta^{18}O$ values tracking this immense variability with relative precision. Secondly, we demonstrate that juvenile snappers from mangroves in the Baja California Peninsula grow faster in warmer waters than in colder waters, but there is a temperature threshold beyond which their growth is reduced (~ 28 – 32 °C). This species is potentially experiencing detrimental conditions for growth and development, with important implications for their long-term sustainability. Furthermore, the ongoing and rapid warming rate adjacent to all mangrove sites in the Gulf of California is concerning and might accentuate changes in the function and services provided by mangrove ecosystems. Otoliths are truly "flight recorders" of yellow snapper juvenile inhabitance in mangrove lagoons of Baja California and can shed light on how climate change affects these nursery sites and other economically and ecologically important marine life associated.

Acknowledgements

We are grateful to Carlos Sanchez for sampling permits and to Amilcar Huelgas and Oscar Pena for their assistance during field work in Baja California Peninsula. We thank Alfredo Girón for assistance in creating SST maps. This research was supported by the Tegner 2016 Fellowship awarded to LMC. LMC was supported by CNPq grant 213540/2014-2.

Chapter 1, in part, is being prepared for submission of the material. Cavole L.M., Zwolinski J., Castro-Falcón G., Johnson A.F., Hertwig A., Ming-Chang L., McKeegan K.D., Aburto-Oropeza O. The dissertation author was the primary investigator and author of this material.

Literature Cited

Aburto-Oropeza, O., Ezcurra, E., Danemann, G., Valdez, V., Murray, J., & Sala, E. (2008). Mangroves in the Gulf of California increase fishery yields. *Proceedings of the National Academy of Sciences*, *105*(30), 10456-10459.

Aburto-Oropeza, O., Dominguez-Guerrero, I., Cota-Nieto, J., & Plomozo-Lugo, T. (2009). Recruitment and ontogenetic habitat shifts of the yellow snapper (*Lutjanus argentiventris*) in the Gulf of California. *Marine biology*, *156*(12), 2461-2472.

Allen G. R. (1985) FAO species catalogue. Vol. 6. Snappers of the world. An annotated and illustrated catalogue of lutjanid species known to date. FAO *Fisheries Synopsis*, *125*(6), 60–61.

Alongi, D. M. (2008). Mangrove forests: resilience, protection from tsunamis, and responses to global climate change. *Estuarine, Coastal and Shelf Science*, *76*(1), 1-13.

Beck, M. W., Heck, K. L., Able, K. W., Childers, D. L., Eggleston, D. B., Gillanders, B. M., Halpern, B., Hays, C. G., Hoshino, K., Minello, T. J., Orth, R. J., Sheridan, P. F. & Weinstein, M. P. (2001). The identification, conservation, and management of estuarine and marine nurseries for fish and invertebrates: a better understanding of the habitats that serve as nurseries for marine species and the factors that create site-specific variability in nursery quality will improve conservation and management of these areas. *Bioscience*, *51*(8), 633-641.

Black, B. A., Matta, M. E., Helser, T. E. & Wilderbuer, T. K. (2013). Otolith biochronologies as multidecadal indicators of body size anomalies in yellowfin sole (*Limanda aspera)*. *Fisheries Oceanography, 22*(6), 523–532

Cheung, W. W., Lam, V. W., Sarmiento, J. L., Kearney, K., Watson, R. E. G., Zeller, D., & Pauly, D. (2010). Large-scale redistribution of maximum fisheries catch potential in the global ocean under climate change. *Global Change Biology*, *16*(1), 24-35.

Cheung, W. W., Watson, R., & Pauly, D. (2013). Signature of ocean warming in global fisheries catch. *Nature, 497*(7449), 365-368.

Contreras-Espinosa, F., & Warner, B. G. (2004). Ecosystem characteristics and management considerations for coastal wetlands in Mexico. *Hydrobiologia 511*(1), 233–245.

Coplen, T. B., Kendall, C., & Hopple, J. (1983). Comparison of stable isotope reference samples. *Nature, 302*(5905), 236-238.

Drinkwater, K. F. (2005). The response of Atlantic cod (*Gadus morhua*) to future climate change. *ICES Journal of Marine Science 62*(7), 1327 -1337.

Erisman, B., Mascarenas, I., Paredes, G., de Mitcheson, Y. S., Aburto-Oropeza, O., & Hastings, P. (2010). Seasonal, annual, and long-term trends in commercial fisheries for aggregating reef fishes in the Gulf of California, Mexico. *Fisheries Research*, *106*(3), 279-288.

Ezcurra, P., Ezcurra, E., Garcillán, P. P., Costa, M. T., & Aburto-Oropeza, O. (2016). Coastal landforms and accumulation of mangrove peat increase carbon sequestration and storage. *Proceedings of the National Academy of Sciences*, *113*(16), 4404-4409.

Gabitov, R. I. (2013). Growth-rate induced disequilibrium of oxygen isotopes in aragonite: An in situ study. *Chemical Geology*, *351*, 268-275.

Galland, G. R., Hastings, P. A., & Leichter, J. J. (2019). Fluctuating thermal environments of shallow-water rocky reefs in the Gulf of California, Mexico. *Scientific Reports*, *9*(1), 1-10.

Green, B. S., Mapstone, B. D., Carlos, G., & Begg, G. A. (Eds.). (2009). *Tropical fish otoliths: information for assessment, management and ecology* (Vol. 11). Springer Science & Business Media.

Handeland, S. O., Imsland, A. K., & Stefansson, S. O. (2008). The effect of temperature and fish size on growth, feed intake, food conversion efficiency and stomach evacuation rate of Atlantic salmon post-smolts. *Aquaculture*, *283*(1-4), 36-42.

Høie, H., Otterlei, E., & Folkvord, A., 2004. Temperature-dependent fractionation of stable oxygen isotopes in otoliths of juvenile cod (*Gadus morhua*). *ICES Journal of Marine Science, 61*(2), 243–251.

Houde, E. D. (1989). Comparative growth, mortality, and energetics of marine fish larvae: temperature and implied latitudinal effects. *Fishery Bulletin*, *87*(3), 471-495.

Houde, E. D. (2002). Mortality. In: Fishery Science: The Unique Contributions of Early Life Stages: Edited by Fuiman, L. A. & Werner, R. G. Blackwell Science Ltd. Oxford, UK. 64-87.

IPCC. (2013). Climate Change 2013: The Physical Science Basis. Contribution of Working Group I to the Fifth Assessment Report of the Intergovernmental Panel on Climate Change [Stocker, T. F., Qin, D., Plattner, G. -K., Tignor, M., Allen, S. K., Boshung, J.,

Nauels, A., Xia, Y., Bex, V., & Midgley P. M. (eds.)]. Cambridge University Press, Cambridge, United Kingtom and New York, NY, USA, 1535 pp.

IPCC. (2019). IPCC Special Report on the Ocean and Cryosphere in a Changing Climate [Pörtner, H.-O., Roberts, D. C., Masson-Delmotte, V., Zhai, P., Tignor, M., Poloczanska, E., Mintenbeck, K., Alegría, A., Nicolai, M., Okem, A., Petzold, J., Rama, B., & Weyer, N. M. (eds.)]. In press.

Jones, J. B., & Campana, S. E. (2009). Stable oxygen isotope reconstruction of ambient temperature during the collapse of a cod (*Gadus morhua*) fishery. *Ecological applications*, *19*(6), 1500-1514.

Jørgensen, K. E. M., Neuheimer, A. B., Jorde, P. E., Knutsen, H., & Grønkjær, P. (2020). Settlement processes induce differences in daily growth rates between two co-existing ecotypes of juvenile cod *Gadus morhua*. *Marine Ecology Progress Series*, *650*, 175-189.

Kalish, J. M. (1991a). Oxygen and carbon stable isotopes in the otoliths of wild and laboratory-reared Australian salmon (*Arripis trutta*). *Marine Biology*, *110*(1), 37-47.

Kalish, J. M. (1991b). 13C and 18O isotopic disequilibria in fish otoliths: metabolic and kinetic effects. *Marine Ecology Progress Series*, *75*(2–3), 191-203.

Kassambara, A. (2020). ggpubr: 'ggplot2' Based Publication Ready Plots. R package version 0.2.5. https://CRAN.R-project.org/package=ggpubr

Kim, S. T., & O'Neil, J. R. (1997). Equilibrium and nonequilibrium oxygen isotope effects in synthetic carbonates. *Geochimica et cosmochimica acta*, *61*(16), 3461-3475.

Lluch-Cota, S. E., Parés-Sierra, A., Magaña-Rueda, V. O., Arreguín-Sánchez, F., Bazzino, G., Herrera-Cervantes, H., & Lluch-Belda, D. (2010). Changing climate in the Gulf of California. *Progress in Oceanography*, *87*(1-4), 114-126.

Munday, P. L., Jones, G. P., Pratchett, M. S., & Williams, A. J. (2008). Climate change and the future for coral reef fishes. *Fish and Fisheries*, *9*(3), 261-285.

Nagelkerken, I. S. J. M., Blaber, S. J. M., Bouillon, S., Green, P., Haywood, M., Kirton, L. G., Meynecke, J. O., Pawlik, J., Penrose, H. M., Sasekumar, A. & Somerfield, P. J. (2008). The habitat function of mangroves for terrestrial and marine fauna: a review. *Aquatic botany*, *89*(2), 155-185.

NOAA. (2019). National Centers for Environmental Information, State of the Climate: Global Climate Report for Annual 2019, published online January 2020, retrieved on March 24, 2020 from https://www.ncdc.noaa.gov/sotc/global/201913.

NOAA. (2020). National Centers for Environmental information, Climate at a Glance: Global Time Series, published online March 2020, retrieved on March 24, 2020 from https://www.ncdc.noaa.gov/cag/

Páez-Osuna, F., Sanchez-Cabeza, J. A., Ruiz-Fernández, A. C., Alonso-Rodríguez, R., Piñón-Gimate, A., Cardoso-Mohedano, J. G., Flores-Verdugo, F. J., Carballo, J. L., Cisneros-Mata, M. A., & Álvarez-Borrego, S. (2016). Environmental status of the Gulf of California: A review of responses to climate change and climate variability. *Earth-Science Reviews*, *162*, 253-268.

Pankhurst, N. W., & Munday, P. L. (2011). Effects of climate change on fish reproduction and early life history stages. *Marine and Freshwater Research*, *62*(9), 1015-1026.

Parmesan, C., & Yohe, G. (2003). A globally coherent fingerprint of climate change impacts across natural systems. *Nature*, *421*(6918), 37.

Parmesan, C. (2006). Ecological and evolutionary responses to recent climate change. *Annual Review of Ecology, Evolution and Systematics*, *37*, 637-669.

Pedersen, E. J., Miller, D. L., Simpson, G. L., & Ross, N. (2019). Hierarchical generalized additive models in ecology: an introduction with mgcv. *PeerJ*, *7*, e6876.

Pepin, P. (1991). Effect of temperature and size on development, mortality, and survival rates of the pelagic early life history stages of marine fish. *Canadian Journal of Fisheries and Aquatic Sciences*, *48*(3), 503-518.

Perry, A. L., Low, P. J., Ellis, J. R., & Reynolds, J. D. (2005). Climate change and distribution shifts in marine fishes. *Science*, *308*(5730), 1912-1915.

Planque, B., Fromentin, J. M., Cury, P., Drinkwater, K. F., Jennings, S., Perry, R. I., & Kifani, S. (2010). How does fishing alter marine populations and ecosystems sensitivity to climate? *Journal of Marine Systems*, *79*(3), 403-417.

Pörtner, H. O., & Knust, R. (2007). Climate change affects marine fishes through the oxygen limitation of thermal tolerance. *Science*, *315* (5808), 95-97.

Pörtner, H. O., & Peck, M. A. (2010). Climate change effects on fishes and fisheries: towards a cause-and-effect understanding. *Journal of fish biology*, *77*(8), 1745-1779.

Przeslawski, R., Byrne, M., & Mellin, C. (2015). A review and meta-analysis of the effects of multiple abiotic stressors on marine embryos and larvae. *Global change biology*, *21*(6), 2122-2140.

Righton D. A., Andersen K. H., Neat F., Thorsteinsson V., Steingrund, P., Svedäng, H., Michalsen, K., Hinrichsen, H. H., Bendall, V., Neuenfeldt, S. & Wright, P. 2010.

Thermal niche of Atlantic cod *Gadus morhua*: limits, tolerance and optima. *Marine Ecology Progress Series*, *420*, 1-13.

Rijn, I., Buba, Y., DeLong, J., Kiflawi, M., & Belmaker, J. (2017). Large but uneven reduction in fish size across species in relation to changing sea temperatures. *Global Change Biology*, *23*(9), 3667-3674.

Rowell, K., Flessa, K. W., Dettman, D. L., & Román, M. (2005). The importance of Colorado River flow to nursery habitats of the Gulf corvina (*Cynoscion othonopterus*). *Canadian Journal of Fisheries and Aquatic Sciences*, *62*(12), 2874-2885.

Rowell K. (2006). Isotopic logs of the Sea of Cortez: Oxygen and carbon stable isotopes in otoliths from marine fish record the impact of diverting the Colorado River from the sea. PhD Dissertation, University of Arizona.

Shiao, J. C., Sui, T. D., Chang, N. N., & Chang, C. W. (2017). Remarkable vertical shift in residence depth links pelagic larval and demersal adult jellynose fish. *Deep Sea Research Part I: Oceanographic Research Papers*, *121*, 160-168.

Stephenson, P. C., Edmons, J. S., Moran, M. J., & Caputi, N. (2001). Analysis of stable isotope ratios to investigate stock structure of red emperor and Rankin cod in northern Western Australia. *Journal of Fish Biology*, *58*(1), 126-144.

Thomas, C. D., Cameron, A., Green, R. E., Bakkenes, M., Beaumont, L. J., Collingham, Y. C., Erasmus, B. F. N., de Siqueira, M. F., Grainger, A., Hannah, L., Hughes, L., Huntley, B., van Jaarsveld, A. S., Midgley, G. F., Miles, L., Ortega-Huerta, M. A., Peterson, A. T., Phillips, O. L., & Williams, S. E. 2004. Extinction risk from climate change. *Nature 427*(6970), 145–148.

Walden, G., Noirot, C., & Nagelkerken, I. (2019). A future 1.2° C increase in ocean temperature alters the quality of mangrove habitats for marine plants and animals. *Science of the Total Environment*, *690*, 596-603.

Weidman, C. R., & Millner, R. (2000). High-resolution stable isotope records from North Atlantic cod. *Fisheries Research*, *46*(1-3), 327-342.

Wenger, A. S., Whinney, J., Taylor, B., & Kroon, F. (2016). The impact of individual and combined abiotic factors on daily otolith growth in a coral reef fish. *Scientific Reports*, *6*(1), 1-10.

Whitmore, R. C., Brusca, R. C., León de la Luz, J. L., González- Zamorano, P., Mendoza-Salgado, R., Amador-Silva, E. S., Holguín, G., Galván-Magaña, F., Hastings, P. A., Cartron, J.- L. E., Felger, R. S., Seminoff, J. A. & McIvor, C. C. (2005). The ecological importance of mangroves in Baja California Sur: conservation implications for an endangered ecosystem. In: Cartron, J.E., Ceballos, G. & Felger, R.S. (eds.) Biodiversity,

ecosystems and conservation in northern Mexico. *Oxford University Press, New York, NY, US*. pp. 298–332.

Wickham, H. (2016). ggplot2: Elegant Graphics for Data Analysis. Springer-Verlag New York, 2016.

Wood, S.N. (2017) Generalized Additive Models: An Introduction with R. Chapman and Hall/CRC.

Zgliczynski, B. J. (2015). *The direct and indirect effects of predators on coral reef fish assemblages*. PhD Dissertation, University of California, San Diego.

TABLES

Table 1.1. Yellow snapper samples used for thermal reconstruction. The *in-situ* temperature was recorded for one year (*in-situ* T) inside each mangrove site. The age of juveniles was estimated as the number of daily growth increments (Age), and standard length (SL) and total weight (TW) are provided for each individual. Spots are number of $\delta^{18}O$ measurements in two opposing transects along the otolith (except by juvenile #47, with one transect). $\delta^{18}O$ values (‰ vs. VSMOW) for seawater were estimated based on outermost spot and temperature at the time of fish capture.

Fish ID	Mangrove	Location	*In situ* T (°C)	Age (DGI)	$\delta^{18}O_{sw}$	SL (mm)	TW (g)	Spot (*n*)	Collection date
104	Los Cocos	26.74°N 111.89°W	16.59 - 33.86	178	-2.59	114	39.58	33	27-Jan-19
103	Los Cocos	26.74°N 111.89°W	16.59 - 33.86	152	-2.55	102	31.46	22	27-Jan-19
47	Santispac	26.77°N 111.89°W	15.84 - 33.55	156	-1.89	88	12.23	14	24-Jan-18
141	Balandra	24.32°N 110.31°W	18.13 - 30.32	173	-2.35	90	17.2	27	1-Feb-19

Table 1.2. Yellow snapper samples used in the GAM model. Number of otoliths used (*n*) at each mangrove site is presented. Range for standard length (SL), age based on daily growth increment count (Age) and the width of daily growth increments (DGW) are provided.

Mangrove	*n*	SL (mm)	Age (DGR)	DGW (µm)
Balandra	14	39-95	79-155	5.26-16.27
Los Cocos	17	24-94	46-124	4.83-13.17
Santispac	22	48-103	73-157	4.81-22.09

Table 1.3. Yellow snapper samples used for the estimate of growth rates along a latitudinal SST gradient. Growth rates (mm day^{-1}) of juveniles from eight mangrove sites collected in June and October of 2003 and 2004. Number of otoliths used in age estimation (*n*) is shown. Mean sea surface temperature (SST) and mean chlorophyll *a* (chl *a*) experienced during juvenile's lifetime are presented. Range for the age based on daily growth increment count (Age) and the standard lengths of fish (SL) are listed.

Mangrove site	Location	coast	*n*	SST (°C)	Chl *a* (mg m^{-3})	Age (DGI)	SL (mm)	Growth rate (mm day^{-1})
San Lucas	27.22°N 112.21°W	Peninsula	23	25.06	3.03	87-215	37.5-99	0.25
Puerto Escondido	25.82°N 111.31°W	Peninsula	22	25.17	2.31	33-195	17.9-87.6	0.35
Los Gatos	25.27°N 110.93°W	Peninsula	30	29.27	1.02	33-179	22.9-102.5	0.35
San Jose	24.83°N 110.56°W	Peninsula	23	26.01	1.10	93-290	35.9-131.3	0.52
Balandra	24.32°N 110.31°W	Peninsula	29	26.49	1.46	17-176	22.8-94.7	0.41
Tajce	29.02°N 112.17°W	Mainland	22	25.17	6.60	58-294	32-136.2	0.4
Islote Bojorquez	25.00°N 108.15°W	Mainland	5	30.67	3.20	118-156	66.2-80.9	0.34
Barra de Piaxtla	24.32°N 110.31°W	Mainland	15	29.64	2.38	16-95	18-62.4	0.63

Chapter 1 Appendix

The role of temperature on fish growth: insights from mangrove microcosms

Supplementary Information

by

LETICIA MARIA CAVOLE[1,*], JUAN ZWOLINSKI[2,3], GABRIEL CASTRO FALCÓN[1], HAYLE SUE[1], ANDREW FREDERICK JOHNSON[1,4], ANDREAS HERTWIG[5,6], MING-CHANG LIU[5], KEVIN D. MCKEEGAN[5], OCTAVIO ABURTO-OROPEZA[1]

[1]Scripps Institution of Oceanography, University of California San Diego, 9500 Gilman Drive, La Jolla, CA 92093, USA

[2] University of California Santa Cruz, Santa Cruz, California, CA 95064, USA

[3] NOAA Southwest Fisheries Science Center, La Jolla, CA 92037, USA

[4] The Lyell Centre, Institute of Life and Earth Sciences, School of Energy, Geoscience, Infrastructure and Society, Heriot-Watt University, Edinburgh, EH14 4AS, UK

[5] Department of Earth, Planetary, and Space Sciences, University of California - Los Angeles, Los Angeles, CA, 90095, USA

[6] Institute of Earth Sciences, Heidelberg University, 69120 Heidelberg, Germany

*Corresponding Author: lcavole@ucsd.edu

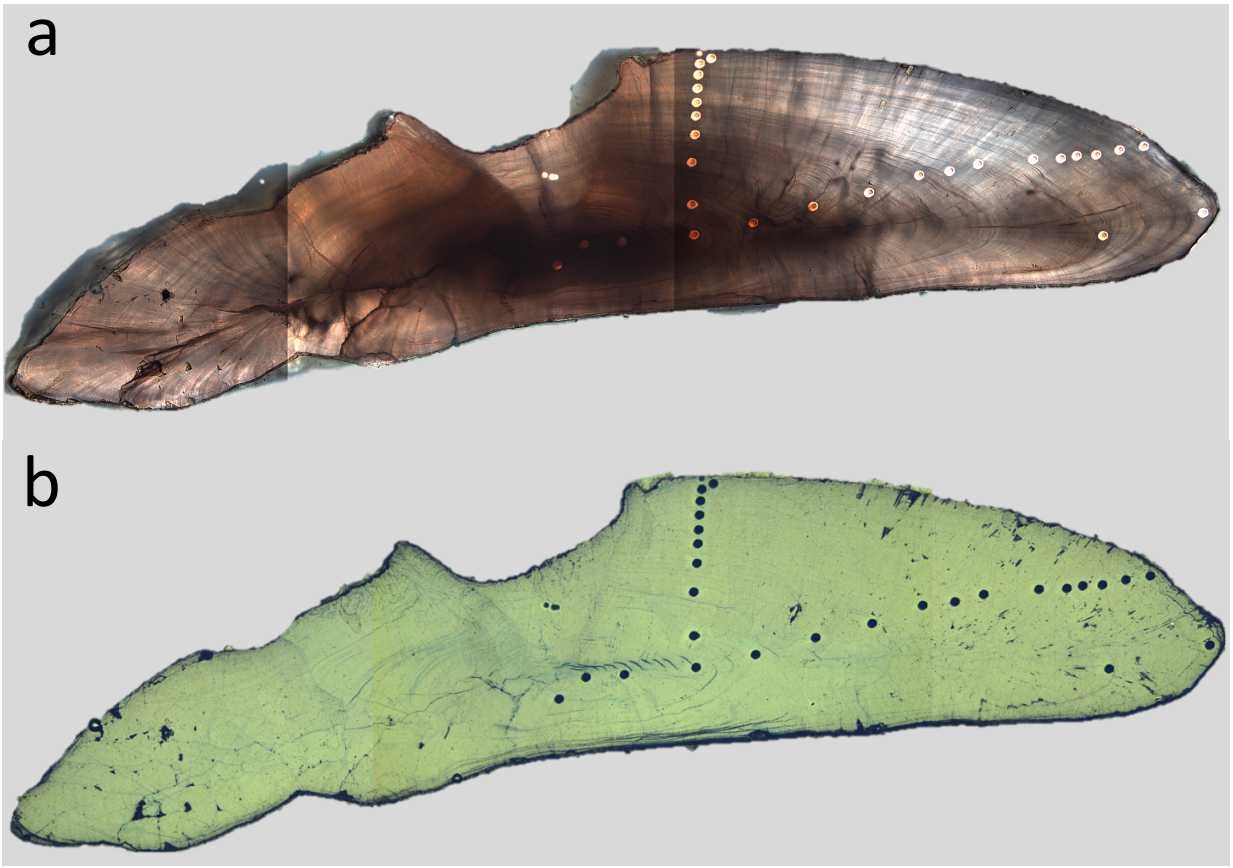

Figure 1.S1. Otolith section showing the location of spots where $\delta^{18}O$ values were measured. A picture of the section using (a) transmitted light and (b) reflected light. $\delta^{18}O$ values follow the juvenile ontogeny from the core area to the edge of the otolith.

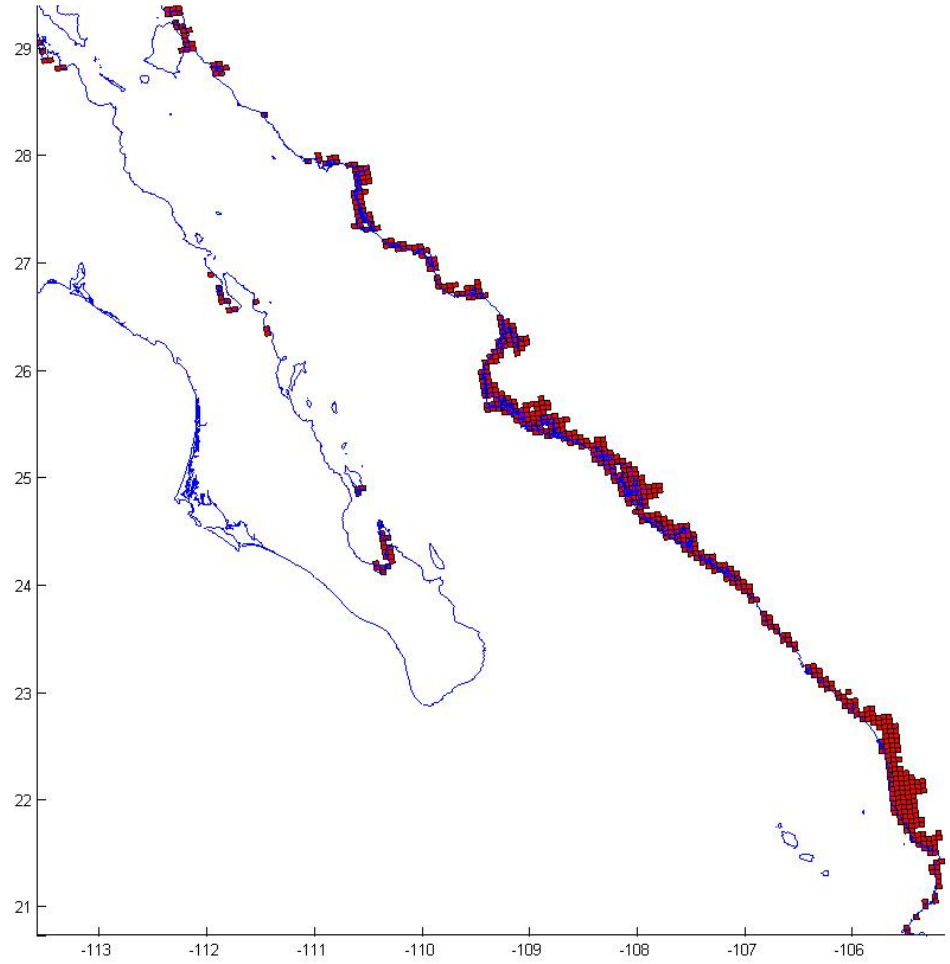

Figure 1.S2. Polygons of 25 km^2 overlap the map of mangrove distribution inside the Gulf of California, generating a total of 624 polygons (red). The sea surface temperature available for each of these polygons were downloaded to examine trends of water temperature adjacent to these ecosystems.

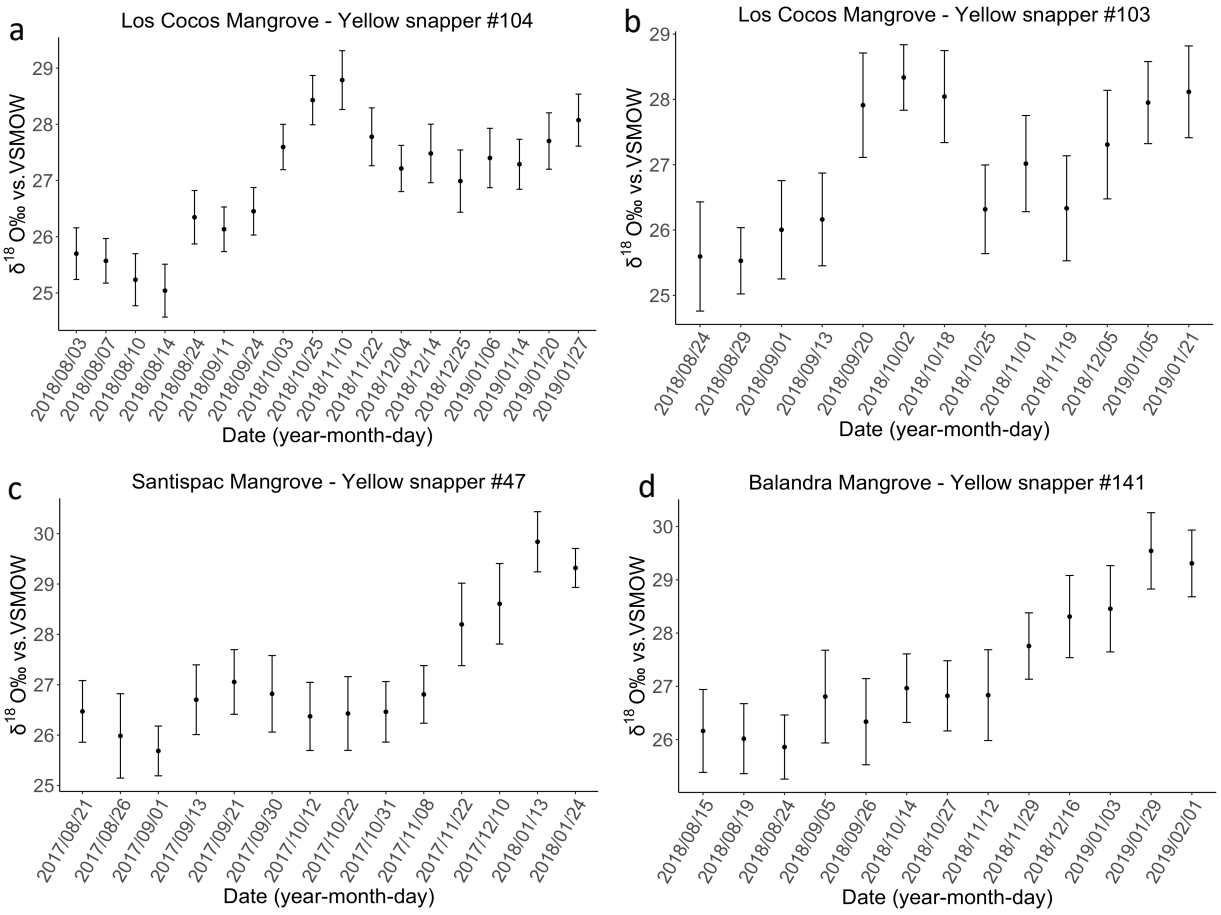

Figure 1.S3. Measurements of $\delta^{18}O$ values (‰ vs. VSMOW) in four otoliths of yellow snappers *Lutjanus argentiventris*. Error bars indicate 2σ. X-axis represent time from birth (left) to death (right). Dates were back calculated based on the alignment between daily growth increments and the spots for $\delta^{18}O$ values obtained from secondary ion mass spectrometry (SIMS).

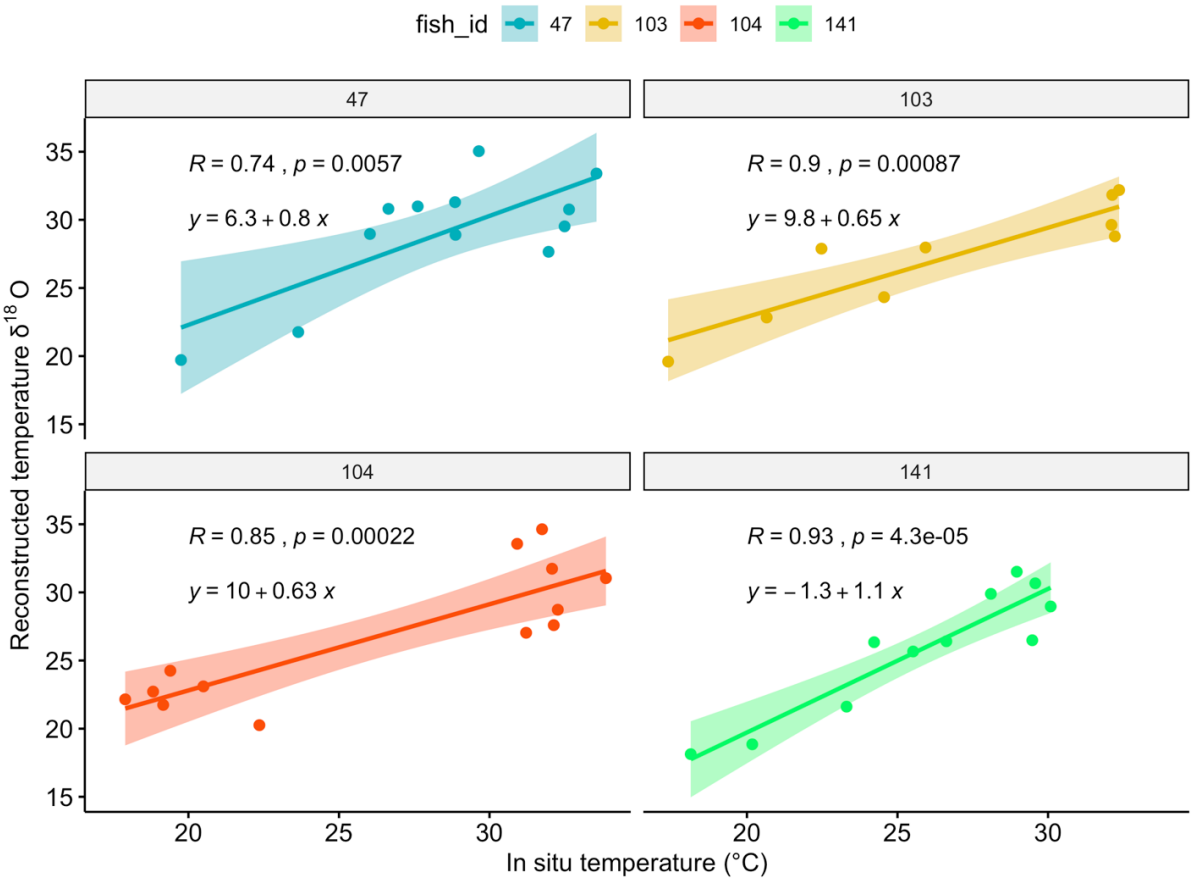

Figure 1.S4. Relationship between reconstructed temperature using otolith $\delta^{18}O$ values and *in situ* temperature recorded by HOBO loggers. Pearson correlation coefficient (*R*) and significance level (*p*) are displayed for four juveniles. Outliers attributed to the Hurricane season of 2018 in Baja California for the juveniles # 103 and #104 were removed.

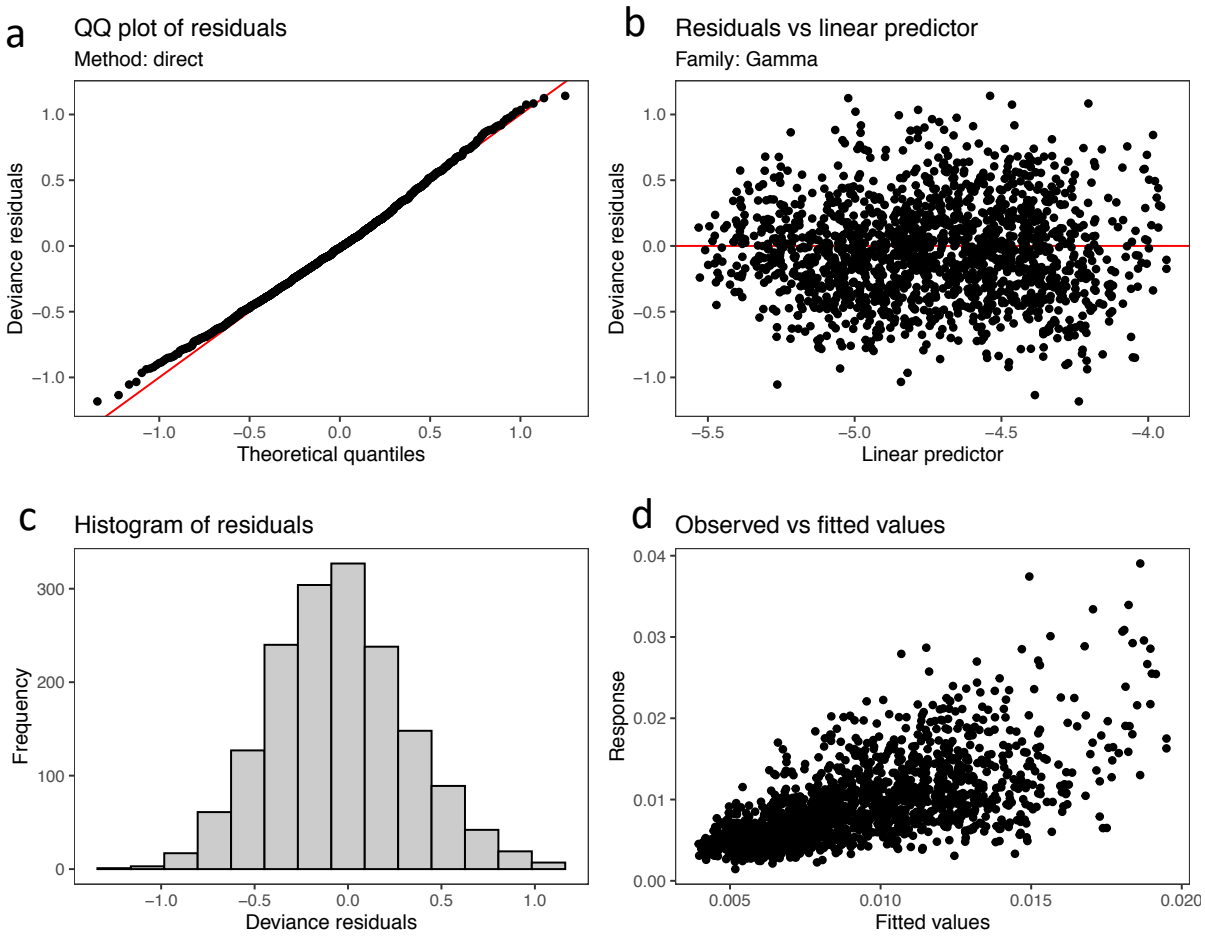

Figure 1.S5. Diagnostic plots for Santispac Global GAM model, where (a) = Normal quantile-quantile, (b) = Linear predictor values plotted against residuals, (c) = Histogram plot of residuals, and (d) = Fitted values plotted against response variable.

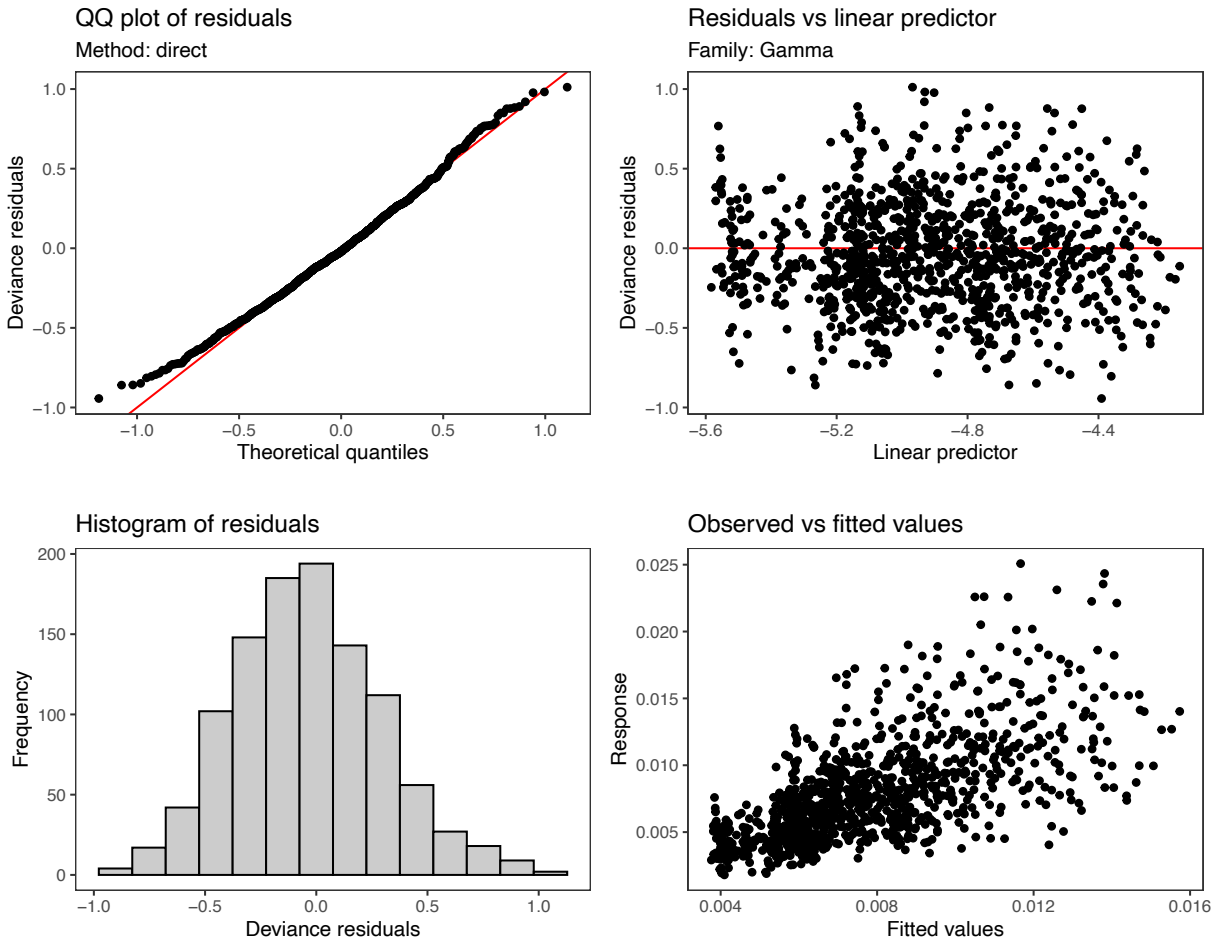

Figure 1.S6. Diagnostic plots for Los Cocos Global GAM model, where (a) = Normal quantile-quantile, (b) = Linear predictor values plotted against residuals, (c) = Histogram plot of residuals, and (d) = Fitted values plotted against response variable.

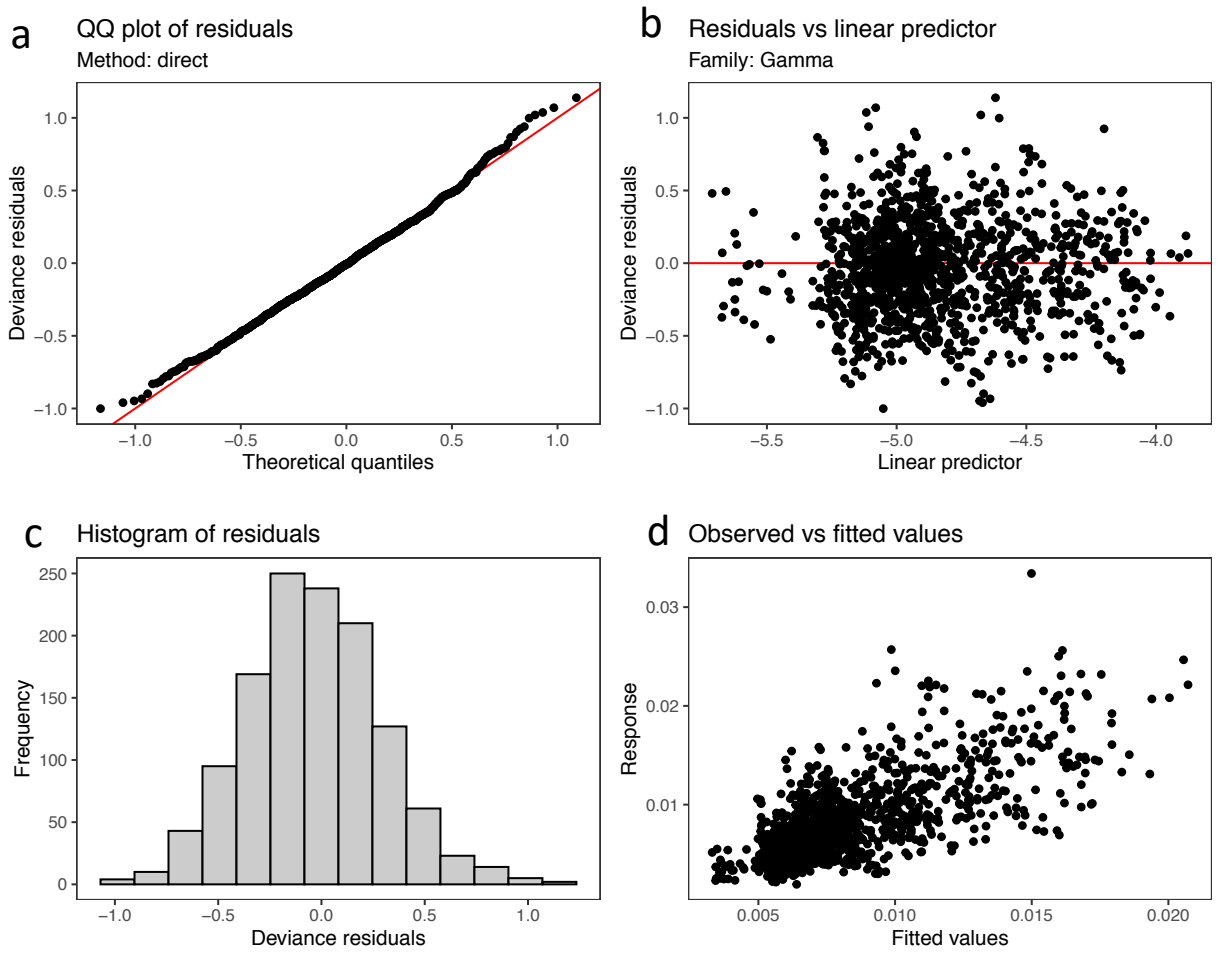

Figure 1.S7. Diagnostic plots for Balandra Global GAM model, where (a) = Normal quantile-quantile, (b) = Linear predictor values plotted against residuals, (c) = Histogram plot of residuals, and (d) = Fitted values plotted against response variable.

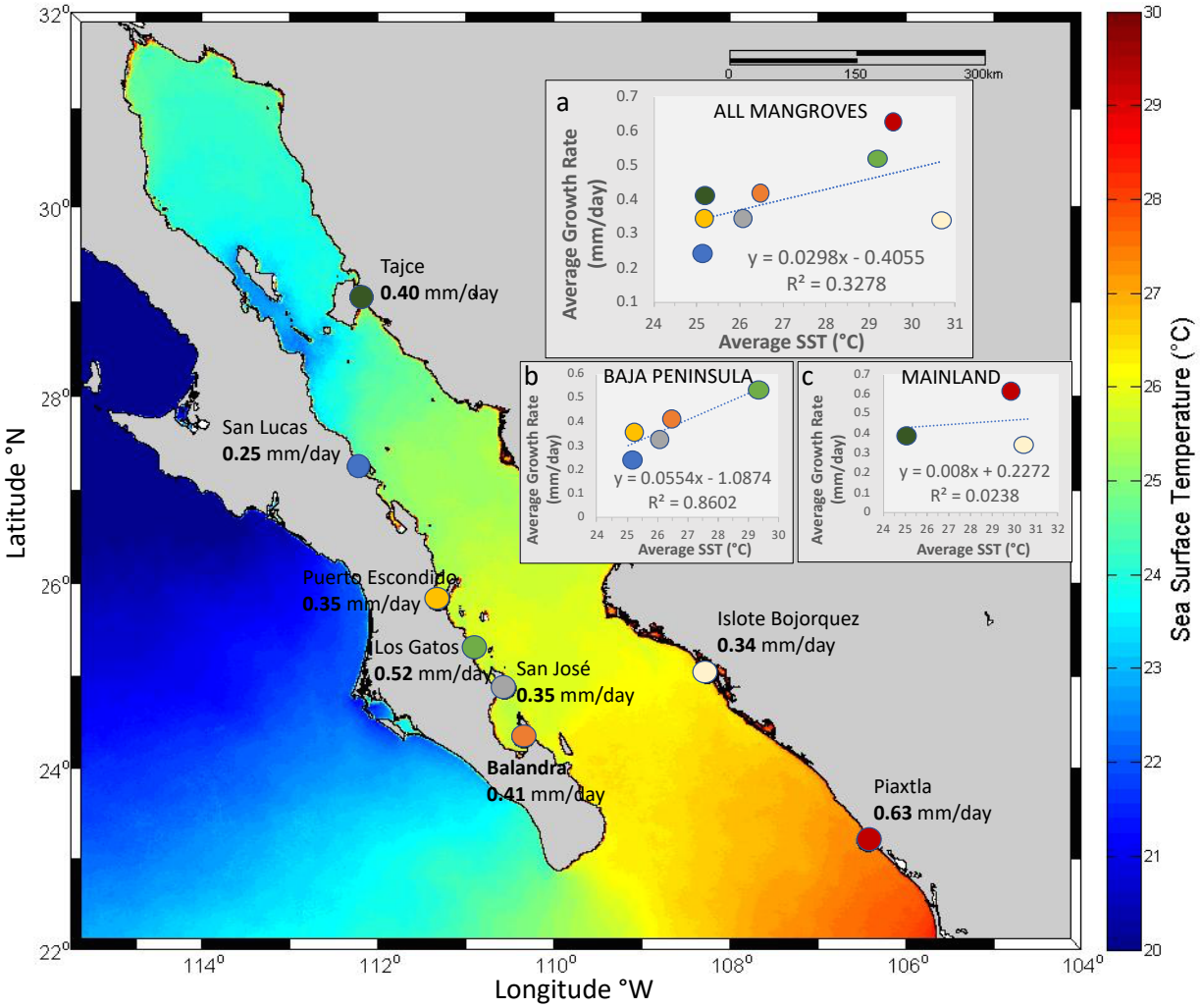

Figure 1.S8. Colorful dots correspond to mangrove sites where juveniles of yellow snapper were collected in 2003-2004, and their correspondent growth rates based on the number of daily growth increments. Inset plots show: (a) the relationship between juvenile's average growth rate and average SST in each mangrove site, (b) for juveniles in mangroves at Baja peninsula, and (c) for juveniles in mangroves at Mexico's mainland. The site colors in the map correspond to the dot colors in the plots. *For Los Gatos mangrove, the average SST experienced by snapper juveniles is higher than what is displayed at the map, since these juveniles lived during the warmest season of the year.

Figure 1.S9. Number of days in a year above water temperature thresholds (28, 30 and 32°C). The water temperature was calculated based on the SST adjacent to all mangrove lagoons in the Gulf of California for the past 20 years.

CHAPTER 2:

The role of extrinsic variation – cohabiting juvenile fish species exhibit similar otolith elemental signatures

LETICIA MARIA CAVOLE, JESSICA A. MILLER, PELAYO SALINAS-DE-LEÓN, OCTAVIO ABURTO-OROPEZA, JOSE R. MARIN JARRIN AND ANDREW FREDERICK JOHNSON

Abstract

The effect of extrinsic (environmentally-based) and intrinsic (physiologically-based) controls on otolith elemental signatures remains poorly understood. We evaluated the relative importance of both extrinsic and intrinsic factors using juvenile fish in Eastern Tropical Pacific (ETP) mangroves. To assess extrinsic influences, we compared the cohabiting yellow snapper *Lutjanus argentiventris* and sailfin grouper *Mycteroperca olfax* from the Galápagos Archipelago. To evaluate intrinsic influences, we compared yellow snapper from the Gulf of California (Mexico) and the Galápagos Archipelago (Ecuador). The 2 cohabiting species in the Galápagos exhibited very similar otolith elemental signatures, with no significant differences observed for Li, Cu, Mg, Mn, Rb, and Sr (univariate ANOVAs, $p > 0.05$), and a small separation achieved between these species (ANOSIM test, $R = 0.01$, P: 0.038). The yellow snappers from Galápagos and the Gulf of California exhibited distinct elemental signatures increasing from Rb, Cu, Mn, Sr, Li to Ba (univariate ANOVAs, $p < 0.05$), with a large separation between them (ANOSIM test, $R = 0.55$, P: 0.001). The present study suggests that extrinsic factors (e.g. water chemistry, temperature, salinity) can be more important than intrinsic factors (e.g. physiology, growth rates, genetics) for influencing elemental uptake in the otoliths of juveniles from mangrove waters. However, improved understanding of factors influencing elemental incorporation is still needed to ensure accurate interpretation of field data, especially in dynamic oceanographic systems, which is the case for both the Gulf of California and the Galápagos Archipelago.

Introduction

Otoliths – calcium carbonate structures in the inner ear of teleost fishes – present unique chemical and chronological properties as they can record aspects of both the environment and

fish life history strategy (Campana & Thorrold 2001). The chemistry of otoliths can be influenced either directly by variation in environmental conditions (e.g. ambient water chemistry, salinity, temperature) or indirectly through the environmental effects on fish physiology (e.g. growth, metabolism, stress). Laboratory experiments demonstrating how elemental signatures in otoliths reflect environmental conditions have allowed insight to be gained on various aspects of the life history dynamics of fish including freshwater-marine transitions in anadromous and catadromous species (Kalish 1990, Secor 1992), population connectivity (Chittaro et al. 2004), population structure (Campana et al. 1994, Ashford et al. 2006, Clarke et al. 2011), and utilization of nursery habitats and natal homing (de Pontual et al. 2000, Thorrold et al. 2001, Gillanders et al. 2003, Mateo et al. 2010). Otolith microchemistry has also been useful in developing environmental proxies for hypoxia events (Limburg et al. 2015) and pollution exposure (Geffen et al. 1998, Halden & Friedrich 2008).

Although otolith chemical analyses have become a common research tool in fish ecology and fisheries management, the precise mechanisms governing elemental incorporation into the otoliths are not fully understood (Campana 1999). This is due to the complex interaction of multiple intrinsic (e.g. physiology, growth rates, metabolism, genetics) and extrinsic (e.g. temperature, salinity, dissolved oxygen, water chemistry) factors that can disrupt the simple linear relationships between an element and a single environmental parameter (Grønkjær 2016, Walther 2019). The current discussion on how intrinsic or species-specific "vital effects" affect the use of otolith chemistry as a natural tag has been addressed in several recent studies (Chang & Geffen 2013, Sturrock et al. 2015, Walther 2019), which suggest that the influence of physiological controls may play a key – usually underestimated – role in elemental incorporation (Sturrock et al. 2014, 2015, Thomas et al. 2017, Izzo et al. 2018). Moreover, the degree to which

the relationship between environment and otolith chemistry can be generalized across species with physiological differences remains poorly understood. Comparison of different species experiencing the same environmental variation could provide insights into whether the influence of environmental variation on otolith chemistry remains consistent across species.

In addition to the lack of knowledge of the underlying mechanisms affecting otolith chemical composition, otolith microchemistry work is still not broadly available in developing countries or tropical areas (Avigliano & Volpedo 2016) due to the highs costs and qualified technical knowledge required. This is the case in the Gulf of California (Mexico) and the Galápagos Archipelago (Ecuador), an area for which just 1 microchemistry paper is currently available (Ruttenberg & Warner 2006). Nonetheless, these subtropical regions are particularly interesting from an ecological perspective because they experience high seasonal variation in sea surface temperature (SST) and primary productivity. For example, the intra-annual SST and chlorophyll a vary up to 8°C and 10-fold among bioregions in Galápagos, an archipelago located at the equator (Wellington et al. 2001) and the intra-annual SST varies up to 17°C in the Gulf of California, which is one of the most productive marginal seas in the world (Álvarez-Borrego 2012). In addition, both regions have high percentages of endemic fish – 13.6% for Galápagos (McCosker & Rosenblatt 2010) and 10% for the Gulf of California (Lluch-Cota et al. 2007) – that are subject to fisheries and whose management could use tools such as otolith microchemistry analysis. For example, otolith microchemistry could help to identify and address the contribution of nursery sites for the adult populations (Thorrold et al. 2001, Chittaro et al. 2004, Mateo et al. 2010), and/or to assess stock structure and connectivity patterns (Thorrold et al. 2007).

The present study is the first attempt to evaluate extrinsic and intrinsic influences on the elemental composition of otoliths of juvenile fishes inhabiting mangrove forests in the Eastern Tropical Pacific Ocean (ETP). To evaluate the relative importance of extrinsic drivers we compared different species in the same environment: yellow snapper *Lutjanus argentiventris* and sailfin grouper *Mycteroperca olfax* in Galápagos. We used snappers and groupers as model species because they both have different life histories, growth rates, and diets (Aburto-Oropeza et al. 2009, Usseglio et al. 2015) but both inhabit mangroves during their juvenile stages. If these 2 species exhibit similar elemental fingerprints in Galápagos, then these would both likely reflect the characteristics of the environment, such as water chemistry, temperature and salinity. Conversely, if they exhibit different elemental fingerprints that would indicate an effect of species-specific physiologies, taxonomic differences and/or microhabitat preferences. Furthermore, to improve our understanding of the role that intrinsic variation can play in the elemental composition of the otoliths, we also compared the elemental signatures of yellow snapper *L. argentiventris* occupying 2 different dynamic ecosystems: the Galápagos Archipelago and the Gulf of California. Although this interspecies comparison has a temporal component we cannot control for (snappers were collected in each location ~ 12 yr apart), this comparison provides an initial evaluation of the magnitude of variation in otolith chemistry between yellow snappers at their northern (Mexico) and southern (Ecuador) limits of distribution.

We hypothesized that (1) the water environmental signal in the Galápagos Archipelago – driven by the convergence of 3 major oceanographic currents – is stronger than the taxonomic or physiological factors regulating the incorporation of trace elements into fish otoliths, and (2) physiological factors regulating the incorporation of trace elements into fish otoliths may be minor when comparing the same species across completely distinct ecosystems.

Material and Methods

Model species and data selection

The yellow snapper *Lutjanus argentiventris* occurs throughout the ETP, from southern California to Peru (Allen 1985). In the Gulf of California, adults spawn on the continental shelf, and their larvae are transported to mangroves where they metamorphose and settle at around 19 to 26 d after hatching. The juveniles remain close to the substrate and to the mangrove roots until they are approximately 10 cm in total length (TL) (approx. 150 to 200 d old), when they begin to migrate offshore to join adults on rocky reefs (Aburto-Oropeza et al. 2009). In Galápagos, juvenile yellow snappers are also present in mangroves, but up to a larger size (~20 cm TL), suggesting that they might migrate at larger sizes than the juveniles from the Gulf of California (J. Marin. pers comm. 2017). This species sustains an important artisanal fishery in both the Gulf of California and Galápagos. There are signs of overexploitation, such as a decline in the size-at-capture in the former (Piñón et al. 2009) and reduced abundance and biomass in the latter region (Ruttenberg 2001).

The Galápagos sailfin grouper *Mycteroperca olfax* is endemic to several islands of the ETP and in Galápagos it has a high economic and cultural value (Reck 1983). Despite its importance, the Galápagos sailfin grouper faces severe overexploitation (Usseglio et al. 2016) due to the combination of a strong fishery pressure, the direct targeting of spawning aggregations (Salinas-de-León et al. 2015) and its K-selected life-history strategy of slow growth and high longevity (Usseglio et al. 2015, Usseglio et al. 2016, Eddy et al. 2019).

We examined 70 grouper juveniles and 88 yellow snapper juveniles from the Galápagos Archipelago, and 174 yellow snapper juveniles from the Gulf of California, for a total of 332 fishes (**Figure 2.1**). We selected the juvenile stage of these species because they all come from

mangrove sites and do not have physiological changes induced by reproduction, which is known to affect the chemistry of otoliths (Kalish 1989). Snappers and groupers from Galápagos were collected in 2 sampling events, in April of 2015 and April of 2016, while snappers from the Gulf of California were sampled in 4 collection events, in June and October of 2003 and June and October 2004 (**Table 2.1**). Most of the Galápagos samples (93% of the fishes) were collected in April 2015, while 60% of the Gulf of California samples were collected in June and October 2003, and 40% in June and October 2004.

For the present study, we included only sailfin grouper juveniles under 26 cm of TL (**Table 2.1**), which had not yet formed the first annual ring in their otolith. Since this species begins to reproduce at ~ 6.5 yr old and 65 cm of TL (Usseglio et al. 2016), all groupers collected in this study were immature. All snappers were age-0 (**Figure 2.2, Table 2.1**), estimated from counts of daily growth rings validated by Zapata & Herrón (2002). The snappers from the Gulf of California represented 4 different cohorts - the winter and summer of 2003, and the winter and summer of 2004 - while the snappers from Galápagos represented 2 cohorts – the winter of 2014 and summer of 2015 (**Figure 2.3**).

Otolith preparation and elemental analysis

Otolith sections from all samples were mounted in random order on microscope slides using thermoplastic adhesive (Crystalbond™), cleaned in ultrapure water and dried in a Class 100 clean bench (for details of otolith preparation see Text S1 in the Supplement at www.int-res.com/articles/suppl/mXXXpXXX_supp.pdf). The elemental composition of *L. argentiventris* and *M. olfax* otoliths was quantified using a Thermo Scientific X-series II quadrupole inductively coupled plasma mass spectrometer with a Photon Machines Analyte G2 laser system (LA-

ICPMS) at the Oregon State University WM Keck Collaboratory for Plasma Spectrometry in Corvallis, Oregon (see Text S1 for details on elemental acquisition). Laser transects were positioned along the longest axis of the otoliths, from the outer edge of the core, passing through the core to the opposite edge of the otolith, in order to collect a time series of elemental composition (**Figure 2.4a**). We collected data on lithium (^{7}Li), magnesium (^{24}Mg), calcium (^{43}Ca), manganese (^{55}Mn), copper (^{65}Cu), rubidium (^{85}Rb), strontium (^{86}Sr), barium (^{138}Ba), zinc (^{66}Zn) and lead (^{208}Pb). The trace elements were divided by Ca (Me/Ca, where the Me represents a metallic element) and data were converted to molar ratios based on repeated measurements of the NIST 612 standard. Elemental ratios are presented as mmol mol^{-1} (Mg, Mn, and Sr,) or μmol mol^{-1} (Li, Cu, Zn, Rb, Ba and Pb). The mean percent relative standard deviations (%RSD) of multiple NIST 612 standards (n = 58) were used to evaluate precision (see **Table 2.S1** in the Supplement). Accuracy was estimated with a calcium carbonate standard of known composition (USGS MACS-1, n = 45) and measured values were within 10% of known values for all elements, except for Mg:Ca and Pb:Ca (**Table 2.S1**).

The otolith microchemistry data along each transect were separated into different life stages (i.e. larva, settler, post-settlers and non-migratory immature) to examine stage- and habitat-specific elemental fingerprints. For example, larval snappers and groupers utilize open water habitats, while settlers and non-migratory immature fish (hereafter referred to as "juveniles") reside in mangroves. In order to calculate the average elemental ratio (Me:Ca in μmol mol^{-1} or mmol mol^{-1}) at each life stage of the juvenile fish (i.e. larva, settler, post-settler and immature), we used the relationship between the total length of the fish (TL, cm) and the ablated length in each otolith (AL, μm) (see **Figure 2.S1** in the Supplement).

Lutjanus argentiventris

The yellow snapper juveniles from the Gulf of California ranged from 2.21 to 15.19 cm TL and those from Galápagos were from 2.8 cm to 24 cm TL. The relationship between the TL of yellow snappers and the AL for each of their otoliths (AL, μm) was linear (TL= 0.0088AL, R^2 = 0.92, $p < 0.05$ for the Gulf of California, and TL= 0.0097AL, $R^2 = 0.90$, $p < 0.05$ for Galápagos) (**Figure 2.S1**). The regression slopes were significantly different between fish from the Gulf of California and the Galápagos (Multiple Linear Regression, $p < 0.0001$), partially because Galápagos juveniles were larger than those from the Gulf of California. Using these 2 relationships between fish TL and otolith AL, we calculated the average Me:Ca (μmol mol^{-1} or mmol mol^{-1}) for each section of AL along the otolith that corresponded to a specific range of TL in the fish (**Figure 2.4b**). These specific ranges of TL were based on a previously established classification of juvenile size classes (Aburto-Oropeza et al., 2009), in which larvae were < 2 cm TL, settlers between 2-4 cm TL, post-settlers between 4 and10 cm TL, and immatures between 10 and 20 cm TL. The average number of days and growth rates corresponding to each of these life stages were also calculated (**Table 2.2**).

Mycteroperca olfax

For sailfin groupers, we included unpublished data from adult samples to improve the relationship between TL and the AL for each of their otoliths. By including the adults, we were able to better adjust the intercept for our regression to improve the estimate of the range in lengths and average elemental ratios for the youngest life stages considered (e.g., larvae and settlers). The relationship between the TL of 189 adult and juvenile sailfin groupers from 7.20 to 89.25 cm TL and their otolith AL was linear (TL= 0.0239AL, $R^2 = 0.7426$, $p < 0.05$) (**Figure**

2.S1). The differences in the fit of the linear relationships between TL and AL for the sailfin groupers and yellow snappers indicate differences in growth rates and otolith accretion rates between these species, since the groupers were larger than the snappers. In the microchemistry runs, we only included juveniles (n = 70), between 7.2 and 25.7 cm of TL that were age-0 (**Table 2.1**). Since there was no available literature for the size ranges of *M. olfax* from the larval to the post-settler stages or for the genus *Mycteroperca*, we used size-class range values from a species with similar growth parameters, the Nassau grouper *Epinephelus striatus* (Eggleston 1995). Using those reference values and the linear relationship between TL and AL, we assigned individuals to different life stages, defining larvae as individuals < 2.5 cm TL, Settlers between 2.5 and 3.5 cm TL, Post-Settlers between 3.5 and 15 cm TL, and Immatures between 15 and 65 cm TL. The average Me:Ca (μmol mol^{-1} or mmol mol^{-1}) for each of these life stages was calculated in the same way as for yellow snappers (**Figure 2.4**, **Figure 2.S1**).

To compare only those juveniles that experienced the same temporal variability of the elements in the environment, we subsampled 97 juveniles of similar sizes, ages and hatch dates within each ecosystem. These juveniles included yellow snappers from 5 to 10 cm of TL collected in October 2003 in the Gulf of California (n = 40) and yellow snappers and sailfin groupers of 15 to 20 cm of TL collected in April 2015 in the Galápagos (n = 57).

Sea surface temperature and chlorophyll a adjacent to mangrove sites – Gulf of California and Galápagos

We downloaded daily SST and chl *a* in 64km^2 polygons adjacent to our mangrove sites during the lifetimes of the juveniles at each ecosystem. For the Gulf of California, the full-resolution data products were merged from data from multiple sensors: SeaWiFS (1997 to 2010),

MODIS-Terra (MODIST, 2000 to present), MODIS-Aqua (MODISA, 2002 to present), MERIS (2003 to 7 April 2012). For the overlapping periods, datasets from all available sensors were merged. Corresponding sea-surface temperature (SST) products were created from MODIST (2000 to present) and MODISA (2002 to present). For Galápagos, the data products were from VIIRS-SNPP sensors on NASA satellites (https://oceancolor.gsfc.nasa.gov).

Statistical analysis

To determine how the overall elemental composition of otoliths differed between species or ecosystem of origin, we used a permutational multivariate analysis of variance (PERMANOVA) (see Text S2 in the Supplement for PERMANOVA assumptions). Two PERMANOVA models were run with the average Me:Ca across the entire life of the juveniles (i.e. elemental ratios) as the dissimilarity matrix and species or region as the independent variables (Anderson 2001, McArdle & Anderson, 2001, Anderson 2014). For the 2 species in the same region (*L. argentiventris* from Galápagos vs. *M. olfax* from Galápagos), we used a model where the species was the independent variable. For the same species in different regions (*L. argentiventris* from Galápagos vs. *L. argentiventris* from Gulf of California), we used a model where the region was the independent variable. In addition, univariate ANOVA comparisons and Tukey tests were used to test for significant differences in single trace elemental ratios (see Text S2 for ANOVA assumptions).

In order to complement the PERMANOVA analysis, an analysis of similarity (ANOSIM) was used to test whether there was significant separation based on species (*L. argentiventris* from Galápagos vs. *M. olfax* from Galápagos) or their respective ecosystem of origin (*L.*

argentiventris from Galápagos vs. *L. argentiventris* from Gulf of California) using the average Me:Ca across the entire life of the juveniles (see Text S2 for ANOSIM model interpretation).

To visualize the level of similarity or dissimilarity is the elemental composition of otoliths by species (*L. argentiventris* vs. *M. olfax* from Galápagos) or ecosystem of origin (*L. argentiventris* from Gulf of California vs. *L. argentiventris* from Galápagos), we used Principal Coordinate Analysis (PCoA), also known as Classical Multidimensional Scaling (MDS) (see TextS2 for PCoA model details). We used the average Me:Ca of larval stages to reflect open ocean residence and the average Me:Ca from settlers to immature stages (i.e. "juveniles") to reflect residence inside the mangrove sites. Confidence intervals (CI) of 95% were used to assess the overlap between sampling areas or species and to better visualize the group separation or overlap achieved between the different species-region combinations (*L. argentiventris* from Gulf of California, *L. argentiventris* from Galápagos, and *M. olfax* from Galápagos) of both larval and juvenile stages.

To investigate temporal variability in elemental composition of otoliths for the yellow snappers and sailfin groupers from different cohorts, we used PCoA of the elemental ratios of juveniles (i.e. post-settlers to immature) based on their species (*L. argentiventris* vs. *M. olfax*), ecosystem of origin (Gulf of California vs. Galápagos), and month and year of collections (April of 2015 and 2016 for Galápagos, and June and October of 2003 and 2004 for the Gulf of California) (see Text S2, **Figure 2.S2 & 2.S3** in the Supplement).

To examine the role of growth on the elemental composition of yellow snappers from different ecosystem of origin (Gulf of California vs. Galápagos), we performed a PCoA only using fish with similar ages, sizes and growth rates. For this analysis, we included fish less than 10 cm TL and ~ 150 d old because their growth rates were similar at these sizes and ages

(**Figure 2.2**). All analyses were performed in the program R (R Core Team 2019). We used the package "vegan" (Oksanen et al. 2019) to perform the PERMANOVA, ANOSIM and PCoAs.

Results

The elemental ratios at each life stage of the subset of juveniles (n = 97) (see **Figure 2.S4** in the Supplement) were very similar with the elemental ratios at each life stage including all samples (n = 332) (see **Figure 2.7**), with differences being within 1 standard deviation, with the exception of Li:Ca and Cu:Ca, which were within 2 standard deviations. Therefore, we decided to include all juveniles in our statistical analysis, with the main assumption that the environment in Galápagos as a whole would be important for imparting local chemical signals to "larvae" and "juveniles" inhabiting it, despite likely seasonal variations.

Interspecific differences within the same ecosystem

Within Galápagos, the multi-elemental otolith signatures of the yellow snappers were significantly different from those of the sailfin groupers, but the difference between species explained only 2.1% of the variance (PERMANOVA, $F = 3.59$, $R^2 = 0.021$, $p < 0.02$) (**Table 2.3**). Univariate results indicated that the differences were primarily due to 2 elemental ratios (Ba:Ca and Pb:Ca) (**Table 2.4**, **Figure 2.S5** in the Supplement). The elemental ratios of Sr:Ca, Cu:Ca, Li:Ca, and Rb:Ca, Mn:Ca and Mg:Ca were very similar in the 2 cohabiting species. The ANOSIM test showed little separation achieved between these 2 species from Galápagos (ANOSIM test, $R = 0.016$, $p = 0.038$) (**Figure 2.5a**). The PCoA showed a high degree of overlap among the elemental signatures, irrespective of the life stage (**Figure 2. 6**). Moreover, the pattern

of elemental composition and range of elemental ratio values across all life stages (larvae, settlers, post-settlers and immatures) was similar, with the exception of Pb (**Figure 2.7**).

Spatial differences within the same species

The multi-elemental otolith signatures of the yellow snappers from Galápagos and the Gulf of California were significantly different and the difference between regions explained 32.4% of the variance (PERMANOVA, $F = 126.58$, $R^2 = 0.324$, $p < 0.001$) (**Table 2.3**). The majority of elements were significantly different between regions, except for Mg:Ca, Zn:Ca and Pb:Ca (**Table 2.4**, **Figure 2.S5**). There was a larger separation between the snappers from Galápagos and snappers from the Gulf (ANOSIM test, $R = 0.558$, $p = 0.001$) (**Figure 2.5b**) than between the snappers and groupers from Galápagos. The PCoA partially separated the yellow snappers of Galápagos from those of the Gulf of California (**Figure 2.6**). In addition, the pattern of elemental composition across life stages was different for yellow snappers from the Galápagos and the Gulf of California. For example, Ba:Ca was around 3 times higher in the snappers from the Gulf of California than in those from Galápagos and Li:Ca was almost 9 times lower in the snappers from the Gulf than in those from Galápagos (**Figure 2.7**).

Temporal variation

The PCoA partially separated the yellow snappers and sailfin groupers in the Galápagos from the yellow snappers in the Gulf of California, irrespective of the distinct cohorts from different sampling events (**Figure 2.8**). While it was not possible to test for temporal variation in the otolith elemental fingerprint for Galápagos fishes due to the low number of samples collected in April 2016 ($n = 12$), their elemental fingerprint overlapped well with the remaining fishes

collected the previous year (n = 160) (**Figure 2.8**). However, the multi-elemental otolith signatures of yellow snapper juveniles from the Gulf of California were significantly different between the years of collection, 2003 and 2004 (PERMANOVA, $F = 46.25$, $p < 0.001$), as well as for some of the elemental ratios averaged for different life stages (**Figure 2.9**). For example, Cu:Ca, Rb:Ca and Zn:Ca were approximately 2 times higher in the snappers from 2004 than in those from 2003, while other elemental ratios were within the same range of values (**Figure 2.9**, **Table 2.S2** in the Supplement). There were no significant differences for Ba:Ca, Mg:Ca, Sr:Ca and Pb:Ca and Zn:Ca among the life stages compared across years for the snappers in the Gulf (**Figure 2.9**, **Table 2.S2**).

Growth rate effects

The PCoA still partially separated the yellow snappers from Galápagos from those from the Gulf of California (**Figure 2.S6** in the Supplement) for those individuals with similar growth rates, suggesting that factors beyond growth are driving this separation pattern.

Discussion

Unraveling the effect of extrinsic and intrinsic factors on elemental composition of otoliths is essential for interpreting connectivity patterns, life history exposure and the role of environment and vital effects in fish ecology (Thorrold et al. 2007, Sturrock et al. 2014, 2015). This study demonstrated consistent otolith microchemistry between 2 species sampled in various locations across the Galápagos. Furthermore, our results indicate that the same species under the influence of dynamic ecosystems had different elemental composition in their otoliths. To our knowledge, this is the first time that otolith microchemistry has been used to assess the relative

role of environment and physiology in juvenile fish at their northern and southern distributional limits in the ETP.

Extrinsic vs. intrinsic influences on otolith elemental composition

The factors that affect the quantification and the elemental composition of otoliths include (1) methodology (Ruttenberg & Warner 2006), (2) temperature (affects fish metabolism and growth rate, and can influence how the elements are incorporated into the crystal matrix) (Radtke & Shafer 1992), (3) ontogeny (developmental changes can lead to changes in otolith deposition) (Ruttenberg et al. 2005), (4) phylogeny (species differences may be due to taxonomic changes in otolith composition) (Chang & Geffen 2013), (5) water chemistry (Thorrold et al. 1997), and (6) dietary sources (Buckel et al. 2004, Mathews & Fisher 2009) .

In our study, methodological influence was discarded as an important factor because data collection occurred using calibration controls during the 1 wk of LA-ICPMS analysis. The potential for growth variation to generate the observed variation in elemental composition appears to be limited, because juveniles younger than 150 d old were growing at similar rates during these periods (**Figure 2.2**) and still exhibited marked differences in their elemental signatures (**Figure 2.S6**). Potential ontogenetic effects were reduced by including only immature fishes prior to reproductive investment (Kalish 1989, Sturrock et al. 2015), and by comparing elemental signatures across discrete stages. Phylogenetic effects were also less evident than the region of origin as elemental signatures between the 2 Galápagos species were more similar than those of yellow snapper from Galápagos and Gulf of California, even when separated by life stage.

Most of the snapper juveniles from Galápagos came from the eastern side of the archipelago, whilst most of the sailfin grouper juveniles came from the western side of the archipelago. Nonetheless, both species exhibited more similar elemental signatures compared to snappers from the Galápagos and the Gulf of California. This pattern of similar trace elemental composition in the 2 species might be due to the unique geographic position of the archipelago, being the only tropical archipelago located at the confluence of major warm- and cool-water current systems, including the: (1) warm south-westerly flowing Panama Current; (2) cool north-westerly flowing Peru Current; and (3) cold eastward-flowing subsurface equatorial undercurrent (EUC). In Galápagos, the EUC divides into a northern and southern branch, leading to local upwelling all around the archipelago and a complicated pattern of internal eddies that allows for horizontal interchange and mixing of water masses (Houvenaghel 1978), likely homogenizing the water across the entire archipelago. This homogenous environment would further support the observations made by Ruttenberg & Warner (2006), who found that otolith chemical signatures did not to vary over larger spatial scales (~100 km) across the Galápagos Archipelago but observed some spatial differences at small spatial scales of 10s of km, which they attributed to localized upwelling events and their variation in intensity among the islands.

The similarity of elemental ratios between species (snappers and groupers) observed in Galápagos does not agree with previous studies where interspecific differences were observed for juvenile fishes living in the same environment (Swearer et al. 2003, Hamer & Jenkins 2007, Reis-Santos et al. 2008). The interspecific similarity of elemental ratios for Galápagos fishes may, however, support interspecific classification of natal sources, where otolith microchemistry signatures obtained for one species may be used to predict those of co-occurring species for which natal source otolith microchemistry information is unavailable (Prichard et al. 2018).

These similarities also hold promise for using one species as a proxy for a congener (Patterson et al, 2014).

The differences in elemental concentration observed between snappers from Galápagos and the Gulf might be due to both environmentally and physiologically mediated mechanisms, as temperature and the amount of productivity within the mangrove lagoons can also affect metabolic rates and the rates of growth of somatic tissue and otoliths. For example, the seasonal SST was more variable in the Gulf (~ 16°C) than in Galápagos (~7°C) (**Table 2.S3** in the Supplement), for the juvenile lifetime examined herein (i.e., < 1 yr old). The strong SST seasonality in the Gulf probably led to a higher variability in growth rates of its snapper juveniles compared with those from Galápagos (**Figure 2.2**).

Trace elements as proxies for large-scale environmental processes

Recent experimental and field observations found that fish physiology affects softer elements (Mn, Cu, Zn, and Pb) and quasi-conservative elements (Sr and Ca) more than hard acid metal ions (Li, Mg, Rb and Ba) in otoliths (Sturrock et al. 2012, 2014, Grammer et al. 2017). Partially aligned with these studies, Thomas et al. (2017) observed the occurrence of Li, Mn, and Rb only in the salt fraction of otoliths, which likely reflects changes in the physicochemical environment; Ba and Sr in both the salt and proteinaceous fractions, which likely reflects both endogenous and exogenous processes; and Cu, Zn and Pb only in the proteinaceous fraction, which likely reflects physiologically-mediated mechanisms. In the present study, most hard acid metal ions (e.g., Li, Rb, Ba) and elements occurring only in the salt fraction (e.g., Mn) of otoliths were significantly different between Galápagos and the Gulf (**Table 2.4**), supporting the

hypothesis that those elements are less affected by physiology and were more influenced by the environment.

Ba:Ca and Sr:Ca were higher for the Gulf snappers than the Galápagos snappers, while Li:Ca was higher for the Galápagos fishes than the Gulf snappers (**Figure 2.7**). In marine systems, these hard acid cations tend to be less physiologically influenced and accepted more readily into the otolith crystal lattice, but are relatively homogeneous in seawater (Sturrock et al. 2012). Ba is often used to identify freshwater occupancy due to the commonly observed relationship of increasing ambient and otolith Ba:Ca with decreasing salinity (Walther & Thorrold, 2006), and greater Ba concentrations are also associated with upwelled waters and primary productivity (Kingsford et al. 2009). In our study, Ba:Ca was the most important element defining the spatial pattern observed for the Gulf of California juvenile snappers (**Figure 2.6**), probably associated with the presence of the rivers Sonora, Yaqui and Fuente (mainland side of the Gulf), and also with the high primary productivity in this marginal sea due to upwelling events (Álvarez-Borrego & Lara-Lara 1991) (**Table 2.S3**).

The Sr:Ca ratios for the Gulf of California fishes were significantly higher than Galápagos fishes (e.g. Sr:Ca was ~ 2.71 mmol mol^{-1} in the Gulf and ~ 2.47 mmol mol^{-1} in Galápagos). The Gulf of California is characterized by a positive salinity anomaly due to higher evaporation rates compared to precipitation rates and the current lack of freshwater inflow from the Colorado River. The annual mean salinity in the Gulf of California decreases from 35.26 ± 0.01 at the head to 34.75 ± 0.01 at the mouth (Beron-Vera & Ripa, 2002), which is slightly higher than the Galápagos Archipelago, where our *in situ* salinity measurements at the time of fish collection were ~34.44. However, because these salinities were within a very small range, the significant differences observed for Sr:Ca ratios are probably related to regional variations in

the bedrock geology between these ecosystems or due to differences in the water temperature, as temperature can also significantly affect Sr incorporation (Bath et al. 2000).

For Galápagos, Li:Ca was the most important element defining the spatial pattern observed for its juvenile fishes and presented ratios up to 10 times higher than those reported in the literature for otoliths (Chang & Geffen 2013). The major sources of Li in the ocean are primarily from river input and hydrothermal activity (Edmond et al. 1979). Sailfin groupers and yellow snappers are found among rock walls, underwater lava ridges and all kinds of vertical rock formations. Juveniles can also be found in shallow lava reefs and inland lava ponds. It is possible that the substrates of these habitats are important sources of lithium, since there are no rivers across the archipelago. In addition, Swan et al. (2003) suggest that the higher concentrations of Li, Rb, Cu and Pb in areas with hydrothermal activity can lead to detectable concentrations of those trace elements in otoliths. In agreement with this study, Rb:Ca and Cu:Ca were consistently higher in fishes from the Galápagos and were also important in defining the spatial pattern of elemental ratios observed for this region (**Figure 2.6**). Pb:Ca and Zn:Ca explained less variance on the first axis of our PCoA and were not significantly different between the Gulf and Galápagos snappers. Pb:Ca is highly toxic at higher concentrations, so fish can present specific mechanisms to control its uptake. For instance, Geffen et al. (1998) observed that the relationship between exposure and metal incorporation in otoliths was not always direct for juvenile sand gobies *Pomatoschistus minutus*, plaice *Pleuronectes platessa* and sole *Solea solea*, suggesting that physiological mechanisms operate to regulate lead and that at higher concentrations lead is sequestered or removed from circulation so that it does not reach the growing otolith.

Diet is the primary source of intake for Zn in teleost and elasmobranch fishes (Mathews & Fisher 2009). It is therefore suspected to be an unreliable proxy for ambient environmental conditions (Miller et al. 2006). In the present study, the lack of difference in Zn ratios between species and ecosystems suggest that these juveniles were feeding on similar prey items. Indeed, snappers feed primarily on decapod crustaceans *Upogebia* sp. in the Gulf of California (Vázquez et al., 2008), a food group also found in the Galápagos mangroves.

Temporal variation

Trace element signatures in otoliths can vary between years in the same system, as demonstrated by the differences we measured for snappers captured in consecutive years in the Gulf of California (**Figure 2.9**). Inter-annual variability in otolith signatures has been previously reported for fish inhabiting dynamic environments such as estuaries (Thorrold et al. 1997, Gillanders & Kingsford 2000, Swearer et al. 2003) and mangroves (Chittaro et al. 2004). Mateo et al. (2010), however, reported consistent elemental signatures between consecutive years in otoliths of 2 species inhabiting seagrass and mangrove habitats on Caribbean Islands. Thus, the degree of inter-annual variation appears to be region- and habitat-specific and must be assessed before multi-elemental fingerprints are considered "permanent" markers of any specific nursery ground.

Conclusion

The present study suggests that extrinsic factors (e.g., water chemistry, temperature, salinity) can be more important than intrinsic factors (e.g., physiology, growth rates, and genetics) for influencing elemental uptake in the otoliths of juveniles from the Gulf of California

and Galápagos. In the future, these elements present the potential to be used as proxies for environmental processes that occur within and adjacent to mangroves, such as for the quantification of hydrothermal activity, pollution, hypoxia and primary productivity levels. We postulate that the combination of terrestrial and submarine volcanos in the Galápagos and the convergence of different oceanographic currents act to create a homogenous and distinctive water chemistry across the entire archipelago that is imparted into calcareous structures of fishes and potentially other marine organisms such as corals and mollusk shells. For the Gulf of California, the trace element ratios found in this study (especially Li:Ca, Cu:Ca, Rb:Ca, Zn:Ca, Mn:Ca and Pb:Ca) can serve as a benchmark for future comparison, in light of the potential changes in water chemistry in sediment plumes from planned mining operations. For example, the Clarion-Clipperton Zone boasts one of the world's largest untapped collections of rare-earth elements, stretches from Hawaii to the Baja California Peninsula, and is projected to be explored within the next 10 years with 16 licenses already granted for contractors (Heffernan 2019). Finally, we also hope this simple comparison will set the scene for future interspecific comparisons of fish inhabiting ETP mangroves.

Acknowledgements

We are grateful to the Charles Darwin Foundation and the Galápagos National Park Directorate for the institutional support during this study. We are grateful to the crews of the vessels 'El Primo', 'Pirata' and 'Queen Mabel' for their assistance during field work in Galápagos. We thank Joy Kumagai for the map assistance and Andy Ungerer at the Oregon State University W. M. Keck Collaboratory for Plasma Spectrometry for assistance with otolith analysis. This research was supported by a grant from the Helmsley Charitable Trust to P.S.L.

and O.A.O. L.M.C. was supported by CNPq grant 213540/2014-2. A.F.J. was supported by NSF grant DEB-1632648 (2017/18). The research presented in this manuscript was conducted under permits PC-13-14, and PC-13-15 provided by the Galápagos National Park Directorate. This publication is contribution number 2298 of the Charles Darwin Foundation for the Galápagos Islands.

Chapter 2, in full, is a reprint of the material as it appears in Marine Ecology Progress Series. Cavole L.M., Miller J.A., Salinas-de-Léon P., Aburto-Oropeza O., Jarrin J.R.M., Johnson A.F. The dissertation author was the primary investigator and author of this material.

Literature Cited

Aburto-Oropeza O, Dominguez-Guerrero I, Cota-Nieto J & Plomozo-Lugo T (2009) Recruitment and ontogenetic habitat shifts of the yellow snapper (*Lutjanus argentiventris*) in the Gulf of California. Mari Biol 156: 2461-2472.

Allen GR (1985) FAO species catalogue. Vol. 6. Snappers of the world. An annotated and illustrated catalogue of lutjanid species known to date. FAO Fish. Synop. 125: 60–61

Álvarez-Borrego S (2012) Phytoplankton biomass and production in the Gulf of California: a review. Bot Mar 55:119–128.

Álvarez-Borrego S, Lara-Lara JR (1991) The physical environment and productivity of the Gulf of California. In: Dauphin JP, Simoneit B (eds) The Gulf and peninsular province of the Californias. Am Assoc Pet Geol Mem 47:555 – 567.

Anderson MJ (2001) A new method for non-parametric multivariate analysis of variance. *Austral Ecol* 26: 32–46.

Anderson, MJ (2014). Permutational multivariate analysis of variance (PERMANOVA). Wiley StatsRef: Statistics Reference Online, 1-15.

Ashford JR, Arkhipkin AI, Jones CM (2006) Can the chemistry of otolith nuclei determine population structure of Patagonian toothfish *Dissostichus eleginoides*? J Fish Biol 69: 708-721.

Avigliano E, Volpedo AV (2016) A review of the application of otolith microchemistry toward the study of Latin American fishes. Rev Fish Sci Aquac 24: 369-384.

Bath GE, Thorrold SR, Jones CM, Campana SE, McLaren JW, Lam JW (2000) Strontium and barium uptake in aragonitic otoliths of marine fish. Geochim cosmochim acta 64: 1705-1714.

Beron-Vera FJ, Ripa P. Seasonal salinity balance in the Gulf of California (2002) J Geophys Res 107: C8

Buckel JA, Sharack BL, Zdanowicz VS (2004). Effect of diet on otolith composition in Pomatomus saltatrix, an estuarine piscivore. J Fish Biol 64: 1469-1484.

Campana SE, Fowler AJ, Jones CM (1994) Otolith elemental fingerprinting for stock identification of Atlantic cod (*Gadus morhua*) using laser ablation ICPMS. Can J Fish Aquat Sci 51: 1942-1950.

Campana SE (1999) Chemistry and composition of fish otoliths: pathways, mechanisms and applications. Mar Ecol Prog Ser 188: 263-297.

Campana SE, Thorrold SR (2001) Otoliths, increments, and elements: keys to a comprehensive understanding of fish populations? Can J Fish Aquat Sci 58: 30-38.

Chang MY, Geffen AJ (2013) Taxonomic and geographic influences on fish otolith microchemistry. Fish Fish 14: 458-492.

Chittaro PM, Fryer BJ, Sale PF (2004) Discrimination of French grunts (*Haemulon flavolineatum*, Desmarest, 1823) from mangrove and coral reef habitats using otolith microchemistry. J Exp Mar Biol Ecol 308; 169-183.

Clarke LM, Thorrold SR, Conover DO (2011) Population differences in otolith chemistry have a genetic basis in *Menidia menidia*. Can J Fish Aquat Sci 68: 105-114.

de Pontual H, Lagardere F, Troadec H, Batel A, Desaunay Y, Koutsikopoulos C (2000) Otoliths imprinting of sole (*Solea solea*) from the Bay of Biscay: a tool to discriminate individuals from nursery origins?. Oceanol Acta 23: 497-513.

Eddy TD, Friedlander AM, de León PS 2019. Ecosystem effects of fishing & El Niño at the Galápagos Marine Reserve. PeerJ, *7*, e6878.

Edmond JM, Measures C, McDuff RE, Chan LH, Collier R, Grant B, Gordon LI, Corliss JB (1979) Ridge crest hydrothermal activity and the balances of the major and minor elements in the ocean: the Galápagos data. Earth Planet Sci Lett 46: 1-18.

Eggleston DB (1995) Recruitment in Nassau grouper *Epinephelus striatus*: post-settlement abundance, microhabitat features, and ontogenetic habitat shifts. Mar Ecol Prog Ser 124: 9-22.

Geffen AJ, Pearce NJG, Perkins WT (1998) Metal concentrations in fish otoliths in relation to body composition after laboratory exposure to mercury and lead. Mar Ecol Prog Ser 165: 235-245.

Gillanders BM, Kingsford MJ (2000) Elemental fingerprints of otoliths of fish may distinguish estuarine 'nursery' habitats. Mar Ecol Prog Ser 201:273-286.

Gillanders BM, Able KW, Brown JA, Eggleston DB, Sheridan PF (2003) Evidence of connectivity between juvenile and adult habitats for mobile marine fauna: an important component of nurseries. Mar Ecol Prog Ser 247: 281-295.

Grammer GL, Morrongiello JR, Izzo C, Hawthorne PJ, Middleton JF, Gillanders, BM (2017) Coupling biogeochemical tracers with fish growth reveals physiological and environmental controls on otolith chemistry. Ecol Monogr 87: 487-507.

Grønkjær P (2016). Otoliths as individual indicators: a reappraisal of the link between fish physiology and otolith characteristics. Mar and Freshwater Res 67:881-888.

Halden NM, Friedrich LA (2008) Trace-element distributions in fish otoliths: natural markers of life histories, environmental conditions and exposure to tailings effluence. Mineralogical Mag 72: 593-605.

Hamer PA, Jenkins GP (2007) Comparison of spatial variation in otolith chemistry of two fish species and relationships with water chemistry and otolith growth. J Fish Biol 71: 1035-1055.

Heffernan O (2019) Seabed mining is coming-bringing mineral riches and fears of epic extinctions. Nature 571:465-468.

Houvenaghel GT (1978) Oceanographic conditions in the Galápagos Archipelago and their relationships with life on the islands. In: Boje R, Tomczak M (eds) Upwelling Ecosystems. Springer-Verlag, Berlin, p 181-200.

Izzo C, Reis-Santos P, Gillanders BM (2018) Otolith chemistry does not just reflect environmental conditions: a meta-analytic evaluation. Fish Fish 19: 441-454.

Oksanen J, Blanchet FG, Friendly M, Kindt R, Legendre P, McGlinn D, Minchin PR, O'Hara RB, Simpson GL, Solymos P, Stevens MHH, Szoecs E, Wagner H. (2019). vegan: Community Ecology Package. R package version 2.5-5.

Kalish JM (1989) Otolith microchemistry: validation of the effects of physiology, age and environment on otolith composition. J Exp Mar Bio and Eco 132: 151-178.

Kalish JM (1990) Use of otolith microchemistry to distinguish the progeny of sympatric anadromous and non-anadromous salmonids. Fish Bull 88: 657-666.

Kingsford MJ, Hughes JM, Patterson HM (2009) Otolith chemistry of the non-dispersing reef fish *Acanthochromis polyacanthus*: cross-shelf patterns from the central Great Barrier Reef. Mar Ecol Prog Ser 377: 279-288.

Limburg KE, Walther BD, Lu Z, Jackman G, Mohan J, Walther Y, Nissling A, Weber PK, Schmitt AK (2015) In search of the dead zone: use of otoliths for tracking fish exposure to hypoxia. J Marine Syst 141: 167-178.

Lluch-Cota SE, Aragon-Noriega EA, Arreguín-Sánchez F, Aurioles-Gamboa D, Bautista-Romero JJ, Brusca RC, Cervantes-Duarte R, Cortés-Altamirano R, Del-Monte-Luna P, Esquivel-Herrera A, Fernández G (2007) The Gulf of California: review of ecosystem status and sustainability challenges. Prog Oceanogr 73: 1-26.

Mateo I, Durbin EG, Appeldoorn RS, Adams AJ, Juanes F, Kingsley R, Swart P, Durant D (2010) Role of mangroves as nurseries for French grunt *Haemulon flavolineatum* and schoolmaster *Lutjanus apodus* assessed by otolith elemental fingerprints. Mar Ecol Prog Ser 402: 197-212.

Mathews T, Fisher NS (2009) Dominance of dietary intake of metals in marine elasmobranch and teleost fish. Sci Total Environ 407: 5156-5161.

McArdle, B.H. and M.J. Anderson. (2001). Fitting multivariate models to community data: A comment on distance-based redundancy analysis. Ecology 82: 290–297.

McCosker JE, Rosenblatt RH (2010). The fishes of the Galápagos Archipelago: an update. Proc Calif Acad Sci 61: 167-195.

Miller MB, Clough AM, Batson JN, Vachet RW (2006) Transition metal binding to cod otolith proteins. J Exp Mar Bio Ecol 329: 135-143.

Patterson WF III, Barnett BK, Sluis MZ, Cowan Jr JH, Shiller AM (2014) Interspecific variation in juvenile snapper otolith chemical signatures in the northern Gulf of Mexico. Aquat Biol 21:1-0.

Piñón A, Amezcua F, Duncan N (2009) Reproductive cycle of female yellow snapper *Lutjanus argentiventris* (Pisces, Actinopterygii, Lutjanidae) in the SW Gulf of California: gonadic stages, spawning seasonality and length at sexual maturity. J Appli Ichthyol 25: 18-25.

Prichard CG, Jonas JL, Student JJ, Watson NM, Pangle KL (2018) Same habitat, different species: otolith microchemistry relationships between migratory and resident species support interspecific natal source classification. Environ Biol Fish 101:1025-38.

R Core Team (2019). R: A language and environment for statistical computing. R Foundation for statistical computing, Vienna, Austria. DOI: http://www.R-project.org/

Radtke RL, Shafer DJ (1992) Environmental sensitivity of fish otolith microchemistry. Mar Freshwater Res, 43: 935-951.

Reck G K (1983) The coastal fisheries in the Galápagos Islands, Ecuador: description and consequences for management in the context of marine environmental protection and regional development. PhD dissertation, University of Kiel, Germain.

Reis-Santos P, Vasconcelos RP, Ruano M, Latkoczy C, Günther D, Costa MJ, Cabral H (2008) Interspecific variations of otolith chemistry in estuarine fish nurseries. J Fish Biol 72: 2595-2614.

Ruttenberg BI (2001) Effects of artisanal fishing on marine communities in the Galápagos Islands. Conserv Biol 15: 1691-1699.

Ruttenberg BI, Hamilton SL, Hickford MJ, Paradis GL, Sheehy MS, Standish JD, Ben-Tzvi O, Warner RR (2005) Elevated levels of trace elements in cores of otoliths and their potential for use as natural tags. Mar Ecol Prog Ser 297: 273-281.

Ruttenberg BI, Warner RR (2006) Spatial variation in the chemical composition of natal otoliths from a reef fish in the Galápagos Islands. Mar Ecol Prog Ser 328: 225-236.

Salinas-de-León P, Rastoin E, Acuña-Marrero D (2015) First record of a spawning aggregation for the tropical eastern Pacific endemic grouper *Mycteroperca olfax* in the Galápagos Marine Reserve. J Fish Biol 87: 179-186.

Secor DH (1992) Application of otolith microchemistry analysis to investigate anadromy in Chesapeak Bay striped bass *Morone saxatilis*. Fish Bull (Seattle) 90: 798-806.

Sturrock AM, Trueman CN, Darnaude AM, Hunter E (2012) Can otolith elemental chemistry retrospectively track migrations in fully marine fishes? J Fish Biol 81: 766-795.

Sturrock AM, Trueman CN, Milton JA, Waring CP, Cooper MJ, Hunter E (2014) Physiological influences can outweigh environmental signals in otolith microchemistry research. Mar Ecol Prog Ser 500: 245– 264.

Sturrock AM, Hunter E, Milton JA, Johnson RC, Waring CP, Trueman CN (2015) Quantifying physiological influences on otolith microchemistry. Methods Ecol Evol 6: 806-816.

Swan SC, Gordon JD, Morales-Nin B, Shimmield T, Sawyer T, Geffen AJ (2003) Otolith microchemistry of *Nezumia aequalis* (Pisces: Macrouridae) from widely different habitats in the Atlantic and Mediterranean. J Mar Biol Assoc UK 83: 883-886.

Swearer SE, Forrester GE, Steele MA, Brooks AJ, Lea DW (2003) Spatio-temporal and interspecific variation in otolith trace-elemental fingerprints in a temperate estuarine fish assemblage. Estuar, Coastal and Shelf S 56: 1111-1123.

Thomas ORB, Ganio K, Roberts BR, Swearer SE (2017) Trace element–protein interactions in endolymph from the inner ear of fish: implications for environmental reconstructions using fish otolith chemistry. Metallomics 9: 239-249.

Thorrold SR, Jones CM, Campana SE (1997) Response of otolith microchemistry to environmental variations experienced by larval and juvenile Atlantic croaker (*Micropogonias undulatus*). Limnol Oceanogr 42: 102-111.

Thorrold SR, Latkoczy C, Swart PK, Jones CM (2001) Natal homing in a marine fish metapopulation. Science 291: 297-299.

Thorrold SR, Zacherl DC, Levin LA (2007) Population connectivity and larval dispersal: using geochemical signatures in calcified structures. Oceanography 20: 80-89.

Usseglio P, Friedlander AM, DeMartini EE, Schuhbauer A, Schemmel E, Salinas-de-Léon P (2015) Improved estimates of age, growth and reproduction for the regionally endemic Galápagos sailfin grouper *Mycteroperca olfax* (Jenyns, 1840). PeerJ 3: e1270.

Usseglio P, Friedlander AM, Koike H, Zimmerhackel J, Schuhbauer A, Eddy T, Salinas-de-León P (2016) So Long and Thanks for All the Fish: Overexploitation of the Regionally Endemic Galápagos Grouper *Mycteroperca olfax* (Jenyns, 1840). PloS one 10: e0165167.

Vázquez RI, Rodríguez J, Abitia LA, Galván F (2008) Food habits of the yellow snapper Lutjanus argentiventris (Peters, 1869) (Percoidei: Lutjanidae) in La Paz Bay, Mexico. Rev Biol Mar Oceanogr 43: 295-302.

Walther BD, Thorrold SR (2006) Water, not food, contributes the majority of strontium and barium deposited in the otoliths of a marine fish. Mar Ecol Prog Ser 311: 125–130.

Walther BD (2019) The art of otolith chemistry: interpreting patterns by integrating perspectives. Mar and Freshwater Res 70: 1643-1658.

Wellington GM, Strong AE, Merlen G (2001) Sea surface temperature variation in the Galápagos Archipelago: a comparison between AVHRR nighttime satellite data and in situ instrumentation (1982–1998). Bull Mar Sci 69: 27-42.

Zapata FA, Herron PA (2002) Pelagic larval duration and geographic distribution of tropical eastern Pacific snappers (Pisces: Lutjanidae). Mar Ecol Prog Ser 230:295–300.

FIGURES

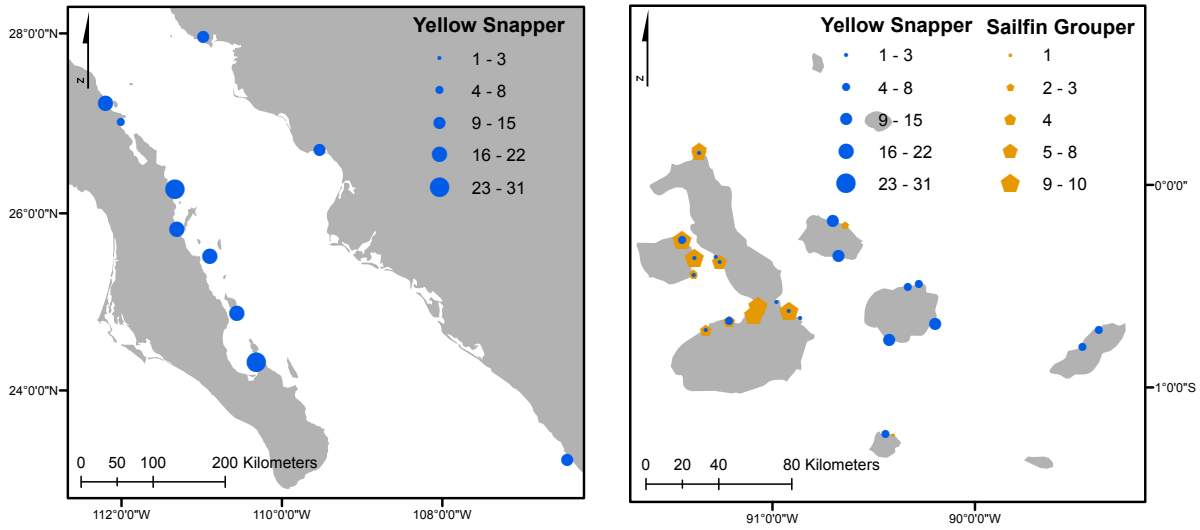

Figure 2.1. Fish collection area in (a) the Gulf of California (n = 174) and (b) the Galápagos Archipelago (n = 158) mangroves.

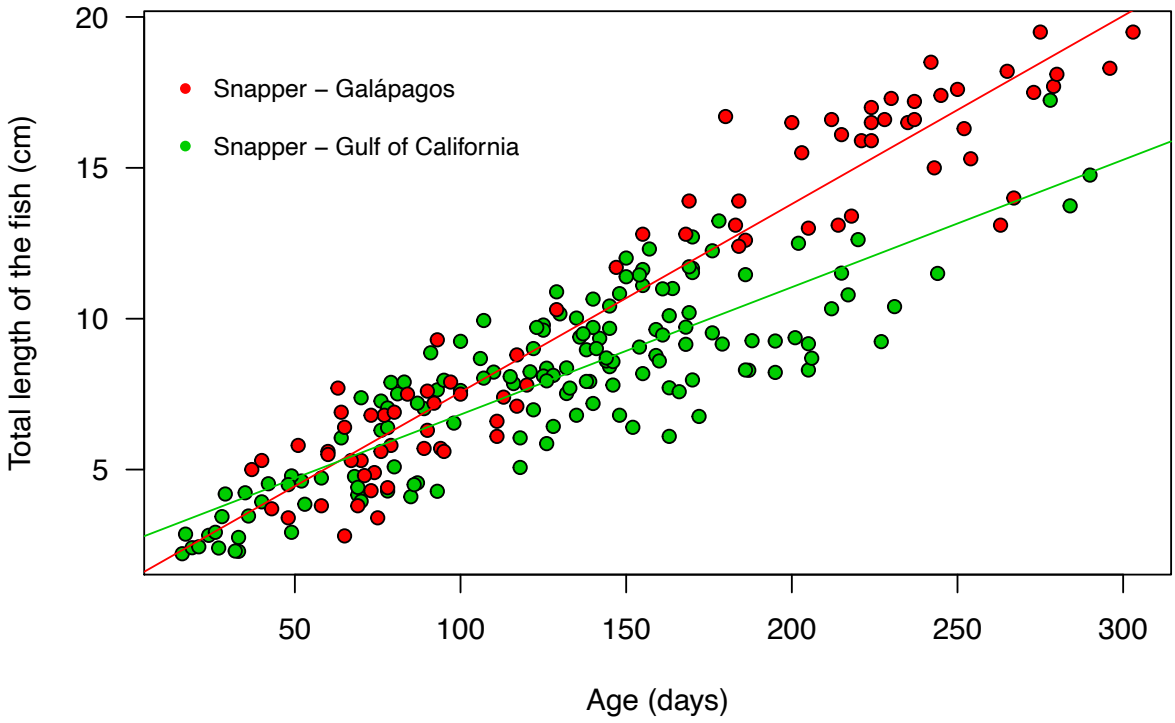

Figure 2.2. Linear regression between the fish total length (cm) and age (days) estimated from the otolith sagittae of yellow snapper *Lutjanus argentiventris* juveniles collected in the Gulf of California (n = 148) and Galápagos (n = 82).

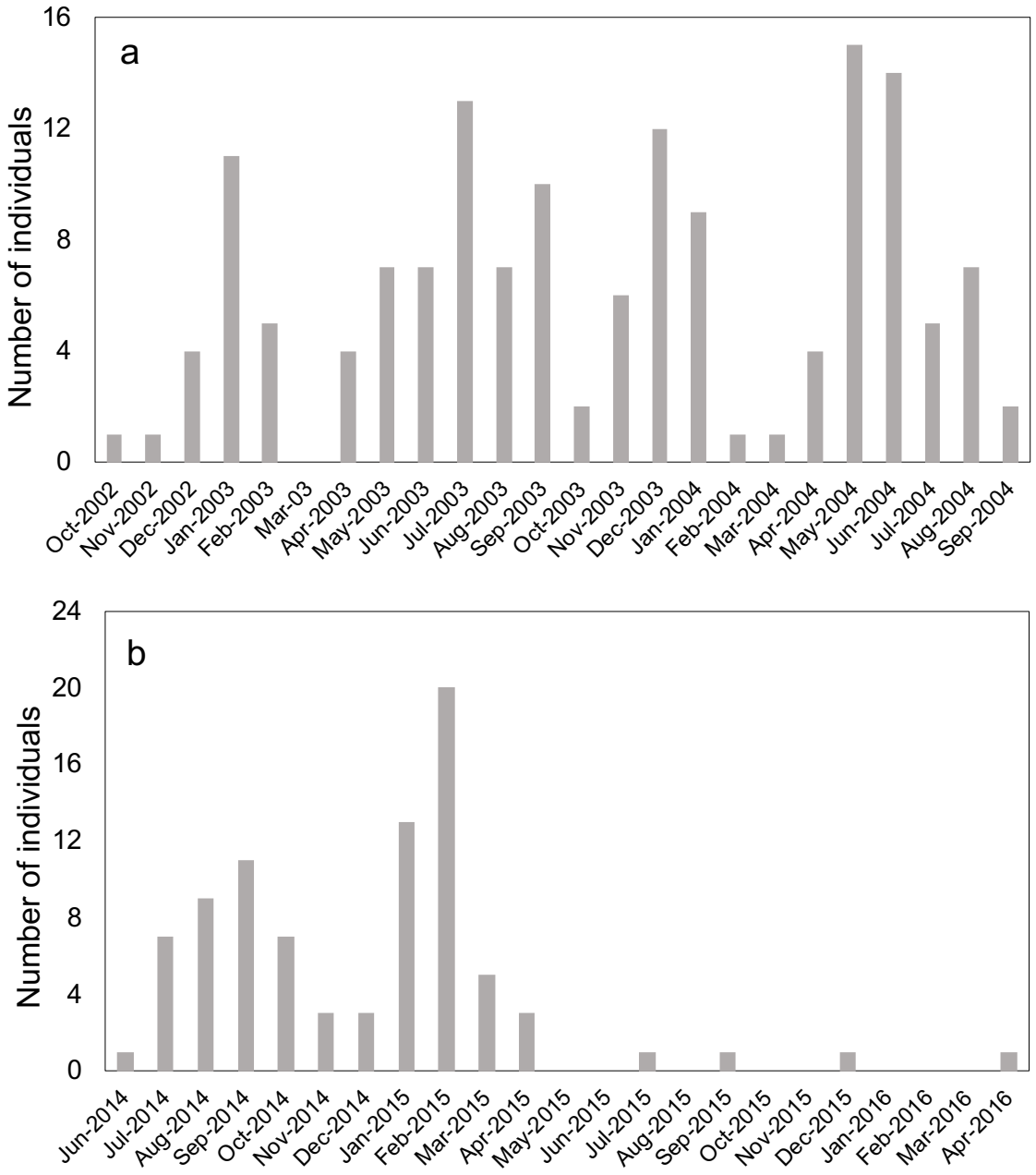

Figure 2.3. Monthly distribution of back-calculated hatch date for the juvenile yellow snapper *Lutjanus argentiventris* collected in (a) the Gulf of California (n = 148) and (b) Galápagos (n = 82). Please note that in the Galápagos Archipelago, the cold season is between July and November and the warm season is between January and May, being June and December transition months.

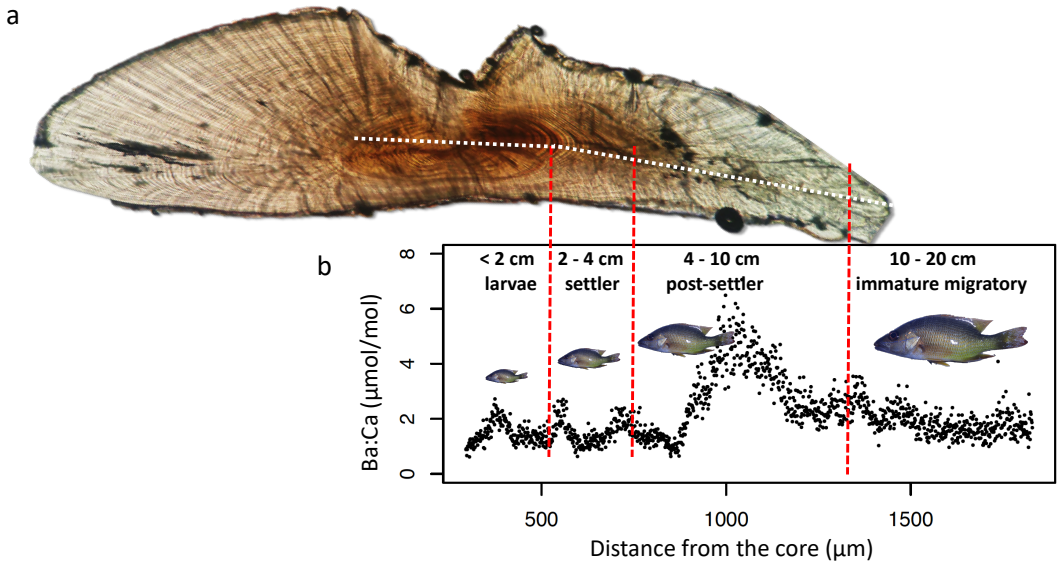

Figure 2.4. (a) Ablated laser transect across a juvenile yellow snapper otolith (white dashed line) (a) and (b) an example of the mean Ba:Ca trace elemental ratio (μmol mol^{-1}) estimated at each life stage.

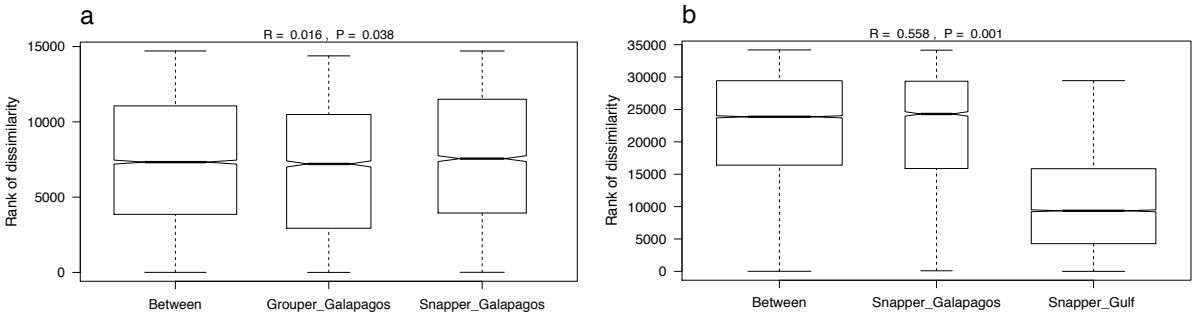

Figure 2.5. ANOSIM test between (a) the sailfin grouper and yellow snapper from the Galápagos Archipelago (ANOSIM test, R = 0.01, p = 0.038), and (b) yellow snapper from Galápagos and yellow snapper from the Gulf of California (ANOSIM test, R = 0.55, p = 0.001). Notched boxplots indicate the dissimilarity rank distributions for between and within species presented in plots.

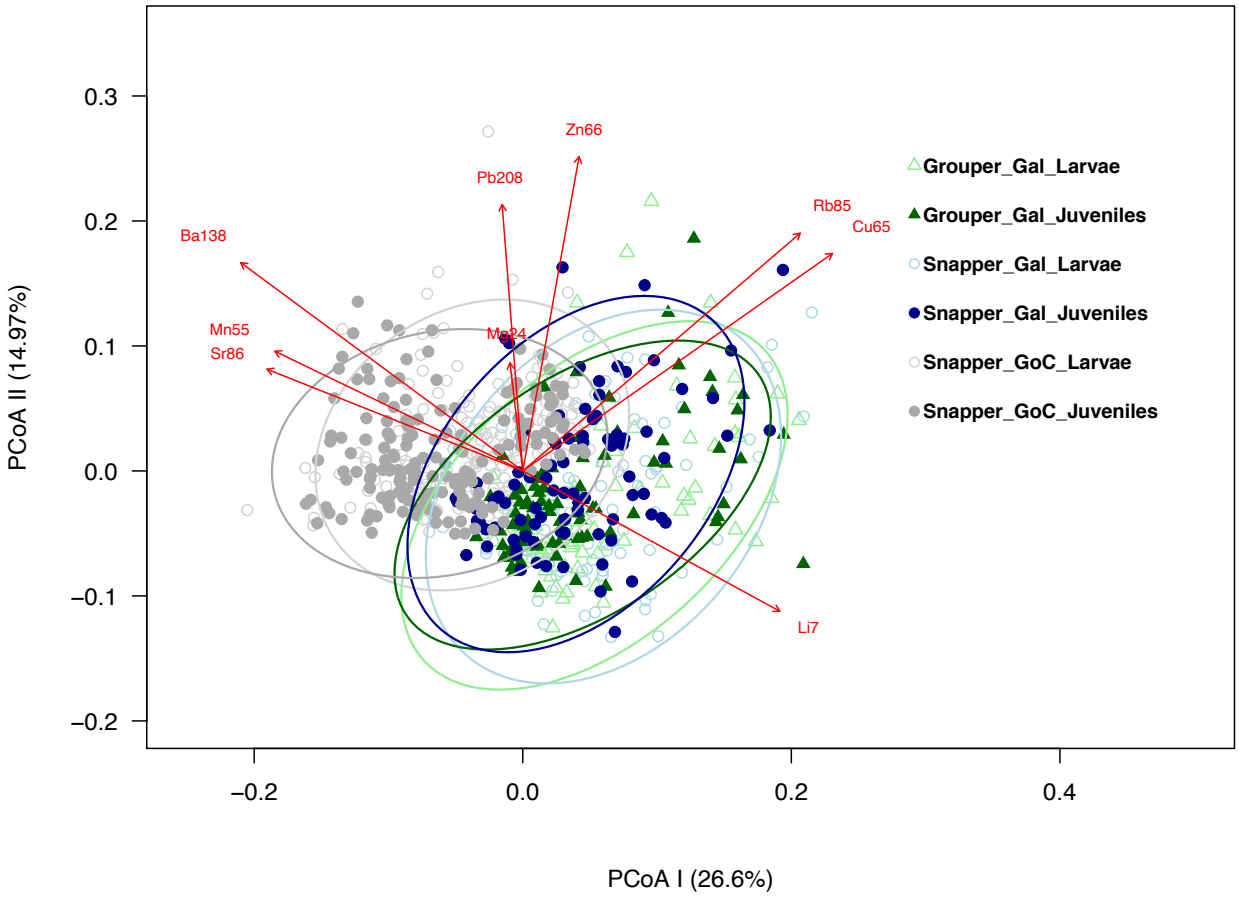

Figure 2.6. Principal Coordinate Analysis (PCoA) of fish otoliths from Galápagos (Gal) and the Gulf of California (GoC). Each symbol represents the elemental ratios (Me:Ca) of a single otolith during the larval stage (open ocean) or the juvenile stage (mangrove sites). Environmental vector correlations are included to indicate relationships between trace element ratios (Me:Ca) and PCoA axes.

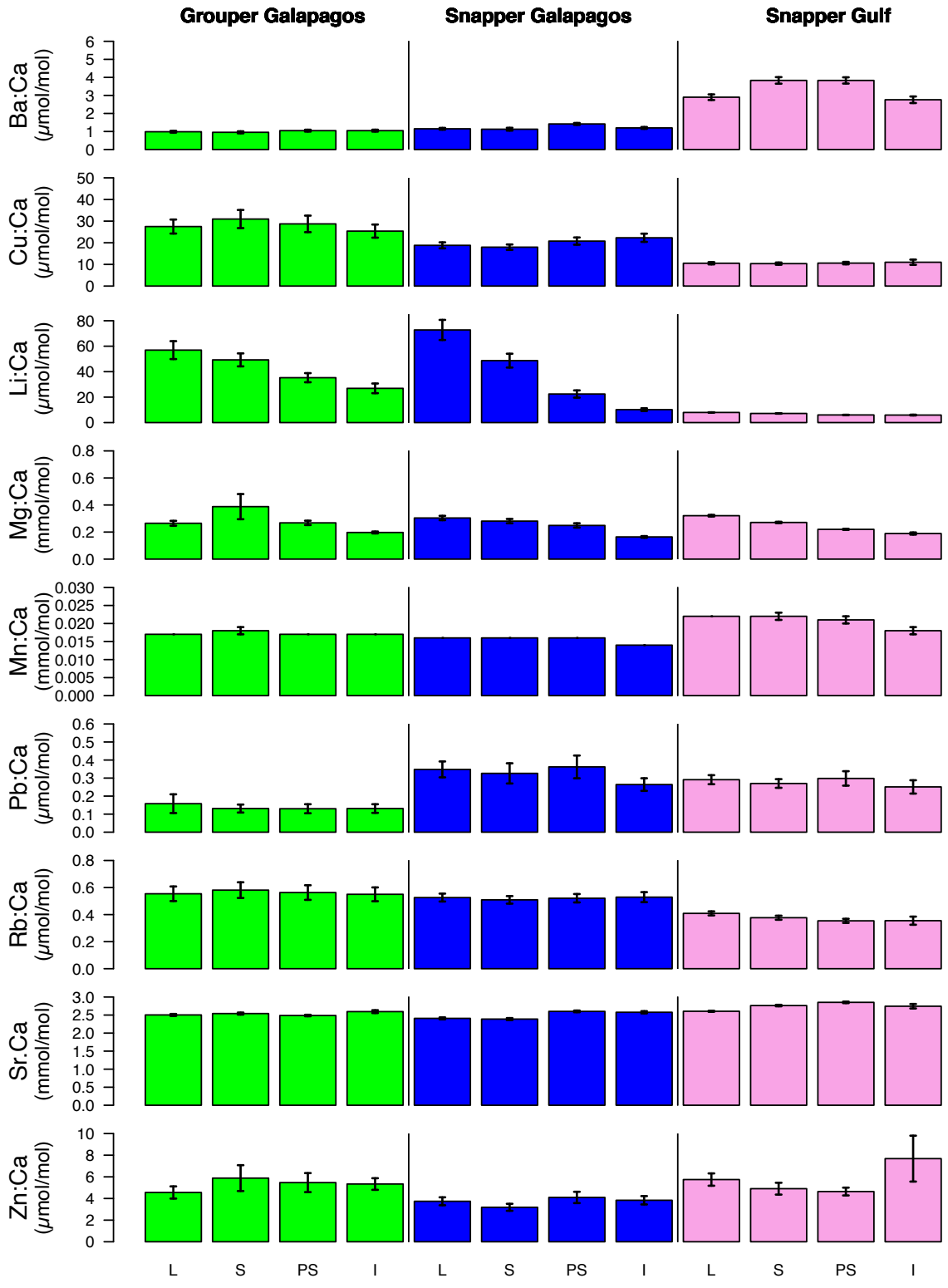

Figure 2.7. Average ± SE of element to calcium ratios per juvenile size class for sailfin grouper from Galápagos, yellow snapper from Galápagos and yellow snappers from the Gulf of California. L: larvae; S: settler; PS: post-settler, and I: immatures.

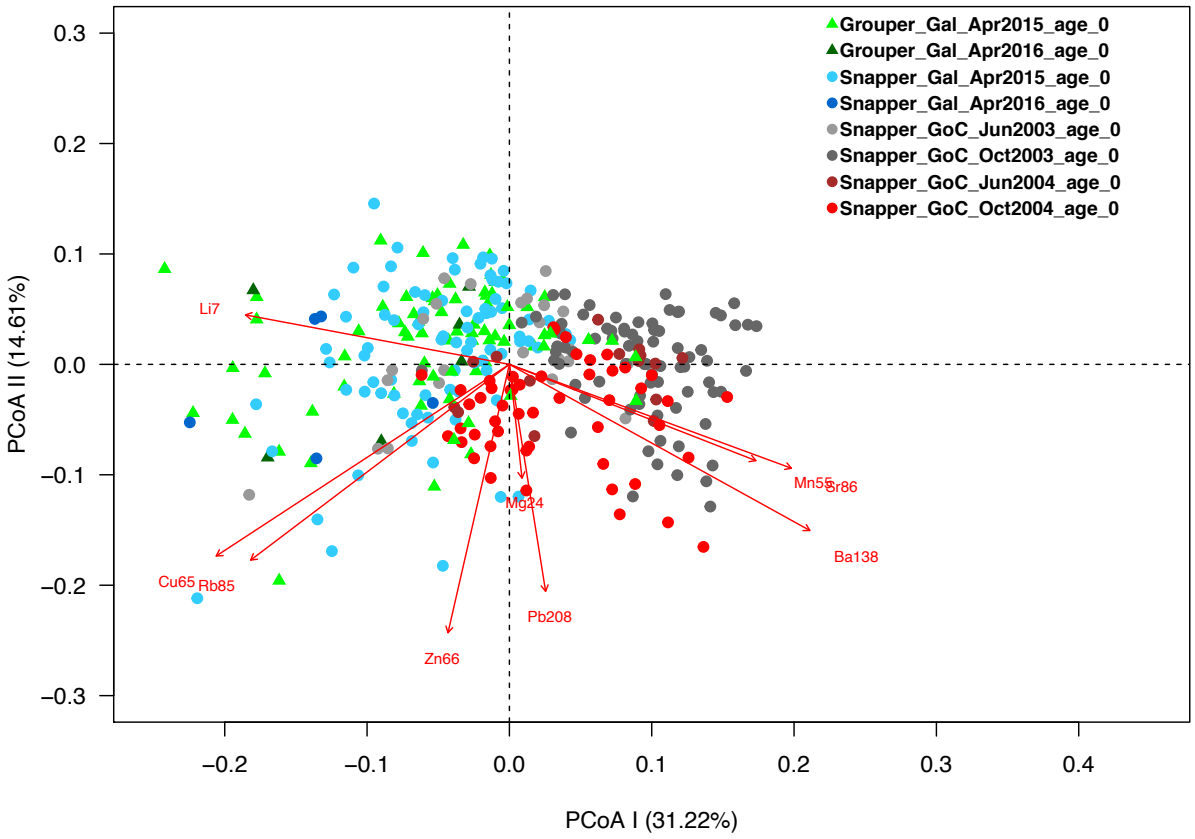

Figure 2.8. Principal Coordinate Analysis (PCoA) of fish otoliths from Galápagos (Gal) and the Gulf of California (GoC). Each symbol represents the elemental ratios (Me:Ca) of the juvenile stage of a single otolith (i.e. representing mangrove waters) across different cohorts. Environmental vector correlations are included to indicate relationships between trace element ratios (Me:Ca) and PCoA axes.

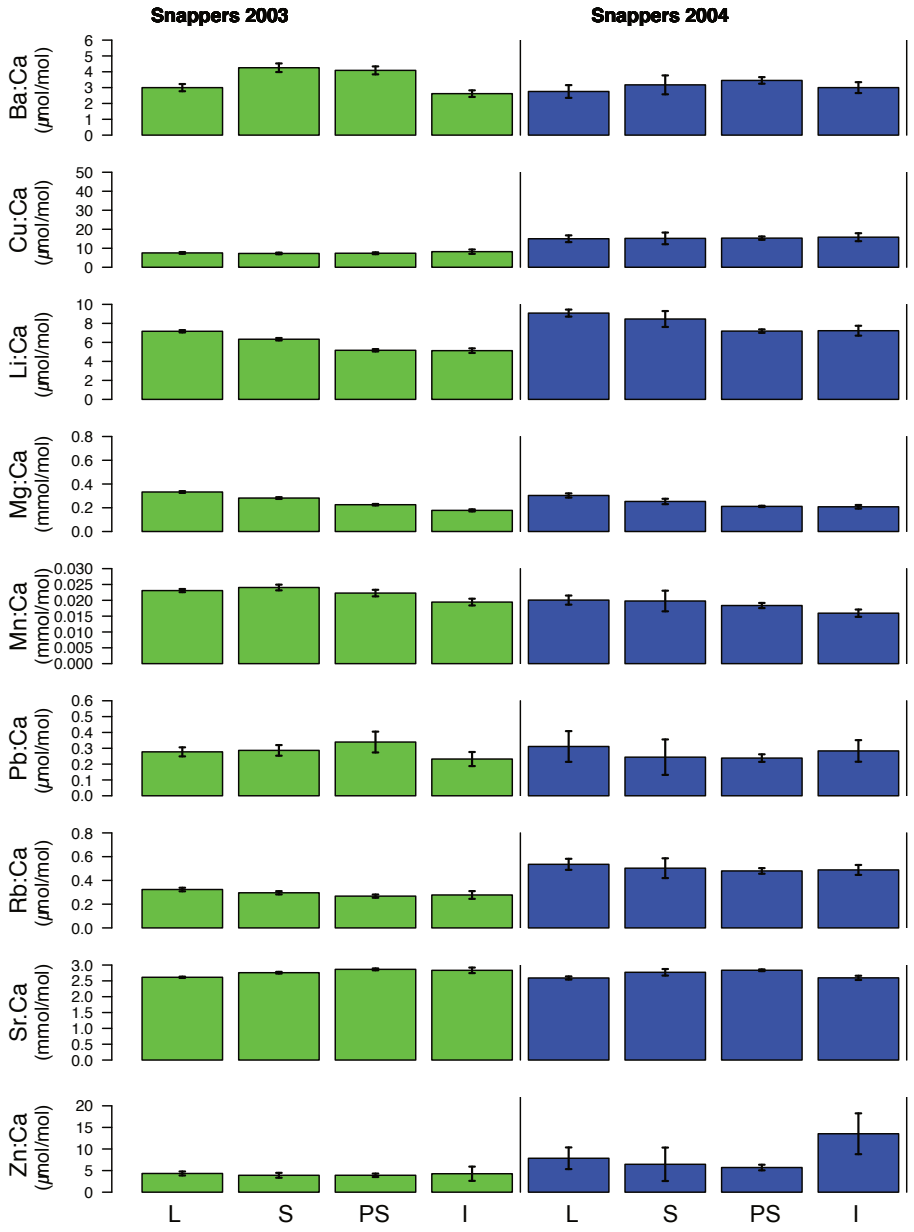

Figure 2.9. Average ± SE of element to calcium ratios per juvenile size classes for yellow snapper collected in 2003 and 2004 from the Gulf of California. See Fig. 7 and Section 2.2.1 for abbreviations and size ranges.

TABLES

Table 2.1. Date of collection, sample size (n) and size range of yellow snapper *Lutjanus argentiventris* and sailfin grouper *Mycteroperca olfax* from the Galápagos and the Gulf of California. TL: Total length.

Ecosystem	Date of collection	Species	*n*	Age (years)	Min TL (mm)	Max TL (mm)
Gulf of California	June-03	Yellow snapper	24	0	5.45	15.19
Gulf of California	October-03	Yellow snapper	80	0	2.7	12.41
Gulf of California	June-04	Yellow snapper	20	0	2.21	11.15
Gulf of California	October-04	Yellow snapper	50	0	2.44	12.02
Galápagos	April-15	Yellow snapper	83	0	2.8	19.5
Galápagos	April-16	Yellow snapper	5	0	10.3	24
Galápagos	April-15	Sailfin grouper	64	0	7.2	25.7
Galápagos	April-16	Sailfin grouper	6	0	11.5	24

Table 2.2. Average (SD in parenthesis) of the total length (TL) and age, and mean growth rate of yellow snapper *Lutjanus argentiventris* in the Gulf of California and Galápagos ecosystems.

Ecosystem	Species	Life Stage	TL (cm)	Age (days)	Mean growth (mm day^{-1})
Gulf of California	Yellow Snapper	Settler	2.93 (0.61)	33 (15)	0.089
		Post-Settler	7.46 (1.67)	124 (43)	0.060
		Immature	11.75 (1.53)	182 (44)	0.065
Galápagos	Yellow Snapper	Settler	3.41 (0.39)	60 (12)	0.057
		Post-Settler	6.36 (1.20)	82 (21)	0.078
		Immature	15.68 (2.25)	224 (41)	0.070

Table 2.3. Results of PERMANOVA comparing trace element signatures in yellow snapper otoliths collected from the Gulf of California (GOC) and Galápagos (GAL) and comparing yellow snapper and sailfin grouper otoliths collected from Galápagos (GAL). Df =Degrees of freedom. Sum0fSqs = Sequential Sum of squares. Pr = p-values based on 999 permutations. *p = 0.05, **p = 0.01, ***p = 0.001).

Species and Region	Factor	df	SS	R^2	F	Pr > F	
Yellow snapper GOC *vs* Yellow snapper GAL	Region	1	1.868	0.324	126.580	0.001	***
Yellow snapper GAL *vs* Sailfin grouper GAL	Species	1	0.084	0.021	3.586	0.027	*

Table 2.4. Results of univariate ANOVA comparing elemental ratios between species (yellow snapper GAL vs. sailfin grouper GAL) and between regions (yellow snapper GOC vs. yellow snapper GAL). p-bonf: p-values adjusted for multiple comparisons using the "Bonferroni" procedure. *p = 0.05, ** p = 0.01, *** p = 0.001; ns: non-significant

Element	Response	df	SS	MS	*F*	p-bonf	
Ba	Species	1	1.94	1.94	20.18	< 0.001	***
	Region	1	50.91	50.91	342.91	< 0.001	***
Cu	Species	1	0.44	0.44	0.82	ns	
	Region	1	21.32	21.32	58.90	< 0.001	***
Li	Species	1	0.99	0.99	1.09	ns	
	Region	1	115.77	115.77	273.62	< 0.001	***
Mg	Species	1	0.77	0.77	5.85	ns	
	Region	1	0.41	0.41	5.12	ns	
Mn	Species	1	0.21	0.21	5.24	ns	
	Region	1	4.67	4.67	68.68	< 0.001	***
Pb	Species	1	33.81	33.81	29.88	< 0.001	***
	Region	1	0.53	0.52	0.49	ns	
Rb	Species	1	0.14	0.14	0.46	ns	
	Region	1	4.70	4.70	20.73	< 0.001	***
Sr	Species	1	0.01	0.01	2.22	ns	
	Region	1	0.47	0.47	94.72	< 0.001	***
Zn	Species	1	1.94	1.94	3.99	ns	
	Region	1	1.52	1.52	2.63	ns	

Chapter 2 Appendix

The role of extrinsic variation – cohabiting juvenile fish species exhibit similar otolith elemental signatures

Supplementary Information

by

LETICIA MARIA CAVOLE[1,*], JESSICA A. MILLER[2], PELAYO SALINAS-DE-LEÓN[3,4], OCTAVIO ABURTO-OROPEZA[1], JOSE R. MARIN JARRIN[3,5] AND ANDREW FREDERICK JOHNSON[1,6,7]

[1]Scripps Institution of Oceanography, University of California San Diego, 9500 Gilman Drive, La Jolla, CA 92093 USA

[2]Oregon State University, 2030 SE Marine Science Drive, Newport, OR 97365, USA

[3]Charles Darwin Research Station, Charles Darwin Foundation, Puerto Ayora 200350, Galapagos Islands, Ecuador

[4] Pristine Seas, National Geographic Society, Washington, DC, USA 20036.

[5]Department of Fisheries Biology, Humboldt State University, 1Harpst St, Arcata, CA 95521

[6]MarFishEco Fisheries Consultants, Llanforda Mead, Oswestry, Shropshire, SY11 1TS, UK

[7]The Lyell Centre, Institute of Life and Earth Sciences, School of Energy, Geoscience, Infrastructure and Society, Heriot-Watt University, Edinburgh, EH14 4AS, UK

*Corresponding Author: lcavole@ucsd.edu

SUPPLEMENTARY MATERIAL

Supplementary information for section 2.2. Otolith preparation and elemental analysis

Sagittae from juveniles collected in the Gulf of California were removed, cleaned and embedded in epoxy blocks and sectioned through the core in the transverse plane with a low-speed diamond saw (Buehler Isomet) and then progressively polished using lapping film until the daily rings and the otolith core were exposed. Sagittae collected in the Galápagos Archipelago were mounted on the edge of microscope slides using thermoplastic adhesive (Crystalbond™) to expose the rostrum but to keep the nucleus of the otolith protected on the slide. The exposed section of each otolith was ground down to the slide edge using a series of polishing paper and diamond lapping film (400 grit or 30μm – 4000 grit or 3μm in decreasing order). The half section of each otolith was then re-heated using a hotplate and flipped so that the post-rostrum was vertically oriented. The post-rostral section was then ground and polished to the nucleus (until the core was visible) in the same sequence as already described. The methodologies to obtain the thin transverse sections of otoliths were different because no low-speed diamond saw was available in Galápagos.

The operating parameters for the LA-ICPMS laser were: pulse rate of 7 Hz with an ablation spot size of 30 μm that translated across the sample at 5 μm/s. A 30-second washout before and after each sample was completed to remove residues from previous samples and to collect background data. Transects were pre-ablated (2 Hz, 50 μm spot size, 100 μm/s) to further reduce potential sample contamination. For the Gulf of California, magnesium (^{24}Mg), calcium (^{43}Ca), manganese (^{55}Mn), strontium (^{86}Sr), lead (^{208}Pb), barium (^{138}Ba) and zinc (^{66}Zn) were consistently above detection limits. For Galápagos, all the elements were consistently above

detection limits. National Institute of Standards and Technology glass (NIST 612), and two calcium carbonate (USGS MACS-1 and MACS-3) standards were measured every 10 otoliths.

Supplementary information for section 2.4. Statistical analysis

We determined the extent to which the yellow snapper from the Galápagos and the Gulf of California, and the grouper *M. olfax* from the Galápagos Archipelago had similar patterns in their elemental signatures. The elemental ratios were transformed using the square root of each mean trace elemental ratio, prior to computing the distance matrix, to improve normality and homoscedasticity of the data.

PERMANOVA assumptions:

PERMANOVA is a semiparametric method that performs a geometric partitioning of multivariate variation in the space of a chosen dissimilarity measure with no assumption of multivariate normality (Anderson 2014) – a feature that is common among otolith microchemistry data. The assumption of homogeneity was tested using betadisper {vegan Package in R} and was met for the interspecific comparisons.

ANOVA assumptions:

For the ANOVA comparisons, we tested for normality and homoscedasticity using Shapiro-Wilk test and Bartlett's test for each elemental ratio (Me:Ca) and factor (species or region), respectively. The Shapiro-Wilk test indicated the data distributions for Pb:Ca and Zn:Ca were not normally distributed between Galápagos species, or Pb:Ca, Rb:Ca and Zn:Ca between snappers from Galápagos vs. those from the Gulf. The Bartlett's test confirmed homoscedasticity for most of the elemental ratios analyzed, with the exception of Pb:Ca, Rb:Ca and Zn:Ca for both

groups. Bonferroni correction was applied to adjust p-values to account for the multiple comparisons. We performed Tukey's post hoc test to examine which group pair (e.g., *L. argentiventris* - Galápagos vs. *M. olfax* - Galápagos) exhibited significant differences for each trace elemental ratio (**Figure 2.S5**).

ANOSIM model interpretation:

This hypothesis test used distance or dissimilarity matrices and significance was evaluated by permutation. The ANOSIM statistic compares the mean of ranked dissimilarities between groups to the mean of ranked dissimilarities within groups. An R value close to "1.0" suggests dissimilarity between groups, or high separation between groups, while an R value close to "0" suggests an even distribution of high and low ranks within and between groups, or no separation between group.

PCoA model:

PCoA is an eigen-analysis of a distance or dissimilarity matrix. A dissimilarity matrix was constructed based on the "Gower" method (Gower, 1966), using a two-dimensional projection of distance between average otolith Me:Ca values. In order to fit the trace elements onto an ordination, we projected the points onto vectors that have maximum correlation with corresponding elemental ratio, using envfit {vegan Package in R}.

Gulf of California temporal comparison:

The yellow snappers from the Gulf of California did not present differences in the elemental ratios (Me:Ca) within the same year of collection (**Figure 2.S2 & 2.S3** in

Supplements). Therefore, these data were grouped per year (2003 vs. 2004) to examine interannual variability on elemental composition across life stages using Welch t-tests, which accounts for unequal variances and *P*-values were Bonferroni-corrected after analysis for multiple comparisons. This analysis was not possible for Galápagos, since only 12 fishes (5 snappers and 7 sailfin groupers) out of a total of 158 were collected in April of 2016.

Table 2.S1. Estimation of accuracy and precision using calcium carbonate standards (MACS-3 and MACS-1) and the mean percent relative standard deviations (%RSD) of the NIST 612. All standards were run at every 10 otoliths for the Galápagos and the Gulf of California samples. NIST: National Institute of Standards and Technology; NA: not applicable.

Ecosystem	Species	Standard	Sr:Ca	Ba:Ca	Cu:Ca	Li:Ca	Mg:Ca	Mn:Ca	Zn:Ca	Pb:Ca	Rb:Ca
Galápagos	Yellow Snapper	MACS3	1.11	1.32	0.82	0.83	1.12	0.97	0.91	1.16	NA
		MACS 1	1.09	1.09	NA	NA	1.45	1.01	0.91	0.80	NA
		NIST 612	6.10	5.07	15.93	18.38	12.76	9.45	19.94	13.43	14.00
Galápagos	Sailfin Grouper	MACS3	1.01	1.25	0.79	0.83	1.02	0.96	0.77	1.24	NA
		MACS 1	1.10	1.07	NA	NA	1.61	1.05	0.92	0.77	NA
		NIST 612	5.72	4.58	13.91	15.68	11.42	9.18	16.55	11.37	12.25
Gulf of California	Yellow Snapper	MACS3	1.09	1.25	0.74	0.76	1.13	0.94	0.78	0.98	NA
		MACS 1	1.12	1.13	NA	NA	1.63	1.02	0.89	0.75	NA
		NIST 612	6.53	4.85	15.87	16.99	12.63	9.23	18.17	12.52	12.56

Table 2.S2. Comparison by t-test of elemental ratio means between 2003 and 2004 years for all life stages (larvae, settlers, post-settlers and immatures) of yellow snappers from the Gulf of California. *P*-values were adjusted for multiple comparisons using the "Bonferroni" procedure (*P*-bonf corr). Bold values indicate significant *P*-values (<0.05). Asterisks denote significance (* = 0.05, ** = 0.01, *** = 0.001). NS: non-significant.

		Mean					
Element	Life stage	Year 2003	Year 2004	*t*	d.f.	*P*- bonf corr	
Ba:Ca	Larvae	2.999	2.755	0.82	171.81	NS	
	Settler	4.255	3.173	3.41	157.16	**0.03**	*
	Post-settler	4.088	3.454	1.95	151.00	NS	
	Immature	2.618	3.000	-0.95	22.60	NS	
Cu:Ca	Larvae	7.538	15.001	-7.71	109.29	**< 0.001**	***
	Settler	7.268	15.193	-8.38	98.30	**< 0.001**	***
	Post-settler	7.377	15.329	-7.93	98.43	**< 0.001**	***
	Immature	8.205	15.819	-3.19	20.87	NS	
Li:Ca	Larvae	7.168	9.081	-8.84	132.10	**< 0.001**	***
	Settler	6.331	8.459	-8.10	103.75	**< 0.001**	***
	Post-settler	5.167	7.186	-9.06	113.64	**< 0.001**	***
	Immature	5.129	7.228	-3.66	18.74	NS	
Mg:Ca	Larvae	0.333	0.303	2.60	155.17	NS	
	Settler	0.282	0.253	2.96	166.57	NS	
	Post-settler	0.226	0.212	1.71	150.91	NS	
	Immature	0.178	0.208	-1.71	22.03	NS	

Table 2.S2. Comparison by t-test of elemental ratio means between 2003 and 2004 years for all life stages (continued).

Element	Life stage	Mean		*t*	d.f.	*P*- bonf corr	
		Year 2003	Year 2004				
Mn:Ca	Larvae	0.023	0.020	3.55	133.98	**0.019**	*
	Settler	0.024	0.020	3.36	158.94	**0.035**	*
	Post-settler	0.022	0.018	2.99	150.65	NS	
	Immature	0.019	0.016	2.24	31.50	NS	
Pb:Ca	Larvae	0.277	0.311	-0.62	119.73	NS	
	Settler	0.287	0.244	0.94	163.91	NS	
	Post-settler	0.339	0.238	1.45	112.49	NS	
	Immature	0.232	0.283	-0.63	23.94	NS	
Rb:Ca	Larvae	0.323	0.535	-7.92	128.16	**< 0.001**	***
	Settler	0.296	0.503	-7.73	111.84	**< 0.001**	***
	Post-settler	0.268	0.480	-7.79	100.34	**< 0.001**	***
	Immature	0.277	0.488	-3.98	27.83	**0.016**	*
Sr:Ca	Larvae	2.613	2.591	0.71	153.45	NS	
	Settler	2.758	2.770	-0.32	154.84	NS	
	Post-settler	2.864	2.835	0.71	148.47	NS	
	Immature	2.833	2.595	2.17	36.00	NS	
Zn:Ca	Larvae	4.331	7.854	-2.74	89.62	NS	
	Settler	3.911	6.458	-2.11	101.64	NS	
	Post-settler	3.913	5.710	-2.36	105.33	NS	
	Immature	4.273	13.528	-1.85	16.21	NS	

Table 2.S3. Mean, standard deviation (SD), minimum and maximum values of sea surface temperature (SST, °C) and chlorophyll-a (Chl-a, mg m3) adjacent to the mangrove sites of Galápagos and the Gulf of California during the lifetime of snappers and grouper juveniles.

Ecosystem	Mangrove Site	Long	Lat	Variable	Mean	SD	Min	Max	Variable	Mean	SD	Min	Max
Galápagos	Punta Espinoza	-91.45	-0.27	**SST**	25.59	1.48	23.12	29.25	**Chl-a**	0.30	0.11	0.12	0.55
	Punta Mangle	-91.39	-0.45		25.11	1.70	22.32	29.36		0.27	0.08	0.16	0.52
	Poza los Patillos	-91.38	-0.36		24.79	1.80	21.67	28.89		0.25	0.07	0.14	0.42
	Baya Post Office	-90.44	-1.23		24.91	1.70	21.40	28.29		0.26	0.09	0.10	0.54
	Urbina Sur	-91.26	-0.38		25.76	1.08	24.06	27.80		0.29	0.11	0.16	0.61
	Urbina Sur 2	-91.28	-0.36		25.13	1.85	21.77	28.51		0.22	0.05	0.14	0.33
	Abaledo	-91.21	-0.67		25.58	1.47	22.28	28.96		0.41	0.24	0.18	1.14
	Punta Moreno	-91.33	-0.72		25.22	1.75	22.44	29.68		0.28	0.07	0.17	0.52
	Cartago Grande	-90.92	-0.62		24.79	1.88	21.57	29.00		0.24	0.07	0.14	0.50
	Cartago Chico	-90.86	-0.66		25.58	1.33	22.92	28.53		0.28	0.10	0.16	0.61
	Cartago North	-90.98	-0.58		24.73	1.95	21.81	29.08		0.25	0.08	0.14	0.48
	Albemarle	-91.36	0.16		25.06	1.79	21.76	28.60		0.27	0.09	0.17	0.65
	Puerto Grande	-89.47	-0.80		24.59	1.90	21.83	28.73		0.30	0.09	0.14	0.46
	Las Sardinas	-89.39	-0.72		24.68	1.96	21.38	28.62		0.24	0.08	0.13	0.50
	Parroquinnos	-90.42	-0.77		25.16	1.45	22.61	28.29		0.29	0.10	0.14	0.66
	Caleta Tortuga Negra	-90.33	-0.50		24.42	1.97	21.23	28.97		0.36	0.16	0.13	0.80
	Itabaca Canal	-90.28	-0.49		24.90	1.73	21.98	28.45		0.31	0.13	0.16	0.97
	East Santa Cruz	-90.20	-0.68		24.38	1.73	20.53	28.73		0.62	0.38	0.20	1.55
	Poza de las azules	-90.67	-0.35		24.94	1.77	21.75	28.59		0.25	0.07	0.13	0.46
	La Bomba	-90.70	-0.18		24.89	1.81	21.46	28.16		0.25	0.07	0.14	0.45
Gulf of California	San Lucas	-112.20	27.23	**SST**	24.42	4.19	15.65	31.70	**Chl-a**	3.08	2.86	0.22	27.81
	Los Mojones	-112.01	27.02		25.14	4.34	16.67	32.29		2.51	2.96	0.18	20.08
	Punta Mangle Baja	-111.33	26.27		25.21	4.01	15.53	32.34		1.68	2.21	0.13	25.20
	Puerto Escondido	-111.31	25.82		25.55	3.86	18.15	32.29		1.94	2.66	0.10	25.41
	Los Gatos	-110.90	25.52		25.69	3.68	18.30	32.55		1.47	2.21	0.04	21.56
	San Jose	-110.56	24.87		25.71	3.52	18.75	32.26		0.97	0.88	0.08	7.80
	Balandra	-110.32	24.32		25.53	3.29	17.44	32.10		1.43	1.93	0.20	20.75
	El Soldado	-110.98	27.96		25.05	5.03	15.17	33.57		3.02	4.08	0.16	29.55
	Punta Yavaros	-109.53	26.71		26.28	4.95	16.54	34.53		3.77	3.70	0.43	28.10
	Barra de Piaxtla	-106.44	23.20		27.27	3.31	19.01	33.90		2.90	2.69	0.13	22.13

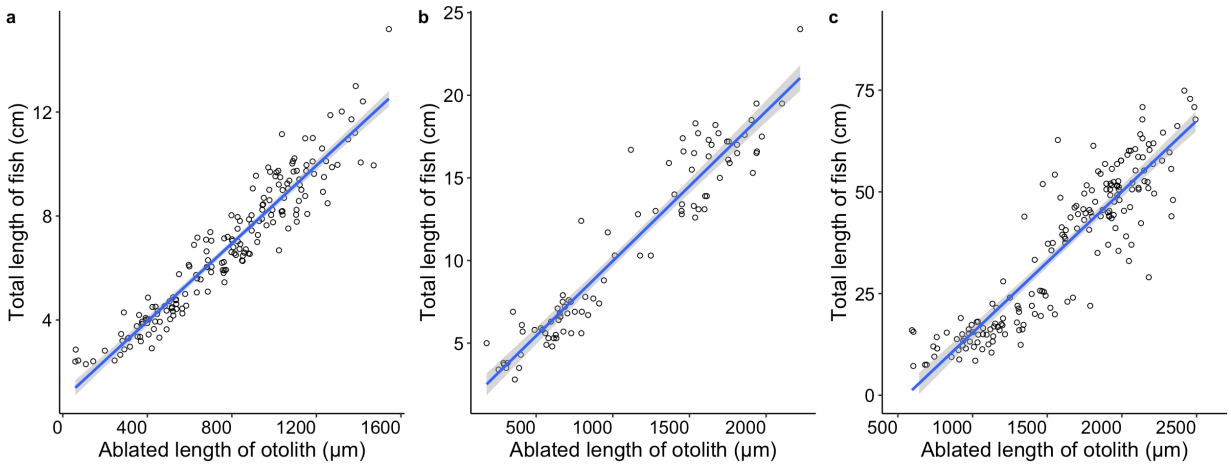

Figure 2.S1. Linear relationship between the total length of fish (mm) and the ablated length of otolith (μm) using the LA-ICPMS for (A) the Gulf of California yellow snapper juveniles, (B) the Galápagos yellow snapper juveniles and (C) the Galápagos sailfin groupers.

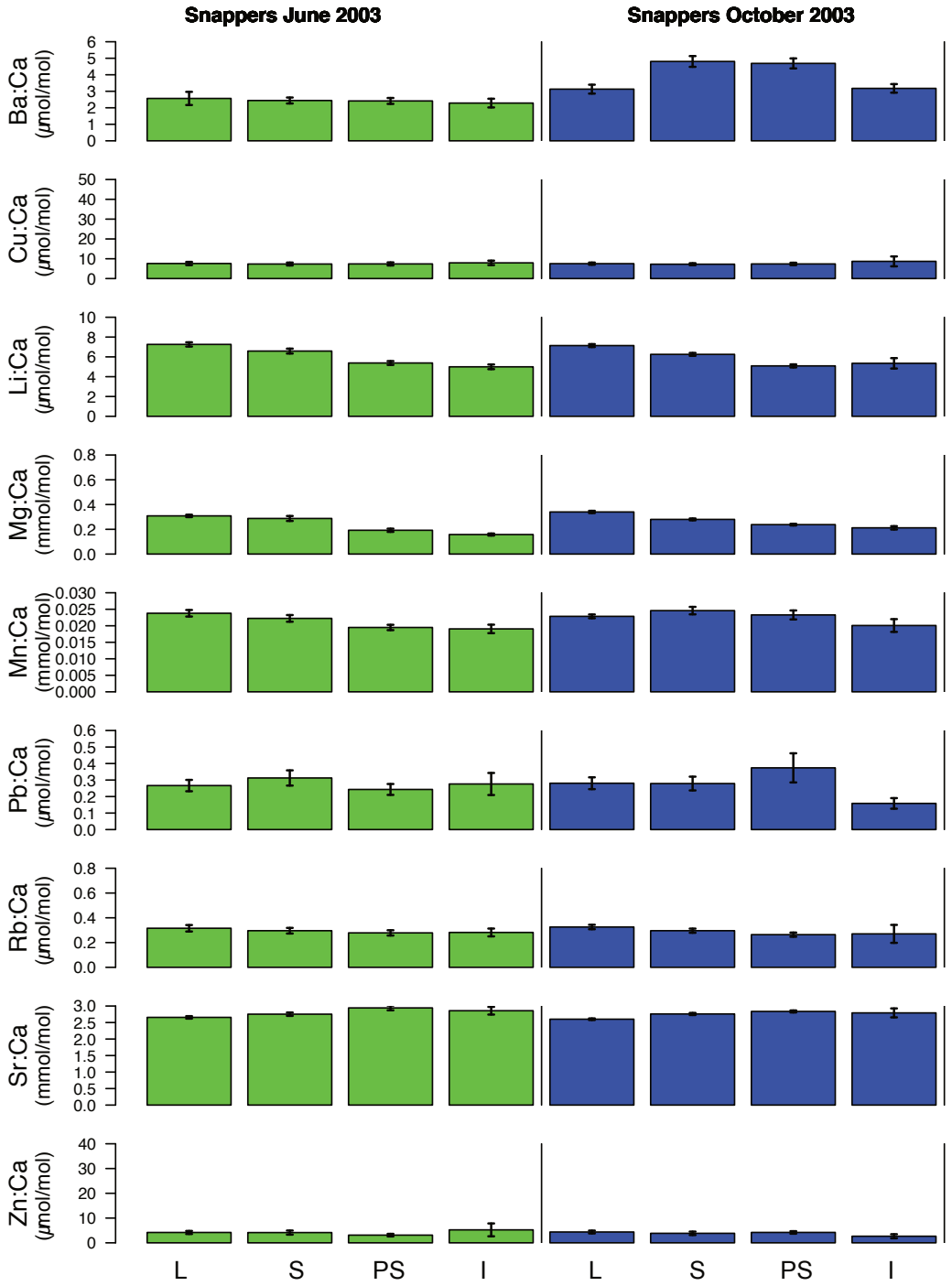

Figure 2.S2. Average ± standard error of element to calcium ratios per juvenile size classes for yellow snapper collected in June of 2003 (green) and October of 2003 (blue) from the Gulf of California. Larvae (L) < 2cm, Settler (S): 2-4 cm, Post-Settler (PS): 4-10 cm, and Immature (I): 10-20 cm for yellow snappers.

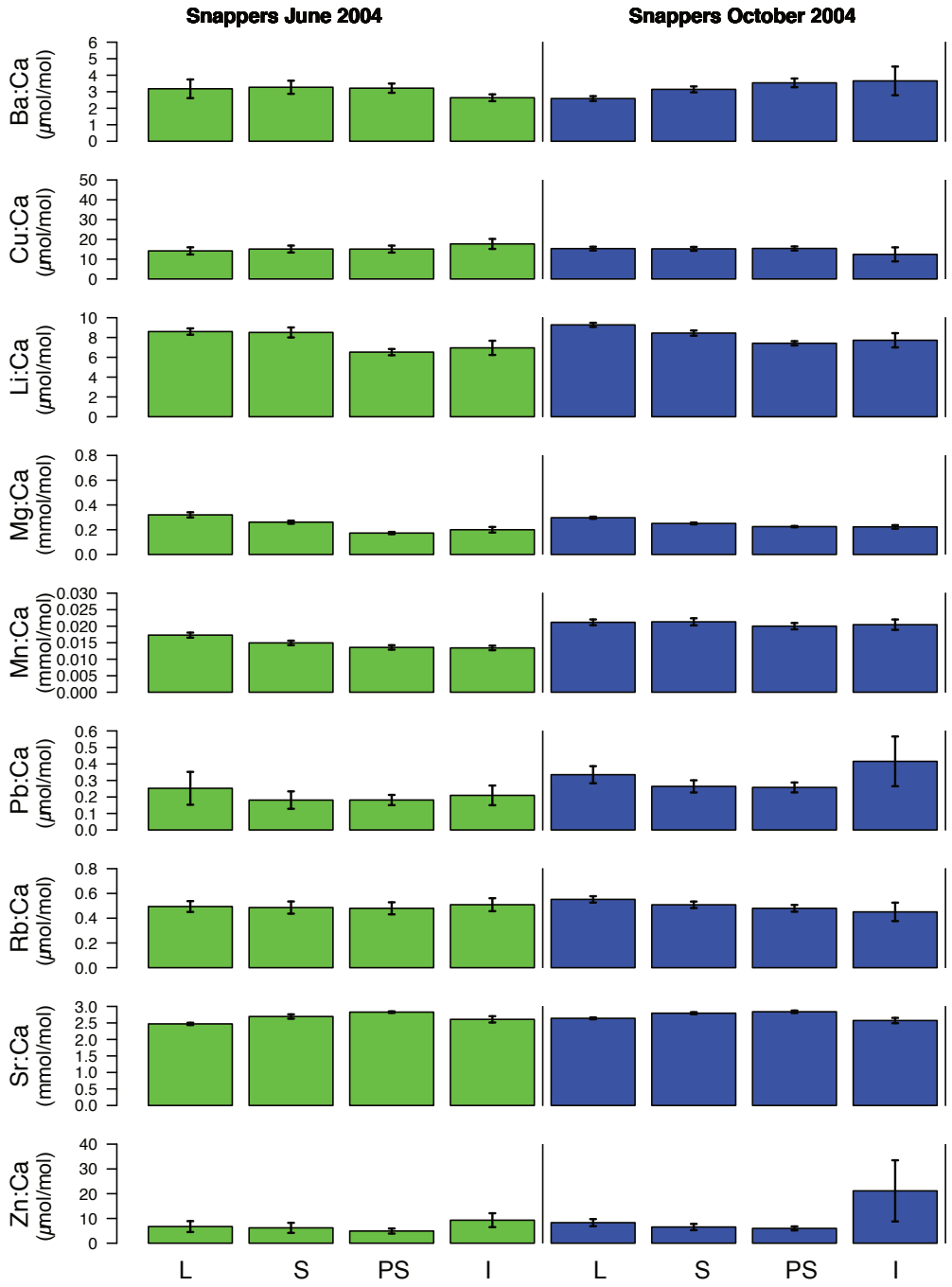

Figure 2.S3. Average ± standard error of element to calcium ratios per juvenile size classes for yellow snapper collected in June of 2004 (green) and October of 2004 (blue) from the Gulf of California. Larvae (L) < 2cm, Settler (S): 2-4 cm, Post-Settler (PS): 4-10 cm, and Immature (I): 10-20 cm for yellow snappers.

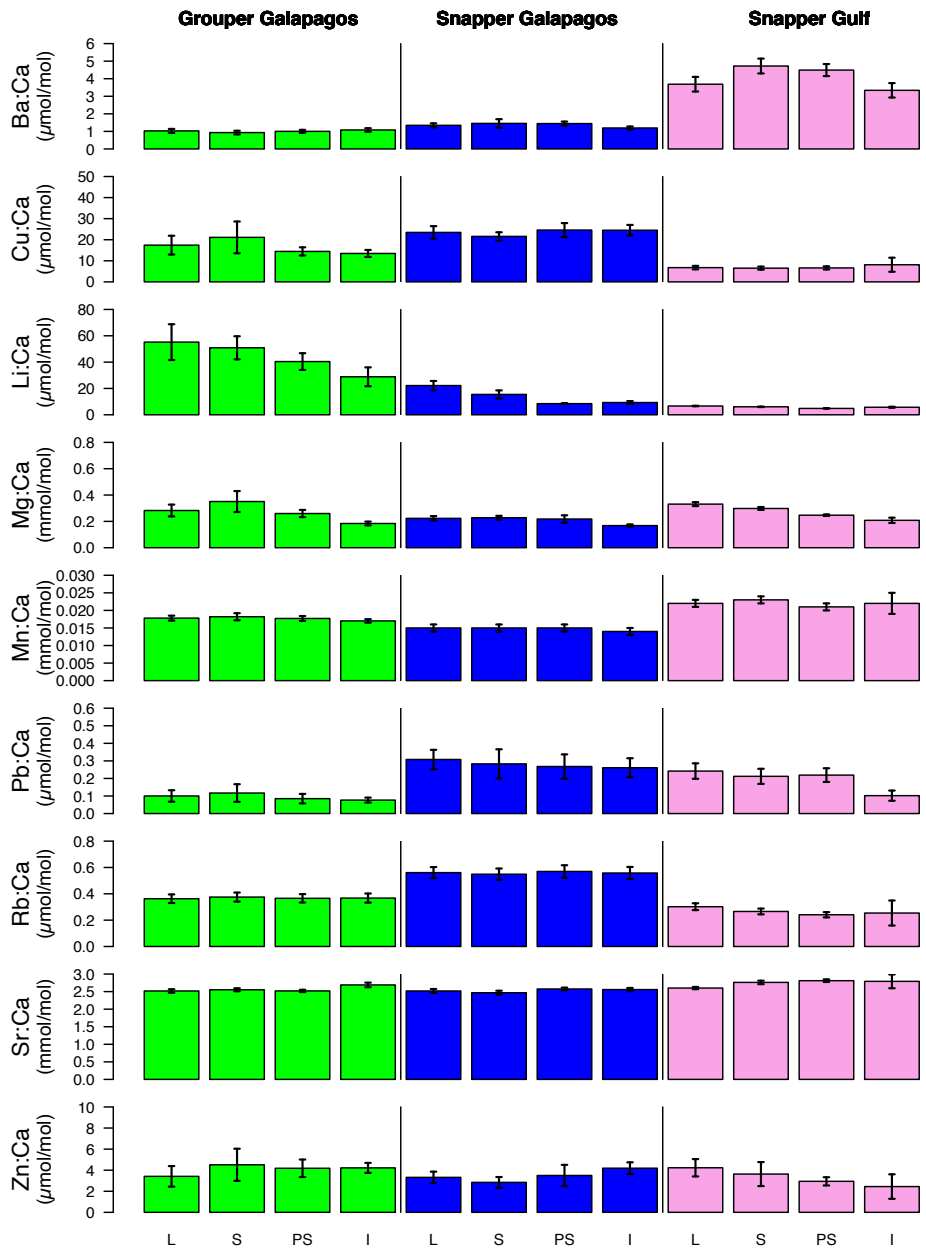

Figure 2.S4. Average ± standard error of element to calcium ratios per juvenile size class for sailfin grouper from Galápagos (green), yellow snapper from Galápagos (blue) and yellow snappers from the Gulf of California (pink) that co-occurred within the same time window (n=97). Larvae (L) < 2cm, Settler (S): 2-4 cm, Post-Settler (PS): 4-10 cm, and Immature (I): 10-20 cm for yellow snappers and Larvae (L) < 2.5cm, Settler (S): 2.5 – 3.5 cm, Post-Settler (PS): 3.5 - 15 cm, and Immature (I): 15-65 cm for sailfin groupers.

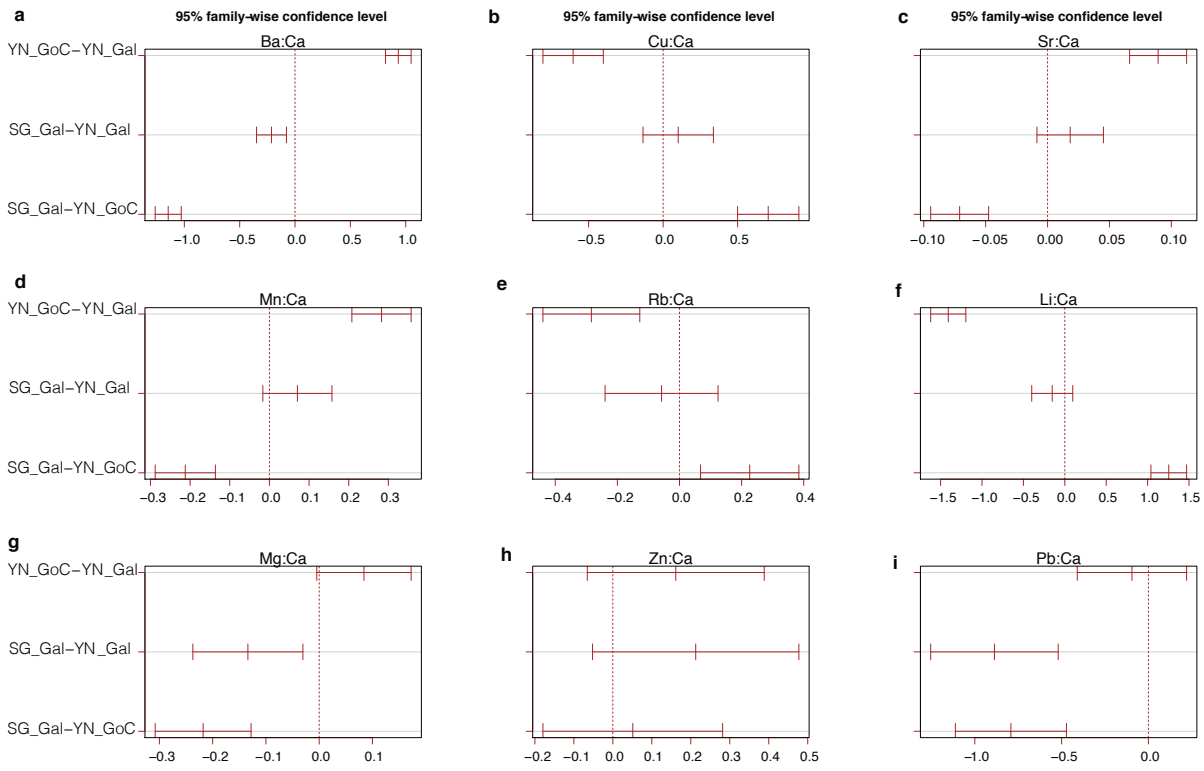

Figure 2.S5. Tukey simultaneous confidence intervals for univariate ANOVAs comparing trace elemental ratios (Me:Ca) among otoliths of yellow snappers from the Gulf of California (YN_GoC), yellow snappers from Galápagos (YN_Gal), and sailfin groupers from Galápagos (SG_Gal). If a 95% confidence interval does not contain zero, the corresponding means are significantly different.

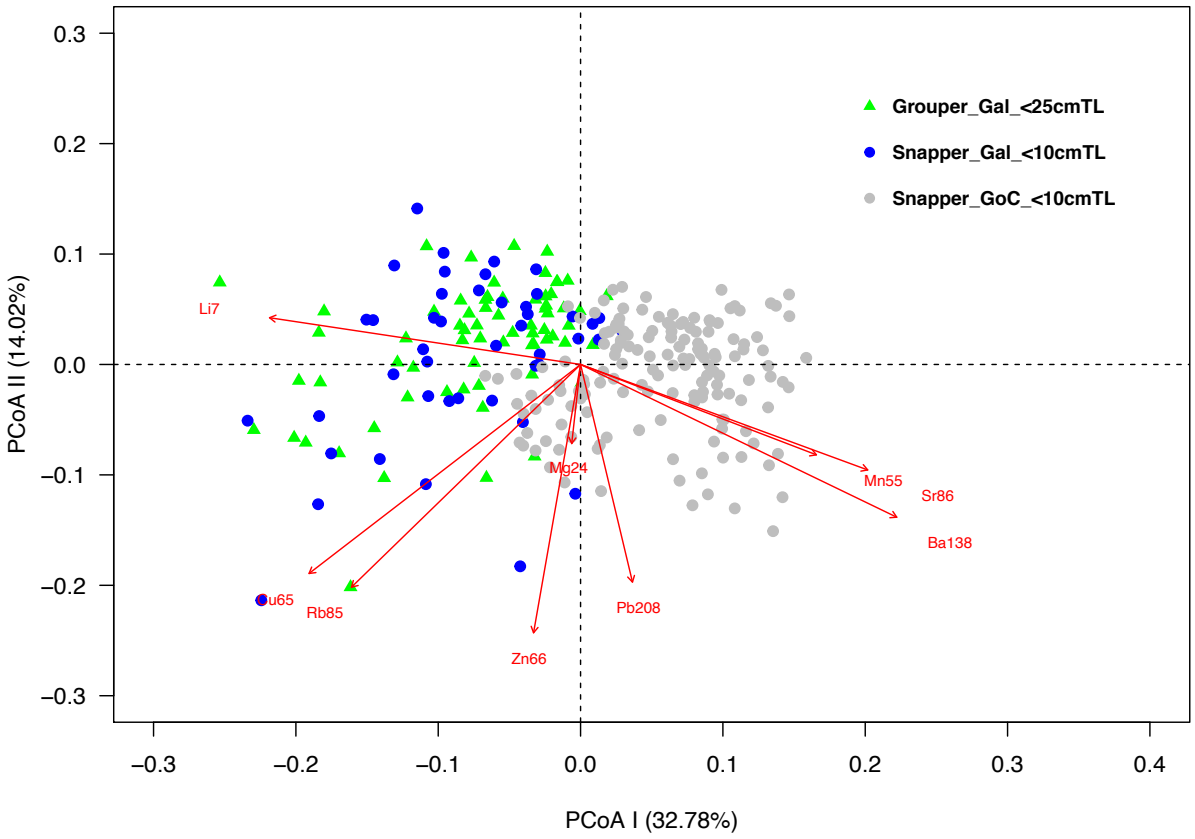

Figure 2.S6. Principal Coordinate Analysis (PCoA) of fish otoliths from Galápagos (Gal) and the Gulf of California (GoC). Each symbol represents the elemental ratios (Me:Ca) of the juvenile stage of a single otolith (i.e. representing mangrove waters) across different cohorts. Environmental vector correlations are included to indicate relationships between trace element ratios (Me:Ca) and PCoA axes. Yellow snappers included are below 10 cm of total length, and sailfin groupers are below 25 cm of total length.

CHAPTER 3:

Fish metapopulation structure changes throughout life stages based on otolith microchemistry and genetic analysis

LETICIA MARIA CAVOLE, ADRIAN MUNGUIA-VEGA, JESSICA A. MILLER, PELAYO SALINAS-DE-LEÓN, JOSE R. MARIN JARRIN, ANDREW FREDERICK JOHNSON, ETIENNE-RASTOIN LAPLANE, ALFREDO GIRÓN-NAVA, OCTAVIO ABURTO-OROPEZA

Abstract

Metapopulation framework in the marine realm contributes to the understanding of spatial processes and structures in populations, providing basic information for conservation biology. However, the extent to which the metapopulation structure differs geographically and across life-history stages is unexplored for most marine fishes. Here, we developed a comparison of population structure and connectivity by contrasting the same species in their northern and southern geographical limits. Juvenile yellow snapper *Lutjanus argentiventris* occurs throughout Eastern Tropical Pacific (ETP) mangrove habitats, experiencing an array of environmental and oceanographic conditions that can produce unique otolith microchemistry signatures and metapopulation structures. In the Galápagos Archipelago (GA), we used otolith microchemistry (embryonic, larval, and juvenile stages) and microsatellite DNA (juvenile stage) in tandem to elucidate the population structure of snappers. For the Gulf of California (GOC), we used self-assignment rates obtained from otolith microchemistry (embryonic, larval, and juvenile stages) to predict the population structure for snappers, and later compared these results with the genetic structure of adult populations from rocky reefs. Otolith microchemistry fingerprints differed between GA and GOC, possibly due to freshwater, salinity, primary productivity, hydrothermal activity and human impact gradients. We observed significant differences in otolith microchemistry at the ecoregion spatial scale (10 - 100 km^2) for GA and GOC (classification accuracy ~ 60%). At the finer mangrove spatial scale (1 km^2), we found larger differences in otolith signatures among the GOC mangroves (classification accuracy ~ 90%) than in GAL (classification accuracy ~ 23%), potentially related to a stronger environmental gradient over a larger latitudinal spatial scale in the GOC. Seventy-five percent of juveniles were migrants among mangroves in GA, in contrast with only ~ 10% of migrants among GOC mangroves. For

GA, both microchemistry and genetics supported the presence of a source-sink metapopulation structure for the yellow snapper, with high levels of connectivity in mangroves within ecoregions. For the GOC, based on otolith microchemistry at early life stages, the yellow snapper has a metapopulation structure characterized by higher rates of self-recruitment that is not compatible with the metapopulation structure found offshore for adults at the rocky reefs. By combining tools that assess connectivity at multiple time scales (microchemistry and genetics) at different life stages and distinct ecosystems, we were able to provide a more holistic metapopulation model for *L. argentiventris*.

Introduction

A metapopulation is defined as a population that occupies distinct habitat patches with several levels of dispersion among individuals, allowing demographic connectivity and population independence to co-occur (Kritzer and Sale 2010). A metapopulation model is applicable to cases in which the spatial structure of populations is determined by habitat patchiness, and therefore, this patchy population structure is pivotal for understanding its population dynamics, conservation of genetic variation and evolutionary responses to natural and/or anthropogenic pressures (e.g., changes in physical-chemical variables, habitat fragmentation and loss). Metapopulation theory also requires that local populations are potentially connected via migration, such that movements among patches are important for their population dynamics and genetic structure (Kritzer and Sale 2010). Metapopulation framework in the marine realm contributes to the understanding of spatial processes and structures in populations as well as basic information for population and conservation biology. However, the extent to which the metapopulation structure differs across ecosystems with varying

oceanographic conditions, or it changes based on the life stage examined, is still a conundrum and unexplored topic for most fish species and marine ecosystems.

Within the context of illuminating the level of connectivity among fish populations, many studies have determined the importance of different nurseries as sources of recruitment into adult populations and the extent of self-recruitment/dispersal among natural populations using otolith microchemistry and genetic markers (Thorrold et al. 2001, Gillanders et al. 2003, Chittaro et al. 2004, Miller et al. 2005, Mateo et al. 2010, Christie et al. 2010, Cook et al. 2014). Using otolith microchemistry techniques, previous studies were usually performed in mangrove sites or estuarine systems under freshwater runoff influence, where discriminatory capabilities are usually greater. This is not the case for the semi-arid mangrove sites in the Gulf of California (GOC) and the Galápagos Archipelago (GA). Nonetheless, the Gulf of California and Galápagos Archipelago have marked seasonal differences in surface water temperatures – up to 8°C in Galápagos, and 20 °C in the Gulf of California – and striking differences over a latitudinal gradient for the Gulf of California (the northern areas are cooler than southern areas) and longitudinal gradient for the Galápagos (the western side of the archipelago is consistently cooler than its eastern side). The Gulf of California and Galápagos are also home to many mangroves that serve as nurseries to several commercially important fish species (Aburto-Oropeza et al. 2008, Llerena et al. 2013). Thus, information on mangrove habitats (i.e., whether they act as sources or sinks for individuals) within these ecosystems can refine the understanding of connectivity patterns between juvenile and adult fish to better manage the stocks associated with them.

Both otolith microchemistry (i.e., minor, trace and major elements in fish otoliths) and microsatellite DNA (i.e., sequence repeats of two to five base pairs in eukaryotic genomes) show

potential to define the spatial structure and connectivity patterns of fish populations (O'Connell and Wright 1997, Campana and Thorrold 2001, Reis-Santos et al. 2018). Otoliths function as natural tags that grow throughout the life of teleost fish, and directly and indirectly record aspects of the environment, such as temperature and primary productivity, within its structure and chemical properties (Radtke and Shaefer 1992, Campana 1999, Martin and Thorrold 2005*)*. Otolith microchemistry can elucidate the metapopulation structure of fish populations by analyzing the signatures acquired during embryonic development, which reflects their natal origin(s), and/or by analyzing the extent of mixing in a population through the comparison of elemental signatures across later life stages from different locations.

Microsatellites DNA base pair sequences experience several mutation rates that can lead to high levels of polymorphism. This feature can be useful for discriminating fine-scale population structure in marine fish (Buonaccorsi et al. 2002) and to quantify levels of connectivity among adjacent populations (Bradbury et al. 2014). Although both otolith microchemistry and genetic methods can be complementary in fish population analyses (Feyrer et al. 2007), they provide information at different time scales; genetics (e.g., microsatellite DNA) can elucidate long-term gene flow and connectivity patterns on evolutionary time scales, whereas chemical tracers in otoliths can reveal connectivity patterns within ecological timescales (i.e., during an individual lifetime) (Fromentin et al. 2009). Depending on the strength and consistency of environmental gradients (e.g., SST, Chl-*a*, salinity, oxygen levels) imposed by the landscape and hydrography (e.g., current mixing, upwelling, freshwater influence, bedrock composition), these two approaches can yield similar metapopulation structures that may reflect the short and long-term population dynamics in a given ecosystem.

Yellow snapper *Lutjanus argentiventris* is a marine fish species with a complex life cycle

that involves ontogenetic migration among distinct habitats during its lifetime. In the Gulf of California, adults spawn during spring-summer season on coastal marine sites, close to rocky reefs, and their larvae are then dispersed for ~ 19-26 days until entering a mangrove lagoon (Aburto-Oropeza et al. 2009). In mangroves, juveniles remain close to the substrate and to the mangrove roots until they are around 10 cm of total length and 300 days-old, when they begin to migrate to the offshore adult rocky reef habitats (Aburto-Oropeza et al. 2009). There is no otolith-based tracking for ontogenetic habitat shifts in the yellow snapper in the Galápagos Archipelago, but juveniles are also observed inside mangrove sites and adults are observed at adjacent coastal sites (Fierro-Arcos et al. 2021).

We hypothesize that marked differences in ocean temperature, primary productivity, and the size and configuration of mangrove lagoons, together with the complex life history of yellow snappers (i.e., ontogenetic migration of oceanic larvae to mangroves, mangrove residence for about one year, and later migration of juveniles to coastal sites), will result in distinct metapopulation structures for the yellow snappers in each of these large ecosystems.

In order to test this, we first examined if there is variation of otolith microchemistry among the *ecoregions* and *mangrove sites* in these large ecosystems. Then, we tested for evidence of genetic structuring in Galápagos' populations (using microsatellite DNA), and if the conclusions observed with otolith microchemistry (i.e., ecological time scale) and microsatellite DNA (i.e., evolutionary time scale) analysis were complementary. After validating the matching between otolith microchemistry and genetic analysis for Galápagos snappers, we assessed the role of the mangroves and adjacent coastal sites (natal origins) as source or sink of individuals and estimated the genetic structure at the mangrove/ecoregion level. For the Gulf of California snappers, by using self-assignment rates obtained from the otolith microchemistry analysis, we

predicted the population structure of snappers (similarly to the population structure based on genetic analysis performed for the Galápagos snappers) and compared these results with a previous study describing the population structure of adults from rocky reefs. In addition, we also examine the use of elements in otoliths as potential indicators of exposure to environmental conditions and processes (e.g., freshwater, salinity, primary productivity, hydrothermal activity) experienced by the juveniles. Unveiling major environmental processes can contribute to the understanding of the unique scenarios of population structure described in this study, from ecological to evolutionary time scales.

To the best of our knowledge, this is the first-time genetic markers and otolith microchemistry are used in concert to assess the population structure and connectivity patterns of a tropical marine species at its northern and southern limits of distribution (Avigliano and Volpedo 2016). We expect that the elucidation of connectivity patterns of yellow snappers from the Galápagos and the Gulf of California will help to optimize the location, size and spacing of marine protected areas (MPAs) in each of these large ecosystems, in order to achieve long-term sustainability of their fish populations.

Materials and Methods

Study site

The Gulf of California (~ 28° N, 112° W) is a semi-enclosed sea in the northern Eastern Tropical Pacific, located between the 1200-km-long Baja California Peninsula to the west and the mainland Mexican states of Sonora and Sinaloa to the east. The Gulf of California has one of the highest environmental extremes among the semi-enclosed seas (Moser et al. 1974, Álvarez-Borrego 1983), with a variability of up to 20°C between February and August, and a high

primary productivity that supports nearly half of Mexico's fisheries production in weight (Cisneros-Mata 2010) due to coastal and tide-driven upwelling events (Lluch-Cota 2000). The Galápagos Archipelago is approximately 4,000 km south of the Gulf of California and ~ 1000 km west of the Ecuadorian coast, at the confluence of three major oceanographic currents: The Equatorial Undercurrent (cold/ nutrient rich/ Western side), a branch of the Peruvian Current (cold/ nutrient-rich/ Southern islands) and the Panama Current (warm/ nutrient poor/ Northern islands). This oceanographic setting creates hydrogeographic and biogeographic regions (Harris 1969, Edgar et al. 2004) where regional differences in SST can exceed 5 - 8°C and primary productivity may vary 10-fold (Wellington et al. 2001, Ruttenberg et al. 2005). Upwelling is more persistent in the West side of the archipelago, while the Northern is influenced by the Panama current, and the Eastern and Southern regions are more influenced by the Peruvian Current.

The Gulf of California and the Galápagos Archipelago offer an interesting comparison since both regions have the interaction of different currents and upwelling events, are home to marine hotspots of biodiversity, and share many common fish species in their mangroves (at least 10 co-occurring species) despite their large geographic separation (~ 4,000 km apart). Although they are hotspots of biodiversity, both the Gulf of California and the Galápagos Archipelago are currently facing severe environmental problems such as fisheries overexploitation (Schiller et al. 2015, Sala et al. 2004), species invasions (Toral-Granda et al. 2017), and strong El Niño events (Robinson and Del Pino 1985, Guilderson and Schrag 1998, Vargas et al. 2006). Furthermore, mangroves in these regions may be particularly vulnerable to climate change, as they are relatively shallow and semi-closed systems, so warmer waters with

long residence times may pose a threat to the physiology of the early life stages of many marine species.

Model species

Yellow snapper *Lutjanus argentiventris* occurs from southern California to Peru, including the Galápagos and Cocos Islands (Allen 1985). The population of yellow snappers in the Gulf of California (Mexico) is probably not connected with the populations of yellow snappers in Galápagos (Ecuador) for single generation events due to their large distance apart (~ 4,000 km), (Palumbi 2003). However, by analyzing this species at its northern and southern limits of distribution, we can better understand of how the population structures of snappers are linked with the landscape configuration and to the environmental conditions in each of these large ecosystems. Since the fishery in both areas has signs of overexploitation (Ruttenberg 2001, Piñón et al. 2009), unveiling the population structure of snappers in these large ecosystems can provide baseline information needed to the maintenance of their populations in the long-term.

Otolith microchemistry analysis - preparation and elemental composition

Juvenile yellow snappers were collected using push nets and small spear guns. In the Gulf of California, 188 juveniles (2.21 to 15.9 cm of total length, TL) were collected inside three ecoregions (Northern, Central, and Southern), encompassing 10 mangrove sites, during four sampling events in June and October 2003 and June and October 2004 (**Figure 3.1a**). In the Galápagos Archipelago, 100 juveniles (2.8 cm to 24 cm TL) were obtained from four ecoregions (Northern, Western, Eastern and Southern), covering 20 mangroves sites during a research expedition in April of 2015 (**Figure 3.1b**, **Table 3.S1**).

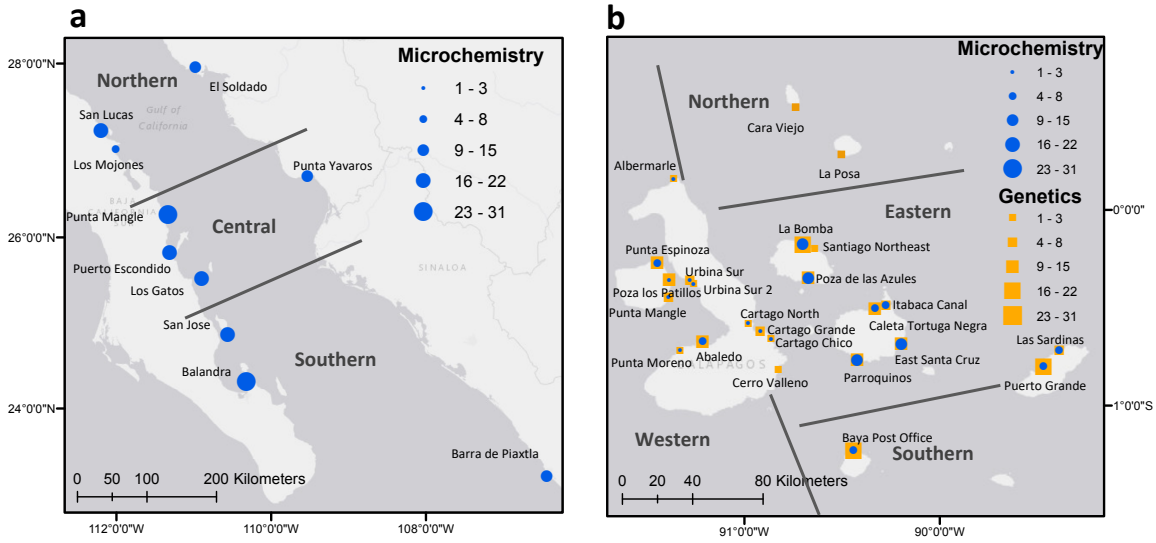

Figure 3.1. Mangrove collection sites for yellow snapper in (a) the Northern, Central and Southern ecoregions of the Gulf of California (n = 174), and in (b) the Western, Eastern, Southern and Northern ecoregions of Galápagos (n = 195). The size of blue circles and orange squares is proportional to the number of juveniles analyzed for otolith microchemistry and microsatellite DNA analysis, respectively.

The preparation of otolith sections and the quantification of minor and trace elements by LA-ICPMS followed the methodology stated in Cavole el at. (2020). Concisely, we collected data on 10 analytes: lithium (^{7}Li), magnesium (^{24}Mg), calcium (^{43}Ca), manganese (^{55}Mn), copper (^{65}Cu), rubidium (^{85}Rb), strontium (^{86}Sr), barium (^{138}Ba), zinc (^{66}Zn) and lead (^{208}Pb). The trace elements were ratioed to Ca (Me/Ca), where the Me represents a metallic element and was converted to molar ratios based on measurements of NIST 612 standard glass (Kent and Ungerer, 2006). Elemental ratios are presented in mmol mol^{-1} (Sr, Mg and Mn) or μmol mol^{-1} (Li, Cu, Zn, Rb, Ba and Pb). The coefficient of variation (CV) of carbonate standards MACS-1 and MACS-3 (United States Geological Survey) (n = 62) and the mean percent relative standard deviations

(%RSD) of multiple NIST 612 standards (n = 43) were used to evaluate accuracy and precision (**Table 3.S2**).

Otolith microchemistry - Spatial division

We examined patterns of elemental signatures at the mangrove site resolution (1 km^2 scale) and at the larger spatial scale of ecoregions (10-100 km^2 scale) using Linear Discriminant Analysis (LDA). The ecoregion separation was based on the sea surface temperature (SST) and primary productivity (chlorophyll *a)* gradients among distinct hydrographic regions (**Figure 3.2**), similarly to the ecoregion division stated in Harris (1969). The classification matrices generated with the LDAs at each life stage (embryos, larvae and juveniles) were posteriorly used to obtain the connectivity network among mangrove sites.

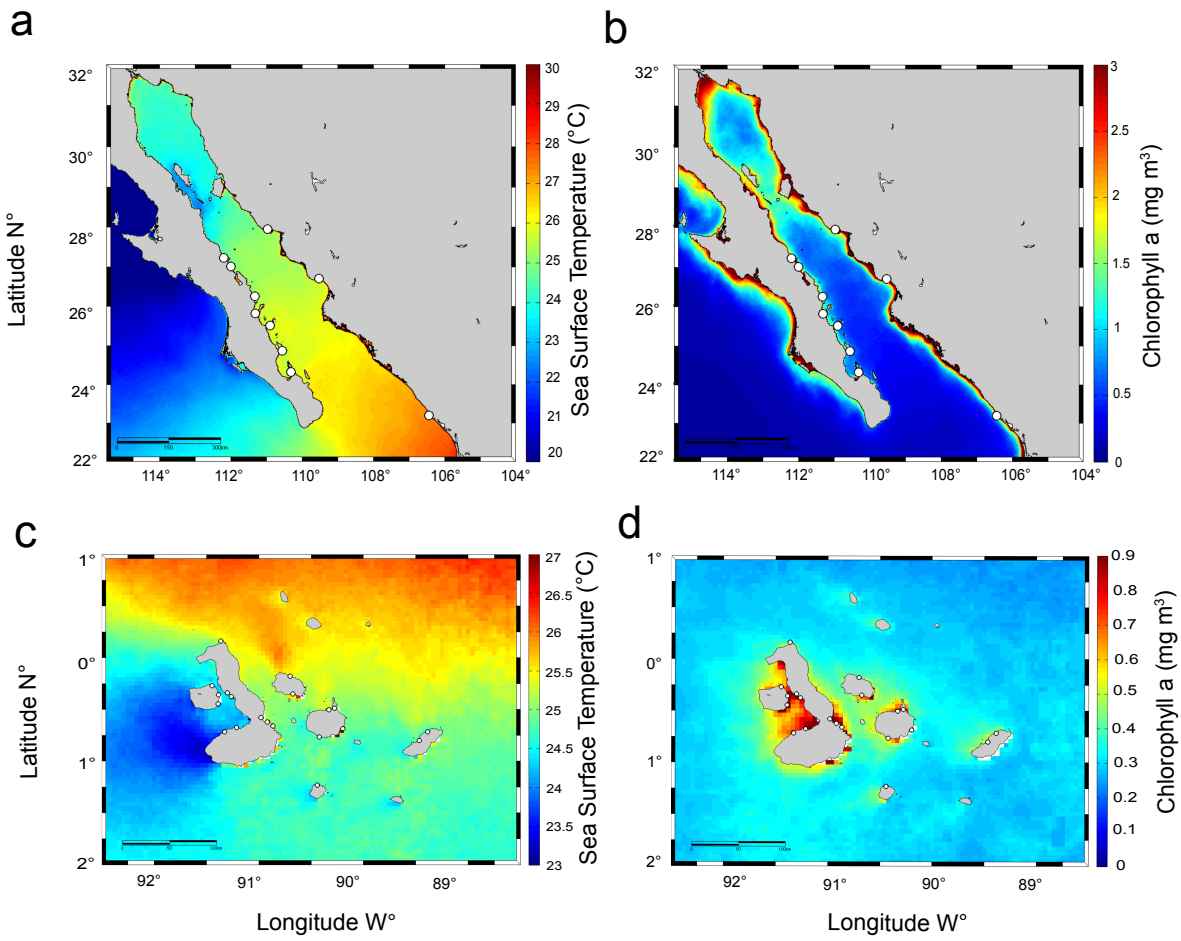

Figure 3.2. Average sea surface temperature (°C) and chlorophyll *a* (mg m^{-3}): (a-b) between October 2002 and October 2004 in the Gulf of California, and (c-d) between April 2014 and April 2015 in the Galápagos Archipelago, based on monthly averages. This time interval covers the fish lifetime used in the present study. White dots are all the mangrove sites where snappers were collected.

To determine how different environmental conditions and processes might affect otolith elemental signatures, we also compared the otolith microchemistry among the Islands in the Galápagos Archipelago (Isabela East, Isabela North, Fernandina, Isabela West, Santa Cruz, Santiago, San Cristóbal and Floreana) and the sub regions of Peninsula and Mainland for the Gulf of California. For Galápagos, the island division was based on the different times of geological formation for each island, which affects their erosion processes and bedrock

composition. For the Gulf of California, this division was based on the lack of rivers on the Peninsula side, whilst some rivers occur in the Mainland – and this is likely to affect the quantification of elements since freshwater input and proximity to the coastline is known to affect otolith microchemistry (Gillanders 2005)

Otolith microchemistry - Trace elemental composition at each life stage

We averaged the elemental ratios at three life stages – embryo, larval and juvenile -in order to understand how natal origins (embryo), dispersal area (larval) and mangrove nursery residence (juvenile) signatures compare among themselves and elucidate the overall population structure for this species. For the Lutjanidae family, it is assumed that some species have relatively small home range sizes (< 8 km^2) (Farmer and Ault 2011) and are composed of local populations, but the extent to which their larvae can disperse or remain close to nursery sites (such as mangroves or estuaries) is unexplored for *L. argentiventris* and can be revealed by analyzing the chemical signatures corresponding to the larval stage, for example.

In order to calculate the average elemental ratio at each previous life stage of the juveniles, we used the relationship between the total length of the fish (TL, cm) and the ablated length in each otolith (AL, μm) (**Figure 3.S1**). The AL was a straight line from the core to the edge of the otolith (**Figure 3.S2a**). The relationship between TL and AL was linear (TL= (AL+1.81)/0.0091, $R^2 = 0.90$ for The Gulf of California, and TL= (AL + 1.18)/0.0074, $R^2 = 0.90$ for Galápagos) (**Figure 3.S1**). The regression slope was significantly different between ecosystems ($p < 0.05$), implying differences in age and/or growth rates among fish groups (Gulf of California *vs*. Galápagos). Using the relationships between fish TL and otolith AL (**Figure 3.S1**), we calculated the average of Me:Ca (μmol mol^{-1} or mmol mol^{-1}) for each AL transect

across the otolith that corresponded to a specific range of TL in the fish (**Figure 3.S2b**) (Cavole et al., 2020). For the embryonic stage, we integrated the elemental signal in the core of the otolith that corresponded to ~ between 0 and 3 mm of the fish TL (**Figure 3.S2b**). Subgroup ranges of TL were based on a previously classification of juvenile size classes (Aburto-Oropeza et al. 2009), in which larvae were < 2 cm TL, settlers between 2 and 4 cm TL, post-settlers between 4 and 10 cm TL, and immatures between 10 and 20 cm TL. The juvenile stage used hereafter integrates the elemental composition between post-settlers to immatures, when the fish was residing in mangrove waters (**Figure 3.S2b**).

Otolith microchemistry classification

We tested for overall variation in elemental ratios between the Galápagos Archipelago and the Gulf of California ecosystems, and among the ecoregions and mangrove sites in each of these large ecosystems using a one-way MANOVA. We used Pillai's trace as the test statistic, because it is robust to deviations from multivariate normality (Quinn and Keough 2002). One-way ANOVA comparisons were used to test for differences in single elemental ratios (Me:Ca) at the ecosystem level (Galápagos Archipelago *vs*. Gulf of California), and also at the ecoregions and mangrove site level for the Gulf of California and Galápagos. For the MANOVA tests, we only included mangrove sites with more than five fish in our analysis. To determine if there was a linear correlation between our multiple continuous variables (Me:Ca), we built scatterplot matrices (**Figure 3.S3**).

For elemental ratios that were significantly different among ecoregions or mangroves sites, we performed a linear discriminant analysis (LDA) to test if there was sufficient variation in elemental ratios to identify the ecoregions or the mangrove sites from which fish were

collected. We performed this analysis at the embryonic (i.e., where individuals were spawned), larval (i.e., when individuals are pelagic in the open ocean environment) and juvenile stages (i.e., when individuals reside in mangrove lagoons), (**Figure 3.3** shows results only for the juvenile stage). For the LDA at the ecoregion level, we included all the fish. For the LDA at the mangrove level, we only included those mangrove sites with more than five fish.

The LDA builds linear discriminant axes of elemental ratios, maximizing the standard deviation between groups while minimizing it within groups (Fisher 1936). Because Galápagos fishes were not evenly distributed among mangrove sites, we set an equal number of samples as an *a priori* information for grouping into the LDA model, in order to correct for unequal sample sizes. The ability to accurately classify individuals based on their ecoregions or mangrove sites of origin was based on the otoliths Me:Ca average data. A jackknife classification matrix was determined for each LDA to indicate the percentage of fish correctly identified to the ecoregions/mangrove site from which they were collected. We used the classification matrix obtained from the microchemistry analysis at the mangroves level for embryos, larvae and juveniles (**Table 3.S4 - 3.S6**) to explore their metapopulation structure in the Galápagos and the Gulf of California. Individuals that were not assigned to the mangrove where they were sampled were identified as migrants and represented in a spatial network using the mangrove sites as nodes and the migrant individuals as directed edges employing the software GEPHI 0.8.2 beta (Bastian et al. 2009). We used GEPHI to calculate in-degree (number of incoming connections), out-degree (number of outgoing connections), degree (total number of connections), and eigenvector centrality, which is a measure of the importance of a node (i.e., mangrove site) as a hub or stepping-stone in the network.

For comparison of elemental ratios between Galápagos and the Mainland and Peninsula sides of the Gulf of California, we calculated the average of Me:Ca (μmol mol^{-1} or mmol mol^{-1}) for the following life stages: larvae (L), settler (S), post-settler (PS) and immature migratory (I) (**Figure 3.4**). The average values for each island of Galápagos are also presented in order to understand the differences in elemental composition observed in this archipelago (**Table 3.S3**). Data were $\log_{10}$ transformed to improve multivariate normality and met the normality assumption. All analyses were conducted on transformed data and performed using the R version 3.4.0 (2017).

Genetic Analyses – Sample preparation for Galápagos samples

We collected tissue samples from 195 yellow snappers from 23 mangrove sites distributed in eight different islands in Galápagos across four main ecoregions (Northern, Southern, Eastern and Western) (**Figure 3.1b, Supplementary Table 3.S1**). Of the 195 juvenile snappers used for genetic analysis, 88 were also used for otolith microchemistry analysis, to allow comparison between these two techniques. We extracted DNA with the Blood and Tissue DNeasy Kit (QIAGEN) and conducted Polymerase Chain Reactions (PCRs) to amplify 12 unlinked polymorphic microsatellite loci. From these loci, five dinucleotide loci (*Larg1*, *Larg4*, *Larg5*, *Larg11*, *Larg19*) and one trinucleotide locus (*Larg27*) were isolated *de-novo* from the species in a previous study (Reguera-Rouzaud et al. 2020), and three tetranucleotide loci (*Lupe01*, *Lupe29*, *Lupe34*) and three dinucleotide loci (*Lupe39*, *Lupe55* and *Lupe62*) were cross-amplified from the related species *L. peru* (Paz-García et al. 2017). To allow fluorescent labeling, we added the universal M13 primer at the 5´ end of all forward primers (Schuelke 2000). We conducted PCRs in 15μL volumes with 40 ng genomic DNA, 1× PCR buffer, 0.2 mM

each dNTP, 1.5 mM $MgCl_2$, 0.2% BSA, 0.5 U *Taq* DNA polymerase (Apex, Bioresearch Products), 0.02μM of the unlabeled M13-tailed forward primer, and 0.2 μM of the fluorescently labeled M13 primer, and 0.2 μM of the reverse primer. We applied a PCR touchdown protocol consisting of 94 °C for 5 min, 15 cycles of 94 °C for 30 s, 65–50 °C for 30 s (1 °C decrease each cycle), 72 °C for 30 s, followed by 40 cycles at 94 °C for 30 s, 55 °C for 30 s, 72 °C for 30 s, and a final extension of 72 °C for 5 min. We genotyped PCR products using an Applied Biosystems' 3730XL sequencer. We scored alleles using GENEMAKER Version 2.6.0 (SoftGenetics LLC), and assigned bins to allele sizes using FLEXIBIN (Amos et al. 2007).

Genetic differentiation and geographic barriers - Galápagos

We calculated observed and expected heterozygosity, number of alleles, allele frequencies, tested for deviations for Hardy-Weinberg equilibrium (HWE) for each locus within each population and performed analyses of molecular variance (AMOVA) among ecoregions using the software GENALEX 6.5 (Peakall and Smouse 2012). We estimated F_{ST} values between pairs of islands with the software GENODIVE 2.0b25 (Meirmans and Van Tienderen 2004). Since F_{ST} values likely decreases as the within-population heterozygosity increases (Meirmans and Hedrick 2011), we calculated an index of genetic differentiation D (Jost 2008) that is not affected by within-population diversity. The significance of pairwise F_{ST} values was assessed with an AMOVA test and 1000 permutations in GENODIVE. We used the software Alleles in Space (Miller 2005) to search for the spatial location of the five most important barriers to gene flow in the area of study with the implementation of the Monmonier's maximum difference algorithm, employing the GPS coordinates of each sample.

First-generation migrants and relatedness – Galápagos

To search for evidence of recent gene flow and explore the role of each mangrove/coastal adjacent site as a source or sink of larvae, we identified first-generation migrants in Galápagos using a Bayesian assignment (Rannala and Mountain 1997) implemented in the software GENECLASS2 (Piry et al. 2004). For each individual, we assessed the likelihood ratio L-home/L-max using Monte Carlo resampling (Paetkau et al. 2004) and simulating 10,000 individuals. Individuals with a probability ≤ 0.01 of belonging to the population where they were sampled were identified as migrants. First-generation migrants were represented in a spatial network using the mangrove/coastal sites as nodes and the migrant individuals as directed edges employing the software GEPHI and we calculated in-degree, out-degree, degree and eigenvector centrality. We compared the agreement in the spatial networks of migrant individuals from both microchemistry (based on the misclassified individuals obtained from the classification matrices of embryos, juveniles and larvae) and genetics via a linear regression analysis of the eigenvector centrality and the node degree values of each mangrove site. The eigenvector centrality measures the "connectedness" and influence of a mangrove site (node) within a network. High score nodes are connected to highly connected nodes and low score nodes are connected to poorly connected nodes (Bonacich and Lloyd, 2001). The node degree is the number of in-coming and out-going edges connected to each mangrove (node), and thus, it measures the number of other mangroves a particular site is connected to, either by export or import of individuals.

We used GENALEX to estimate pairwise individual relatedness values (Queller and Goodnight 1989), which has been proposed as a proxy for levels of local larval retention (Munguia-Vega et al. 2018). For each population, we calculated average pairwise values and

tested for statistical significance for deviations under a scenario of random mating within each population with 1000 permutations and 1000 bootstraps to estimate 95% C.I.

Metapopulation structure scenarios - Galápagos

We tested the statistical support of three different scenarios of metapopulation structure to explain the observed distribution of microsatellite allele frequency data with the software MIGRATE-N (Beerli and Palczewski 2010): 1) all the samples belong to a single population with one population size (panmixia); 2) each of 10 sampled populations show bidirectional migration rates with all other populations (full model with 10 population sizes and 90 migration rates between each pair of sites), 3) a model following the results of the assignment of individuals to mangrove sites based on the microchemistry results (**Table 3.S4**, **Figure 3.3**), including 10 population sizes and 40 directional migration rates. We used a Bayesian inference, a mutation model with Brownian movement, 1,000,000 steps of which 25% was discarded as burn-in, one long and four short chains with static warming, uniform prior and an exchange of trees of 10. To choose the model best supported by the observed data, we used the marginal probability ratios (Bayes factors) following a Bezier approximation.

After identifying the most probable model, we used the distribution of posterior probabilities for the effective size scaled by mutation rate Θ ($4N_e\mu$) and migration scaled by mutation rate M ($m\mu$) to estimate the number of migrants per generation (N_m), as $Nm = \Theta \times M/4$, where Θ corresponds to the recipient population (Beerli 2009). Based on the results of the most likely scenario of metapopulation structure, we estimated in-degree and out-degree for each site. Finally, we estimated the role of each site as either source or sink by subtracting the total N_m received by each site (N_m in) from the total N_m that each site exported (N_m out). Sites with

positive values were considered as sources (net exporters), whereas those with negative values were identified as sinks (net importers).

Results

Otolith microchemistry – Large ecosystem spatial scale

We quantified trace element signatures using otoliths from 262 yellow snapper (*Lutjanus argentiventris*) juveniles inhabiting mangrove forests from two regions of the ETP; the Gulf of California and the Galápagos Archipelago (**Table 3.S1**).

At the ecosystem level, the elemental ratios between the juveniles of the Galápagos and the Gulf of California were significantly different (MANOVA, Pillai's trace = 0.9466, $F = 19.70$, $p < 0.001$). The differences were mainly driven by six elemental ratios (Ba:Ca, Cu:Ca, Li:Ca, Mn:Ca, Rb:Ca, Sr:Ca and Zn:Ca), with Ba:Ca (Univariate ANOVA, $F = 80.10$, $p < 0.001$) and Li:Ca (Univariate ANOVA, $F = 79.01$, $p < 0.001$) contributing most to the differences observed (**Table 3.1**).

Otolith microchemistry patterns - Gulf of California ecoregions and mangroves

At the ecoregion level, the elemental ratios among the Gulf of California's Northern, Central and Southern ecoregions were significantly different (MANOVA, Pillai's trace = 0.6993, $F = 9.79$, $p < 0.001$). All juvenile elemental ratios, with the exception of Mg:Ca, were significantly different among the Gulf's Northern, Central and Southern ecoregions (Univariate ANOVAs, **Table 3.2**).

At the mangrove site level, we also observed significant differences for all elemental ratios together (MANOVA, Pillai's trace = 3.4203, F = 11.17, $p < 0.001$) and individually (Univariate ANOVAs, **Table 3.2**).

Otolith microchemistry patterns - Galápagos ecoregions and mangroves

At the ecoregion level, the elemental ratios among Galápagos' Western, Eastern and Southern ecoregions were not significantly different (MANOVA, Pillai's trace = 0.3534, F= 1.5026, $p = 0.0994$). However, when looking at individual elemental ratios at the juvenile stage, we observed that four elemental ratios were significantly different among ecoregions (Ba:Ca, Mg:Ca, Sr:Ca, and Li:Ca) (Univariate ANOVAs, **Table 3.2**).

At the mangrove site spatial scale, all elemental ratios together were significantly different (MANOVA, Pillai's trace = 1.5291, F= 1.4327, $p < 0.05$), with four elemental ratios contributing most to this pattern (Ba:Ca, Mg:Ca, Sr:Ca, and Li:Ca) (Univariate ANOVAs, **Table 3.2**). We used those elements that were significantly different in the LDA analyses.

Ecoregion's fingerprint

The elemental ratios were relatively useful for discriminating ecoregions among the juveniles. The percentage separation achieved by the first discriminant function was 66.22% for the Gulf of California (LDA, **Figure 3.3a**) and 93.5% for the Galápagos Archipelago fishes (LDA, **Figure 3.3c**). We were able to successfully reclassify 64% of the juveniles to their respective ecoregions from the Gulf of California and 57% of the juveniles to their respective ecoregions from the Galápagos archipelago (Jackknife reclassification success rates, **Table 3.S4**). Juvenile fishes were separated into Northern, Central and Southern Ecoregions for the

Gulf of California and into Western, Eastern, and Southern Ecoregions for the Galápagos Archipelago.

Mangrove fingerprints

The juveniles from the Gulf of California showed a high discriminatory power at the mangrove site resolution, with a percentage separation achieved by the first discriminant function of 88.2% (LDA, **Figure 3.3b**). The assignment success rates were much higher for the Gulf of California (90%), compared to the Galápagos Archipelago (23%) (Jackknife reclassification success rates, **Figure 3.3b-d**, **Table 3.S4**).

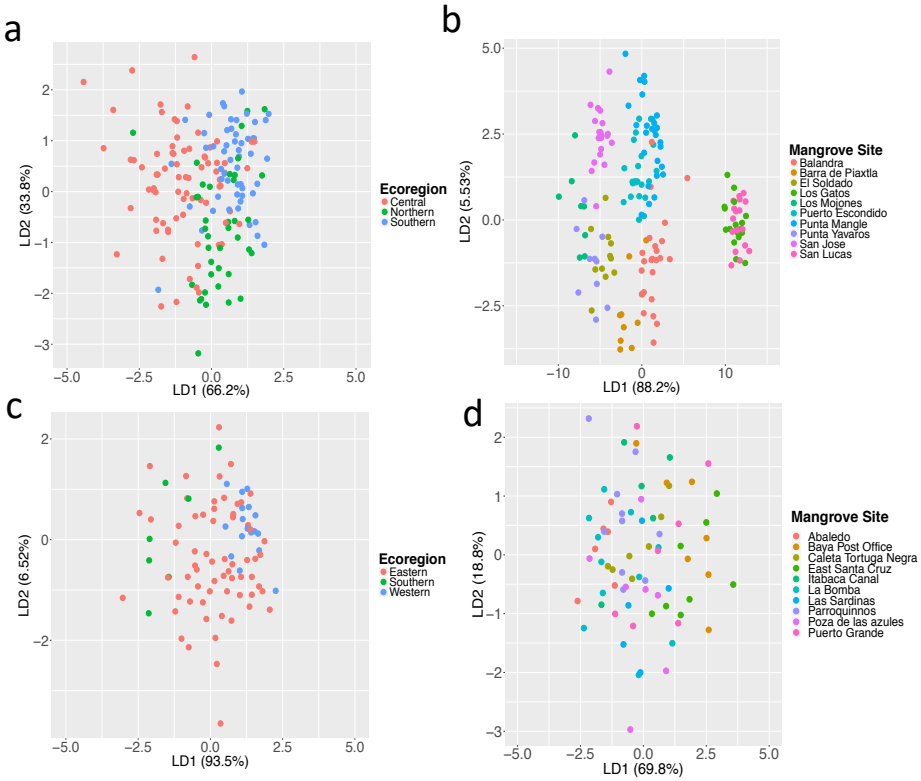

Figure 3.3. Linear Discriminant Analysis of juvenile otoliths. Each point represents a single otolith. (a) Gulf of California Ecoregions, using Li:Ca, Mn:Ca, Cu:Ca, Rb:Ca, Sr:Ca, Ba:Ca, Zn:Ca and Pb:Ca (n = 174). (b) Gulf of California Mangrove Sites, using Li:Ca, Mn:Ca, Cu:Ca, Rb:Ca, Sr:Ca, Ba:Ca, Zn:Ca and Pb:Ca (n = 174). (c) Galápagos Archipelago ecoregions, using Ba:Ca, Mg:Ca, Sr:Ca and Li:Ca (n = 88). (d) Galápagos Archipelago Mangroves Sites, using Ba:Ca, Mg:Ca, Sr:Ca and Li:Ca (n = 73).

Elemental ratios across the fish life stages

There were distinct elemental patterns in the otoliths of yellow snapper juveniles among the Galápagos Archipelago, and the peninsula and mainland sides of the Gulf of California (**Figure 3.4**).

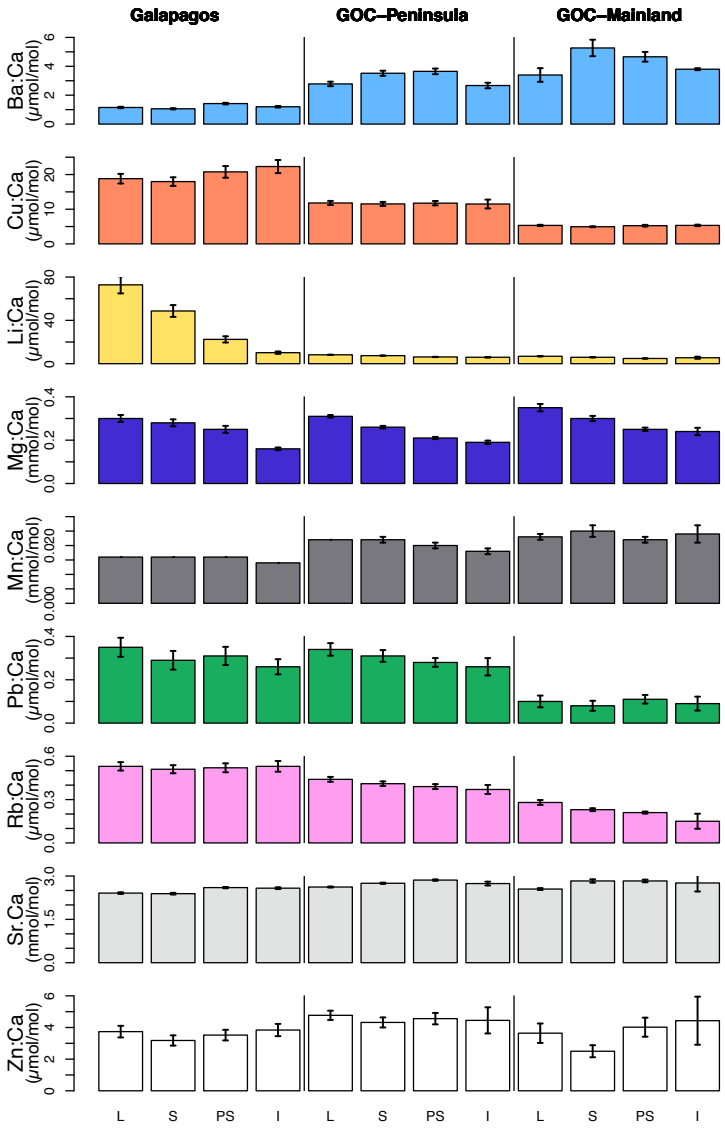

Figure 3.4. Average ± SE of element to calcium ratios for each size class. Larvae (L) < 2cm of TL, settler (S): 2 - 4 cm of TL, post-settler (PS): 4 -10 cm of TL, and immature migratory (I): 10-20 cm of TL in *Lutjanus argentiventris* from the Galápagos (GA), the Gulf of California (GOC) – Peninsula, and the Gulf of California (GOC) – Mainland.

Ba:Ca

Mean Ba: Ca overall ratios were significantly higher for the fishes in the Gulf of California mangroves ($p < 0.001$, $F= 80.10$) (**Table 3.1**). Mean Ba:Ca for each life stage (larvae, settler, post-settler and immature) were higher for the Gulf of California Mainland (Ba_{larvae} = 3.40 μmol mol^{-1} to $Ba_{settler}$ = 5.27 μmol mol^{-1}) and lower for the Galápagos Archipelago ($Ba_{settler}$ = 1.13 μmol mol^{-1} to Ba_{larvae} = 1.15 μmol mol^{-1}) (**Figure 3.4**). Ba:Ca ratios were higher and more variable for the juveniles from the Gulf of California mangroves (**Figure 3.5a**).

Cu:Ca, Li:Ca, Rb:Ca

The average ratios for Cu:Ca, Li:Ca, Rb:Ca were higher for the Galápagos Archipelago at each life stage ($Cu_{immature}$ = 22.31 μmol mol^{-1}, Li_{larvae} = 72.77 μmol mol^{-1}, Rb_{larvae} = 0.53 μmol mol^{-1}), (**Figure 3.4**) and for its mangroves (**Table 3.1**, **Figure 3.5b-d**) in comparison with the Gulf. Lithium averages and variability were much higher for the fishes in the Galápagos mangroves and presented an opposite pattern to Barium (**Figure 3.5a-b**). Lithium and Barium were negatively correlated (R^2 = -0.61) (**Figure 3.S3**). Copper and Rubidium averages presented a similar pattern between the Gulf of California and Galápagos (**Figure 3.4**, **Figure 3.5c-d**) and were positively correlated (R^2 = 0.94) (**Figure 3.S3**).

Mn:Ca, Sr:Ca

The overall ratios of Mn:Ca and Sr:Ca were significantly higher for the fishes in the Gulf of California (**Table 3.1**). Mn:Ca average ratios per life stage presented lower values for the Galápagos Archipelago (Mn_{larvae} = 0.016 mmol mol^{-1} to $Mn_{immature}$ = 0.014 mmol mol^{-1}) than the Gulf of California - Mainland (Mn_{larvae} = 0.023 mmol mol^{-1} to $Mn_{immature}$ = 0.024 mmol mol^{-1})

(**Figure 3.4**, **Figure 3.5e**). Strontium presented higher values for the Gulf of California (Sr_{larvae} = 2.55 mmol mol^{-1} to $Sr_{post\text{-}settler}$ = 2.86 mmol mol^{-1}) than Galápagos ($Sr_{settler}$ = 2.39 mmol mol^{-1} to $Sr_{post\text{-}settler}$ = 2.60 mmol mol^{-1}) (**Figure 3.4**, **Figure 3.5f**). Manganese and Strontium averages per each life stage presented a similar pattern between the Gulf of California and Galápagos (**Figure 3.4**) and were positively correlated (R^2 = 0.37) (**Figure 3.S3**)

Pb:Ca, Mg:Ca, Zn:Ca

Pb:Ca and Mg:Ca average ratios per life stage presented similar values for the Galápagos ($Pb_{immature}$ = 0.26 μmol mol^{-1} to $Pb_{post\text{-}settler}$ = 0.36 μmol mol^{-1}; $Mg_{immature}$ = 0.16 mmol mol^{-1} to Mg_{larvae} = 0.30 mmol mol^{-1}) and Gulf of California – Peninsula ($Pb_{immature}$ = 0.26 μmol mol^{-1} to $Pb_{post\text{-}settler}$ = 0.34 μmol mol^{-1}; $Mg_{immature}$ = 0.19 mmol mol^{-1} to Mg_{larvae} = 0.31 mmol mol^{-1}) (**Figure 3.4**). Pb:Ca, Mg:Ca and Zn:Ca ratios were not significantly different between the fishes from the Gulf of California and Galápagos mangroves (**Table 3.1**, **Figure 3.5g-**i). Zinc had the higher values for the Gulf of California – Peninsula ($Zn_{post\text{-}settler}$ = 4.77 μmol mol^{-1} to $Zn_{immature}$ = 7.97 μmol mol^{-1}) (**Figure 3.4**).

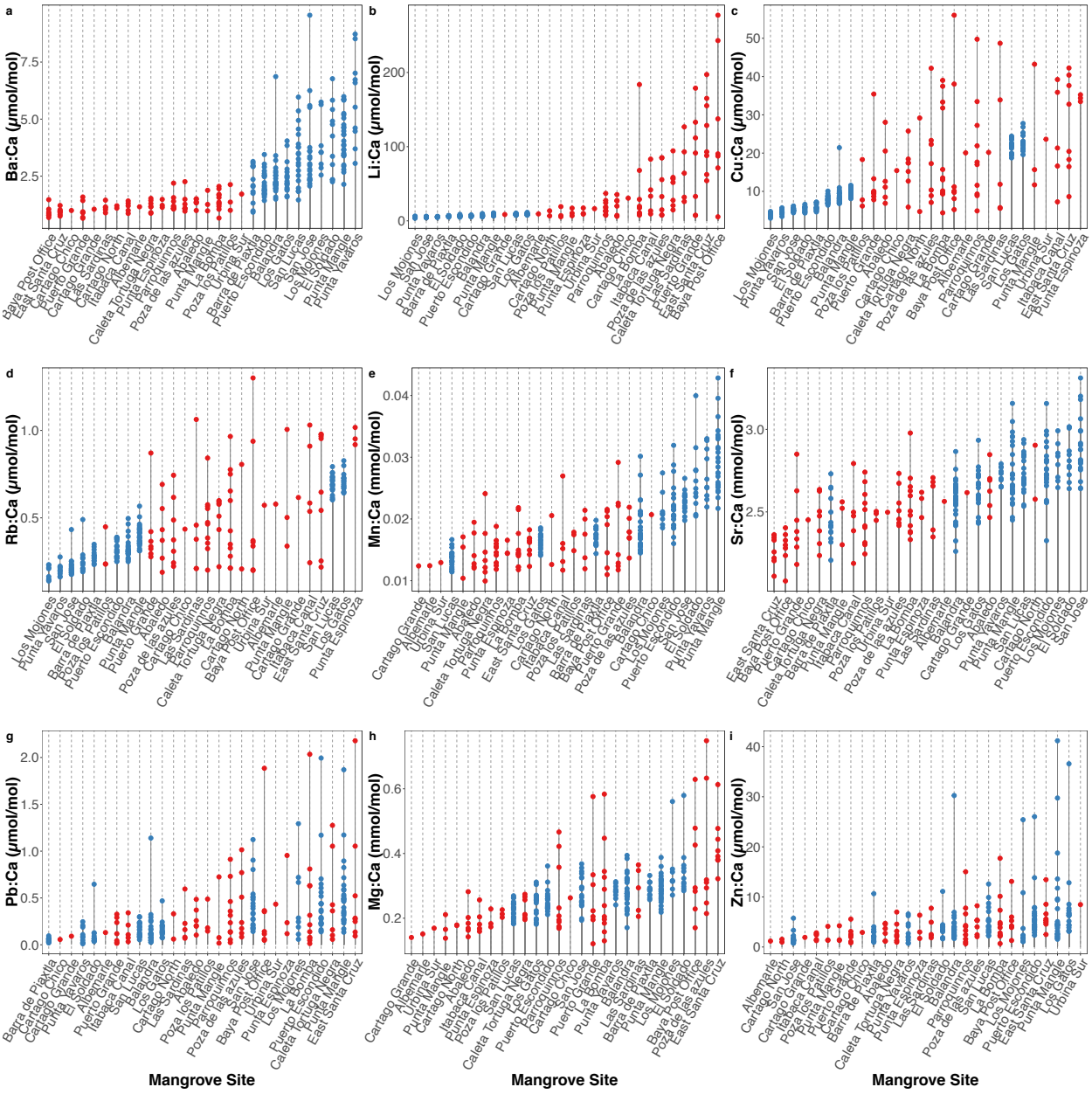

Figure 3.5. Dot plot of average elemental ratios in each juvenile of *Lutjanus argentiventris* from different mangrove sites in the Galápagos (red dots) and the Gulf of California (blue).

Genetic analyses – Galápagos Archipelago

We found high levels of genetic variation among 195 samples that were successfully genotyped from Galápagos islands, with an average of 9.6 observed alleles, 5.6 effective alleles, and mean observed and expected heterozygosities of 0.661 and 0.677, respectively (**Table 3.3**).

The highest allelic diversity was found at Santa Cruz Island (6.3 effective alleles) and the lowest at the East of Isabela island (4.7 effective alleles). The largest frequency of private alleles (alleles that are unique to a single population) was found in Santa Cruz Island (1.0) followed by Santiago Island (0.75), while the lowest was observed in the East of Isabela Island (0). From 84 tests of Hardy-Weinberg equilibrium (HWE) conducted in seven islands with a sample size of 18 individuals or larger, we found only 3 instances of statistically significant deviations of HWE after the Bonferroni correction for multiple tests (adjusted P value = 0.0005). Missing data averaged 1.75% per loci and only 0.21% per individual.

We found low but significant levels of genetic structure among four recognized ecoregions of the Galápagos Islands that were sampled (AMOVA test, Global F_{ST} = 0.006, P = 0.003, **Table 3.4**). The F_{ST} values among pairs of ecoregions ranged from - 0.001 (Southern vs. Western) to 0.025 (North vs. Eastern, **Table 3.5**). However, the sample size for the Northern ecoregion was considerably smaller (n=5), and thus F_{ST} values are likely biased. Beyond the comparisons with the Northern ecoregion, significant differences in allele frequencies were detected between the Western and the Eastern ecoregions (F_{ST} = 0.003, P = 0.041, **Table 3.5**).

We detected the presence of the most important genetic barrier along the north-south axis of Isabela Island that also separates the Western and Eastern ecoregions (Monmonier's algorithm, **Figure 3.6**). The second most important barrier isolated the Pinta and Marchena islands that belong to the Northern ecoregion from the rest. The third and fourth barriers identified were located south of Fernandina island, while the fifth barrier was placed around the south of Santa Cruz island. The F_{ST} values calculated between islands confirmed the largest levels of genetic differentiation were found between Fernandina and all other islands (F_{ST} ranged from 0.002 to 0.014, **Table 3.6**), in particular between Fernandina and San Cristóbal (F_{ST} = 0.014) and also

between Floreana and the East of Isabela island (F_{ST} = 0.004) and between the West and East coasts of Isabela Island (F_{ST} = 0.008), (**Table 3.6**).

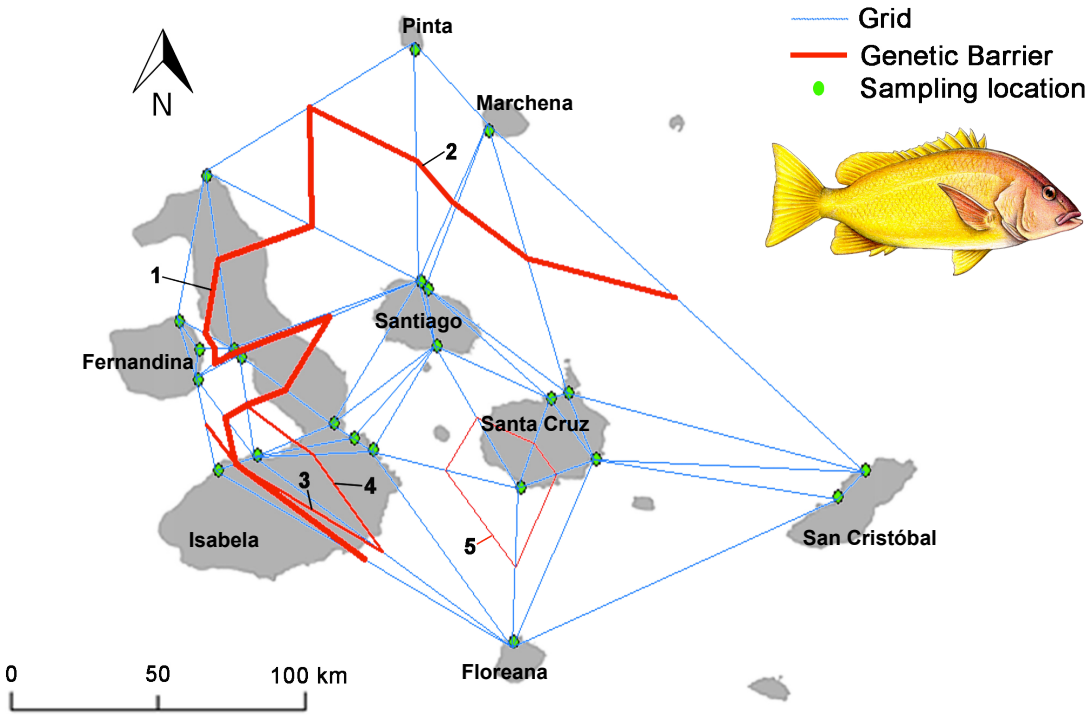

Figure 3.6. The five most important barriers to gene flow among sampled locations identified by Monmonier's maximum difference algorithm. Barriers are labeled 1-5 and their weight reflects their importance.

Based on the otolith microchemistry of juveniles, the jackknife reclassification success rates were higher for the Gulf of California (90%) than the Galápagos Archipelago (23%) (**Table 3.S4**, **Figure 3.3a-d**). Consequently, the genetic analyses identified 17 individuals as migrants among mangroves in the Gulf of California (10% of the total) and 55 individuals as migrants at Galápagos (75.3% of the total) (**Figure 3.7b, d**), where migrants are defines as individuals not assigned to their mangrove of origin. The analysis of first-generation migrants in Galápagos

identified 32 individuals (16.4% from the total of individuals genotyped) that met our threshold probability ($P < 0.01$) (**Figure 3.7e**). Based on the analysis of first-generation migrants, the most important source of larvae identified (7 migrants) was the north of Santiago Island (La Bomba), followed by the north of Floreana Island (Baya Post Office) with 5 migrants exported (Network Genetics: **Table 3.S8**). The analysis of average pairwise genetic relatedness within islands, a proxy for the presence of local larval retention, showed relatedness was higher than expected under random mating at the East of Isabela Island and in San Cristóbal Island (**Figure 3.S4**, $P < 0.05$) and between Itabaca Canal and Puerto Grande mangroves (**Figure 3.S5**, $P < 0.05$).

When we restricted the comparison of the network of first-generation migrants (genetics) to the same 10 mangrove sites analyzed for the microchemistry network derived from the assignment of individuals (**Table 3.S8**), we found a significant correlation between the eigenvector centrality of each site as estimated by both methods, particularly at the juvenile stage ($R^2 = 0.69$, $P = 0.002$) (**Figure 3.S6c**). When we compare the number of connections to each mangrove site (node degree) using both techniques, we observed a higher correlation at the larval stage ($R^2 = 0.55$, $P = 0.0136$), (**Figure 3.**).

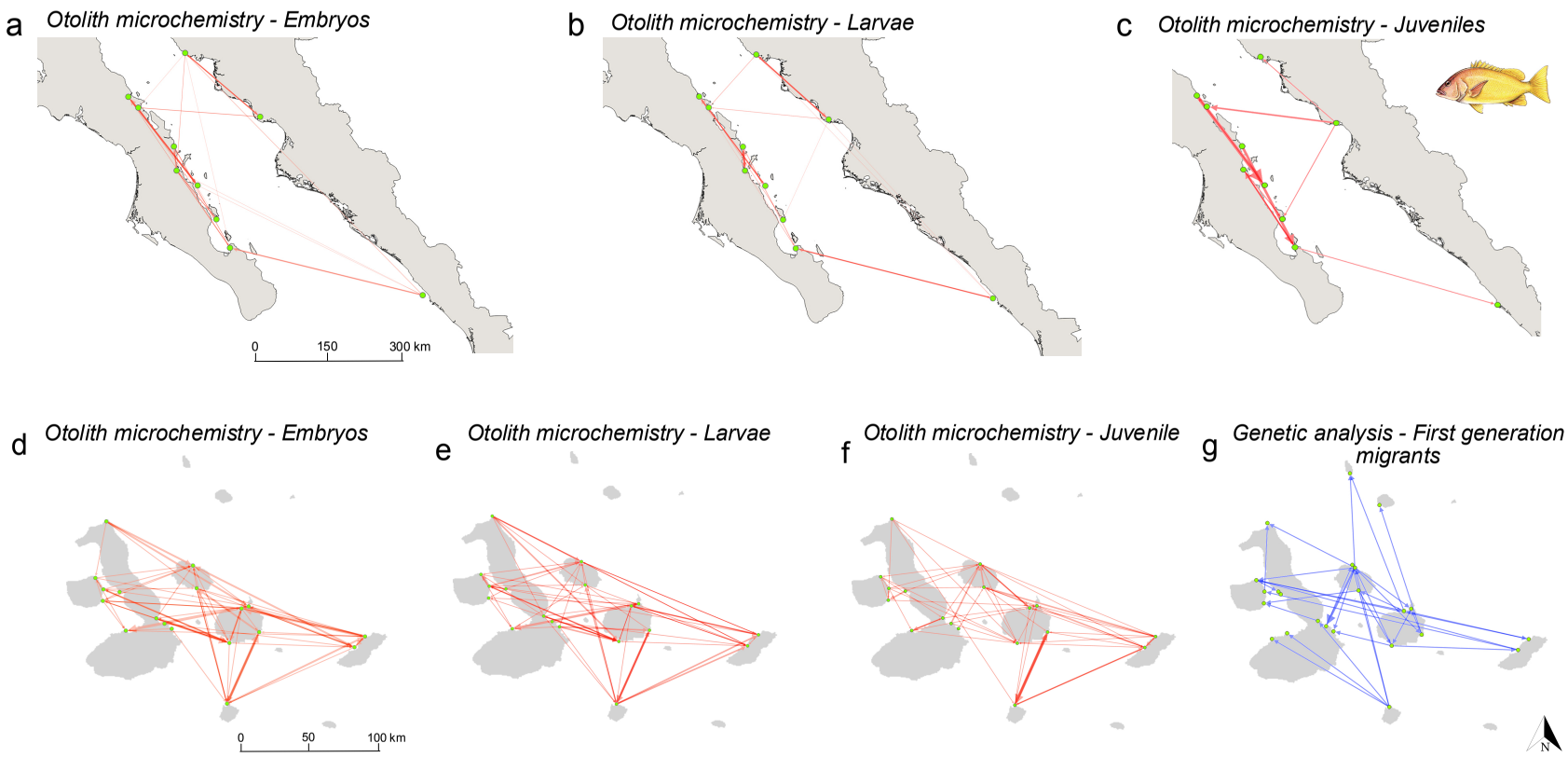

Figure 3.7. Networks showing the direction of larval dispersal events. Networks based on otolith microchemistry assignment of (a) embryos, (b) larvae and (c) juveniles from the Gulf of California, and (d) embryos, (e) larvae and (f) juveniles from the Galápagos. Networks based on (g) genetic analysis of first-generation migrants for the Galápagos. On the genetic network, each link (blue arrow) represents one individual identified as migrant, while on the microchemistry network (red arrow) the thin lines represent one individual, and the bold lines represent up to four individuals.

Metapopulation structure scenarios for yellow snappers in Galápagos

According to the Bayes factors, the most likely underlying metapopulation structure model to explain the empirical genetic data was model 3 (Microchemistry, **Table 3.7**), while the least ranked model was Panmixia. Based on estimates of Θ, M, and Nm for the best-supported model, Parroquinos mangrove (Santa Cruz Island) was the most important source in terms of number of juveniles exported, followed by Itabaca Canal mangrove (Santa Cruz Island), (i.e., Nm out – Nm in), (**Table 3.S9**). Las Sardinas (San Cristóbal Island) and Itabaca Canal (Santa Cruz Island) were important sources of juveniles in terms of number of sites (six) to which individuals were exported to (i.e., Out-degree). Caleta Tortuga Negra (Santa Cruz Island), East Santa Cruz and La Bomba (Santiago Island) were the only net sinks (i.e., Nm out – Nm in), while La Bomba and Parroquinos each received individuals from at least six other sites (i.e., In-degree), (**Table 3.S9**).

Discussion

Otolith microchemistry as proxies for environmental processes

The significant differences in the concentration of 6 elemental ratios (Ba:Ca, Cu:Ca, Li:Ca, Sr:Ca, Mn:Ca, Rb:Ca) between the otoliths of juveniles collected in the Gulf of California and Galápagos were likely due to the presence of different oceanographic processes and geological landscapes between these two regions.

Barium. Ba is a common proxy to identify freshwater occupancy due to a commonly observed relationship of increasing ambient and otolith Ba:Ca with decreasing salinity (Bath et al. 2000, Elsdon and Gillanders, 2005, Walther and Thorrold, 2006) and is also associated with upwelled waters (Kingsford et al. 2009, Grammer et al. 2017). The increasing Ba:Ca ratios

among the Galápagos Archipelago, the Gulf of California Peninsula, and the Gulf of California Mainland follows the natural freshwater gradient observed in these regions (**Table 3.1**, **Figure 3.4, Figure 3.5**). The low Ba:Ca averages found in Galápagos match with the little freshwater accumulation in this archipelago because its basaltic terrain is impermeable and there is low precipitation and high evaporation rates across all islands (d'Ozouville et al. 2008). The freshwater ecosystems are mainly restricted to the most densely populated island of Santa Cruz and are composed of swamps, semi-permanent surface ponds and streams, open coastal fractures known as *grietas* and coastal-back beach lagoons for brackish ones. In contrast, the high Ba:Ca averages found in the Gulf of California – Mainland (**Figure 3.4**) may be due the presence of large rivers such as Sonora, Yaqui and Fuente, and higher precipitation rates on this side of the Gulf than on the Peninsula side (Roden 1958). Upwelled waters also typically leave distinct elemental signatures in otoliths due to differences in water chemistry and associated links to primary productivity (Kingsford et al. 2009). The juveniles from the Gulf of California had Ba:Ca ratios three times higher than the juveniles from Galápagos, potentially associated to differences on Chlorophyll-*a* (mg m^{-3}). For example, the Mainland of the Gulf of California had average Chlorophyll-*a* values up to ten times higher than those found for the western ecoregion of Galápagos Archipelago, which is the most productive region in this archipelago (**Figure 3.2b-d**, **Figure 3.5a**, **Table 3.S7**).

Copper and Lead. High concentration of Pb and Cu in seawater or estuaries usually indicate coastal runoff or anthropogenic pollutants (Geffen et al. 1998, Halden and Friedrich 2008), and airborne sources (Boyle et al. 1977, Chester et al. 1993). We observed decreasing ratios of Cu from the Galápagos Archipelago to the Gulf of California Peninsula and the Gulf of California Mainland (**Figure 3.4**). The pattern observed in our fish otoliths does not seem to be

associated with the size of human population in these places as both Galápagos and the Gulf of California are not densely populated. In Galápagos, the average Cu:Ca ratios measured in otoliths (Cu:Ca = 19.50 μmol mol^{-1}) were higher than the range of those values reported for otoliths in the Mediterranean and North Atlantic (0.34-16.6 μg g^{-1}, converted here in the same unit for comparison; 0.21 – 10.46 μmol mol^{-1}) (Chang and Geffen 2013), and suggest that its terrain may be naturally enriched in this element. In the Gulf of California - Peninsula, copper deposits are abundant and sustain large mining production in this region (Wilson and Rocha 1955), and anomalous high concentrations were previously found in marine sediments due to intense mining activities close to the ocean shore (Shumilin et al. 2000, Rodríguez-Figueroa et al. 2009). Considering this, the relative high concentration of these elements in the water may be the result of sporadic enriched inflows from the adjacent coastal terrain. Since we do not have the water chemistry for our sites, we are unable to establish a direct relationship between the mining activities and the concentration of these elements in the otoliths from the Gulf of California.

Lithium and Rubidium. Hydrothermal activity along mid-oceanic ridges is the main source of Li and Rb in seawater (Edmond et al. 1979) and is also associated with the input of relatively high levels of other trace elements, included Zn, Cu and Pb (Honnorez 1983). For example, on the crest of Galápagos spreading ridge, the fluxes of Lithium and Rubidium exceed the river input balance by factors of between five and ten (Edmond et al. 1979, Honnorez, 1983). Swan et al. (2003) suggests that the higher concentrations of Li, Rb, Cu and Pb in areas with hydrothermal activity can lead to detectable concentrations of those trace elements in otoliths. It is possible that some of our fish were residing in more Li-enriched waters during their egg and larval development and then, as they move progressively toward the coastal mangroves, this

element reduces its concentration (**Figure 3.5**). The Li:Ca ratio values for the Galápagos ($Li_{average}$ = 59.43 ± 39.21 μmol mol^{-1}) (**Table 3.1**) is around double the upper limit value found in the literature review made by Chang and Geffen (2013) (0.01 - 4.6 μg g^{-1}, converted here in the same unit for comparison; 0.05 - 26.55 μmol mol^{-1}). For Galápagos, water samples collected one year later from the same mangroves where our fish were sampled had an average value of 260 ppm for lithium, which is higher than the average global concentration of lithium in seawater (180 ppm), showing that this Archipelago is naturally enriched in such element. Besides the water concentration, negative temperature effects of Li:Ca incorporation into calcite and aragonite have been observed experimentally in some foraminifera, brachiopods, and corals (Delaney et al. 1985, Marriott et al. 2004) and may help to explain why the southernmost Floreana Island (exposed to the Peruvian cold-current) presented the highest values for this element (130.31 ± 97.32 μmol mol^{-1}), followed by San Cristóbal (74.96 ± 55.20 μmol mol^{-1}) and Santa Cruz Island (53.93 μmol ± 50.64 mol^{-1}) (**Table 3.S3**).

Strontium. Sr concentrations in water are related to salinity concentrations (Bath et al. 2000) and regional variations in geology (Walther and Thorrold 2006), making it a potent element for classifying regional patterns of fish populations. The significantly higher concentration of Sr in the Gulf of California was likely associated with the higher salinity of this sea in comparison with the Galápagos Archipelago (**Table 3.1**). The Gulf of California is characterized by a positive salinity anomaly due higher evaporation rates compared to the precipitation rates and the current lack of freshwater inflow from the Colorado River. The annual mean of salinity decreases from 35.26 ± 0.01 at the head to 34.75 ± 0.01 at the mouth (Berón-Vera and Ripa 2002), matching the Sr:Ca found in the otoliths; higher for the Northern areas ($Sr_{average}$ = 2.78 ± 0.13 mmol mol^{-1}) than the Central ($Sr_{average}$ = 2.72 ± 0.16 mmol mol^{-1}) and

Southern Regions ($Sr_{average}$ = 2.66 ± 0.23 mol mol^{-1}) (**Table 3.S3**). In the Galápagos archipelago, the maximum sea surface salinity (34.9) is usually found in the west of Isabela Island (Liu et al. 2014), where our otoliths also presented higher Sr:Ca ratios than the eastern islands (**Table 3.S3**).

Manganese. Mn:Ca is elevated in otoliths of cod inhabiting hypoxic waters of the Baltic sea (Limburg et al. 2011, 2015) because the Mn is released from sediments during low redox conditions. The Gulf of California mangroves presented higher Mn concentrations ($Mn_{average}$ = 0.021 ± 0.005 mmol mol^{-1}) than the Galápagos archipelago ($Mn_{average}$ = 0.016 ± 0.001 mmol mol^{-1}) (**Table 3.1**). Mn:Ca > 0.03 mmol mol^{-1} values were just found for the juveniles inside the Gulf of California mangroves (6 mangroves out of 10), probably associated with more hypoxic conditions and longer water residence in those sites. In the Gulf of California, Aburto-Oropeza et al. (2009) observed that mangrove forests associated with lagoons might remain closed by sand bars during several winter-spring months, leading to anoxic conditions. The mangrove sites with the highest manganese values in otoliths were in the Gulf of California-Mainland, suggesting that the larger rivers in this system may be associated with episodic hypoxic conditions inside those mangroves (**Figure 3.5e**). In addition, these mangroves are the only ones close to agriculture, aquaculture and industrial activities, suggesting anthropogenic eutrophication influences the oxygen levels in those sites.

In all biological systems there are underlying physical and biological mechanisms that are ultimately responsible for the quantity of a particular trace element that is incorporated into the aragonite matrix of an otolith (Kinsman and Holland 1969). Some trace elements found in the snapper otoliths were particularly interesting and might be useful environmental proxies, such as Li:Ca for hydrothermal activity in Galápagos (Edmond et al. 1979), Ba:Ca for freshwater and

upwelling occupancy and Mn:Ca for hypoxic conditions in the Gulf of California Mainland. The Li:Ca ratios found for the yellow snapper larval stages ($Li_{average}$ = 80 μmol mol^{-1}) in Galápagos were the highest ever reported in marine fish otoliths. This opens an exciting line of research, suggesting the impact of deep-sea processes in the marine life accumulation of trace elements in shallower waters. Interestingly, both Li:Ca and Ba:Ca literature supports the idea that these elements are environmentally influenced (Grammer et al. 2017). Future research may shed light on how other oceanographic and anthropogenic processes (e.g., upwelling and coastal human activities) might affect the traceability of chemical signatures in the otoliths, therefore future water samples from the same site and time of fish collections will be indispensable.

Population structure of yellow snappers across mangrove and ecoregional spatial scales – combining otolith microchemistry and genetic analysis

Places with large gradients in temperature and primary productivity can generate differences in the elemental composition of otoliths, such as the ones observed here for the yellow snappers from the Galápagos (GA) and the Gulf of California (GOC) ecosystems. The LDA reclassified the otoliths to an ecoregion level (~60%) for the Gulf of California and the Galápagos Archipelago, implying that the otolith chemical signatures vary over large ecoregional scales (> 100 km). Ecoregions in both ecosystems are defined by distinct oceanographic features that translate into characteristic temperatures, productivity, biotas, etc., and our results corroborate that larval dispersal of juvenile fish within ecoregions is greater than exchange among ecoregions.

The results in the assignment of individuals as locals or migrants based on otolith microchemistry or genetic fingerprints need to be evaluated in light of the magnitude of

differences among mangrove site fingerprints, where the larger the differences among sites, the greater the power of our analyses to identify migrant or self-recruited individuals. Also, otolith chemistry provides information over ecological time frames (i.e., fish lifespan), while genetic analyses are based on changes in allele frequencies (e.g., Fst, AMOVA, genetic barrier identification, migration rates) and provide information on gene flow over multiple generations (i.e., evolutionary time scales).

The classification accuracy of our juveniles at the mangrove sites based on otolith microchemistry was higher for the Gulf of California (90%), likely driven by a larger spatial scale of sampling (~ 1000 km) and the presence of a stronger gradient in environmental factors that explains larger differences in the elemental fingerprints among mangroves. The unique elemental fingerprint among GOC mangrove sites seems related to the high heterogeneity in seawater temperature (**Figure 3.2a**, **Table 3.S7**), chlorophyll *a* (proxy for primary productivity) (**Figure 3.2b**, **Table 3.S7**), and potentially the water chemistry among these sites. In the Gulf of California, the shallow and semi-enclosed bays show greater variations than the open Gulf and the trace elements in water may vary substantially due to the processes of heating, cooling, mixing, evaporation, precipitation, runoff and biological activities. For example, the range of SST observed for our Gulf of California mangrove sites was up to 18 °C (for the northernmost mangrove site "El Soldado" at the Mainland coast) between October 2002 and October 2004, which encompass the time span the juveniles lived in (**Table 3.S7**).

Based on otolith microchemistry, our results suggest that about 10% of the yellow snapper juveniles from the GOC are migrants from other mangrove sites, which implies that most local populations within mangroves might be self-sufficient. This result is in line with a recent study showing evidence of high levels of local larval retention for this species, as inferred

from high levels of relatedness at mangroves in the Central Gulf of California (Reguera-Rouzaud et al. 2020). For the Gulf of California, the migration events inferred from the otolith classification matrices (**Table 3.S4**, **Figure 3.7b**) matched the pattern expected for the transport of larvae by oceanic currents during the reproductive period of the species. Yellow snappers in the central GOC spawn during spring-summer (Aburto-Oropeza et al. 2009, Erisman et al. 2010) when an anti-cyclonic eddy transports larva northward on the eastern (mainland) coast and southward on the western (Peninsula) coast (Munguia-Vega et al. 2018). Notably, the large differences in elemental fingerprints and high power to resolve migrant individuals (embryos, larvae and juveniles) among mangroves in the GOC contrast with very low levels of population genetic structure and a metapopulation structure with a source-sink dynamics according to microsatellite analyses of late juveniles and adult populations from rocky reefs in the Gulf of California (Reguera-Rozaud et al. 2020), where individuals from multiple mangroves (and their genes) might mix at a single rocky reef. Similar contrasting results were observed for the migratory fish *Prochilodus mariae*, where genetic analysis suggested that their populations had high levels of connectivity, whereas otolith microchemistry suggested the presence of different breeding sites (Collins et al. 2013).

For the Galápagos Archipelago, the variation in otolith elemental signatures among the western, eastern and southern ecoregions was slightly less consistent. This is in line with observations made by Ruttenberg et al. (2006), who demonstrated relatively poor discrimination in otolith elemental signatures for the damselfish (*Stegastes beebei*) over spatial scales of 100 to 150 km. Galápagos also has a smaller gradient in water temperature and primary productivity than the Gulf (**Table 3.S7**). The otolith fingerprint in Galápagos fishes were more homogeneous among the mangroves, probably reflecting the high mixing rates in the region over a smaller

geographical scale, driven by the constant convergence of water masses and oceanographic currents in the middle of the archipelago (Harris 1969, Wellington et al. 2001). For example, the Equatorial Undercurrent (EUC) subdivides itself into northern and southern branches, leading to local upwelling throughout the archipelago and a complicated pattern of internal eddies that allows for horizontal interchange and mixing of water masses (Pak and Zaneveld 1973, Houvenaghel 1978), which might homogenize the water chemistry over the entire archipelago, hence diluting consistent spatial differences. Galápagos snapper juveniles lived within the mangroves between April 2014 and April 2015, where the observed range of SST was up to 7 °C and the chlorophyll *a* values were around 10 times lower than the average values found for the Gulf of California (**Table 3.S7**). The largest genetic differences found between Western and Eastern ecoregions (**Table 3.5**) were supported both by the analyses of genetic barriers (**Figure 3.6**) and the proportion of assigned individuals based on microchemistry among ecoregions at the juvenile stage (**Table 3.S4, Figure 3.3**). Here, genetic data clearly identified significant differences among ecoregions, and the analysis of genetic barriers recovered almost the exact boundaries of the recognized ecoregions **(Figure 3.6**), suggesting population genetic analyses of juvenile fish might show high power to detect population structure, compared to analyses of adult fish after they have recruited to their habitats in rocky reefs (Reguera-Rouzaud et al. 2020).

The elemental fingerprint of GA snappers suggested that about 75% of the juveniles were migrants from other mangrove sites, a proportion much larger than the estimates for the GOC, but consistent with the smaller spatial scale and higher levels of larval exchange in GA. Interestingly, the metapopulation structure model that best explained the population genetic data was precisely the migration model inferred from the microchemistry assignments (**Table 3.7**), further supporting the presence of a source-sink metapopulation structure with high levels of

connectivity in GA mangroves, particularly within the Eastern ecoregion. This result also suggests that both microchemistry and population genetics might be influenced by related oceanographic processes that operate on similar temporal and spatial scales at the Galápagos archipelago.

The yellow snappers in Galápagos exhibited low, but significant differences for allele frequencies among ecoregions (**Table 3.5**). These results are not unexpected since marine species are often characterized by high gene flow that leads to weak genetic structure (Bradbury et al. 2008) and genetic approaches are sensitive to extremely low rates of exchange (Thorrold et al. 2001). For example, Muss et al. (2001) contrasted the genetic signatures of blennies between the Atlantic and eastern Pacific oceans and observed a reduced genetic structure in the eastern Pacific population likely due to the unstable circulation and dynamic oceanography and geology of this large ocean basin. Alongside these findings, the local oceanography in Galápagos Archipelago involves the convergence of different currents that would allow higher connectivity patterns among the snapper populations, especially in the Eastern ecoregion, as Isabela Island behaves as a geographic barrier.

At the island spatial level, juveniles sampled in Fernandina Island (**Table 3.6**) showed the most distinct genetic patterns. Juveniles at Fernandina Island also exhibited the highest concentration of copper and rubidium and lowest concentration of lithium in their otoliths. This distinctiveness in the microsatellite DNA and otolith microchemistry data might be associated to a combination of factors; this island is the youngest and most volcanically active in the Archipelago and is also located at the coldest and most productive waters in the archipelago.

At the mangrove site spatial level, the metapopulation role of each mangrove site was correlated between the genetics and microchemistry results, especially at the juvenile stage

(**Figure 3.7**; **Figure 3.S6**). Larvae can travel over greater distances in open waters, compared to juveniles that have settled and resided inside mangroves, so they are likely to be exposed to a wide range of chemical variation in the water, hence diluting any spatial pattern. In summary, it seems that the metapopulation structure based on the juvenile stages is well aligned with the local oceanography and landscape configuration at both the GOC and GA ecosystems.

Conclusions

In summary, this work showed the complementarity of otolith microchemistry and genetic methods to elucidate the population structure of yellow snapper across large ecosystems, ecoregions and mangrove sites – and, therefore, these approaches in combination are potentially useful for management at such spatial scales. For example, the finer spatial structure of juveniles from the GOC mangroves (e.g., juvenile reclassification rates to mangrove sites of up to 90% based on otolith microchemistry) might allow the estimation of the most important nurseries for the adult stock, ultimately helping with the implementation of marine protected areas. The restricted connectivity of GOC snappers compared to GA snappers suggest that they are more vulnerable to local depletion where fishing effort is concentrated. Therefore, the evidence for self-recruitment population structure in the GOC should be factored into fishing exploitation strategies to prevent local depletion of this species. For the Galápagos archipelago, the high connectivity of yellow snappers among mangroves and fish migration rates suggests that effects on a single juvenile population might have effects cascading into adjacent areas. Accordingly, the evidence of a source-sink metapopulation structure for GA snappers should leverage the inclusion of its mangrove sites into a network of Marine Protected Areas. This study also suggests that the inference of metapopulation structure in fish may differ based on the life stage

considered (embryo, larval, juvenile and adult). The use of complementary approaches, such as otolith microchemistry and microsatellite DNA, when tested at various life stages of a species of interest, can advance the understanding of fish species with complex population dynamics and residence in different habitats, with the ultimate goal of maintaining the sustainability of their populations.

Acknowledgements

We are grateful to the Charles Darwin Foundation and the Galápagos National Park Directorate for the institutional support during this study. We are grateful to the crews of the vessels El Primo, Pirata and Queen Mabel for their assistance during field work in Galápagos. We thank Joy Kumagai for the map assistance and Andy Ungerer at the Oregon State University W. M. Keck Collaboratory for Plasma Spectrometry for assistance with otolith analysis. We thank Comunidad y Biodiversidad A.C. for support in obtaining permits for importing genetic samples, and Sociedad de Historia Natural Niparaja A.C. for providing access to the illustration of the yellow snapper adult fish. This research was supported by a grant from the Helmsley Charitable Trust to PSL and OAO. LMC was supported by CNPq grant 213540/2014-2. AFJ was supported by NSF grant DEB-1632648 (2017/18). The research presented in this manuscript was conducted under permits PC-13-14, and PC-13-15 provided by the Galapagos National Park Directorate. This publication is contribution number 2299 of the Charles Darwin Foundation for the Galapagos Islands.

Chapter 3, in part, is being prepared for submission of the material. Cavole L.M., Munguia-Vega A., Miller J.A., Salinas-de-Léon P., Jarrin J.R.M., Johnson A.F., Rastoin-Laplane

E., Girón-Nava A., Aburto-Oropeza O. The dissertation author was the primary investigator and author of this material.

Literature Cited

Amos, W., J. I. Hoffman, A. Frodsham, L. Zhang, S. Best, and A. V. S. Hill. 2007. Automated binning of microsatellite alleles: problems and solutions. Molecular Ecology Notes 7:10-14.

Aburto-Oropeza, O., E. Ezcurra, G. Danemann, V. Valdez, J. Murray, and E. Sala. 2008. Mangroves in the Gulf of California increase fishery yields. Proceedings of the National Academy of Sciences 105:10456-10459.

Aburto-Oropeza, O., I. Dominguez-Guerrero, J. Cota-Nieto, and T. Plomozo-Lugo. 2009. Recruitment and ontogenetic habitat shifts of the yellow snapper (*Lutjanus argentiventris*) in the Gulf of California. Marine biology 156:2461-2472.

Allen, G. R. 1985. FAO species catalogue. Vol. 6. Snappers of the world. An annotated and illustrated catalogue of lutjanid species known to date. FAO Fish. Synopses 125:60–61.

Álvarez-Borrego, S. 1983. Gulf of California. Ecosystems of the World 26:427-449.

Avigliano, E., and A. V. Volpedo. 2016. A review of the application of otolith microchemistry toward the study of Latin American fishes. Reviews in Fisheries Science & Aquaculture 24:369-384.

Bath, G. E., S. R. Thorrold, C. M. Jones, S. E. Campana, J. W. McLaren, and J. W. Lam. 2000. Strontium and barium uptake in aragonitic otoliths of marine fish. Geochimica et cosmochimica acta 64:1705-1714.

Bastian, M., S. Heymann, and M. Jacomy, M. 2009. Gephi: an open source software for exploring and manipulating networks. International AAAI Conference on Weblogs and Social Media 8:361-362.

Beerli P. 2009. How to use migrate o why are markov chain Monte Carlo programs di cult to use? In: Bertorelle G, Bruford MW, Hau e HC, Rizzoli A, Vernesi C (eds) Population genetics for animal conservation. Cambridge University Press, Cambridge, pp 42–79.

Beerli, P., and M. Palczewski. 2010. Unified framework to evaluate panmixia and migration direction among multiple sampling locations. Genetics 185:313-326.

Berón-Vera, F. J., and P. Ripa. 2002. Seasonal salinity balance in the Gulf of California. Journal of Geophysical Research: Oceans 107:15-1.

Boyle, E. A., F. R. Sclater, and J. M. Edmond. 1977. The distribution of dissolved copper in the Pacific. Earth and planetary science letters 37:38-54.

Bradbury, I.R., S. E. Campana, and P. Bentzen. 2008. Estimating contemporary early life-history dispersal in an estuarine fish: integrating molecular and otolith elemental approaches. Molecular Ecology 17:1438-1450.

Bradbury, I. R., L. C. Hamilton, M. J. Robertson, C. E. Bourgeois, A. Mansour and J. B. Dempson. 2014. Landscape structure and climatic variation determine Atlantic salmon genetic connectivity in the Northwest Atlantic. Canadian Journal of Fisheries and Aquatic Sciences 71:246-258.

Bonacich, P. and Lloyd, P., 2001. Eigenvector-like measures of centrality for asymmetric relations. Social networks 23:191-201.

Buonaccorsi, V. P., C. A. Kimbrell, E. A. Lynn and R. D. Vetter. 2002. Population structure of copper rockfish (*Sebastes caurinus*) reflects postglacial colonization and contemporary patterns of larval dispersal. Canadian Journal of Fisheries and Aquatic Sciences 59:1374-1384.

Campana, S. E. 1999. Chemistry and composition of fish otoliths: pathways, mechanisms and applications. Marine Ecology Progress Series 188:263-297.

Campana, S. E., and S. R. Thorrold. 2001. Otoliths, increments, and elements: keys to a comprehensive understanding of fish populations? Canadian Journal of Fisheries and Aquatic Sciences 58:30–38.

Cavole, L. M., J. A. Miller, P. Salinas-de-Léon, O. Aburto-Oropeza, J. R. Marin Jarrin, Johnson A. F. 2020. The role of extrinsic variation – cohabiting juvenile fish species exhibit similar otolith elemental signatures. Marine Ecology Progress Series. 646:109-125.

Chang, M. Y., and A. J. Geffen. 2013. Taxonomic and geographic influences on fish otolith microchemistry. Fish and Fisheries 14:458-492.

Chester, R., G. F. Bradshaw, C. J. Ottley, R. M. Harrison, J. L. Merrett, M. R. Preston, A. R. Rendell, M. M. Kane and T. D. Jickells. 1993. The atmospheric distributions of trace metals, trace organics and nitrogen species over the North Sea. Philosophical Transactions of the Royal Society of London. Series A: Physical and Engineering Sciences 343:543-556.

Chittaro, P. M., B. J. Fryer, and P. F. Sale. 2004. Discrimination of French grunts *(Haemulon flavolineatum*, Desmarest, 1823) from mangrove and coral reef habitats using otolith microchemistry. Journal of Experimental Marine Biology and Ecology 308:169-183.

Christie, M. R., D. W. Johnson, C. D. Stallings, and M. A. Hixon. 2010. Self-recruitment and sweepstakes reproduction amid extensive gene flow in a coral-reef fish. Molecular ecology 19:1042-1057.

Cisneros-Mata, M. A. 2010. The importance of fisheries in the Gulf of California and ecosystem-based sustainable co-management for conservation. The Gulf of California: biodiversity and conservation. Arizona-Sonora Desert Museum Studies in Natural History. The University of Arizona Press, Tucson, Arizona, USA, 119-134.

Collins, S. M., N. Bickford, P. B. McIntyre, A. Coulon, A. J. Ulseth, D. C. Taphorn, and A. S. Flecker. 2013. Population structure of a neotropical migratory fish: contrasting perspectives from genetics and otolith microchemistry. Transactions of the American Fisheries Society 142:1192-1201.

Cook, G.S., P.E. Parnell, L.A. Levin. 2014. Population connectivity shifts at high frequency within an open-coast marine protected area network. PloS one 9: p.e103654

Delaney M. L., A. W. H. Bé, and E. A. Boyle. 1985. Li, Sr, Mg, and Na in foraminiferal calcite shells from laboratory culture, sediment traps, and sediment cores. Geochimica et Cosmochimica Acta 49:1327-1341.

d'Ozouville, N., B. Deffontaines, J. Benveniste, U. Wegmüller, S. Violette and G. De Marsily. 2008. DEM generation using ASAR (ENVISAT) for addressing the lack of freshwater ecosystems management, Santa Cruz Island, Galápagos. Remote Sensing of Environment 112:4131-4147.

Edgar, G. J., S. Banks, J. M. Fariña, M. Calvopiña and C. Martínez. 2004. Regional biogeography of shallow reef fish and macro-invertebrate communities in the Galápagos archipelago. Journal of Biogeography 31:1107-1124.

Edmond, J. M., C. Measures, R. E. McDuff, L. H. Chan, R. Collier, B. Grant, L. I. Gordon and J. B. Corliss. 1979. Ridge crest hydrothermal activity and the balances of the major and minor elements in the ocean: the Galápagos data. Earth and Planetary Science Letters 46:1-18.

Elsdon, T. S., and B. M. Gillanders. 2005. Alternative life-history patterns of estuarine fish: barium in otoliths elucidates freshwater residency. Canadian Journal of Fisheries and Aquatic Sciences 62:1143-1152.

Erisman, B., I. Mascarenas, G. Paredes, Y. S. de Mitcheson, O. Aburto-Oropeza, and P. Hastings. 2010. Seasonal, annual, and long-term trends in commercial fisheries for aggregating reef fishes in the Gulf of California, Mexico. Fisheries Research 106:279-288.

Farmer, N.A. and J. S. Ault. 2011. Grouper and snapper movements and habitat use in Dry Tortugas, Florida. Marine Ecology Progress Series 433:169-184.

Feyrer, F., J. Hobbs, M. Baerwald, T. Sommer, Q. Z. Yin, K. Clark, B. May, and W. Bennett. 2007. Otolith microchemistry provides information complementary to microsatellite DNA for a migratory fish. Transactions of the American Fisheries Society 136:469-476.

Fierro-Arcos, D., Marín Jarrín, J. R., Aburto-Oropeza, O., Harvey, E. S., Rastoin-Laplane, E., Salinas-de-Léon, P. 2021. Mangrove fish assemblages reflect the environmental diversity of the Galapagos Islands. Marine Ecology Progress Series. *In press*.

Fisher, R. A. 1936. The use of multiple measurements in taxonomic problems. Annals of eugenics 7:179-188.

Fromentin, J. M., B. Ernande, R. Fablet, and H. De Pontual. 2009. Importance and future of individual markers for the ecosystem approach to fisheries. Aquatic Living Resources 22:395-408.

Geffen, A. J., N. J. G. Pearce, and W. T. Perkins. 1998. Metal concentrations in fish otoliths in relation to body composition after laboratory exposure to mercury and lead. Marine Ecology Progress Series 165:235–245.

Gillanders, B. M., K. W. Able, J. A. Brown, D. B. Eggleston, and P. F. Sheridan. 2003. Evidence of connectivity between juvenile and adult habitats for mobile marine fauna: an important component of nurseries. Marine Ecology Progress Series 247:281-295.

Gillanders, B.M. 2005. Otolith chemistry to determine movements of diadromous and freshwater fish. Aquatic Living Resources 18:291-300.

Grammer, G. L., J. R. Morrongiello, C. Izzo, P. J. Hawthorne, J. F. Middleton, and B. M. Gillanders. 2017. Coupling biogeochemical tracers with fish growth reveals physiological and environmental controls on otolith chemistry. Ecological Monographs 87:487-507.

Guilderson, T. P., and D. P. Schrag. 1998. Abrupt shift in subsurface temperatures in the tropical Pacific associated with changes in El Niño. Science 281:240-243.

Halden, N. M., and L. A. Friedrich. 2008. Trace-element distributions in fish otoliths: natural markers of life histories, environmental conditions and exposure to tailings effluence. Mineralogical Magazine 72:593-605.

Harris, M. P. 1969. Breeding seasons of sea-birds in the Galápagos Islands. Journal of Zoology 159:145-165.

Honnorez, J. 1983. Basalt—Seawater Exchange: A Perspective from an Experimental Viewpoint. In *Hydrothermal Processes at Seafloor Spreading Centers* (pp. 169-176). Springer, Boston, MA.

Houvenaghel, G. T. 1978. Oceanographic conditions in the Galápagos Archipelago and their relationships with life on the islands. In *Upwelling ecosystems* (pp. 181-200). Springer, Berlin, Heidelberg.

Jost, L. 2008. G_{st} and its relatives do not measure differentiation. Molecular Ecology 17:4015-4026.

Kent, A. J., and C. A. Ungerer. 2006. Analysis of light lithophile elements (Li, Be, B) by laser ablation ICP-MS: Comparison between magnetic sector and quadrupole ICP-MS. American Mineralogist 91:1401-1411.

Kingsford, M. J., J. M. Hughes and H. M. 2009. Otolith chemistry of the non-dispersing reef fish *Acanthochromis polyacanthus*: cross-shelf patterns from the central Great Barrier Reef. Marine Ecology Progress Series 377:279-288.

Kinsman, D. J., and H. D. Holland. 1969. The co-precipitation of cations with CaCO3—IV. The co-precipitation of Sr^{2+} with aragonite between 16° and 96° C. Geochimica et Cosmochimica Acta 33:1-17.

Kritzer, J. P., & Sale, P. F. (2010). *Marine metapopulations*. Elsevier. Burlington, MA: Academic. 544 pp.

Limburg K. E., C. Olson, Y. Walther, D. Dale, C. P. Slomp C. P., and H. Høie. 2011. Tracking Baltic hypoxia and cod migration over millennia with natural tags. Proceedings of the National Academy of Sciences 108:E177-E182.

Limburg, K. E., B. D. Walther, Z. Lu, G. Jackman, J. Mohan, Y. Walther, A. Nissling, P. K. Weber, and A. K. Schmitt. 2015. In search of the dead zone: use of otoliths for tracking fish exposure to hypoxia. Journal of Marine Systems 141:167-178.

Liu, Y., L. Xie, J. M. Morrison, D. Kamykowski, and W. V. Sweet. 2014. Ocean circulation and water mass characteristics around the Galápagos archipelago simulated by a multiscale nested ocean circulation model. International Journal of Oceanography 2014:1-16.

Llerena, Y., C. Peñaherrera, E. Espinoza, M. Hirschfeld, M. Wolff, and L. R. Vinueza. 2013. Nursery grounds of blacktip sharks (*Carcharhinus limbatus*) in mangrove-fringed bays in the central part of the Galapagos Archipelago. Galapagos Report, 2014:102-110.

Lluch-Cota, S.E., 2000. Coastal upwelling in the eastern Gulf of California. *Oceanologica Acta*, *23*(6), pp.731-740.

Marriott C. S., G. M. Henderson, N. S. Belshaw, and A. W. Tudhope. 2004 Temperature dependence of δ^7 Li, δ^{44}Ca and Li/Ca during growth of calcium carbonate. Earth and Planetary Science Letters 222:615-624.

Martin, G. B., and S. R. Thorrold. 2005. Temperature and salinity effects on magnesium, manganese, and barium incorporation in otoliths of larval and early juvenile spot *Leiostomus xanthurus*. Marine Ecology Progress Series 293:223–232.

Mateo, I., E. G. Durbin, R. S. Appeldoorn, A. J. Adams, F. Juanes, R. Kingsley, P. Swart, and D. Durant. 2010. Role of mangroves as nurseries for French grunt *Haemulon flavolineatum* and schoolmaster *Lutjanus apodus* assessed by otolith elemental fingerprints. Marine Ecology Progress Series 402:197-212.

Meirmans, P.G., and P. W. Hedrick. 2011. Assessing population structure: FST and related measures. Molecular ecology resources 11:5-18.

Meirmans, P.G., and P. H. Van Tienderen. 2004. Genotype and Genodive: two programs for the analysis of genetic diversity of asexual organisms. Molecular Ecology Notes 4:792-794.

Miller, J. A., Banks, M. A., Gomez-Uchida, D., & Shanks, A. L. 2005. A comparison of population structure in black rockfish (*Sebastes melanops*) as determined with otolith microchemistry and microsatellite DNA. Canadian Journal of Fisheries and Aquatic Sciences 62:2189-2198.

Miller, M.P. 2005. Alleles in space (AIS): computer software for the joint analysis of interindividual spatial and genetic information. Journal of Heredity 96:722-724.

Moser, H. G., E. H. Ahlstrom, D. A. V. I. D. Kramer, and E. G. Stevens. 1974. Distribution and abundance of fish eggs and larvae in the Gulf of California. CalCOFI Report 17:112-128.

Munguia-Vega, A., S. G. Marinone, D. A. Paz-Garcia, A. Giron-Nava, T. Plomozo-Lugo, O. Gonzalez-Cuellar, A. H. Weaver, F. J. García-Rodriguez, and H. Reyes-Bonilla. 2018. Anisotropic larval connectivity and metapopulation structure driven by directional oceanic currents in a marine fish targeted by small-scale fisheries. Marine Biology 165:16.

Muss, A., D. R. Robertson, C. A. Stepien, P. Wirtz, and B. W. Bowen. 2001. Phylogeography of *Ophioblennius*: the role of ocean currents and geography in reef fish evolution. Evolution 55:561-572.

O'Connell, M., and J. M. Wright. 1997. Microsatellite DNA in fishes. Reviews in Fish Biology and Fisheries 7:331–363.

Paetkau, D., R. Slade, M. Burdens, and A. Estoup. 2004. Genetic assignment methods for the direct, real-time estimation of migration rate: a simulation-based exploration of accuracy and power. Molecular Ecology 13:55-65.

Pak, H., and J. R. V. Zaneveld. 1973. The Cromwell Current on the east side of the Galapagos Islands. Journal of Geophysical Research 78:7845-7859.

Palumbi, S.R. 2003. Population genetics, demographic connectivity, and the design of marine reserves. Ecological applications 13:146-158.

Paz-García, D.A., A. Munguía-Vega, T. Plomozo-Lugo, and A. H. Weaver. 2017. Characterization of 32 microsatellite loci for the Pacific red snapper, *Lutjanus peru*, through next generation sequencing. Molecular Biology Reports 44:251-256.

Peakall, R., and P.E. Smouse. 2012. GenAlEx 6.5: genetic analysis in Excel. Population genetic software for teaching and research--an update. Bioinformatics 28:2537-2539.

Piñón, A., F. Amezcua, and N. Duncan. 2009. Reproductive cycle of female yellow snapper *Lutjanus argentiventris* (Pisces, Actinopterygii, Lutjanidae) in the SW Gulf of California: gonadic stages, spawning seasonality and length at sexual maturity. Journal of Applied Ichthyology 25:18-25.

Piry, S., A. Alapetite, J. M. Cornuet, D. Paetkau, L. Baudouin, and A. Estoup. 2004. GENECLASS2: a software for genetic assignment and first-generation migrant detection. Journal of Heredity 95: 536-539.

Queller, D.C., and K. F. Goodnight. 1989. Estimating relatedness using genetic markers. Evolution 43:258-275.

Quinn, G. P., and M. J. Keough. 2002. Experimental design and data analysis for biologists. Cambridge University Press.

Radtke, R. L., and D. J. Shafer. 1992. Environmental sensitivity of fish otolith microchemistry. Marine and Freshwater Research 43:935-951.

Rannala, B., and J. L. Mountain. 1997. Detecting immigration by using multilocus genotypes. Proceedings of the National Academy of Sciences 94:9197-9201.

Reguera-Rouzaud, N., N. Díaz-Viloria, L. Sánchez-Velasco, A. L. Flores-Morales, A. Parés-Sierra, O. Aburto-Oropeza, and A. Munguía-Vega. 2020. Yellow snapper (*Lutjanus argentiventris*) connectivity in the Southern Gulf of California. Marine Biodiversity 50:1-14.

Reis-Santos, P., S.E. Tanner, M.A. Aboim, R.P. Vasconcelos, J. Laroche, G. Charrier, M. Pérez, P. Presa, B.M. Gillanders and H.N. Cabral. 2018. Reconciling differences in natural tags to infer demographic and genetic connectivity in marine fish populations. Scientific reports 8:1-12.

Robinson, G. and E. M. Del Pino. 1985. El Niño in the Galápagos Islands: the 1982–1983 event. Charles Darwin Foundation, Quito, Ecuador, 38:50-54.

Roden, G. I. 1958. Oceanographic aspects of Gulf of California. Pacific Science 12:21-45

Rodríguez-Figueroa, G. M., E. Shumilin, and I. Sánchez-Rodríguez. 2009. Heavy metal pollution monitoring using the brown seaweed *Padina durvillaei* in the coastal zone of the Santa Rosalía mining region, Baja California Peninsula, Mexico. Journal of Applied Phycology 21:19-26.

Ruttenberg, B. I. 2001. Effects of artisanal fishing on marine communities in the Galápagos Islands. Conservation Biology 15:1691-1699.

Ruttenberg, B. I., A. J. Haupt, A. I. Chiriboga, and R. R. Warner. 2005. Patterns, causes and consequences of regional ecological variation in a reef fish. Oecologia 145:394–403.

Ruttenberg, B. I., and R. R. Warner. 2006. Spatial variation in the chemical composition of natal otoliths from a reef fish in the Galápagos Islands. Marine Ecology Progress Series 328:225-236.

Sala E., O. Aburto-Oropeza, M. Reza, G. Paredes, and L. G. López-Lemus. 2004. Fishing down coastal food webs in the Gulf of California. Fisheries 29:19–25.

Schuelke, M. 2000. An economic method for the fluorescent labeling of PCR fragments. Nature Biotechnology 18:233-234.

Schiller, L., Alava, J. J., Grove, J., Reck, G., and D. Pauly. 2015. The demise of Darwin's fishes: evidence of fishing down and illegal shark finning in the Galápagos Islands. Aquatic Conservation: Marine and Freshwater Ecosystems 25:431-446.

Shumilin, E. N., G. Rodríguez-Figueroa, O. M. Bermea, E. L. Baturina, E. Hernández, and G. D. R. Meza. 2000. Anomalous trace element composition of coastal sediments near the copper mining district of Santa Rosalia, Peninsula of Baja California, Mexico. Bulletin of environmental contamination and toxicology 65:261-268.

Swan, S. C., J. D. Gordon, B. Morales-Nin, T. Shimmield, T. Sawyer, and A. J. Geffen. 2003. Otolith microchemistry of *Nezumia aequalis* (Pisces: Macrouridae) from widely different habitats in the Atlantic and Mediterranean. Journal of the Marine Biological Association of the United Kingdom 83:883-886.

Toral-Granda, M.V., Causton, C. E., Jäger, H., Trueman, M., Izurieta, J. C., Araujo, E., Cruz, M., Zander, K. K., Izurieta, A. and S. T. Garnett. 2017. Alien species pathways to the Galapagos Islands, Ecuador. PloS one 12(9): p.e0184379.

Thorrold, S. R., C. Latkoczy, P. K. Swart, and C. M Jones. 2001. Natal homing in a marine fish metapopulation. Science 291:297-299.

Vargas, F. H., Harrison, S., Rea, S. and D. W. Macdonald. 2006. Biological effects of El Niño on the Galápagos penguin. Biological Conservation 127:107-114.

Walther, B.D. and S. R. Thorrold. 2006. Water, not food, contributes the majority of strontium and barium deposited in the otoliths of a marine fish. Marine Ecology Progress Series 311:125–130.

Wellington, G. M., A. E. Strong, and G. Merlen. 2001. Sea surface temperature variation in the Galápagos Archipelago: a comparison between AVHRR nighttime satellite data and in situ instrumentation (1982–1998). Bulletin Marine Science 69:27–42.

Wilson, I. F., and V. S. Rocha. 1955. Geology and mineral deposits of the Boleo copper district, Baja California, Mexico. US Government Printing Office.

TABLES

Table 3.1. Results of univariate ANOVA for 9 elemental ratios in juvenile otoliths of *Lutjanus argentiventris* between the Gulf of California and Galápagos Archipelago. NS denotes non-significant. MS denotes mean square. Asterisks denote significance (* = 0.05, ** = 0.01, *** = 0.001).

Elemental ratio to calcium	Df	MS	F value	*p*		Galápagos avg (sd)	Gulf of California avg (sd)
Ba	1,18	0.9963	80.1080	<0.001	***	1.17 (0.17)	3.42 (1.17)
Cu	1,18	0.7255	17.8500	<0.001	***	19.50 (4.13)	9.63 (6.99)
Li	1,18	3.7165	79.0150	<0.001	***	59.43 (39.21)	6.83 (1.47)
Mg	1,18	0.0000	0.0048	0.9457	NS	0.29 (0.08)	0.28 (0.03)
Mn	1,18	0.0633	10.0250	0.0053	**	0.016 (0.001)	0.021 (0.005)
Pb	1,18	0.1847	2.3246	0.1447	NS	0.35 (0.14)	0.26 (0.17)
Rb	1,18	0.1826	7.6831	0.0125	*	0.50 (0.11)	0.35 (0.19)
Sr	1,18	0.0084	19.5190	<0.001	***	2.47 (0.11)	2.71 (0.12)
Zn	1,18	0.0193	0.5483	0.4686	NS	4.10 (1.42)	4.91 (2.04)

Table 3.2. Results of univariate ANOVA comparisons among ecoregions and mangroves for 9 elemental ratios in juvenile otoliths of *Lutjanus argentiventris* from the Galápagos and the Gulf of California. NS denotes non-significant. MS denotes mean square. Asterisks denote significance (* = 0.05, ** = 0.01, *** = 0.001)

Ecosystem	Element	Spatial Scale	df	MS	*F*	*p*	
Galapagos Archipelago	Ba	Ecoregion	2	0.047	3.581	< 0.05	*
		Mangrove	9	0.003	2.761	< 0.01	**
	Cu	Ecoregion	2	0.041	0.489	0.616	
		Mangrove	9	0.059	0.693	0.712	
	Li	Ecoregion	2	0.812	4.078	< 0.05	*
		Mangrove	9	0.647	4.187	< 0.001	***
	Mg	Ecoregion	2	0.105	3.340	< 0.05	*
		Mangrove	9	0.088	3.452	< 0.01	**
	Mn	Ecoregion	2	0.005	0.554	0.577	
		Mangrove	9	0.007	0.694	0.711	
	Pb	Ecoregion	2	0.016	0.063	0.939	
		Mangrove	9	0.234	0.964	0.478	
	Rb	Ecoregion	2	0.020	0.388	0.680	
		Mangrove	9	0.036	0.791	0.705	
	Sr	Ecoregion	2	0.007	7.140	< 0.05	**
		Mangrove	9	0.003	3.875	< 0.001	***
	Zn	Ecoregion	2	0.020	0.920	0.403	
		Mangrove	9	0.155	1.654	0.119	

Ecosystem	Element	Spatial Scale	df	MS	*F*	*p*	
Gulf of California	Ba	Ecoregion	2	0.228	6.950	< 0.01	**
		Mangrove	9	0.308	15.235	< 0.001	***
	Cu	Ecoregion	2	0.713	13.180	< 0.001	***
		Mangrove	9	1.123	322.810	< 0.001	***
	Li	Ecoregion	2	0.116	13.793	< 0.001	***
		Mangrove	9	0.139	54.447	< 0.001	***
	Mg	Ecoregion	2	0.007	1.121	0.300	
		Mangrove	9	0.046	10.341	< 0.001	***
	Mn	Ecoregion	2	0.186	14.903	< 0.001	***
		Mangrove	9	0.207	54.142	< 0.001	***
	Pb	Ecoregion	2	1.513	9.020	< 0.001	***
		Mangrove	9	1.935	22.180	< 0.001	***
	Rb	Ecoregion	2	0.465	13.773	< 0.001	***
		Mangrove	9	0.661	143.290	< 0.001	***
	Sr	Ecoregion	2	0.005	5.887	0.003	**
		Mangrove	9	0.006	12.107	< 0.001	***
	Zn	Ecoregion	2	1.529	15.934	< 0.001	***
		Mangrove	9	0.697	8.661	< 0.001	***

Table 3.3. Average sample size (N), number of alleles (Na), number of effective alleles (Ne), observed heterozygosity (Ho), expected heterozygosity (He), and proportion of private alleles (Pa) for each sampled island and overall.

Pop		N	Na	Ne	Ho	He	Pa
Fernandina	Mean	20.000	9.333	5.879	0.696	0.682	0.500
	SE	0.000	1.856	1.345	0.074	0.075	0.195
Floreana	Mean	17.917	8.583	5.658	0.684	0.683	0.250
	SE	0.083	1.897	1.385	0.078	0.065	0.131
Isabela East	Mean	12.833	7.250	4.776	0.659	0.642	0.0
	SE	0.167	1.321	0.972	0.081	0.076	0.0
Isabela West	Mean	27.833	9.833	5.606	0.610	0.686	0.083
	SE	0.112	2.212	1.362	0.090	0.066	0.083
San Cristobal	Mean	25.667	9.500	5.139	0.655	0.661	0.333
	SE	0.333	1.889	1.158	0.060	0.070	0.142
Santa Cruz	Mean	48.583	12.417	6.307	0.672	0.688	1.000
	SE	0.260	2.748	1.547	0.070	0.071	0.326
Santiago	Mean	35.833	10.833	5.975	0.680	0.684	0.750
	SE	0.112	2.576	1.548	0.077	0.068	0.429
Total	Mean	26.969	9.656	5.640	0.661	0.677	
	SE	1.078	0.720	0.455	0.026	0.024	

Table 3.4. Summary results of the AMOVA analysis among Galápagos ecoregions. Df denote degrees of freedom. SS denotes sum of squares. MS denotes mean of square. Est Var denotes estimated variance and % indicates the percentage of variance attributed to each data partition (Fst = among ecoregions, Fis = among individuals, Fit = within individuals).

Source	df	SS	MS	Est. Var.	%
Among Ecoregions	3	17.959	5.986	0.024	1%
Among Individuals	190	829.528	4.366	0.211	5%
Within Individuals	194	765.000	3.943	3.943	94%
Total	387	1612.487		4.179	100%
F-Statistics	Value	P (rand >= data)			
Fst	0.006	0.003			
Fis	0.051	0.001			
Fit	0.056	0.001			

Table 3.5. F_{ST} values among yellow snappers sampled from four Galápagos ecoregions (below diagonal) and associated *P* values (above diagonal). Statistically significant values are highlighted in bold.

	North	Eastern	Southern	Western
North	--	**0.019**	0.086	0.061
Eastern	0.025	--	0.964	**0.041**
Southern	0.02	-0.005	--	0.578
Western	0.019	0.003	-0.001	--

Table 3.6. F_{ST} values among yellow snappers sampled in Galápagos Islands (below diagonal) and associated *P* values (above diagonal). Statistically significant values are highlighted in bold.

	Fernandina	Floreana	Isabela East	Isabela West	San Cristobal	Santa Cruz	Santiago
Fernandina	_	0.24	0.066	0.364	**0.004**	0.076	0.263
Floreana	0.003	_	0.25	0.888	0.881	0.993	0.88
Isabela East	0.01	0.004	_	0.115	0.556	0.265	0.283
Isabela West	0.001	-0.006	0.008	_	0.413	0.605	0.704
San Cristobal	0.014	-0.005	-0.001	0.001	_	0.267	0.33
Santa Cruz	0.005	-0.008	0.003	-0.001	0.002	_	0.919
Santiago	0.002	-0.005	0.003	-0.002	0.001	-0.003	_

Table 3.7. Natural log Bayes Factors and log marginal likelihoods for each metapopulation scenario estimated with MIGRATE-N using multilocus genotypes for 10 populations and 12 microsatellite markers in *Lutjanus argentiventris* from the Galápagos archipelago.

#	Model	Bezier lmL	Rank	Model probability
1	Full model	-1144816.45	2.00	0.00
2	Panmixia	-3038141.97	3.00	0.00
3	Microchemistry	-1020906.91	1.00	1.00

Chapter 3 Appendix

Metapopulation structure changes throughout life stages based on otolith microchemistry and genetic analysis

Supplementary Information

by

LETICIA MARIA CAVOLE[1,*], ADRIAN MUNGUIA-VEGA[2,3], JESSICA A. MILLER[4], PELAYO SALINAS-DE-LEÓN[5,6], JOSE R. MARIN JARRIN [5,7], ANDREW FREDERICK JOHNSON[1,8], ETIENNE-RASTOIN LAPLANE [5,9], ALFREDO GIRÓN-NAVA[10], OCTAVIO ABURTO-OROPEZA[1]

[1]Scripps Institution of Oceanography, University of California San Diego, 9500 Gilman Drive, La Jolla, CA 92093, USA

[2]School of Natural Resources and the Environment, University of Arizona, Tucson, AZ, 85721, USA

[3]@ Lab Applied Genetics Research, La Paz, Baja California Sur, 23000, Mexico

[4]Oregon State University, 2030 SE Marine Science Drive, Newport, OR 97365, USA

[5]Charles Darwin Research Station, Puerto Ayora 200350, Ecuador

[6] Pristine Seas, National Geographic Society, Washington, DC, USA.

[7]Department of Fisheries Biology, Humboldt State University, 1Harpst St, Arcata, CA 95521, USA

[8] The Lyell Centre, Institute of Life and Earth Sciences, School of Energy, Geoscience, Infrastructure and Society, Heriot-Watt University, Edinburgh, EH14 4AS, UK

[9] School of Molecular and Life Sciences, Curtin University, Perth, Australia

[10] National Center for Ecological Analysis and Synthesis, University of California Santa Barbara, 735 State Street, Suite 300, Santa Barbara, CA 93101, USA

*Corresponding Author: lcavole@ucsd.edu

APPENDIX - Figures related with otolith microchemistry analysis

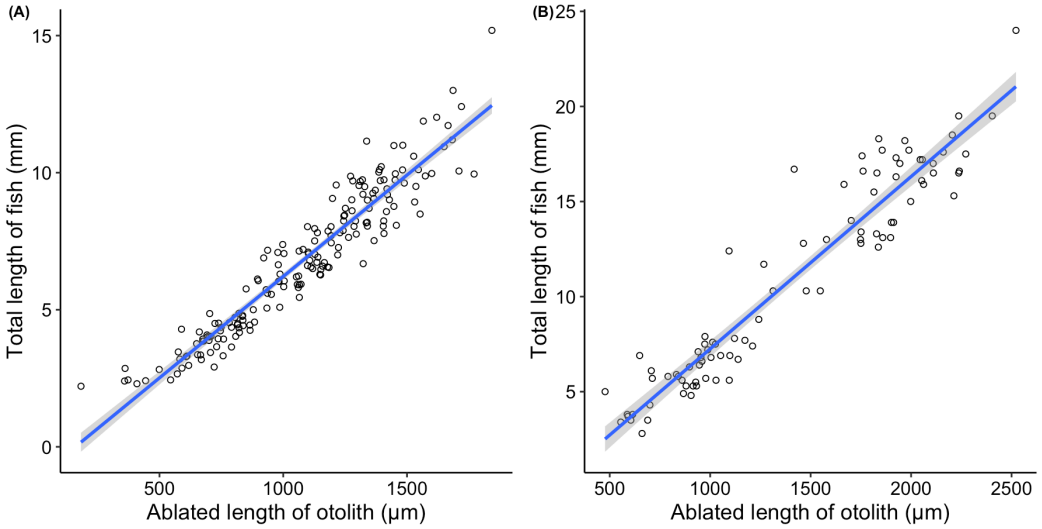

Figure 3.S1. Linear relationship between the total length of fish (mm) and the ablated length of otolith (μm) using LA-ICPMS for *Lutjanus argentiventris* from the (A) Gulf of California and (B) Galápagos.

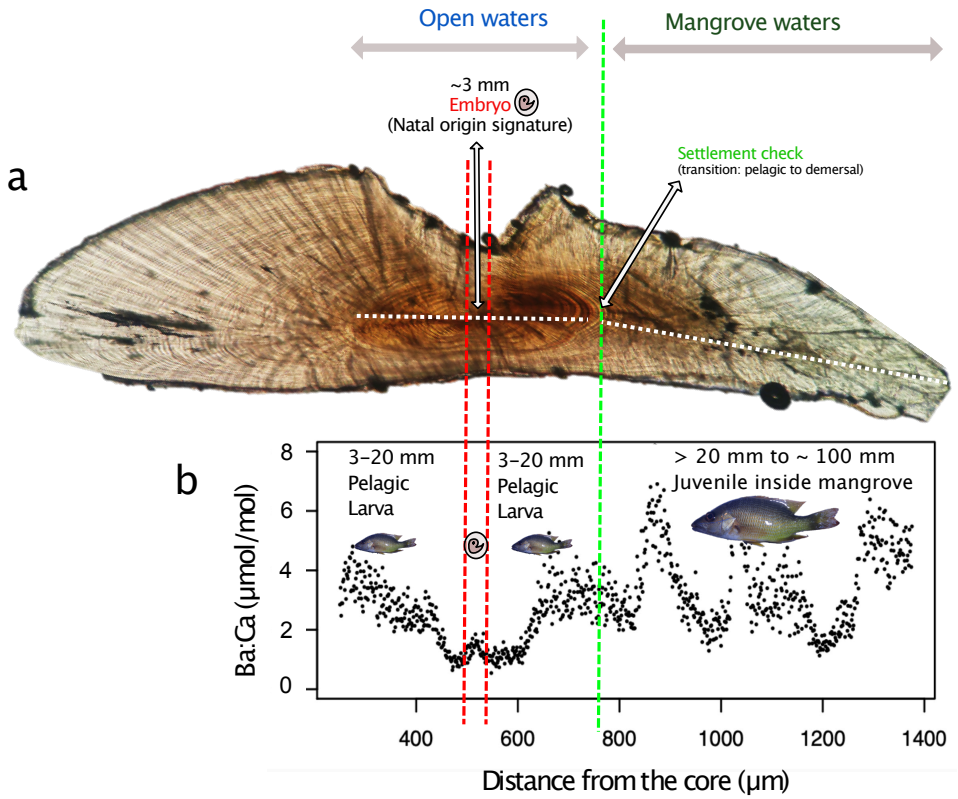

Figure 3.S2. (a) Example of an ablated laser transect across a juvenile *Lutjanus argentiventris* otolith and (b) an example of the mean Ba:Ca trace-elemental ratio back calculated for each life stage (embryo, larval, and post-settlement juvenile) .

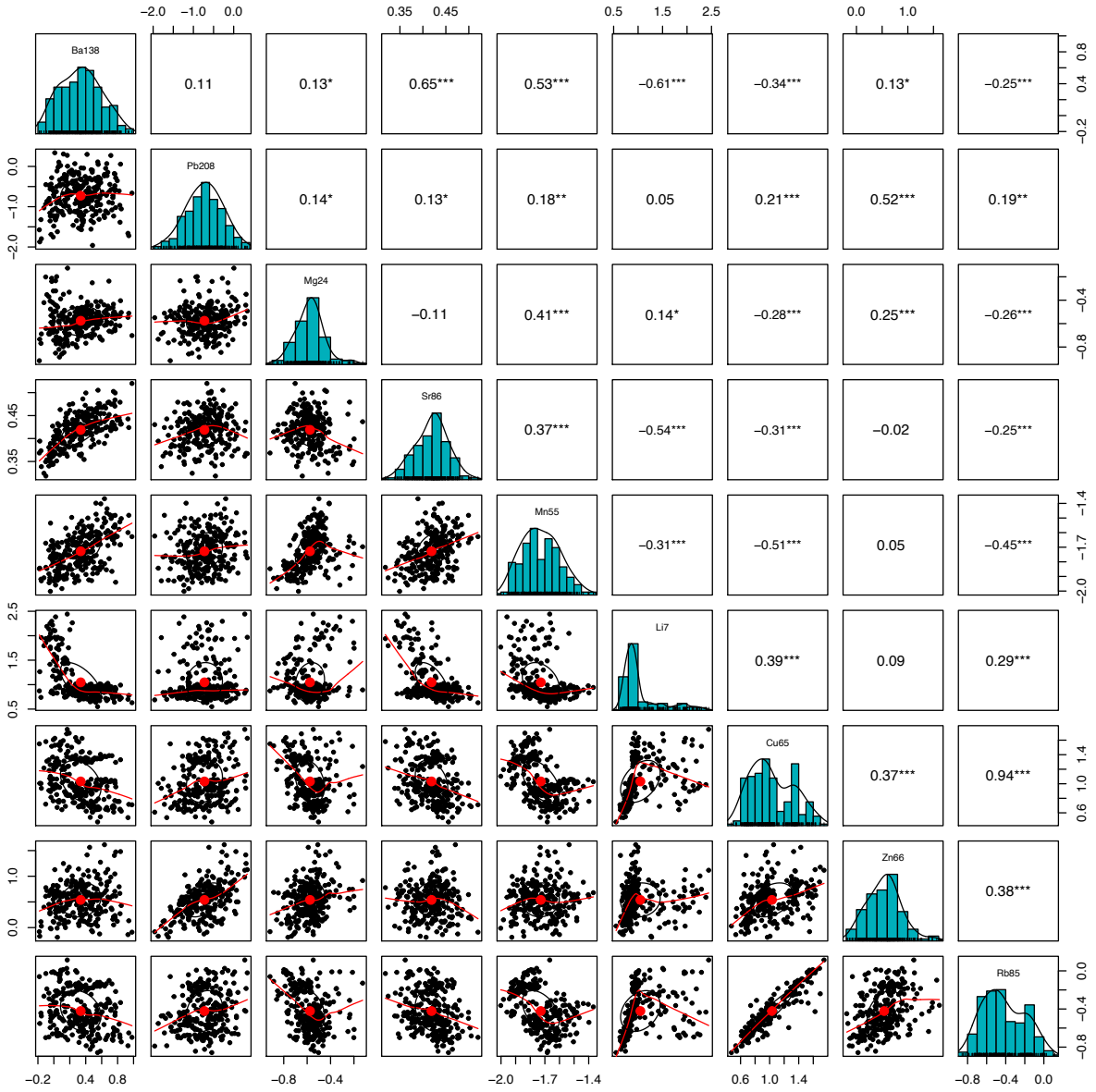

Figure 3.S3. Scatterplot matrices for all pair of elemental ratios (Me:Ca) of *Lutjanus argentiventris* from the Gulf of California and Galápagos Archipelago. Bivariate scatter plots are below the diagonal, histograms are on the diagonal, and the Pearson correlations with significance levels (* = 0.05, ** = 0.01, *** = 0.001) are above the diagonal.

APPENDIX - Figures of genetic analysis/microsatellite DNA markers

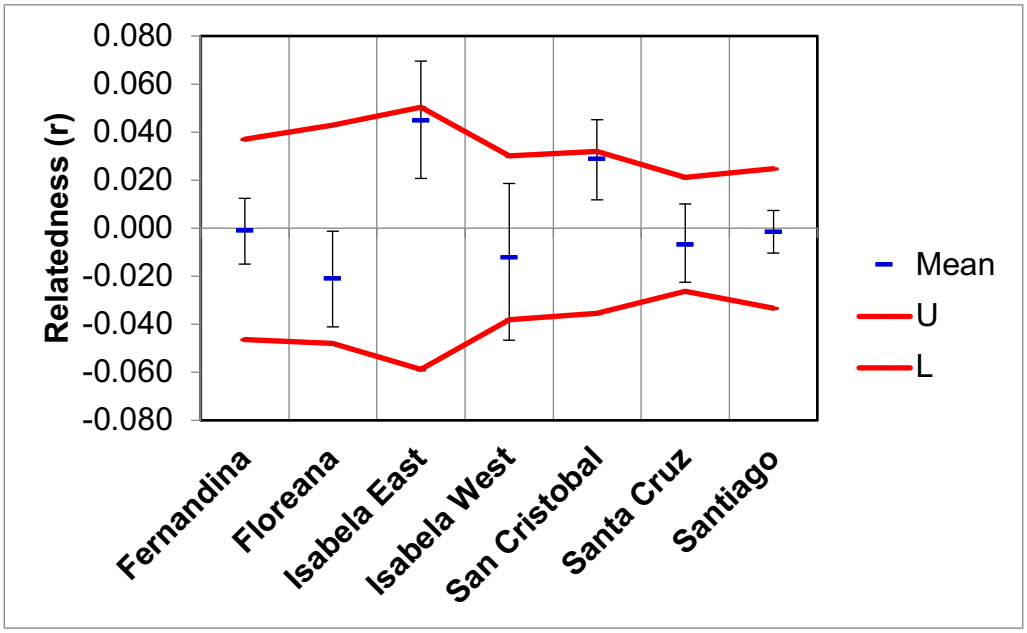

Figure 3.S4. Yellow snapper relatedness among Galápagos' Islands. Mean within population pairwise relatedness (r) values (%95%confidenceintervals) compared with bootstrapped upper (U) and lower (L) 95% confidence intervals assuming random mating (1,000 bootstrap replicates).

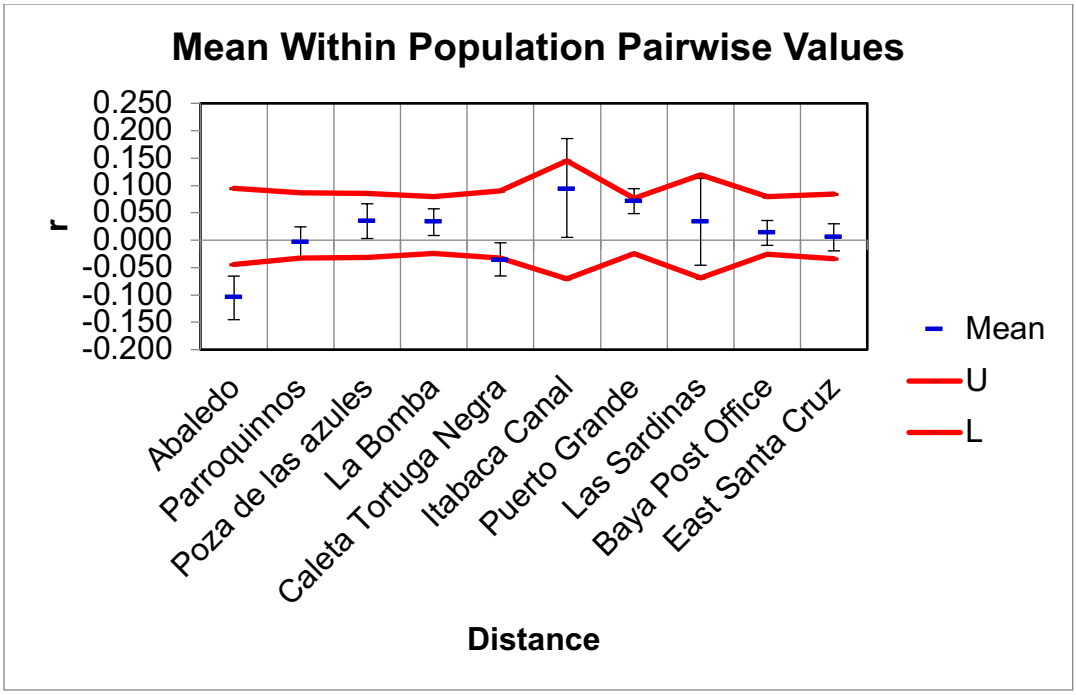

Figure 3.S5. Mean within population pairwise relatedness (r) values (%95%confidenceintervals) compared with bootstrapped upper (U) and lower (L) 95% confidence intervals assuming random mating (1,000 bootstrap replicates).

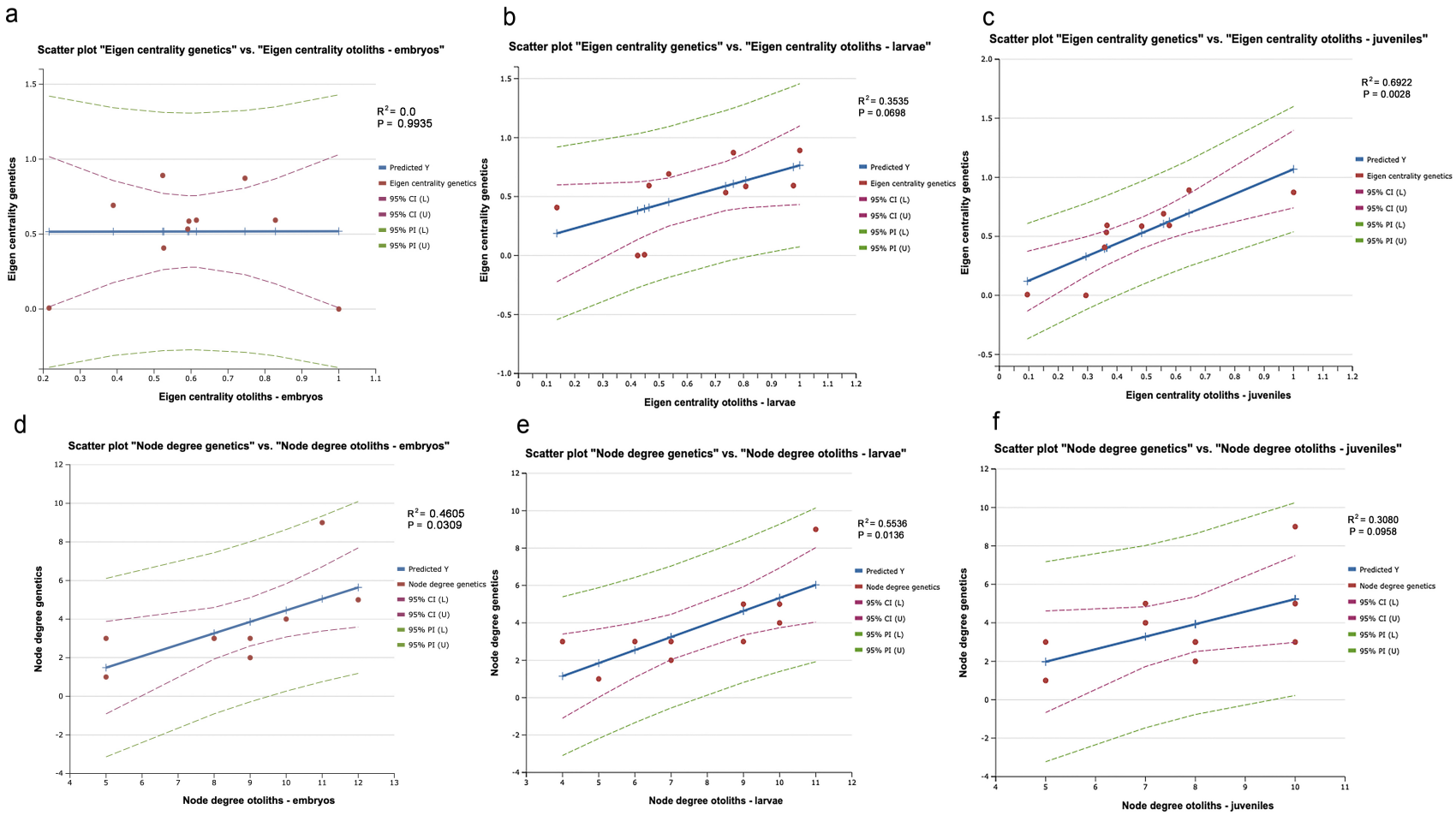

Figure 3.S6. Scatter plots showing the agreement of genetic (first-generation migrants) and microchemistry networks for *Lutjanus argentiventris* in 10 mangrove sites. The relationship between the eigen vector centrality of (a) genetics and embryo microchemistry (b) genetics and larval microchemistry, and (c) genetics and juvenile microchemistry. The relationship between the node degree of (d) genetics and embryo microchemistry, (e) genetics and larvae microchemistry and (f) genetics and juvenile microchemistry.

APPENDIX (Tables related with otolith microchemistry analysis and sample information)

Table 3.S1. Sample size and size range of *Lutjanus argentiventris* used for otolith microchemistry and genetic analyses.

Ecosystem	Ecoregion	Mangrove site	Otolith microchemistry *n*	Max TL (mm)	Min TL (mm)	Genetics *n*
Galápagos	Eastern	Cartago Grande	1	15	15	7
Galápagos	Eastern	Cartago Chico	1	16.3	16.3	3
Galápagos	Western	Albemarle	1	16.5	16.5	2
Galápagos	Western	Urbina Sur	1	17.4	17.4	5
Galápagos	Eastern	Cartago North	2	19.5	15.3	3
Galápagos	Western	Punta Mangle Galápagos	3	17.7	15.9	4
Galápagos	Western	Punta Espinoza	3	19.5	16.5	11
Galápagos	Western	Poza los Patillos	3	24	13.9	11
Galápagos	Eastern	Las Sardinas	5	7.9	3.4	7
Galápagos	Eastern	Itabaca Canal	5	12.6	7.5	6
Galápagos	Western	Abaledo	6	17.5	12.8	11
Galápagos	Eastern	Caleta Tortuga Negra	7	15.5	5.3	14
Galápagos	Eastern	Puerto Grande	7	15.9	2.8	19
Galápagos	Eastern	Poza de las azules	7	17.2	5.5	15
Galápagos	Southern	Baya Post Office	7	17.3	3.4	18
Galápagos	Eastern	East Santa Cruz	8	6.8	3.5	15
Galápagos	Western	Punta Moreno				3
Galápagos	Eastern	Cerro Valleno				1
Galápagos	Eastern	Santiago Norteast				2
Galápagos	Northern	Cara de Viejo				2
Galápagos	Northern	La posa				3
Gulf of California	Northern	Los Mojones	8	9.74	2.91	
Gulf of California	Central	Punta Yavaros	10	10.22	8.42	
Galápagos	Eastern	Parroquinnos	10	17	7.7	14
Gulf of California	Northern	El Soldado	11	6.73	4.17	
Galápagos	Eastern	La Bomba	11	18.5	5	19
Gulf of California	Southern	Barra de Piaxtla	13	7.96	2.3	
Gulf of California	Central	Los Gatos	17	11.88	2.66	
Gulf of California	Southern	San Jose	20	10.95	3.35	
Gulf of California	Northern	San Lucas	20	15.19	4.86	
Gulf of California	Central	Puerto Escondido	22	13	2.44	
Gulf of California	Southern	Balandra	26	11.72	2.82	
Gulf of California	Central	Punta Mangle	27	9.36	2.87	

Table 3.S2. Instrumental accuracy and precision for measurements of trace elements based on calcium carbonate standards (MACS-3 and MACS-1) and the mean percent relative standard deviations (%RSD) of the NIST 612. All standards were run at every 10 otoliths. NIST: National Institute of Standards and Technology; NA: not applicable.

Ecosystem	Standard	Sr:Ca	Ba:Ca	Cu:Ca	Li:Ca	Mg:Ca	Mn:Ca	Zn:Ca	Pb:Ca	Rb:Ca
Galápagos	MACS3	1.11	1.32	0.82	0.83	1.12	0.97	0.91	1.16	NA
	MACS 1	1.09	1.09	NA	NA	1.45	1.01	0.91	0.80	NA
	NIST 612	6.10	5.07	15.93	18.38	12.76	9.45	19.94	13.43	14.00
Gulf of California	MACS3	1.09	1.25	0.74	0.76	1.13	0.94	0.78	0.98	NA
	MACS 1	1.12	1.13	NA	NA	1.63	1.02	0.89	0.75	NA
	NIST 612	6.53	4.85	15.87	16.99	12.63	9.23	18.17	12.52	12.56

Table 3.S3. The average (avg) and standard deviation (sd) for each trace element analyzed in *Lutjanus argentiventris*. Data are provided for the ecoregions (Western, Eastern and Southern) and islands (Fernandina, Isabela, Santiago, Santa Cruz, San Cristóbal and Floreana) in the Galapagos and for ecoregions (northern, central and southern) and the coastal type (Mainland or Peninsula) in the Gulf of California. Western (W), Eastern (E) and Southern (S) ecoregions are specified for each one of the Galapagos Islands.

Ecosystem	Spatial Resolution	Ba:Ca		Cu:Ca		Li:Ca		Mg:Ca		Mn:Ca		Pb:Ca		Rb:Ca		Sr:Ca		Zn:Ca	
		avg	sd	avg	sd	avg	sd	avg	sd	avg	sd	avg	sd	avg	sd	avg	sd	avg	sd
Galápagos Archipelago	Western	1.37	0.31	19.78	11.48	14.75	8.70	0.19	0.04	0.01	0.00	0.29	0.25	0.55	0.28	2.55	0.12	3.04	2.07
	Eastern	1.20	0.34	19.59	12.12	50.76	50.17	0.29	0.13	0.02	0.00	0.35	0.40	0.51	0.25	2.48	0.19	4.08	3.31
	Southern	0.94	0.26	19.77	19.43	130.31	97.32	0.36	0.16	0.02	0.00	0.42	0.66	0.53	0.42	2.28	0.10	5.40	3.69
	Isabela (E)	1.09	0.09	17.38	10.18	14.87	10.88	0.19	0.05	0.02	0.00	0.14	0.13	0.52	0.26	2.64	0.19	1.84	0.81
	Fernandina (W)	1.38	0.39	22.86	13.80	11.39	5.16	0.19	0.03	0.02	0.00	0.32	0.32	0.63	0.34	2.50	0.09	2.73	1.83
	Isabela (W)	1.39	0.22	15.77	8.05	19.84	10.70	0.19	0.05	0.01	0.00	0.28	0.14	0.44	0.18	2.62	0.13	3.70	2.39
	Santa Cruz (E)	1.15	0.28	21.57	11.91	53.93	50.64	0.28	0.12	0.02	0.00	0.39	0.41	0.57	0.25	2.42	0.17	4.25	3.34
	Santiago (S)	1.39	0.41	19.34	12.23	37.31	45.11	0.33	0.17	0.02	0.00	0.44	0.50	0.48	0.23	2.55	0.16	5.08	3.97
	San Cristobal (E)	1.06	0.30	15.77	13.39	74.96	55.20	0.28	0.12	0.02	0.01	0.17	0.17	0.43	0.26	2.49	0.21	2.93	1.94
	Floreana (S)	0.94	0.26	19.77	19.43	130.31	97.32	0.36	0.16	0.02	0.00	0.42	0.66	0.53	0.42	2.28	0.10	5.40	3.69
Gulf of California	Northern	3.68	1.33	13.55	8.78	7.41	1.78	0.29	0.09	0.02	0.01	0.21	0.24	0.47	0.24	2.78	0.13	4.97	4.41
	Central	3.44	1.65	11.59	6.47	7.61	1.50	0.27	0.04	0.02	0.01	0.36	0.35	0.42	0.17	2.72	0.16	6.64	7.23
	Southern	2.78	1.42	6.84	2.54	6.28	1.18	0.28	0.05	0.02	0.00	0.22	0.25	0.28	0.07	2.66	0.23	3.17	3.97
	Mainland	3.90	2.09	5.30	0.92	6.06	0.88	0.31	0.06	0.02	0.01	0.09	0.11	0.25	0.06	2.66	0.20	3.28	2.40
	Peninsula	3.12	1.34	11.66	6.87	7.37	1.61	0.27	0.05	0.02	0.01	0.32	0.32	0.41	0.19	2.72	0.18	5.53	6.37

Table 3.S4. Classification matrix based on otolith microchemistry (juvenile stage) for the assignment of *Lutjanus argentiventris* to each mangrove and ecoregion of Galápagos and the Gulf of California.

Galápagos-Mangroves	Abaledo	Baya PostOffice	CaletaTortuga Negra	East Santa Cruz	Itabaca Canal	La Bomba	Las Sardinas	Parroquinnos	Poza de las azules	Puerto Grande
Abaledo	4	0	0	0	0	1	0	1	0	0
Baya Post Office	0	1	0	4	1	0	0	0	0	1
Caleta Tortuga Negra	1	1	1	0	0	2	1	0	0	1
East Santa Cruz	0	3	0	3	0	0	1	0	1	0
Itabaca Canal	0	1	1	0	1	1	0	0	0	1
La Bomba	3	0	1	0	1	2	1	1	2	0
Las Sardinas	0	0	0	0	1	0	3	0	0	1
Parroquinnos	1	0	0	0	4	2	1	0	1	1
Poza de las azules	0	0	0	0	1	1	2	1	2	0
Puerto Grande	0	2	0	1	1	0	2	0	1	0

GOC-Mangroves	Balandra	Barra de Piaxtla	El Soldado	Los Gatos	Los Mojones	Pto Escondido	Punta Mangle	Punta Yavaros	San Jose	San Lucas
Balandra	21	0	0	0	0	1	3	0	0	0
Barra de Piaxtla	1	8	0	0	0	0	0	0	0	0
El Soldado	0	0	10	0	0	0	0	1	0	0
Los Gatos	0	0	0	13	0	0	0	0	0	4
Los Mojones	0	0	0	0	6	0	0	2	0	0
Pto Escondido	2	0	0	0	0	20	0	0	0	0
Punta Mangle	0	0	0	0	0	0	27	0	0	0
Punta Yavaros	0	0	0	0	0	0	0	10	0	0
San Jose	0	0	0	0	0	1	0	1	18	0
San Lucas	0	0	0	1	0	0	0	0	0	19

Table 3.S4. Classification matrix based on otolith microchemistry (juvenile stage) for the assignment of *Lutjanus argentiventris* (continued)

Galáoagos-Ecoregions	Eastern	Southern	Western
Eastern	31	12	21
Southern	1	5	1
Western	3	0	14
GOC-Ecoregions	Central	Northern	Southern
Central	46	14	16
Northern	6	24	9
Southern	7	10	37

Table 3.S5. Classification matrix based on otolith microchemistry (larval stage) for the assignment of *Lutjanus argentiventris* to each mangrove of Galápagos and the Gulf of California.

Galápagos-Mangroves	Abaledo	Baya PostOffice	CaletaTortuga Negra	East Santa Cruz	Itabaca Canal	La Bomba	Las Sardinas	Parroquinnos	Poza de las azules	Puerto Grande
Abaledo	0	0	0	1	3	1	0	1	0	0
Baya Post Office	0	1	2	3	0	0	0	1	0	0
Caleta Tortuga Negra	0	0	2	0	1	1	1	1	0	1
East Santa Cruz	0	3	0	5	0	0	0	0	0	0
Itabaca Canal	0	0	1	0	2	2	0	0	0	0
La Bomba	1	1	2	0	3	0	1	0	2	1
Las Sardinas	0	2	1	0	0	1	0	0	0	1
Parroquinnos	1	0	3	0	1	1	0	1	2	1
Poza de las azules	1	2	0	1	0	1	0	0	1	1
Puerto Grande	0	2	1	0	1	0	1	1	1	0

GOC-Mangroves	Balandra	Barra de Piaxtla	El Soldado	Los Gatos	Los Mojones	Pto Escondido	Punta Mangle	Punta Yavaros	San Jose	San Lucas
Balandra	17	5	0	0	0	0	3	0	0	1
Barra de Piaxtla	3	10	0	0	0	0	0	1	0	0
El Soldado	0	1	4	0	2	0	0	4	0	0
Los Gatos	0	0	0	14	0	0	0	0	0	3
Los Mojones	0	0	0	0	6	0	0	2	0	0
Pto Escondido	1	0	0	0	0	15	6	0	0	0
Punta Mangle	0	0	0	0	0	7	20	0	0	0
Punta Yavaros	0	0	6	0	0	0	0	4	0	0
San Jose	0	0	0	0	2	0	0	1	17	0
San Lucas	0	0	0	6	0	0	0	0	0	14

Table 3.S6. Classification matrix based on otolith microchemistry (embryonic stage) for the assignment of *Lutjanus argentiventris* to each mangrove of Galápagos and the Gulf of California.

Galápagos-Mangroves	Abaledo	Baya PostOffice	CaletaTortuga Negra	East Santa Cruz	Itabaca Canal	La Bomba	Las Sardinas	Parroquinnos	Poza de las azules	Puerto Grande
Abaledo	0	0	0	1	3	0	0	2	0	0
Baya Post Office	0	0	2	2	0	0	0	1	1	1
Caleta Tortuga Negra	0	1	0	0	1	1	3	1	0	0
East Santa Cruz	0	3	1	3	0	0	1	0	0	0
Itabaca Canal	0	0	0	0	2	2	1	0	0	0
La Bomba	0	1	2	0	4	0	0	0	2	2
Las Sardinas	1	2	0	0	0	0	0	1	0	1
Parroquinnos	1	0	4	0	0	1	0	3	1	0
Poza de las azules	0	2	0	1	1	1	1	0	1	0
Puerto Grande	0	0	0	0	2	0	2	2	1	0

GOC-Mangroves	Balandra	Barra de Piaxtla	El Soldado	Los Gatos	Los Mojones	Pto Escondido	Punta Mangle	Punta Yavaros	San Jose	San Lucas
Balandra	15	5	1	0	0	2	2	0	0	1
Barra de Piaxtla	1	12	0	1	0	0	0	0	0	0
El Soldado	0	2	4	0	1	1	0	3	0	0
Los Gatos	0	0	0	12	0	0	0	0	0	5
Los Mojones	0	0	0	0	5	0	0	2	1	0
Pto Escondido	1	1	1	0	0	16	1	0	2	0
Punta Mangle	1	0	0	0	0	5	20	0	1	0
Punta Yavaros	0	0	5	0	1	0	0	4	0	0
San Jose	0	0	0	0	1	2	0	0	17	0
San Lucas	1	0	0	7	0	0	0	0	0	12

Table 3.S7. Mean, standard deviation (SD), minimum and maximum values of sea surface temperature (SST, °C) and chlorophyll-a (Chl-a, mg m^{-3}) for the mangrove sites of Galápagos between April 2014 and April 2015 and the Gulf of California between October 2002 and October 2004

Ecosystem	Mangrove Site	Long	Lat	Variable	Mean	SD	Minimum	Maximum
Galápagos	Punta Espinoza	-91.45	-0.27	SST	25.59	1.48	23.12	29.25
	Punta Mangle	-91.39	-0.45		25.11	1.70	22.32	29.36
	Poza los Patillos	-91.38	-0.36		24.79	1.80	21.67	28.89
	Baya Post Office	-90.44	-1.23		24.91	1.70	21.40	28.29
	Urbina Sur	-91.26	-0.38		25.76	1.08	24.06	27.80
	Urbina Sur 2	-91.28	-0.36		25.13	1.85	21.77	28.51
	Abaledo	-91.21	-0.67		25.58	1.47	22.28	28.96
	Punta Moreno	-91.33	-0.72		25.22	1.75	22.44	29.68
	Cartago Grande	-90.92	-0.62		24.79	1.88	21.57	29.00
	Cartago Chico	-90.86	-0.66		25.58	1.33	22.92	28.53
	Cartago North	-90.98	-0.58		24.73	1.95	21.81	29.08
	Albemarle	-91.36	0.16		25.06	1.79	21.76	28.60
	Puerto Grande	-89.47	-0.80		24.59	1.90	21.83	28.73
	Las Sardinas	-89.39	-0.72		24.68	1.96	21.38	28.62
	Parroquinnos	-90.42	-0.77		25.16	1.45	22.61	28.29
	Caleta Tortuga Negra	-90.33	-0.50		24.42	1.97	21.23	28.97
	Itabaca Canal	-90.28	-0.49		24.90	1.73	21.98	28.45
	East Santa Cruz	-90.20	-0.68		24.38	1.73	20.53	28.73
	Poza de las azules	-90.67	-0.35		24.94	1.77	21.75	28.59
	La Bomba	-90.70	-0.18		24.89	1.81	21.46	28.16
Gulf of California	San Lucas	-112.20	27.23	SST	24.42	4.19	15.65	31.70
	Los Mojones	-112.01	27.02		25.14	4.34	16.67	32.29
	Punta Mangle Baja	-111.33	26.27		25.21	4.01	15.53	32.34
	Puerto Escondido	-111.31	25.82		25.55	3.86	18.15	32.29
	Los Gatos	-110.90	25.52		25.69	3.68	18.30	32.55
	San Jose	-110.56	24.87		25.71	3.52	18.75	32.26
	Balandra	-110.32	24.32		25.53	3.29	17.44	32.10
	El Soldado	-110.98	27.96		25.05	5.03	15.17	33.57
	Punta Yavaros	-109.53	26.71		26.28	4.95	16.54	34.53
	Barra de Piaxtla	-106.44	23.20		27.27	3.31	19.01	33.90

Table 3.S7. Mean, standard deviation (SD), minimum and maximum values (continued)

Ecosystem	Mangrove Site	Long	Lat	Variable	Mean	SD	Minimum	Maximum
Galápagos	Punta Espinoza	-91.45	-0.27	Chl-a	0.30	0.11	0.12	0.55
	Punta Mangle	-91.39	-0.45		0.27	0.08	0.16	0.52
	Poza los Patillos	-91.38	-0.36		0.25	0.07	0.14	0.42
	Baya Post Office	-90.44	-1.23		0.26	0.09	0.10	0.54
	Urbina Sur	-91.26	-0.38		0.29	0.11	0.16	0.61
	Urbina Sur 2	-91.28	-0.36		0.22	0.05	0.14	0.33
	Abaledo	-91.21	-0.67		0.41	0.24	0.18	1.14
	Punta Moreno	-91.33	-0.72		0.28	0.07	0.17	0.52
	Cartago Grande	-90.92	-0.62		0.24	0.07	0.14	0.50
	Cartago Chico	-90.86	-0.66		0.28	0.10	0.16	0.61
	Cartago North	-90.98	-0.58		0.25	0.08	0.14	0.48
	Albemarle	-91.36	0.16		0.27	0.09	0.17	0.65
	Puerto Grande	-89.47	-0.80		0.30	0.09	0.14	0.46
	Las Sardinas	-89.39	-0.72		0.24	0.08	0.13	0.50
	Parroquinnos	-90.42	-0.77		0.29	0.10	0.14	0.66
	Caleta Tortuga Negra	-90.33	-0.50		0.36	0.16	0.13	0.80
	Itabaca Canal	-90.28	-0.49		0.31	0.13	0.16	0.97
	East Santa Cruz	-90.20	-0.68		0.62	0.38	0.20	1.55
	Poza de las azules	-90.67	-0.35		0.25	0.07	0.13	0.46
	La Bomba	-90.70	-0.18		0.25	0.07	0.14	0.45
Gulf of California	San Lucas	-112.20	27.23	Chl-a	3.08	2.86	0.22	27.81
	Los Mojones	-112.01	27.02		2.51	2.96	0.18	20.08
	Punta Mangle Baja	-111.33	26.27		1.68	2.21	0.13	25.20
	Puerto Escondido	-111.31	25.82		1.94	2.66	0.10	25.41
	Los Gatos	-110.90	25.52		1.47	2.21	0.04	21.56
	San Jose	-110.56	24.87		0.97	0.88	0.08	7.80
	Balandra	-110.32	24.32		1.43	1.93	0.20	20.75
	El Soldado	-110.98	27.96		3.02	4.08	0.16	29.55
	Punta Yavaros	-109.53	26.71		3.77	3.70	0.43	28.10
	Barra de Piaxtla	-106.44	23.20		2.90	2.69	0.13	22.13

APPENDIX (Tables of genetic analysis/microsatellite DNA markers)

Table 3.S8. In-degree, out-degree, total degree and eigenvector centrality (EC) of the microchemistry and genetic networks shown in Figure 3.7, including the self-assignment percentage (SA) and the average genetic relatedness (GR) of individuals within each mangrove site. Mangrove sites with more than 5 fish are in bold.

Network Microchemistry-Individual Assignment-Larvae								
ID	Mangrove	Latitude	Longitude	In-Degree	Out-Degree	Degree	EC	SA (%)
1	**Abaledo**	-0.67247	-91.2133	4	1	5	0.447902	0
2	Albemarle	0.16087	-91.36199	0	5	5	0	0
3	**Baya Post Office**	-1.22958	-90.44119	4	5	9	0.423544	0.1428
4	**Caleta Tortuga Negra**	-0.50359	-90.33087	5	5	10	1	0.2857
5	Cartago Chico	-0.65825	-90.86309	0	5	5	0	0
6	Cartago Grande	-0.6195	-90.91866	0	1	1	0	0
7	Cartago North	-0.57869	-90.98064	2	5	7	0.236282	0
8	**East Santa Cruz**	-0.68371	-90.19605	2	2	4	0.136511	0.5
9	**Itabaca Canal**	-0.48788	-90.27606	3	3	6	0.534189	0.4
10	**La Bomba**	-0.17611	-90.7008	9	2	11	0.977408	0
11	**Las Sardinas**	-0.71701	-89.38812	3	4	7	0.736607	0
12	**Parroquinnos**	-0.76666	-90.4233	6	4	10	0.764025	0
13	**Poza de las azules**	-0.3489	-90.67307	5	2	7	0.463903	0.1428
14	Poza los Patillos	-0.35773	-91.38438	3	5	8	0.4571	0
15	**Puerto Grande**	-0.79902	-89.46877	6	3	9	0.807919	0
16	Punta Espinoza	-0.27074	-91.44552	3	2	5	0.522277	0
17	Punta Mangle Galapagos	-0.44557	-91.38865	3	1	4	0.396145	0
18	Urbina Sur	-0.37787	-91.2607	0	3	3	0	0

Table 3.S8. In-degree, out-degree, total degree and eigenvector centrality (EC) (continued)

Network Microchemistry-Individual Assignment-Juveniles								
ID	**Mangrove**	**Latitude**	**Longitude**	**In-Degree**	**Out-Degree**	**Degree**	**EC**	**SA (%)**
1	**Abaledo**	-0.67247	-91.2133	2	3	5	0.094998626	**0.5**
2	Albemarle	0.16087	-91.36199	0	4	4	0	0
3	**Baya Post Office**	-1.22958	-90.44119	3	4	7	0.294254805	0.1428
4	**Caleta Tortuga Negra**	-0.50359	-90.33087	5	2	7	0.64466799	0.1428
5	Cartago Chico	-0.65825	-90.86309	0	1	1	0	0
6	Cartago Grande	-0.6195	-90.91866	0	2	2	0	0
7	Cartago North	-0.57869	-90.98064	2	3	5	0.125722534	0
8	**East Santa Cruz**	-0.68371	-90.19605	3	2	5	0.357405251	0.375
9	**Itabaca Canal**	-0.48788	-90.27606	5	3	8	0.558079451	0
10	**La Bomba**	-0.17611	-90.7008	7	3	10	0.57769292	0.1818
11	**Las Sardinas**	-0.71701	-89.38812	2	6	8	0.364021507	0.6
12	**Parroquinnos**	-0.76666	-90.4233	10	0	10	1	0
13	**Poza de las azules**	-0.3489	-90.67307	4	4	8	0.365870865	0.2857
14	Poza los Patillos	-0.35773	-91.38438	2	4	6	0.094867292	0.3333
15	**Puerto Grande**	-0.79902	-89.46877	5	5	10	0.483826848	0
16	Punta Espinoza	-0.27074	-91.44552	2	3	5	0.218970616	0.3333
17	Punta Mangle Galapagos	-0.44557	-91.38865	2	3	5	0.007043855	0
18	Urbina Sur	-0.37787	-91.2607	0	2	2	0	0

Table 3.S8. In-degree, out-degree, total degree and eigenvector centrality (EC) (continued)

		Network Genetics-First Generation Migrants						
ID	Mangrove	Latitude	Longitude	In-Degree	Out-Degree	Degree	EC	SA (%)
1	**Abaledo**	-0.67247	-91.2133	1	0	1	0.006669723	-0.103
2	Albemarle	0.16087	-91.36199	2	0	2	0.662564784	
3	**Baya Post Office**	-1.22958	-90.44119	0	5	5	0	0.014
4	**Caleta Tortuga Negra**	-0.50359	-90.33087	2	2	4	0.891165527	-0.036
5	Cartago Chico	-0.65825	-90.86309	2	0	2	0.993206617	
6	Cartago Grande	-0.6195	-90.91866	1	1	2	0.40700161	
7	Cartago North	-0.57869	-90.98064	1	1	2	0.006669723	
8	**East Santa Cruz**	-0.68371	-90.19605	1	2	3	0.40700161	0.006
9	**Itabaca Canal**	-0.48788	-90.27606	2	1	3	0.691743667	0.093
10	**La Bomba**	-0.17611	-90.7008	2	7	9	0.59287473	0.034
11	**Las Sardinas**	-0.71701	-89.38812	1	1	2	0.533635509	0.034
12	**Parroquinnos**	-0.76666	-90.4233	2	3	5	0.872606873	-0.004
13	**Poza de las azules**	-0.3489	-90.67307	1	2	3	0.59299839	0.035
14	Poza los Patillos	-0.35773	-91.38438	1	1	2	0.386779736	
15	**Puerto Grande**	-0.79902	-89.46877	1	2	3	0.586205007	0.072
16	Punta Espinoza	-0.27074	-91.44552	2	3	5	0.793781346	
17	Punta Mangle Galapagos	-0.44557	-91.38865	2	0	2	0.41579152	
18	Urbina Sur	-0.35745	-91.27911	1	0	1	0.533635509	
19	Cara de Viego	0.53718	-90.73818	2	0	2	1	
20	La Posa	0.29773	-90.51536	1	0	1	0.284742057	
21	Punta Moreno	-0.71536	-91.32817	1	0	1	0.006669723	
22	Santiago Northeast	-0.15592	-90.72097	2	0	2	0.29141178	

Table 3.S9. Estimates of Θ ($4N_e\mu$) for the 10 sites, M ($m\mu$) and Nm (Number of migrants) between populations according to the most probable gene flow scenario (Model # 3, Microchemistry). We show the role of each site with respect to the number of sites from which it receives (in-degree) and those to which it exports (out-degree) migrants. Nm in = total number of migrants received, Nm out = total number of migrants exported. Nm out-Nm in = net number of migrants.

Parameter	Mean	Nm	Nm in	In-degree	Nm out	Out-degree	Nm out - Nm in
Θ 1 Abaledo	0.098		0.872	2	1.813	3	0.942
Θ 2 Baya Post Office	0.098		1.329	3	1.594	4	0.265
Θ 3 Caleta Tortuga Negra	0.096		5.528	5	2.102	2	-3.426
Θ 4 East Santa Cruz	0.097		2.648	3	1.438	2	-1.21
Θ 5 Itabaca Canal	0.097		3.075	4	4.114	6	1.039
Θ 6 La Bomba	0.097		7.057	6	6.786	5	-0.271
Θ 7 Las Sardinas	0.097		2.934	2	3.365	6	0.431
Θ 8 Parroquinos	0.097		3.157	6	4.952	3	1.795
Θ 9 Poza de las azules	0.098		3.105	4	3.4	4	0.295
Θ 10 Puerto Grande	0.097		3.285	5	3.425	5	0.14

Table 3.S9. Estimates of Θ ($4N_e\mu$) for the 10 sites, M ($m\mu$) and Nm (Number of migrants) (continued)

Parameter	Mean	Nm	Nm in	In-degree	Nm out	Out-degree	Nm out - Nm in
M_1->3	30.81	0.742					
M_1->6	19.67	0.479					
M_1->8	24.47	0.592					
M_2->10	14.87	0.362					
M_2->3	19.01	0.458					
M_2->4	16.03	0.388					
M_2->5	15.9	0.386					
M_3->5	57.3	1.391					
M_3->6	29.24	0.712					
M_4->10	42.35	1.032					
M_4->2	16.63	0.406					
M_5->10	20.98	0.511					
M_5->2	18.24	0.445					
M_5->6	30.88	0.752					
M_5->7	50.67	1.228					
M_5->8	13.74	0.333					
M_5->9	34.59	0.845					
M_6->1	18.23	0.444					
M_6->3	143.04	3.446					
M_6->5	32.48	0.788					
M_6->8	43.25	1.047					
M_6->9	43.4	1.06					
M_7->10	19.81	0.483					
M_7->3	24	0.578					
M_7->4	31.79	0.769					
M_7->6	7.11	0.173					
M_7->8	17.87	0.433					
M_7->9	38.05	0.93					
M_8->1	17.53	0.427					
M_8->6	174.82	4.255					
M_8->9	11.05	0.27					
M_9->10	36.79	0.897					
M_9->4	61.67	1.491					
M_9->6	28.23	0.687					
M_9->8	13.43	0.325					
M_10->2	19.63	0.479					
M_10->3	12.6	0.304					
M_10->5	21.01	0.51					
M_10->7	70.33	1.705					
M_10->8	17.68	0.428					

CHAPTER 4:

Marine fish as mobile monitors of low oxygen, temperature and pH conditions

LETICIA MARIA CAVOLE, KARIN LIMBURG, NATALYA D. GALLO, ANNE GRO VEA SALVANES, ARTURO RAMÍREZ-VALDEZ, LISA A. LEVIN, OCTAVIO ABURTO OROPEZA, ANDREAS HERTWIG, MING-CHANG LIU, KEVIN D. MCKEEGAN

Abstract

The ocean is rapidly losing oxygen, with profound implications for marine organisms. Within Eastern Boundary Upwelling Systems, such as the California and the Benguela Current Ecosystems, an important question is how the ongoing expansion, intensification and shoaling of Oxygen Minimum Zones (OMZs) will affect fish throughout their lifetimes. One of the first steps to filling this knowledge gap is through the development of tools and techniques to track fishes' exposure to hypoxic (< 22-45 μmol kg^{-1}) and low-pH (~ 7.5) waters when inhabiting OMZs. Here, we examine if the otoliths of fish living in OMZs exhibit distinct patterns of elemental and isotopic composition, which could be used to monitor their exposure history to severely hypoxic and low-pH waters. We hypothesize that the unique biogeochemistry of OMZs (i.e., low-oxygen, low-pH, and the presence of dissolved elements) will impart unique elemental and isotopic signatures upon the otoliths of both long-lived and short-lived fishes living within it. We analyzed the otoliths of six fish species from three OMZ regions: the Southern California Bight and the Gulf of California in the Northeast Pacific Ocean, and the Namibian shelf in the Southeast Atlantic Ocean, using three complementary techniques: laser ablation inductively coupled plasma mass spectrometry, secondary ion mass spectrometry and scanning X-ray fluorescence microscopy. We observed that OMZ-dwelling fishes spanning a range of life-history traits (e.g. longevity, maximum size, growth rate, parental investment and thermal history inferred by $\delta^{18}O$) exhibited a common elemental fingerprint (with respect to Sr:Ca, Mn:Ca, Zn:Ca, B:Ca, Ba;Ca and Mg:Ca) when compared to a shallow-water marine fish from better oxygenated waters. In addition, we observed that boron ratios in otoliths seem to work as a tracer of low-pH seawater (~ 7.5) characteristic of OMZs. Our findings suggest that the underlying mechanism for the common elemental fingerprinting of otoliths of OMZ-dwelling fishes is

attributed to the unique biogeochemistry found on the margins of these highly productive upwelling systems as well as the physiological constraints resident organisms are perennially exposed to, including reduced oxygen and low pH conditions.

Introduction

The rapid loss of oxygen in the global oceans

Ocean deoxygenation is the loss of oxygen (O_2) in the ocean (Keeling and Garcia et al., 2002). This phenomenon has resulted in the loss of 77 billion metric tons, or approximately 2% of the O_2 content in the open ocean since the 1960s (Schmidtko et al., 2017), as well as the development of hypoxic zones in more than 500 coastal sites across the globe (Breitburg et al., 2018).

Global warming is likely the primary cause of continuing deoxygenation in the open ocean. The increase of temperature decreases seawater solubility of O_2, and it increases stratification in the upper ocean, reducing the supply of O_2 to the ocean's interior (Sarmiento et al., 1998; Keeling and Garcia, 2002). Global warming can also increase microbial, plant and animal respiration processes. Ocean models forecast declines in the global ocean O_2 inventory between 1 to 7% by the end of this century, mainly due to reduced transport of O_2 into the ocean interior (Keeling et al., 2010). This is expected to alter ocean productivity, biogeochemical cycles, marine habitats and marine biodiversity (Keeling and Garcia 2002; Breitburg et al., 2018).

These predictions are particularly concerning for regions known as Oxygen Minimum Zones (OMZs). These permanent midwater features occur between 100-1500 meters, mainly along the Eastern Boundary Upwelling Systems (EBUS), where there is high primary

productivity in surface waters, high carbon export to the deep, and slow advection of oxygen-rich deep-currents (Gilly et al., 2013). OMZs are defined by oxygen concentrations < 20 μmol kg^{-1} in the Pacific and Indian Oceans and < 45 μmol kg^{-1} in the Atlantic Ocean (Gilly et al., 2013). OMZs correspond to 8% of total oceanic area and contain the largest reservoir of hypoxic waters in the world (Helly and Levi, 2004; Paulmier and Ruiz-Pino, 2009). Immediately above or below an OMZ, there is an oxygen limited zone (OLZ) characterized by oxygen concentration < 60 μmol kg^{-1} in the Pacific and Indian Oceans and < 90 μmol kg^{-1} in the Atlantic (Gilly et al., 2013). The oxygen concentrations commonly observed in OMZs and OLZs are lower than the range shown by physiological studies to be limiting for many marine organisms (60-120 μmol kg^{-1}) (Vaquer-Sunyer and Duarte 2008), placing these ecosystems as ideal regions to study severe hypoxia. OMZs are also Carbon maximum Zones (CMZs), due to their high concentrations of dissolved inorganic carbon (DIC) and, as such, can function as "natural laboratories" to understand the interplay between low O_2, low pH and high CO_2 (Paulmier et al. 2011). The rapid, ongoing and ubiquitous deoxygenation trends increase the need to identify which regions and marine organisms are most vulnerable to or tolerant of low oxygen levels.

Gulf of California, Namibian shelf and Southern California Bight OMZs: unique places to study fish exposure to severe hypoxia

OMZs are not only midwater features; they intercept the shelf and slope of continental margins to create extensive severely hypoxic seafloor habitats (< 20 μmol kg^{-1}) – an area estimated globally of 1,148,000 km^2 (Helly and Levin, 2004). In the California Current Ecosystem, the Southern California Bight (SCB) OMZ occurs from about 450 to 1250 m deep and is characterized by the presence of low oxygen levels on the outer continental shelf that are

unfavorable to demersal and epibenthic communities (Levin 2003; McClatchie et al., 2010; Sato et al., 2018; Gallo et al., 2018) and may have already compressed the habitat for midwater fish (Koslow et al., 2011). For example, declines of up to ~ 2.1 μmol kg^{-1} y^{-1} (up to 21 %) from 1984 to 2006 at several stations off the coast of Southern California were associated with a shoaling of the hypoxia boundary (~ 60 μmol kg^{-1}) by up to 100 m, particularly in the nearshore regions (Bograd et al., 2008), potentially driven by the advection of modified source water, such as the California Undercurrent (Bograd et al., 2015).

The Gulf of California (GOC) OMZ occurs roughly from 100 to1300 m deep, with dissolved oxygen concentrations consistently below 22 μmol kg^{-1}, and suboxic conditions (i.e., $O_2 < 5$ μmol kg^{-1}) present for more than 500 m of the water column (Zamorano et al., 2007; Hendrickx and Serrano 2014; Gallo et al., 2020). The southern Gulf of California OMZ sits above the outer continental shelf and the upper slope, with extremely low oxygen concentrations (i.e., $O_2 < 2$ μmol kg^{-1}) that excludes most invertebrate species (Zamorano et al., 2007; Hendrickx and Serrano 2014). A surprising exception is the ophidiid black brotula *Cherublema emmelas*, a low-oxygen extremophile fish which thrives at $O_2 \sim 2$ μmol kg^{-1} (Gallo et al., 2019).

About 15,000 km away from the Southern California Bight and the Gulf of California OMZs, the Namibian shelf OMZ is part of the northern Benguela Current Ecosystem and is characterized as one of the most extreme marine habitats in the world due to its perennial hypoxia and anoxic conditions as well as its high hydrogen sulphide concentrations (Hutchings et al., 2009; Salvanes et al., 2011). In this geologically mature shelf upwelling system, the bearded goby *Sufflogobius bibartus* exhibits remarkable adaptations to the extreme environmental conditions (Salvanes et al., 2011) and acts as a keystone species, coupling the

inhospitable benthic environment with the pelagic system above (Utne-Palm et al., 2010; Currie et al., 2018).

The expansion of hypoxic zones is expected to alter the range distributions and decrease the biodiversity of fishes (Levin et al., 2009; Stramma et al., 2010, 2012; Gallo and Levin 2016; Gallo et al., 2020). Overall, demersal fish have higher oxygen requirements than benthic invertebrates (Vaquer-Sunyer and Duarte, 2008), potentially making them more vulnerable to deoxygenation. While ecological sampling methods such as trawls or remotely operated vehicles (ROVs) can shed light on community-level patterns, often fine-scale, data on how individual fish interact with hypoxic areas is lacking. Identifying tools that can track hypoxia, anoxia and low-pH seawater exposure during fishes' lifetimes can help fill this gap. The chemical analysis of fish otoliths – the calcium carbonate structures that grow periodically throughout the life of a fish - might help to understand fish exposure to hypoxic and/or anoxic conditions (Limburg et al., 2011; 2015) and fish exposure to low pH waters characteristic of OMZs-CMZs (Levin et al. 2015; Paulmier et al., 2011). Currently, understanding of how OMZs-CMZs environments affect otolith microchemistry remains largely unexplored.

Hypoxia and low pH exposure in OMZ-CMZ fish – looking at otolith chemistry

The elemental composition of otoliths, especially for elements that are redox-sensitive, such as iron (Fe) and manganese (Mn), and which are likely bioavailable inside OMZs (Morford and Emerson, 1999; Hopkinson and Barbeau 2007), have the potential to be used as proxies for hypoxia exposure in deep-water OMZ fish. During anoxic conditions, hydrogen sulfate (H_2S) is depleted in sulfur isotopes ($\delta^{34}S$), and this low $\delta^{34}S$ signature might be incorporated into otoliths

of fish exposed to suboxic (oxygen concentrations < 5 μmol kg^{-1}) or anoxic conditions (Weber et al., 2002; Limburg et al., 2015).

OMZs contain more acidic waters (pH ~ 7.5) compared to oceanic surface waters (pH ~ 8.1) (Paulmier and Ruiz-Pino, 2009; Paulmier et al. 2011), and elemental ratios, such as boron to calcium (B:Ca) (commonly analyzed in foraminifera and corals (Levin et al. 2015)), might provide insights about the range of pH conditions experienced by fish in the wild. Temperature is understood to interact with oxygen and CO_2 to set tolerance limits of fish (Pörtner 2001, 2021) and oxygen isotopes ($\delta^{18}O$) can allow the reconstruction of the thermal history of deep-sea fishes when living in OMZs-CMZs conditions (Gerringer et al., 2018). Therefore, elemental and isotopic analysis can shed light on how hypoxia, hypercapnia (i.e., excess of CO_2 in the blood) and temperature interactively affect fish.

We hypothesize that the unique biogeochemistry of OMZs-CMZs (i.e., low-oxygen, low-pH, and bioavailable elements) will impart distinctive elemental and isotopic signatures upon the otoliths of both long-lived and short-lived fishes living within it. The goals of this study are to: (i) compare the trace and minor elemental fingerprints in otoliths across fishes from OMZs in the Northeast Pacific and Southeast Atlantic; (ii) identify trace and minor elements as suitable proxies for exposure to severe hypoxia in fully marine fishes (< 20 μmol kg^{-1} in the Pacific, and < 45 μmol kg^{-1} in the Atlantic); and (iii) examine the thermal history of these species when inhabiting OMZs using oxygen isotope ratios. We also explore the suitability of using sulfur isotope ratios as a proxy for exposure to suboxic and/or anoxic conditions and boron to calcium ratios (B:Ca) as a proxy for pH inside OMZs-CMZs. The potential effects of the NE Pacific 2013-2015 warm-water anomaly, referred to as "the Blob" hereafter (Bond et al., 2015), on the chemical composition of deep-sea fish otoliths is also analyzed to shed light on how marine heat

waves (MHW) might affect the deep sea. We anticipate that finding new proxies for hypoxia and low-pH occurrence in fully marine species – relatively far from terrigenous influences known to affect the chemistry of otoliths - will be fundamental for understanding how individual fish respond to the continuing deoxygenation, acidification and warming of global oceans.

Material and Methods

Otolith chemistry, including minor and trace elements and isotopic composition, was quantified through the use of several instruments (**Supplementary Table 4. S1**).

LA-ICPMS analysis

We analyzed the otoliths of demersal fishes that live inside three different OMZs; Dover sole *Microstomus pacificus* (*n = 8*), shortspine thornyhead *Sebastolobus alascanus* (*n* = 10), longspine thornyhead *Sebastolobus altivelis* (*n = 8*) and rubynose brotula *Cataetyx rubrirostris* (*n = 8*) from the Southern California Bight, black brotula *Cherublemma emmelas* (*n* = 1) from the Gulf of California, and bearded goby *Sufflogobius bibarbatus* (*n* = 24) from the Namibian shelf (**Figure 4.1**). For Dover sole specimens, only the blind-side otoliths were used for analytical consistency, since they were in close contact with the hypoxic sediment. We also analyzed the otoliths of the giant sea bass *Stereolepis gigas* (*n = 10*), a shallow-water species (usually found < 30 meters deep) from coastal sites of the Northeast Pacific, which presumably do not live in an oxygen depleted and low pH environment (**Figure 4.1**). The selection of deep-sea fish from different OMZs and one shallow-water fish offer interesting contrasts of how distinct oxygen and pH levels affect otolith chemical patterns.

We quantified minor and trace elements in all fish otoliths (n = 79) using laser ablation inductively coupled plasma mass spectrometry (LA-ICPMS) at the College of Environmental Science and Forestry at Syracuse, NY. All otoliths were immersed in epoxy resin, dried for 48 hours, and transversally sectioned to about 0.5 mm width. For all the species, except the Dover sole, laser transects spanned from the otolith core to the edge. For the Dover sole otoliths, the laser transects extended from edge to edge, crossing the core. We collected data on 10 analytes: lithium (^{7}Li), boron (^{11}B), magnesium (^{24}Mg), calcium (^{43}Ca), manganese (^{55}Mn), copper (^{65}Cu), zinc (^{66}Zn), rubidium (^{85}Rb), strontium (^{86}Sr), barium (^{138}Ba), and lead (^{208} Pb) and. An in-house standard of $CaCO_3$ pellet (Limburg et al., 2015), NIST 612 and MACS-3 (USGS, 2013) were used as standards and were run after every 3-5 otoliths. The trace elements concentrations were analyzed as ratios with Ca (Me/Ca, where Me represents a metallic element), and data were converted to concentration ratio based on measurements of the NIST 612 standard. Elemental ratios are presented in mmol mol^{-1} (Sr, Mg and Mn) or μmol mol^{-1} (Li, B, Cu, Zn, Rb, Ba, and Pb).

Scanning X-ray fluorescence microscopy (SFXM)

We analyzed otolith thin sections by scanning x-ray fluorescence microscopy (SXFM) (n = 15) at the Cornell High Energy Synchrotron Source (CHESS) in Ithaca, NY (**Supplementary Table 4. S1**). This method is based on the use of high-energy X-rays generated by a synchrotron, as described in Limburg et al. (2011). In summary, a monochromator produces a 16.1 keV X-ray beam that is uniformly focused on a spot from 18 to 100 μm, contingent to the resolution desired and the area of the otolith surface. The data collected were calibrated based on an in-house standard prepared with compressed otolith powder (Limburg et al., 2011). Spectral analysis was

performed by using a Python multichannel analyzer - PyMCA (Solé et al., 2007) and software developed at CHESS in order to visualize the mass fractions of elements and generate 2D-elemental maps.

We compared the elemental maps of fish collected before and after "the Blob" (Bond et al., 2015) to test for a potential anomalous chemical signal at the edge of the otolith. This event reduced the primary productivity of surface waters, which led to dramatic changes in the distribution and biomass of several marine species from Alaska to Baja California (Cavole et al., 2016) and potential effects in the deep sea community.

SIMS analysis – Fish thermal history reconstruction using otolith $\delta^{18}O$

In situ $\delta^{18}O$ values were measured from the core of the otolith (i.e., the fish's larval stage) to the edge (i.e., the fish's adult stage) by using secondary ion mass spectrometry (SIMS) (n = 10) representing at least one specimen of each of the species previously analyzed by the LA-ICPMS (**Supplementary Table 4. S1**). Otoliths were cleaned in methanol and mounted on epoxy resin in aluminum rings together with reference materials for isotope measurements. Samples were polished progressively using silicon carbide grinding papers (600, 800, 1200 grit sizes) to flatten the otolith surface to the μm scale. Polished sections were sonicated in methanol, dried, and gold coated. Otolith sections were examined visually with optical microscopy (Olympus BX51, USA). Pictures were taken at 100, 200 and 400x total magnification using transmitted and reflected light to assist in location of analytical spots for the isotope measurements at the otolith's surface.

Oxygen isotope compositions across the otolith sections were measured using the Cameca IMS-1290-HR ion microprobe at the W.M. Keck Foundation Center for Isotope

Geochemistry, UCLA, during two analytical sessions (May-2019, Nov-2019). A Cs^+ primary ion beam of ~2 nA (Nov-2019) or ~3 nA (May-2019) was rastered (5×5 μm^2) over the sample surface (Gaussian beam, ion probe pits of ~10 μm). A normal-incidence electron flood gun was used for charge compensation. Following 30 s (May-2019) or 45 s (Nov-2019) of pre-sputtering and subsequent beam centering routines, measurements were made by simultaneously collecting $^{16}O^-$ and $^{18}O^-$ using two Faraday cups in the multicollection detector array. Data were acquired in 6 (Nov-2019) or 10 (May-2019) cycles; counting time for each of the cycles was 10 s. Mass resolving power was set to 2500 for both sessions.

To correct for instrumental mass fractionation (IMF) and to monitor instrumental drift, in-house reference materials (Joplin calcite, $\delta^{18}O$ = 5.8 ‰ and optical calcite $\delta^{18}O$ = 11.1 ‰ (Shiao et al., 2017), relative to Vienna Standard Mean Ocean Water (VSMOW)) were measured throughout the analytical sessions. The average isotope ratio of the reference material measured throughout that day was used to correct for IMF when no instrumental drift was detected over the course of 24 hrs. However, in the case where instrumental drift was observed, a standard-unknown-standard bracketing approach was applied. The reproducibility (2 standard deviation) of $\delta^{18}O$ values of reference materials was: Joplin calcite, 0.4 ‰, over two days; optical calcite, 0.3 - 2.0 ‰, range of values for several brackets.

Measurement errors are given as 2σ and reflect both the in-spot measurement precision (2 standard error) for each analysis and the reproducibility (2 standard deviation) of standard measurements on the analysis day. Data are reported as δ values in parts per thousand (permil; ‰) relative to VSMOW, (**Eq. (1)**).

$$\textbf{Eq. 1} \qquad \delta^{18}O = 1000 * \left(\frac{\frac{^{18}O}{^{16}O}_{sample}}{\frac{^{18}O}{^{16}O}_{VSMOW}} - 1 \right)$$

Habitat temperatures were estimated from $\delta^{18}O$ values according to the equations presented by Høie et al. (2004) (**Eq. (2) and (3)**), based on otolith carbonate chemistry. Since there were no $\delta^{18}O$ values recorded for seawater ($\delta^{18}O_{sw}$), we calculated it based on the outermost $\delta^{18}O$ values of each otolith, which were presumed to reflect the near-bottom temperature recorded by CTD-O_2 sensors (Sea-Bird Scientific, Bellevue, WA, USA) at the time of fish capture. For the giant sea bass, the temperature at the time of fish collection was estimated based on the World Ocean Atlas 2018 database (**Supplementary Table 4. S1**):

Eq. 2 $$\alpha = \frac{\delta^{18}O_{otolith}+1000}{\delta^{18}O_{seawater}+1000}$$

Eq. 3 $$1000 \ln \alpha = 16.75 \left(\frac{1000}{T}\right) - 27.09$$ (Høie et al., 2004)

We replicated $\delta^{18}O$ values at points at similar distances from the core, and the general trend of increasing $\delta^{18}O$ values was consistent for both growth axes. We aligned each otolith $\delta^{18}O$ value with a calendar date based on the counting of daily growth increments (short-lived species) or annual rings (long-lived species) from the otolith core to the edge of each $\delta^{18}O$ point.

We estimated the age of our fishes by counting the number of clear opaque rings in long-lived species with previously validated annual rings (Hunter et al., 1990; Kline et al., 1996; Allen and Andrews, 2012) and by counting the number of marked daily growth increments in short-lived species. For the daily growth increments, otolith sections were examined using transmitted light microscopy at 400x magnification and the microscope focus was frequently adjusted in order to discriminate daily rings from subdaily rings (Campana and Jones, 1992).

Data analyses for thermal history reconstruction were performed using R (R Core Team, 2015) and figures were generated using the package *ggplot2* (Wickham 2016) and *ggpubr* (Kassambara 2020).

SIMS analysis - otolith $\delta^{34}S$

Sulfur isotopic analysis was performed in four otoliths from a subset of species captured under the most extreme low oxygen conditions (Dover sole, rubynose brotula, black brotula and bearded goby) using the Cameca IMS-1290-HR ion microprobe at the W.M. Keck Foundation Center for Isotope Geochemistry, UCLA. A ~4 nA Cs^+ primary ion beam focused to a ~10 μm analysis spot on the sample was used, generating secondary $^{32}S^-$ and $^{34}S^-$ to be collected simultaneously with an off-axis Faraday cup and the axial electron multiplier, respectively. A normal-incidence electron gun was used for charge compensation during the ion probe analysis. Since there is no proper matrix-matching standard for sulfur isotopes in otoliths, measured raw $^{34}S/^{32}S$ ratios were simply compared to the first spot analysis of each sample, which is located in the core, and per-mil deviations were then calculated:

$$\delta^{34}S = \left[\frac{\left(\frac{^{34}S}{^{32}S}\right)_m}{\left(\frac{^{34}S}{^{32}S}\right)_{first-spot}} - 1 \right] \times 1000\ (‰)$$

The reported uncertainties are two standard errors of the mean. It should be noted that $\delta^{34}S$ values should not be compared between different samples and does not reflect the true sulfur isotopic compositions of the otoliths. Instead, they should only be interpreted as a relative change to the sulfur isotopic composition in the core of an otolith.

Statistical analysis

Principal coordinate analysis

Using a Principal Coordinate Analysis PCoA, we tested if otolith elemental composition (average Me:Ca ratios) and the environmental conditions at the time of fish capture (temperature, salinity, oxygen and depth) enabled discrimination among taxonomic groups (seven species) and/or collection site (Namibian shelf, Southern California Bight and Gulf of California OMZs and surface waters off the Peninsula of Baja California). The variables were standardized using the square root of the average Me:Ca, prior to computing the distance matrix. A dissimilarity matrix was constructed based on the "Gower" method (Gower, 1966). In order to fit Me:Ca ratios onto an ordination plot, we projected the points into vectors that have maximum correlation with corresponding trace elements, using envfit function (vegan Package in R). Confidence intervals (CI) of 95% were used to assess the overlap between species or sampling areas and to better visualize group separation or overlap between the different species-region combinations; the further the distance between two groups, the greater the dissimilarity.

Flow duration curves to determine the duration of hypoxia events in fish life

We performed an analysis known as "flow duration curve" (fdc) to assess the history of hypoxia recorded in each otolith. This analysis is used in hydrology to calculate the frequency of occurrence of stream-flow discharges in a hydrologic time series (Vogel et al., 1994). The fdc analysis can be adjusted to the elemental time-series data on otolith transects (e.g., those obtained with LA-ICPMS) to estimate fish exposure to hypoxia based on chosen Mn:Ca thresholds (Limburg et al., 2015). We calculated the concentration exceedance curves (cumulative distribution functions) of otolith Mn:Ca ratios for all fishes using the "fdc" function

(hydroTSM Package in R). The flow duration curve allows us to estimate the percentage of data that exceed a certain threshold for Mn:Ca, which is presumed to correspond to the relative duration of hypoxia exposure experienced by a fish.

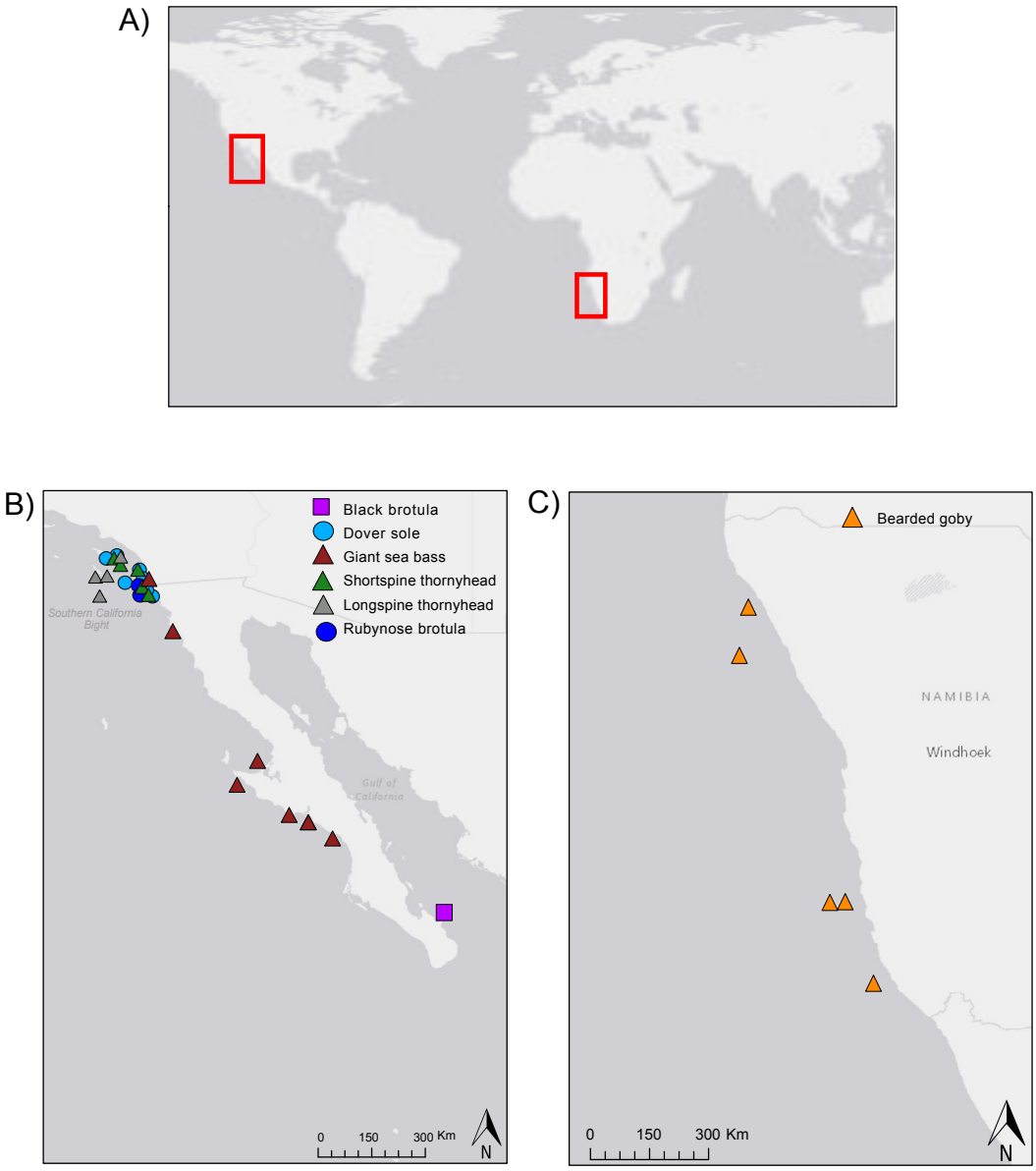

Figure 4.1. A) Fish collection sites in the Pacific and Atlantic ocean basins. B) Northeast Pacific: Dover sole, shortspine thornyhead, longspine thornyhead and rubynose brotula (Southern California Bight, U.S.), black brotula (Gulf of California, Mexico), and giant sea bass (west coast of Baja California peninsula, Mexico). B) Southeast Pacific: Bearded-goby (Namibian shelf).

Kruskal-Wallis test

We performed a non-parametric Kruskal-Wallis test by rank since most of our elemental data (Me:Ca) were not normally distributed (**Supplementary Figure 4.S1**). We tested whether there was a significant difference in average Mn:Ca and B:Ca ratios among deep-sea fishes from the Southern California Bight OMZ, the bearded goby from the Namibian shelf OMZ, and the shallow-water giant sea bass from waters off Pacific Baja California (**Supplementary Figure 4.S2**).

Results

Otoliths transect analysis - LA-ICPMS

Based on ten minor and trace elements analyzed by LA-ICPMS, the species from the Southern California Bight OMZ (Dover sole, thornyheads, rubynose brotula), the Namibian OMZ (bearded goby) and the Gulf of California OMZ (black brotula) all grouped together in a PCoA analysis (**Figure 4.2A**). The six species were living under hypoxic (< 60 μmol kg^{-1} in the Pacific, and < 90 μmol kg^{-1} in the Atlantic) and severely hypoxic conditions (< 20 μmol kg^{-1} in the Pacific, and < 45 μmol kg^{-1} in the Atlantic) during most of their lifetimes (**Supplementary Table 4. S1**). For example, the bearded goby, Dover sole, and the black brotula are all under the same ellipse (95% confidence level) (**Figure 4.2A**) and are correlated with the manganese (Mn 55) and strontium vectors (Sr 86). The Sr:Ca, Mn:Ca and Cu:Ca ratios were higher in OMZ fish (irrespective of location) than in the giant sea bass from shallower, better oxygenated waters in the Northeastern Pacific (**Figure 4.3A-D***)*.

When we incorporate the environmental factors (e.g., depth, temperature, oxygen and salinity) obtained at the time of fish collection as part of our analysis, we find similar results

(**Figure 4.2B**) but observe a larger separation between the demersal fish from the SCB OMZ and the bearded gobies from the Namibian OMZ, driven mainly by differences in temperature and depth at the time of collection (i.e., longer red arrows in **Figure 4.2B**). The giant sea bass separates out from all of the other species (**Figure 4.2A, B**). This species does not live in perennial oxygen-depleted areas, and usually experiences oxygen concentrations above 200 μmol mol^{-1} (**Table 4.1**), although hypoxic events might occur within areas shallower than 50 meters in certain years, particularly associated with red tides (Clements et al., 2020). The B:Ca, Ba:Ca and Mg:Ca ratios were higher for the giant sea bass otoliths than for the deeper water fish from the SCB, the GOC, and the Namibian shelf OMZs (**Figure 4.3F-H***)*.

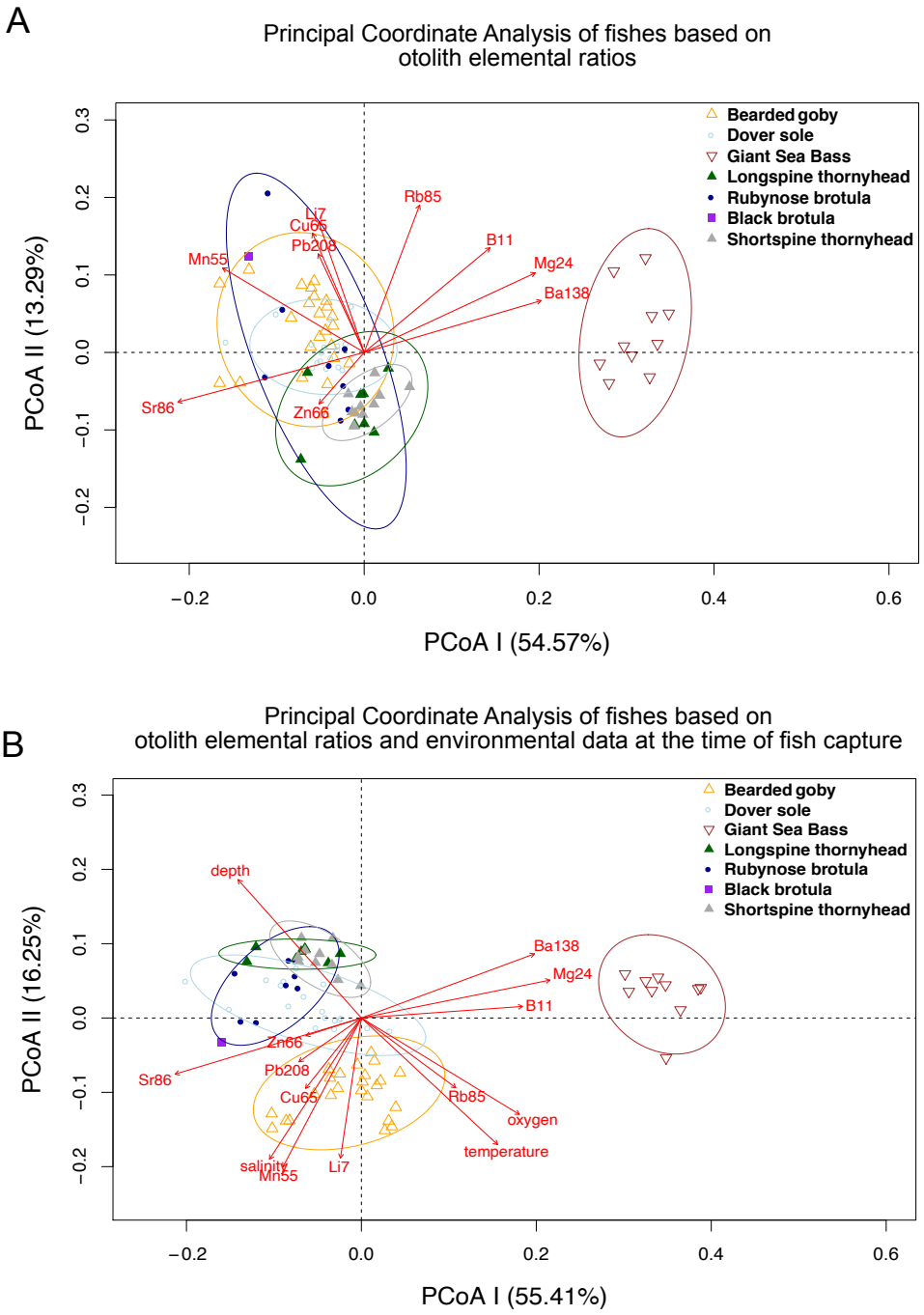

Figure 4.2. Principal Coordinate Analysis (PCoA) of microchemistry data from fish otoliths (n = 79). Each symbol represents an average elemental ratio (Me:Ca) over the lifetime of the fish (i.e., birth-to-death transect of the otolith). Environmental vectors (red arrows) are included to indicate (A) relationships between trace element ratios (Me:Ca) and PCoA axes and (B) relationships between trace element ratios (Me:Ca) and environmental factors (e.g. depth, temperature, salinity and oxygen at the time of fish collection) with PCoA axes.

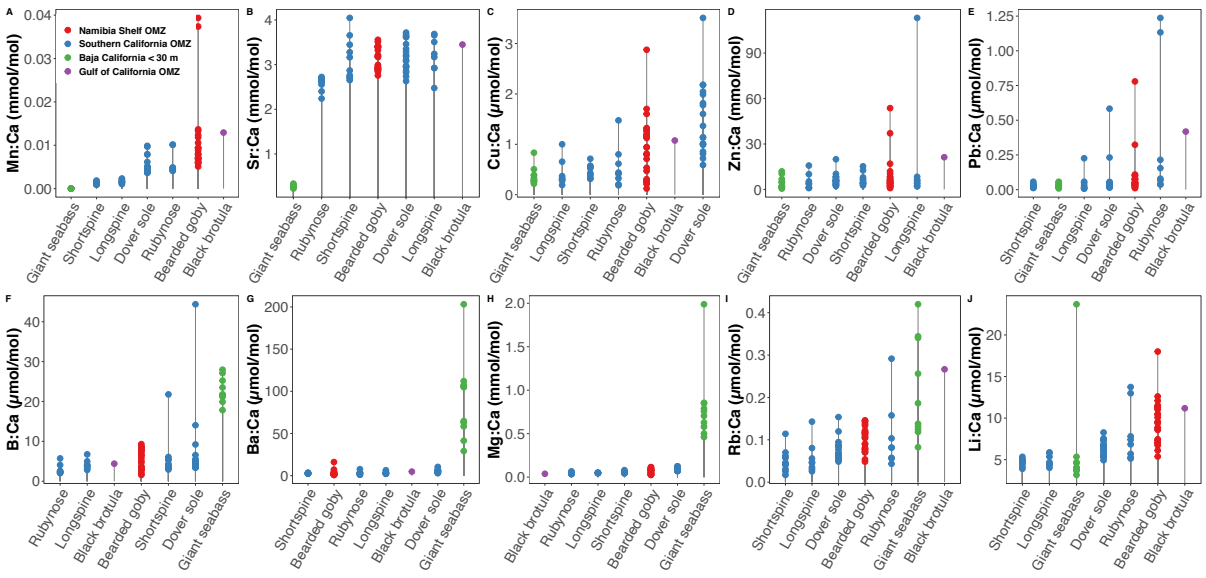

Figure 4.3. Elemental ratios for marine fish species. Each dot represents the average elemental ratio (Me:Ca) over the life of the fish (i.e., birth-to-death transect of the otolith). The blue dots correspond to fishes from the Southern California Bight OMZ, the purple dot is one black brotula specimen collected with a ROV from the Gulf of California OMZ, the red dots are the bearded gobies off the Namibian shelf OMZ, and the green dots are the shallow giant sea bass off the Baja California Peninsula.

Flow duration curves

Flow duration curves (fdc) were used to calculate the duration of hypoxia exposure based on the Mn:Ca otolith transects. Using a hypoxia threshold of 0.01 mmol mol^{-1} Mn:Ca (**Figure 4.4**) (similar to the hypoxic thresholds used for coastal species by Limburg et al. 2015), we found that only the bearded gobies from Namibia and the black brotula from the GOC have experience severe hypoxia exposure (**Table 4.2**). Using a lower hypoxia threshold of 0.0001 mmol mol^{-1} Mn:Ca (**Figure 4.4**), we observed that most of the deep-sea fish spend the majority of their lives under hypoxic conditions (**Table 4.2**). Conversely, it appears as though the giant sea basses we sampled never experienced hypoxia (based on thresholds we defined). When examining the duration of hypoxia exposure among individuals, the fish that seem to have experienced the most prolonged exposure to hypoxia were the black brotula from the GOC (oxygen concentration at collection site = 1.7 μmol kg^{-1}; Gallo et al., 2019), and two female bearded gobies from the

northern stations of Namibia (oxygen concentration = 23.56 μmol kg^{-1}). These females are noted in **Figure 4.3A** as outliers for average Mn:Ca ratios.

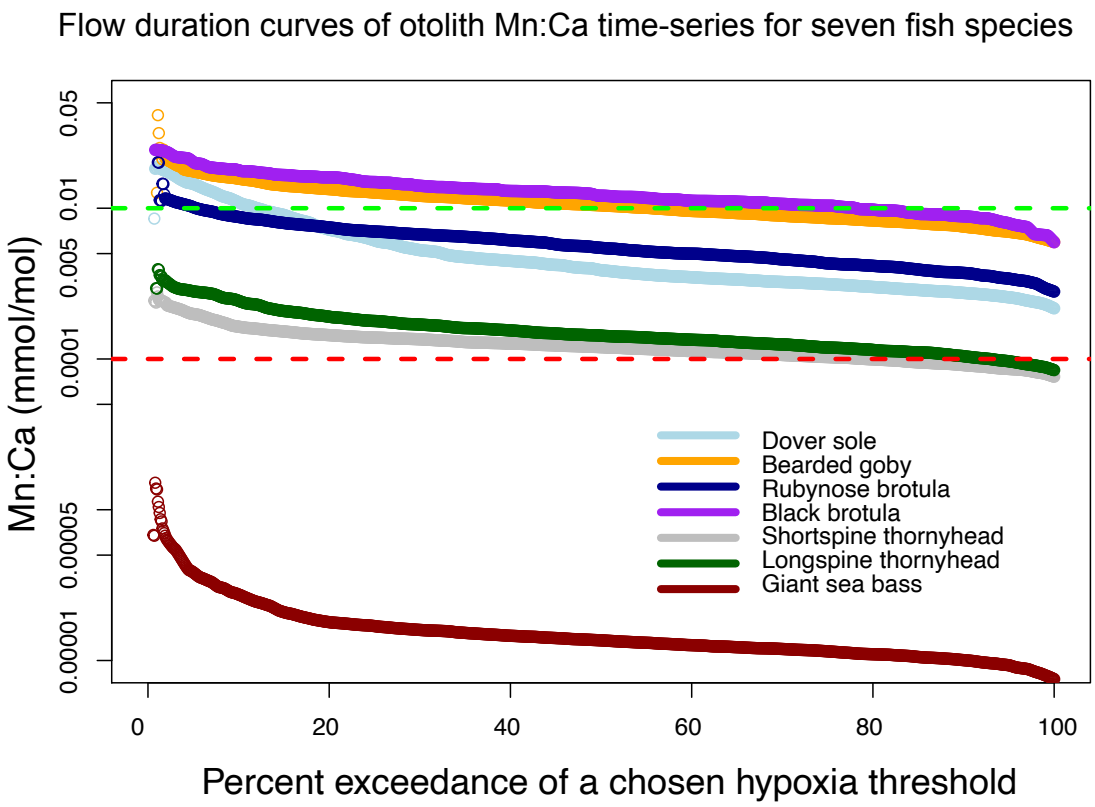

Figure 4.4. Mn:Ca (mmol mol^{-1}) exceedance curves for Dover sole, bearded goby, rubynose brotula, black brotula, shortspine thornyhead, longspine thornyhead and giant sea bass above 0.01 mmol mol^{-1} Mn:Ca ratios (dotted green line) and above 0.001 mmol mol^{-1} Mn:Ca ratios (dotted red lines) hypoxia thresholds. Exceedance curves are calculated as measurements of Mn:Ca above a chosen Mn:Ca threshold, divided by the birth-to-death otolith transects.

Spatial analysis of OMZ fish otoliths – SXFM

The 2-D elemental maps allowed us to observe fine-scale patterns in environmental conditions throughout the lifetime of deep-sea fish, including changes during "the Blob" (**Figure 4.5**). Potentially related with the fish exposure to hypoxic conditions, Fe:Ca was higher outside the core region for both longspine thornyheads, corresponding to adult stages after settlement in deep waters (~ 600 m), although very low concentrations for this element make visualization

difficult. Out of eight bearded gobies analyzed, one individual (#3269), a territorial male (identified by its morphological features) collected at 280 m deep and 23.53 μmol kg^{-1}, showed higher Fe:Ca at the core of the otolith. The longspine thornyheads, shortspine thornyheads, Dover soles and the one black brotula examined here presented well-defined Zn:Ca rings in their otoliths.

We observed subtle differences at the edges of the otoliths of the longspine thornyhead, shortspine thornyhead and Dover sole collected in July 2014 ("Pre-blob LST 705 m"; "Pre-blob SST 705 m"; "Pre-blob Dover sole 698 m") compared to specimens collected in September 2015 ("Post-blob LST 703 m"; "Post-blob SST 703"; "Post-blob Dover sole 703 m") (**Figure 4.5**). For example, Br:Ca was higher and Sr:Ca was lower at the edge of the otoliths collected after "the Blob".

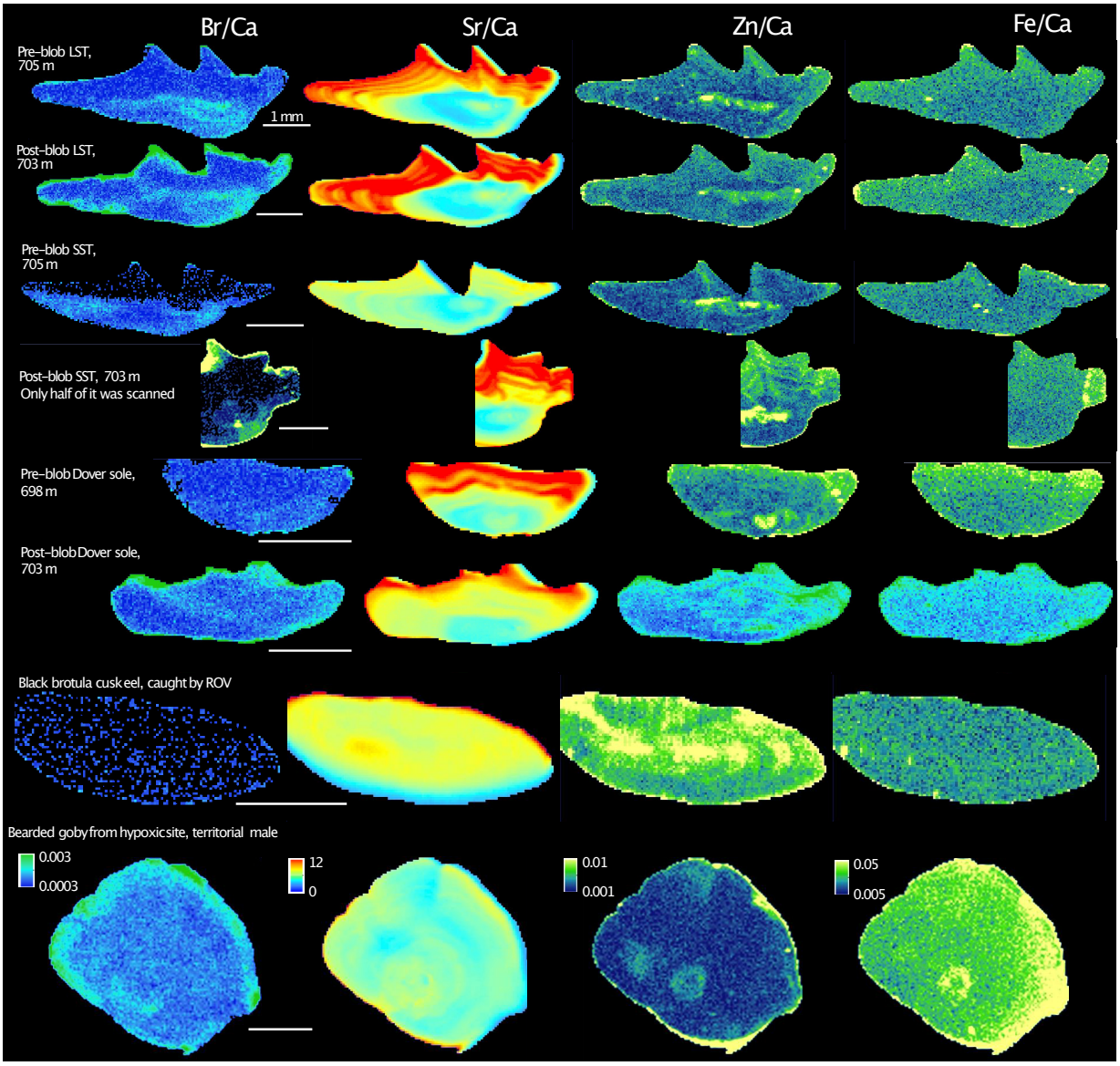

Figure 4.5. Two-D elemental maps of otolith sections from OMZ-dwelling fishes analyzed by SXFM. Bromine to calcium (Br/Ca), strontium to calcium (Sr/Ca), zinc to calcium (Zn/Ca) and iron to calcium (Fe/Ca) maps are presented for a shortspine thornyhead (SST), longspine thornyhead (LST) and Dover sole collected in Southern California Bight before and after the NE Pacific 2013-2015 "Blob", for a black brotula collected in the Gulf of California and for a bearded goby collected in Namibian shelf.

Thermal history reconstruction based on otolith $\delta^{18}O$

The thermal history reconstruction based on $\delta^{18}O$ allowed us to: 1) assess whether temperature played a role on patterns of elemental composition of fish otoliths from the NE Pacific and SE Atlantic OMZs (**Figure 4.2**), 2) infer at which life stages, and for how long, the deep-sea fishes were living under colder waters characteristic of OMZs, 3) better understand the patterns of ontogenetic migration during the life cycle of deep-sea species and the shallow-water giant sea bass.

Overall, the relative changes in seawater temperatures calculated across each fish's otolith (representing lifetime archives) were sufficiently pronounced to produce distinct otolith $\delta^{18}O$ signatures. The $\delta^{18}O$ values ranged from 28.41 to 36.34 ‰ relative to VSMOW for all deep-sea fish, and from 27.99 to 31.85 ‰ for the giant sea bass (**Table 4.3**). The standard errors (2σ) of individual point measurements ranged from ± 0.31 to ± 0.94 ‰. The highest values for otolith $\delta^{18}O$, which correspond to lower habitat temperatures and OMZs-CMZs residency, were consistently observed for all deep-sea fish, with the exception of rubynose brotula (**Figure 4.6**). Fishes from OMZs generally exhibited a $\delta^{18}O$ pattern that suggests a pelagic larval phase in warmer, shallower waters, followed by a progressive ontogenetic migration into colder, deeper waters. For example, the longspine thornyhead may have experienced high temperatures at the larval stage (~ 23 °C), before settling at greater depths in colder waters (~ 5 °C), where it remained for the rest of its life (**Figure 4.6A**). This pattern was less prominent for the Dover sole, rubynose brotula and black brotula, since they seem to be moving more frequently in the water column at younger ages, before being consistently exposed to cooler conditions as adults within the OMZ (**Figure 4.6B, E-F**).

The shortspine thornyhead showed a thermal history that suggests cyclical movements up and down the continental margin throughout its relatively long ontogeny (40 years) (**Figure 4.6C**, **Table 4.3**). Off the Namibian shelf, we analyzed two bearded goby otoliths that exhibited markedly distinct habitat temperature trends. The bearded goby #3081 was a sneaker male that underwent a large temperature variation of almost 18 °C (**Figure 4.6G**), whereas the bearded goby #3044, a female, seems to have been exposed to much smaller temperature variation (~10°C) (**Figure 4.6H**). The thermal history reconstruction for two giant sea bass specimens (**Figure 4.6I-J**) revealed a similar trend to that of the shortspine thornyhead of recurrent changes in depth, although the giant se bass do not live in the deep OMZs-CMZs.

Sulfur stable isotopes in otoliths

The $\delta^{34}S$ in the otoliths was measured to potentially indicate exposure to severe hypoxia, or anoxia, in four of our deep-sea fish species. The specimens analyzed via secondary ion mass spectrometry (SIMS) exhibited patterns of variation in $\delta^{34}S$ different from reconstructed temperatures based on $\delta^{18}O$ along the same otolith transects (blue lines on **Figure 4. 6B, D, F, H**). The bearded goby and black brotula presented the highest $\delta^{34}S$ variability of 9.95 and 10.86 (‰ vs. CDT) respectively, whilst the Dover sole and rubynose brotula presented the lowest $\delta^{34}S$ variability of 7.87 and 4.77 (‰ vs. CDT). There is an inverse relationship between the otolith $\delta^{34}S$ and the reconstructed habitat temperature in the Dover sole and black brotula, while the otolith $\delta^{34}S$ and the reconstructed habitat temperature in the rubynose brotula and bearded goby seem to track each other.

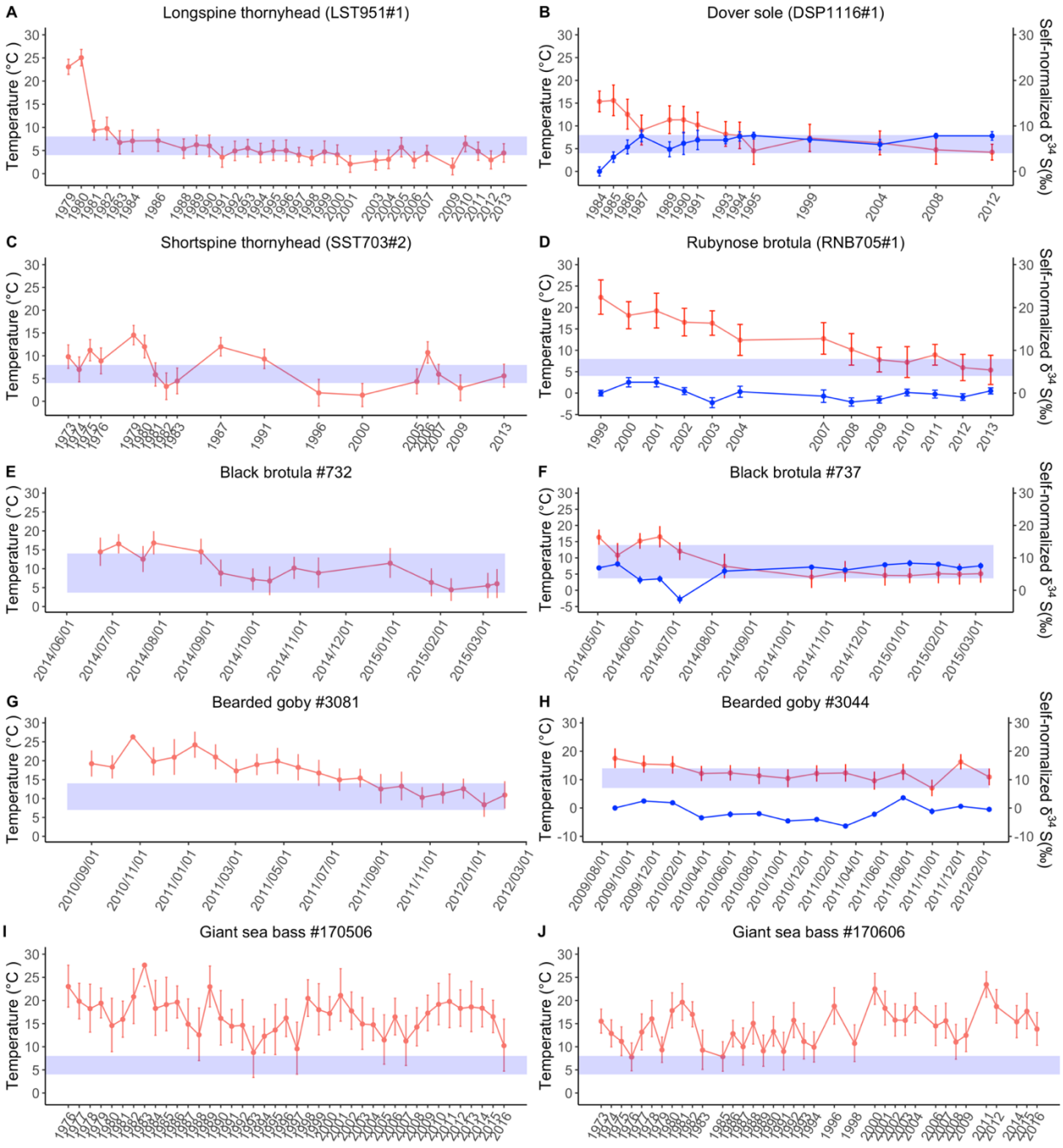

Figure 4.6. Thermal history reconstruction for fishes based on $\delta^{18}O$ values from otoliths (red line). Transects of $\delta^{34}S$ (blue lines) compared to estimated temperatures are provided for four individuals. For all fishes, SIMS spots were aligned with the corresponding calendar date estimated at an annual and/or daily resolution. For secondary y-axis, self-normalized $\delta^{34}S$ means that all values were normalized to the first data point of each otolith. Blue rectangles indicate the temperature ranges of OMZs-CMZs in each ecosystem.

Discussion

Similar elemental composition in fish otoliths from distant OMZs

Our results suggest that fishes that live in OMZs from the NE Pacific and SE Atlantic oceans experience similar environmental and physiological conditions that are reflected in distinctive minor and trace elemental composition in their otoliths (**Figure 4.2**). It is possible that the biogeochemistry of the OMZs-CMZs waters modulate the amount of minor and trace elements dissolved in seawater as well as fishes' physiological responses to extreme hypoxia. Indeed, the California and Benguela Current Ecosystems are two of the four major Eastern Boundary Upwelling Systems (EBUS) in the world (Mackas et al., 2006; Chavez and Messié 2009). EBUS are very productive systems (Carr, 2002), with OMZs-CMZs characterized by similar biogeochemical mechanisms (remineralization processes leading to high DIC and low O_2) (Paulmier et al. 2011) and by similar redox mechanisms that regulate the bioavailability of metals such as iron, copper and manganese (Morford and Emerson, 1999; Hopkinson and Barbeau 2007).

The patterns of elemental composition in otoliths were markedly similar among the Dover sole *Microstomus pacificus* from the Southern California Bight, the bearded goby *Sufflogobius bibartus* from the Namibian shelf and the black brotula *Cherublemma emmelas* from the Gulf of California (**Figure 4.2A**), despite having different life-history traits. Off the coast of California, Dover sole can grow to ~ 50 cm in length, live up to 58 years (estimated), and undergo a remarkable ontogenetic migration from surface waters into deeper waters (Hunter et al., 1990). Ninety-eight percent of their spawning biomass is found at depths of 640 -1000 m (Hunter et al., 1990), where extremely low oxygen levels can depress growth potential (Brodziak and Mikus, 2000). The bearded goby is endemic to west Africa (from South Africa to southern

Angola), occur from the shore to 400 m depth (Staby and Krakstad, 2006), are short-lived (6 years) (Melo and Le Clus, 2005), and undergo diel vertical migrations from hypoxic and anoxic seabed into more oxygen-rich midwaters (Utne-Palm et al., 2010). The abundance of bearded gobies seems to increase with the decrease in oxygen concentration (Salvanes et al., 2015). This species can withstand anoxia and hydrogen sulfide through metabolic depression and high capacity for anaerobic ATP production (Utne-Palm et al., 2010), and can perform rapid escape responses after a five-hour complete anoxia exposure (Salvanes et al., 2011). The one black brotula analyzed herein was caught in the lowest oxygen concentrations measured in this study ($O_2 = 1.73\ \mu mol\ kg^{-1}$), and individuals were frequently observed with their heads buried in the sediment (Gallo et al., 2019). Black brotulas are present in high densities in the southern Gulf of California (Zamorano et al., 2014), are short-lived (i.e., 5 years) (Morales-Azpeitia et al., 2018), and are dominant members of the demersal fish community under the most hypoxic conditions (Gallo et al., 2020).

Notably, the bearded gobies on the Namibian shelf, and the Dover soles and the longspine thornyheads in the Southern California Bight appear to associate with microbial mats on the ocean floor. For the bearded goby, fatty acid and stable isotope signatures in tissues have revealed that the diatom- and bacteria-rich sulphidic sediments play an important role in their diet (Van der Bank et al, 2011). In the California Current Ecosystem, frequent remotely operated vehicle (ROV) observations of Dover soles and longspine thornyheads resting on microbial mats at methane seeps at depths ~ 720-1020 m (Grupe et al., 2015; Levin et al. 2016) indicate that they can withstand suboptimal conditions and potentially feed on benthic invertebrates adapted to these microhabitats. Alternatively, microbes present may detoxify the sulfur, making the environment more habitable. Although the mechanisms driving the common elemental

fingerprints are unclear, the close contact of Dover soles, bearded goby and longspine thornyhead with the substrate might influence their otolith microchemistry similarly.

The shortspine thornyhead *Sebastolobus alascanus* and longspine thornyhead *Sebastolobus altivelis* displayed similar elemental signatures to one another (**Figure 4.2A**). These species are sympatric in the northeast Pacific and inhabit depths of 600 to 1000 m. Thornyheads have long lifespans, of over 100 years in the shortspine and over 45 years in the longspine thornyheads (Butler et al., 1995; Kline 1996; Kastelle et al., 2000). Lastly, the rubynose brotula, *Cataetyx rubirostris*, a small deep-sea bythid (Nielsen et al., 1999; Gibbs 1999) whose population dynamics and ecological role have remained relatively unknown, presented a variable pattern for its otolith elemental composition, with some individuals similar to the bearded gobies and Dover soles and others similar to thornyheads (**Figure 4.2A**).

All the deep-dwelling fishes' elemental signatures were significantly distinct from the giant sea bass, *Stereolepis gigas*. The giant sea bass occurs within relatively shallow waters up to ~ 30-40 m deep (Ramírez-Valdez et al., 2021). At this depth, oxygen and pH conditions vary, but values are consistently higher than those found for our OMZ fishes (**Table 4.1**). Despite the similarity of otolith chemistry among fishes from two EBUS and the one black brotula from the Gulf of California OMZ (**Figure 4. 2**), much uncertainty remains in understanding these complex ecosystems. In particular, determining the mechanisms that affect the amount of minor and trace elements in deep waters is not well understood, and it is of paramount importance to interpret the main processes responsible for their bioavailability. Despite the similarities among the OMZs off the Namibian coast, Southern California Bight and Gulf of California, such as low oxygen, pH and temperature conditions (**Table 4.1**), physiological controls might also play an important role in determining the amount of minor and trace elements that are incorporated into

the otolith matrix (Sturrock et al., 2014, 2015). Following this rationale, we hypothesize that the unique biogeochemistry of OMZs, along with similar physiological constraints related to low oxygen, pH and temperature conditions, have jointly played an important role in the final uptake of elements in these fishes' otoliths.

What processes affect the water chemistry in different OMZs?

Marine autochthonous and terrestrial allochthonous sources supply organic matter and trace elements in marine ecosystems (Dailey et al., 1993). Modern sediments accumulating beneath areas of coastal upwelling are known to have higher concentrations of organic material often enriched with minor and trace elements. Off the California coast, for instance, sediments in the nearshore basins contain up to 6% organic carbon, and in deeper basins up to 11% (Emery, 1960), while on the Namibian wide and deep shelf platform, the organic- and diatom-rich mud can contain up to 22.3% of organic carbon (Calvert and Price, 1970). In the Gulf of California, organic carbon values can be greater than 10% (Calvert, 1966).

In the Southern California Bight, the organic matter and trace elements in seawater derives largely from primary production and natural oil seepage whilst the contributions of terrestrial origin include domestic and industrial discharges, rivers, atmospheric fallout, and the erosion of shales from coastal areas (Dailey et al., 1993). Off the Namibian shelf, the sediments on the modern shelf are comprised primarily of organic matter, diatomaceous silica and calcium carbonate, and the distributions of Cu, Pb and Zn follow the distribution of organic matter and are enriched in the diatom ooze as a consequence of coastal upwelling (Calvert and Price, 1983).

These two EBUS have marine sediments produced by a reduced dilution of planktonic and skeletal materials, since the coastal region is arid or semi-arid and perennial rivers are few or

absent, and by the deposition of organic material with a short transport time from surface waters to the seabed (Calvert and Price, 1983). Thus, the bioavailability of trace elements that can be incorporated into the otoliths of deep-sea fish seems to be related to the composition of the marine seabed, which is sensitive to both changes in the bottom-water oxygen and organic carbon flux.

Manganese as a proxy for hypoxia in fish. Does it work for deep-sea species?

In the search for suitable elemental proxies for hypoxia exposure in fish, manganese is currently the most promising (Limburg et al., 2011, 2015). Manganese is bioavailable from the substrate to the water column under low oxygen conditions and has been found to occur at relatively high concentrations in the Baltic sea cod *Gadus morhua,* Baltic flounder *Platichthys flesus*, Atlantic croaker *Micropogonias undulatus*, and Yellow perch *Perca flavescens* (Limburg et al, 2011, 2015; Altenritter et al.; 2018, Limburg and Casini 2018). Compared to these estuarine and coastal species of the Atlantic Ocean, we only detected high ratios of manganese in the otoliths of the bearded gobies (Namibia) and the one black brotula (Gulf of California OMZ) whereas all other deep-sea fish from Southern California OMZ had much lower average Mn:Ca in their otoliths (**Supplementary Table 4. S2**). However, these lower than expected Mn:Ca values may be due to the lower concentrations of manganese in the Southern California Bight. At the northern range of the SCB OMZ (35°N) between 400-1000 m, manganese concentrations are extremely low at approximately 1.25 nM, which is around 10,000 times lower than in the Baltic sea (Johnson et al., 1992). Therefore, it is important to take into consideration the hypoxia characteristics specific to coastal ecosystems and enclosed seas *vs*. open OMZs. In our case, this is especially relevant for SCB, where fishes were collected between 200 and 1280 m deep,

relatively far from terrigenous input of Mn, in comparison with coastal bays, estuaries and lagoons. Despite low Mn:Ca ratios observed for all fishes in this study, all of our OMZ specimens still exhibited higher Mn:Ca than the shallower giant sea bass (**Figure 4.3A**), which is an unexpected result, since the concentration of manganese in surface waters off California (2-2.5 nM) is twice as much as the waters within its OMZ (1-1.25 nM) (Johnson et al., 1992). Dissolved manganese must be bioavailable in order to be incorporated into the otolith structure and its bioavailability may increase under reducing conditions (i.e., low O_2) (Limburg et al., 2015), thus both background concentrations, as well as elemental bioavailability, must be considered when interpreting otolith patterns.

In order to detect exposure to hypoxia in deep-sea species, the value chosen for the Mn:Ca hypoxia threshold may need to be lower than that used for coastal, estuarine and enclosed sea species. Use of both of our low (0.0001 mmol mol^{-1}) and higher (0.01 mmol mol^{-1}) manganese ratio thresholds for hypoxia suggested that black brotula, bearded gobies, rubynose brotulas and Dover soles are the species experiencing the most hypoxic conditions in their respective environments (**Figure 4.4**). For the bearded gobies, four females experienced hypoxia during most of their lifetimes. These females were captured at 23.56 μmol kg^{-1} of O_2, indicating that females may be particularly exposed to hypoxia in Namibian waters.

Other elements as proxies for hypoxia in fish. Does it work for deep-sea fish?

Other elements analyzed by LA-ICPMS that follow a similar trend to that of manganese were strontium, copper and, to a lesser extent, zinc (**Figure 4.3B-D**). Although recent literature suggests that zinc and copper appear to be mostly controlled by physiological mechanisms before being incorporated into otoliths (Hüssy et al., 2020), the fact that these elements are

enriched in the seabed with high organic matter (Calvert and Price, 1970) suggests that the environment may also play an important role in their final uptake into otoliths. The SXFM analysis (2D-elemental maps) of sectioned otoliths showed interesting results (**Figure 4.5**), complementary to the ones obtained with the LA-ICPMS transects (**Figure 4.3**). Particularly for the black brotula and the Dover sole, the 2D-elemental maps showed a clear ring pattern for Zn:Ca, which demonstrates that this element is incorporated periodically within the calcified structure (**Figure 4.5**). For the shortspine thornyhead, longspine thornyhead, and the Dover sole, although the current resolution of 2D-elemental maps for Sr:Ca (**Figure 4.5**) cannot resolve annual rings, the increasing Sr:Ca ratios from the otolith core to the edge is potentially related to the fishes' ontogenetic migration from surface waters (low salinity/warmer) to deeper waters (higher salinity/colder). Interestingly, we also observed Fe:Ca in the otolith of a bearded goby territorial male, suggesting that it has incorporated the reduced iron (Fe^{+2}) after its larval stage. Together with Fe:Ca, the Zn:Ca outer core ring suggests that this goby had spent a few weeks under very low oxygen waters. Iron and zinc elemental ratios show promise for tracking low oxygen exposures of OMZs-dwelling fishes but increased instrumental resolution in otolith mapping (i.e., dwell-time/pixel) and water analysis for trace, minor and major elements are needed to extensively test these relationships.

Which elements could be a proxy for fish exposure to low pH waters in OMZs-CMZs?

OMZs-CMZs have naturally low pH waters because microbial respiration produces carbon dioxide (CO_2) and carbonic acid (H_2CO_3) while consuming oxygen, causing pH and oxygen levels covary in these systems (Brewer and Peltzer, 2009; Paulmier et al., 2011). In the search for differences in elemental composition at different pH levels, Moreau et al (1986)

observed that manganese, zinc and strontium were 1.6, 1.3 and 1.2 higher in the opercula and scales of brook trout *Salvelinus fontinalis* in acidified lakes (pH 5.2-5.5) than in nonacidified lakes (pH 6.8-7.0). We observed higher ratios of zinc, manganese and strontium for the OMZ fishes, which coincides with Moreau et al. (1986) observations. Remarkably, we also observed lower ratios of boron in the otoliths of OMZ-dwelling fish (~5-10 μmol mol^{-1}) compared to the giant sea bass (20-30 μmol mol^{-1}) (**Figure 4.3F**). Of the boron species in seawater, borate is the dominant form incorporated in marine carbonates, and theoretically δ^{11}B and the boron concentration in carbonates should increase as seawater pH increases (Hemming and Hanson, 1992; Levin et al., 2015), as observed in planktonic foraminifera (Allen et al., 2011) and in cold-water corals (Gagnon et al., 2021). In our study, this indicates that the giant sea bass were encountering consistently higher pH waters than the deep-sea fish caught in the OMZs. Higher B:Ca ratios in giant sea bass were expected because this species lives in shallower, more alkaline waters relative to all other species analyzed herein (~ pH= 8 versus pH= 7.5), (Alin et al., 2012). Since low-oxygen conditions are correlated with acidified conditions, this may explain the significant negative correlation (R = - 0.46) between Mn:Ca and B:Ca observed in our fish otoliths (**Figure 4.S1**, in Supplementary materials). The B:Ca ratios in the giant sea bass (20-30 μmol mol^{-1}) are lower than those observed in shallow planktonic foraminifers *Globigerina bulloides* and *Globorotalia inflata* (30-80 μmol mol^{-1}) and tropical corals (400-600 μmol mol^{-1}) (Sinclair, 2005; Yu et al., 2007). Controlled experiments investigating the effect of pH and pCO_2 on otolith chemistry are scarce, limited to a diadromous species (Martino et al., 2017), early life stages (Munday et al., 2011; Hurst et al., 2012) and with the measurement of only a few trace elements (^{7}Li, ^{25}Mg, ^{43}Ca, ^{55}Mn, ^{88}Sr and ^{138}Ba). Although these studies did not detect significant variation in elemental concentrations between ambient and elevated pCO_2 treatments, they did

not quantify boron. Our analysis suggests that boron, together with manganese, may work as indicators of fish exposure to low-pH and low-O_2 typical of OMZs-CMZs, but future experimental work is necessary to test the B:Ca - pH dependency. If this dependency relationship is validated in fish otoliths, this will have extensive applications for estimating pH histories of wild fish and is particularly important in places like the SCB. In this region, an upwelling within 50 km of the coast brings relatively cold, salty, nutrient-rich, oxygen-deficient, and low-pH waters from depth to the surface (Sverdrup, 1938; Feely et al., 2008) and there is an ongoing and rapid pH decrease over the past 30 years, at rates of 0.001-0.0015 yr^{-1} at 500 m depth (Meinvielle and Johnson, 2013).

Could Marine Heat Waves alter the chemistry of otoliths?

The differences observed at the edge of fish otoliths collected before and after "the Blob" are intriguing, especially for the redox sensitive element bromine (**Figure 4.5**). Since "the Blob" was a superficial phenomenon and has affected water temperatures down to ~ 100 m deep (Bond, et al. 2015), its potential effects in OMZ fishes would be mainly through indirect pathways affecting oxygen levels and/or food availability at depth. For example, during the Blob, primary productivity at surface was reduced (Gómez-Ocampo et al., 2018), which would decrease microbial remineralization process and thus increase O_2 levels inside the OMZs, similarly to what occurs during El Niño years. Indeed, oxygen levels were higher in 2015 at least down to ~ 100 m deep (Brodeur et al., 2019). Reductions in phytoplankton biomass in surface waters likely also reduced food inputs to deeper habitats, thus affecting the metabolism of higher trophic levels, including thornyheads. How the interaction of elevated oxygen levels and reduced food

sources interactively affected the chemistry of deep-fish otoliths remains unclear and could be the focus of future research.

Thermal history reconstruction based on $\delta^{18}O$ and its relationship with sulfur isotopes

Using otolith $\delta^{18}O$ ratios, we reconstructed the habitat temperature experienced by each species in this study. To the best of our knowledge, the lifetime temperature variation experienced by these species had never been estimated before. This is mainly because of the impracticability of tagging deep-sea fish, which can suffer barotrauma, or due the fact that large species are often hard to find because of their low biomass, such as the giant sea bass. In addition, tagging methods cannot track individuals for long periods of time (e.g., many decades) while otolith $\delta^{18}O$ can provide finer temporal resolution to depict the thermal range of exposure and the thermal preferences of any fish species.

The thermal histories of our species were considerably different, especially for the bearded gobies from Namibia and the demersal fish from SCB, suggesting that indeed low oxygen conditions and potentially the low pH waters typical of OMZs-CMZs (blue rectangles on **Figure 4.6**) led to the resemblance of their otolith elemental composition (**Figure 4.2A**).

Although thornyheads support a commercially important fishery, there is little information about their ecology, growth rates, movement patterns, life histories and capacity to withstand fishing pressure (Jacobson and Vetter, 1996; Pearson and Gunderson, 2003; Echave 2017). Our reconstruction of local temperatures using the otolith of longspine thornyhead is consistent with literature on their biology and life history (**Figure 4.6A**). Longspine thornyheads are oviparous and produce gelatinous egg sacs that float to the surface waters where hatching and larval development occurs at warmer water temperatures. Juveniles of longspines remain in

surface waters for approximately 20 months, prior to their settlement at depths between 600 and 1200 m deep (Moser 1974; Wakefield 1990); as adults, they are OMZ specialists, found only in deep waters (600-1400 m) (Jacobson and Vetter, 1996). However, the estimated habitat temperature observed for the shortspine thornyhead was somewhat variable, suggesting at least three major migrations into different water depths for this individual (**Figure 4.6C**). This species is believed to settle at ~ 100 m on the shelf and perform a relatively steady ontogenetic migration into deeper waters (Moser, 1974; Jacobson and Vetter, 1996). For shortspine thornyhead, previous research has debated its main bathymetric demography, finding centers of abundance at shallower waters at approximately 180-440 m (Moser, 1974) or at 600-1000 m (Jacobson and Vetter, 1996). The estimated habitat temperature herein reconciles both views, as this species can remain for longer periods of time either at shallower or deeper depths.

The estimated habitat temperature for the Dover sole (**Figure 4.6B**) agreed with the known life-history strategy for this species; they are born in shallow waters of the continental shelf and, as they grow, they gradually move down the continental slope in deeper waters to reproduce (Jacobson and Hunter, 1993).

The short-lived specimens observed were the black brotulas from the Gulf of California (< 1 years), the bearded gobies (~2-3 years) from the Namibian shelf and the rubynose brotulas (~ 10 years) from Southern California Bight. Information about the population dynamics for the black brotulas and rubynose brotulas are scarce (Gibbs, 1991; Morales-Azpeitia et al., 2018; Gallo et al., 2019,), despite their incredible abilities to withstand hypoxic and conditions closer to anoxia. The rubynose brotula is believed to spend its larval and juvenile stages in the deep scattering layer (300-500 m deep) before moving to the benthos (> 800 m) as adults (Gibbs, 1991, 1999). This assumption does not match our temperature data (**Figure 4.6D**), which

indicated that this species undergoes an ontogenetic migration from surface into deeper waters. The two black brotulas presented similar ranges of habitat temperature from around 4 °C to 16.5 °C (**Figure 4.6E-F**). These temperature ranges match recent data that observed eggs and larvae at surface waters and juveniles and adults up to ~ 1000 m deep (Zamorano et al., 2014). This species likely plays a crucial ecological role, since its larvae have been reported as the most abundant during an extensive exploration of the continental slope off the Mexican Pacific margin (Zamorano et al., 2014). Recently, both the black brotula and rubynose brotula were observed at 1,097 and 2,000 m around Vancouver Island, in British Columbia, Canada (Hanke, 2015), revealing how little we still know about the basic biology of these species.

Bearded gobies reproduce on the seabed in nests, usually during spring and summer in the southern hemisphere. Territorial males are assumed to remain at the bottom for parental care of the eggs longer than females and sneaker males as experiments have demonstrated that territorial males cared for egg clutches for at least six days at 17 °C (Skrypzeck et al., 2014), whereas assumed sneakers that have similar morphology of females (Salvanes et al., 2018) would be "free" to undertake diel vertical migrations and thus visit better oxygenated upper waters. After hatching, larvae and juvenile are pelagic and abundant in the upper 50 m layer, experiencing between 16 and 22.5 °C in the north of Namibia (O'Toole, 1978). As the juveniles grow and mature, they move further offshore to the seabed to reproduce, usually under very low oxygen conditions (Salvanes et al., 2015; Salvanes et al., 2018). This life-history strategy agrees with the thermal history reconstructed based on otolith $\delta^{18}O$ values (**Figure 4.6G-H)**. Intriguingly, we also observed a much higher temperature exposure for the sneaker male (#3081). This individual was collected during the strong Benguela Niño in 2010/2011. This event began in November 2010, lasted five months, and peaked in January 2011, resulting in

monthly water temperatures anomalies up to 4 °C above the average (Rouault et al., 2018). This El Niño imparted the lowest otolith $\delta^{18}O$ values and highest reconstructed temperatures of up to ~ 25 °C on this male's otolith (#3081). The female goby (#3044) was mature at the time of collection (3 years old) and her otolith did not indicate such an anomalous warm pattern, suggesting that it may remain closer to the substrate, perhaps to reproduce under low temperatures and oxygen conditions. This is also supported by the highest Mn:Ca ratios observed for two female gobies among all 24 gobies analyzed (**Figure 4.3A**).

The giant sea bass were the oldest individuals analyzed, thus allowing the reconstruction of habitat temperature back to the early 1970s. Specimen #170506 showed a maximum temperature (~ 27°C) in the year 1983, while the specimen #170606 exhibited maximum temperatures in the years 1999 and 2011. These patterns were potentially associated to the very strong El Niño events of 1983 and 1997/98. These individuals were caught off the coast of Guerrero Negro, in Baja California Sur (Mexico). Fishermen have observed individuals at shallower bays, which can explain the relatively warm temperatures for some years in the otolith record. Overall, otoliths from both individuals presented high temperature variability across years, with an overall negative trend over time for specimen #170506 and a positive trend for #170606 (**Figure 4.6I-J**).

Reconstructing the thermal histories of these fishes can provide a baseline for future comparisons of fish exposed to warmer ocean conditions due to climate change. Because the deep-sea fish analyzed here are believed to be less motile, they may accurately reflect the environmental temperatures of the deep, although the shortspine thornyhead is relatively mobile.

Finally, we explored otolith $\delta^{34}S$ in an attempt to track suboxic and anoxic events. Under normoxic conditions, the S in the otoliths is obtained from marine sulfate SO_4^{-2} ($\delta^{34}S \approx 21‰$),

through the diet ($\delta^{34}S \approx 18‰$) (Limburg et al. 2015). However, under suboxic or anoxic conditions, sulfate (SO_4^{-2}) is reduced by bacteria, and the resulting hydrogen sulphide (H_2S) is depleted in ^{34}S (Limburg et al. 2015). This low $\delta^{34}S$ signature can end up in the otoliths of fish exposed to anoxic waters, and also through dietary sources. In Limburg et al (2015), differences up to 13 ‰ were observed for the Atlantic croaker *Micropogonias undulates,* consistent with the hypothesis that low otolith $\delta^{34}S$ could be a proxy for fish exposure to suboxic/anoxic conditions or for the consumption of prey that were exposed to these conditions. Herein, we did not observe a clear trend of low otolith $\delta^{34}S$ in presumed suboxic/anoxic conditions for the species from the SCB. For example, the $\delta^{34}S$ in the rubynose brotula otolith remained moderately stable across the entire transect and did not show the expected decline when the fish was inside the OMZ. For the Dover sole and black brotula, we observed an inverse relationship between $\delta^{34}S$ and temperature (i.e., low $\delta^{34}S$ in high temperature and oxygen conditions), suggesting that these animals fed on prey items with normal marine sulfur isotopic composition. For the bearded goby, the $\delta^{34}S$ follow the temperature trend, consistent with the idea that $\delta^{34}S$ decreases as temperature and oxygen levels drop. The unique $\delta^{34}S$ observed in the goby otolith is probably related to their diet enriched in diatoms and sulphidic bacteria in the extensive anoxic, diatomaceous ooze seafloor that they inhabit (Van der Bank et al, 2011). Namibia's shelf is incredibly hostile, with episodic occurrences of anoxic and sulphidic bottom water (Brüchert et al., 2009) that can be reflected in milky surface waters observable from space (Weeks et al., 2002) **(Supplementary Figure 4.S3)**.

Conclusion

Fishes from different ocean basins (i.e. the Northeast Pacific and the Southeast Atlantic) and with different life history traits (such as longevity and thermal histories) exhibited similar

elemental composition in their otoliths driven largely by Sr:Ca, Mn:Ca, Zn:Ca, B:Ca, Ba:Ca and Mg:Ca ratios. These fishes have in common the extremely low oxygen conditions they have experienced for most of their lives beneath waters marked by extremely high levels of primary productivity. We hypothesize that the Oxygen Minimum Zones associated with the EBUS have a unique biogeochemistry that can affect otolith chemistry in similar ways. Our results suggest boron as a potential tracer for pH in fishes, with lower boron ratios in otoliths associated with lower pH waters in OMZs. New proxies for hypoxic and acidic water conditions are particularly important in economically important EBUS such as the Southern California Bight, where dissolved oxygen and pH have been decreasing for the past 30 years, and the Namibian shelf, where warming trends and intensification of upwelling winds can extend the already massive hypoxic and sulphidic area of the continental shelf.

Acknowledgements

We thank Debra Driscoll at SUNY-ESF for support during the LA-ICPMS analyses, and Louisa Smieska at the Cornell High Energy Synchrotron Source for support during the SXFM analyses. This work is based upon research conducted at the Cornell High Energy Synchrotron Source (CHESS) which is supported by the National Science Foundation under award DMR-1332208. Analyses at the W.M. Keck Center for Isotope Geochemistry at UCLA were supported by a grant from the NSF Instrumentation and Facilities Program. Fish were collected on research cruises supported by UC Ship Funds, the CCE LTER Program, the NOAA Groundfish Trawl Survey, and MBARI. We thank the crew on the RV Blue Sea and RV Dr. Fridtjof Nansen, Frank Midtøy and Bronwen Currie for help to collect the bearded goby samples, and the University of Bergen and the National Research Foundations of Norway and South Africa (Grant number

180329/S50) for funding. Giant sea bass samples were obtained under research supported by Mia J. Tegner Research Fellowship at Scripps Institution of Oceanography and PADI Foundation (2017, 2018) to ARV. ARV thanks the support of UC Mexus-CONACYT doctoral fellowship 160083, and Shirley Boyd Memorial Endowment at SIO – UCSD. LAL was supported by NSF OCE1829623 and NOAA CHRP award NA18NOS4780172. NDG was funded by a QUEST grant to Brice X. Semmens. LMC was supported by CNPq grant 213540/2014-2.

Chapter 4, in part, is being prepared for submission of the material. Cavole L.M., Limburg K., Gallo N., Salvanes A.G.V., Ramírez-Valdez A., Levin L.A, Aburto-Oropeza O., Hertwig A., Ming-Chang L., McKeegan K.D. The dissertation author was the primary investigator and author of this material.

Literature Cited

Alin, S.R., Feely, R.A., Dickson, A.G., Hernández-Ayón, J.M., Juranek, L.W., Ohman, M.D. and Goericke, R., 2012. Robust empirical relationships for estimating the carbonate system in the southern California Current System and application to CalCOFI hydrographic cruise data (2005–2011). *Journal of Geophysical Research: Oceans*, *117*(C5).

Allen, K.A., Hönisch, B., Eggins, S.M., Yu, J., Spero, H.J. and Elderfield, H., 2011. Controls on boron incorporation in cultured tests of the planktic foraminifer Orbulina universa. *Earth and Planetary Science Letters*, *309*(3-4), pp.291-301.

Allen, L.G. and Andrews, A.H., 2012. Bomb radiocarbon dating and estimated longevity of Giant Sea Bass (Stereolepis gigas). *Bulletin, Southern California Academy of Sciences*, *111*(1), pp.1-14.

Altenritter, M.E., Cohuo, A. and Walther, B.D., 2018. Proportions of demersal fish exposed to sublethal hypoxia revealed by otolith chemistry. *Marine Ecology Progress Series*, *589*, pp.193-208.

Bograd, S.J., Castro, C.G., Di Lorenzo, E., Palacios, D.M., Bailey, H., Gilly, W. and Chavez, F.P., 2008. Oxygen declines and the shoaling of the hypoxic boundary in the California Current. *Geophysical Research Letters*, *35*(12).

Bograd, S.J., Buil, M.P., Di Lorenzo, E., Castro, C.G., Schroeder, I.D., Goericke, R., Anderson, C.R., Benitez-Nelson, C. and Whitney, F.A., 2015. Changes in source waters to the Southern California Bight. *Deep Sea Research Part II: Topical Studies in Oceanography*, *112*, pp.42-52.

Bond, N.A., Cronin, M.F., Freeland, H. and Mantua, N., 2015. Causes and impacts of the 2014 warm anomaly in the NE Pacific. *Geophysical Research Letters*, *42*(9), pp.3414-3420.

Breitburg, D., Levin, L.A., Oschlies, A., Grégoire, M., Chavez, F.P., Conley, D.J., Garçon, V., Gilbert, D., Gutiérrez, D., Isensee, K. and Jacinto, G.S., 2018. Declining oxygen in the global ocean and coastal waters. *Science*, *359*(6371), p.eaam7240.

Brewer, P.G. and Peltzer, E.T., 2009. Limits to marine life. *Science*, *324*(5925), pp.347-348.

Brodeur, R.D., Auth, T.D. and Phillips, A.J., 2019. Major shifts in pelagic micronekton and macrozooplankton community structure in an upwelling ecosystem related to an unprecedented marine heatwave. *Frontiers in Marine Science*, *6*, p.212.

Brodziak, J. and Mikus, R., 2000. Variation in life history parameters of Dover sole, *Microstomus pacificus*, off the coasts of Washington, Oregon, and northern California. *Fishery Bulletin*, *98*(4), pp.661-661.

Brüchert, V., Currie, B. and Peard, K.R., 2009. Hydrogen sulphide and methane emissions on the central Namibian shelf. *Progress in Oceanography*, *83*(1-4), pp.169-179.

Butler, J.L., Kastelle, C., Rubin, K., Kline, D., Heijins, H., Jacobson, L., Andrews, A. and Wakefield, W.W., 1995. *Age determination of shortspine thornyhead, Sebastolobus alascanus, using otolith sections and 210Pb: 226Ra ratio. Admin. Rep. No.* LJ-95-12. National Marine Fisheries Service, Southwest Fisheries Science Center, La Jolla, Calif.

Calvert, S.E., 1966. Accumulation of diatomaceous silica in the sediments of the Gulf of California. *Geological Society of America Bulletin*, *77*(6), pp.569-596.

Calvert, S.E. and Price, N.B., 1970. Minor metal contents of recent organic-rich sediments off South West Africa. *Nature*, *227*(5258), pp.593-595.

Calvert, S.E. and Price, N.B., 1983. Geochemistry of Namibian shelf sediments. In *Coastal Upwelling Its Sediment Record* (pp. 337-375). Springer, Boston, MA.

Campana, S.E. & Jones, C.M. 1992. Analysis of otolith microstructure data. In Otolith Microstructure Examination and Analysis. Canadian Special Publication of Fisheries Aquatic Sciences 117 (Stevenson, D. K. & Campana, S. E., eds), pp. 73–100. Ottawa: Department of Supply and Services.

Carr, M.E., 2002. Estimation of potential productivity in Eastern Boundary Currents using remote sensing. *Deep Sea Research Part II: Topical Studies in Oceanography*, *49*(1-3), pp.59-80.

Cavole, L.M., Demko, A.M., Diner, R.E., Giddings, A., Koester, I., Pagniello, C.M., Paulsen, M.L., Ramirez-Valdez, A., Schwenck, S.M., Yen, N.K. and Zill, M.E., 2016. Biological impacts of the 2013–2015 warm-water anomaly in the Northeast Pacific: winners, losers, and the future. *Oceanography*, *29*(2), pp.273-285.

Chavez, F.P. and Messié, M., 2009. A comparison of eastern boundary upwelling ecosystems. *Progress in Oceanography*, *83*(1-4), pp.80-96.

Clements, S.C., Takeshita Y., Dickson A., Martz T., and Smith J.E. 2020. Scripps Ocean Acidification Real-time (SOAR) Dataset, Scripps Institution of Oceanography, La Jolla, CA. https://coralreefecology.sioword.ucsd.edu/wp-content/uploads/sites/431/2020/05/SOAR_SP2020_Report_draftFinal-2.jpg

Currie, B., Utne-Palm, A.C. and Salvanes, A.G.V., 2018. Winning ways with hydrogen sulphide on the Namibian shelf. *Frontiers in Marine Science*, *5*, p.341.

Dailey, M.D., Reish, D.J. and Anderson, J.W. eds., 1993. *Ecology of the Southern California Bight: a synthesis and interpretation*. Univ of California Press.

Echave, K.B., 2017. First results of the tagging of shortspine thornyhead, *Sebastolobus alascanus*, in Alaska. *Fisheries Research*, *195*, pp.46-51.

Emery, K.O., 1960. The sea off southern California, a modern habitat of petroleum. 366 pp. New York: John Wiley & Sons

Feely, R.A., Sabine, C.L., Hernandez-Ayon, J.M., Ianson, D. and Hales, B., 2008. Evidence for upwelling of corrosive" acidified" water onto the continental shelf. *science*, *320*(5882), pp.1490-1492.

Gagnon, A.C., Gothmann, A.M., Branson, O., Rae, J.W. and Stewart, J.A., 2021. Controls on boron isotopes in a cold-water coral and the cost of resilience to ocean acidification. *Earth and Planetary Science Letters*, *554*, p.116662.

Gallo, N.D., 2018. Influence of ocean deoxygenation on demersal fish communities: Lessons from upwelling margins and oxygen minimum zones. PhD. Dissertation, University of California, San Diego, 2018.

Gallo, N.D., Levin, L.A., Beckwith, M. and Barry, J.P., 2019. Home sweet suboxic home: remarkable hypoxia tolerance in two demersal fish species in the Gulf of California. *Ecology*, *100*(3), p.e02539.

Gallo, N.D., Beckwith, M., Wei, C.L., Levin, L.A., Kuhnz, L. and Barry, J.P., 2020. Dissolved oxygen and temperature best predict deep-sea fish community structure in the Gulf of California with climate change implications. *Marine Ecology Progress Series*, *637*, pp.159-180.

Gerringer, M.E., Andrews, A.H., Huss, G.R., Nagashima, K., Popp, B.N., Linley, T.D., Gallo, N.D., Clark, M.R., Jamieson, A.J. and Drazen, J.C., 2018. Life history of abyssal and hadal fishes from otolith growth zones and oxygen isotopic compositions. *Deep Sea Research Part I: Oceanographic Research Papers*, *132*, pp.37-50.

Gibbs, M.A., 1991. Notes on the distribution and morphology of the rubynose brotula *(Cataetyx rubrirostris*) off central California. *California Fish Game 77*:149–152.

Gibbs, M.A., 1999. Lateral line morphology and cranial osteology of the rubynose brotula, *Cataetyx rubrirostris*. *Journal of morphology*, *241*(3), pp.265-274.

Gilly, W.F., Beman, J.M., Litvin, S.Y. and Robison, B.H., 2013. Oceanographic and biological effects of shoaling of the oxygen minimum zone. *Annual review of marine science*, *5*, pp.393-420.

Gómez-Ocampo, E., Gaxiola-Castro, G., Durazo, R. and Beier, E., 2018. Effects of the 2013-2016 warm anomalies on the California Current phytoplankton. *Deep Sea Research Part II: Topical Studies in Oceanography*, *151*, pp.64-76.

Gower, J.C., 1966. Some distance properties of latent root and vector methods used in multivariate analysis. *Biometrika*, *53*(3-4), pp.325-338.

Grupe, B.M., Krach, M.L., Pasulka, A.L., Maloney, J.M., Levin, L.A. and Frieder, C.A., 2015. Methane seep ecosystem functions and services from a recently discovered southern California seep. *Marine Ecology*, *36*, pp.91-108.

Hanke, G., Gillespie, G., Fong, K., Boutillier, J., Nielsen, J., Møller, P., Bedard, J. and Riley, J., 2015. New records of seven cusk-eels (Ophidiidae) and brotulas (Bythitidae) in coastal waters of British Columbia, Canada. *Northwestern Naturalist*, *96*(1), pp.71-80.

Helly, J.J. and Levin, L.A., 2004. Global distribution of naturally occurring marine hypoxia on continental margins. *Deep Sea Research Part I: Oceanographic Research Papers*, *51*(9), pp.1159-1168.

Hemming, N.G., and G.N. Hanson. 1992. Boron isotopic composition and concentration in modern marine carbonates. *Geochimica et Cosmochimica Acta 56*:537–543.

Hendrickx, M. and Serrano, D., 2014. Effects of the oxygen minimum zone on squat lobster distributions in the Gulf of California, Mexico. *Open Life Sciences*, *9*(1), pp.92-103.

Høie, H., Otterlei, E., Folkvord, A., 2004. Temperature-dependent fractionation of stable oxygen isotopes in otoliths of juvenile cod (*Gadus morhua*). *ICES Journal of Marine Science, 61*, 243–251.

Hopkinson, B.M. and Barbeau, K.A., 2007. Organic and redox speciation of iron in the eastern tropical North Pacific suboxic zone. *Marine Chemistry*, *106*(1-2), pp.2-17.

Hunter, J.R., Butler, J.L., Kimbrell, C.A.R.O.L. and Lynn, E.A., 1990. Bathymetric patterns in size, age, sexual maturity, water content, and caloric density of Dover sole, Microstomus pacificus. *CalCOFI Invest. Rep*, *31*, pp.132-144.

Hurst, T.P., Fernandez, E.R., Mathis, J.T., Miller, J.A., Stinson, C.M. and Ahgeak, E.F., 2012. Resiliency of juvenile walleye pollock to projected levels of ocean acidification. *Aquatic Biology*, *17*(3), pp.247-259.

Hüssy, K., Limburg, K.E., de Pontual, H., Thomas, O.R., Cook, P.K., Heimbrand, Y., Blass, M. and Sturrock, A.M., 2020. Trace Element Patterns in Otoliths: The Role of Biomineralization. *Reviews in Fisheries Science & Aquaculture*, pp.1-33.

Hutchings, L., Van der Lingen, C.D., Shannon, L.J., Crawford, R.J.M., Verheye, H.M.S., Bartholomae, C.H., Van der Plas, A.K., Louw, D., Kreiner, A., Ostrowski, M. and Fidel, Q., 2009. The Benguela Current: An ecosystem of four components. *Progress in Oceanography*, *83*(1-4), pp.15-32.

Jacobson, L.D. and Hunter, J.R., 1993. Bathymetric demography and management of Dover sole. *North American Journal of Fisheries Management*, *13*(3), pp.405-420.

Jacobson, L.D. and Vetter, R.D., 1996. Bathymetric demography and niche separation of thornyhead rockfish: *Sebastolobus alascanus* and *Sebastolobus altivelis*. *Canadian Journal of Fisheries and Aquatic Sciences*, *53*(3), pp.600-609.

Johnson, K.S., Berelson, W.M., Coale, K.H., Coley, T.L., Elrod, V.A., Fairey, W.R., Iams, H.D., Kilgore, T.E. and Nowicki, J.L., 1992. Manganese flux from continental margin sediments in a transect through the oxygen minimum. *Science*, *257*(5074), pp.1242-1245.

Kassambara, A. (2020). ggpubr: 'ggplot2' Based Publication Ready Plots. R package version 0.2.5. https://CRAN.R-project.org/package=ggpubr

Kastelle, C.R., Kimura, D.K. and Jay, S.R., 2000. Using 210Pb/226Ra disequilibrium to validate conventional ages in Scorpaenids (genera Sebastes and Sebastolobus). *Fisheries Research*, *46*(1-3), pp.299-312.

Keeling, R.F. and Garcia, H.E., 2002. The change in oceanic O_2 inventory associated with recent global warming. *Proceedings of the National Academy of Sciences*, *99*(12), pp.7848-7853.

Keeling, R.F., Körtzinger, A. and Gruber, N., 2010. Ocean deoxygenation in a warming world. *Annual Review Marine Science 2*, 199–229.

Kline, D.E., 1996. Radiochemical age verification for two deep-sea rockfishes: *Sebastolobus altivelis* and *S. alascanus*. M.S. Thesis, Moss Landing Marine Laboratories, San Jose State University, CA, 124 pp.

Koslow, J.A., Goericke, R., Lara-Lopez, A., and Watson, W. (2011). Impact of declining intermediate-water oxygen on deepwater fishes in the California Current. *Marine Ecology Progress Series*, *436*, 207-218.

Levin, L.A. 2003. Oxygen minimum zone benthos: Adaptation and community response to hypoxia. In *Oceanography and Marine Biology*, vol. 41, pp. 1–45. London: Taylor & Francis.

Levin, L.A., Ekau, W., Gooday, A.J., Jorissen, F., Middelburg, J.J., Naqvi, S.W.A., Neira, C., Rabalais, N.N. and Zhang, J., 2009. Effects of natural and human-induced hypoxia on coastal benthos.

Levin, L.A., B. Hönisch, and C.A. Frieder. 2015. Geochemical proxies for estimating faunal exposure to ocean acidification. *Oceanography 28(2):*62–73,

Levin, L. A., Girguis, P. R., German, C. R., Brennan, M. L., Tüzün, S., Wagner, J., Smart, C., Kruger, A., Inderbitzen, K., Le, J. and Martinez, M., 2016. Exploration and discovery of methane seeps and associated communities in the California Borderland, in *New Frontiers in Ocean Exploration: The E/V Nautilus and NOAA Ship Okeanos Explorer 2015 Field Season*, eds K. L. C. Bell, M. L. Brennan, J. Flanders, N. A. Raineault, and K. Wagner (Rockville, MD: The Oceanography Society), 40–43. Doi: 10.5670/oceanog.2016.supplement.01

Limburg, K.E., Olson, C., Walther, Y., Dale, D., Slomp, C.P. and Høie, H., 2011. Tracking Baltic hypoxia and cod migration over millennia with natural tags. *Proceedings of the National Academy of Sciences*, *108*(22), pp.E177-E182.

Limburg, K.E., Walther, B.D., Lu, Z., Jackman, G., Mohan, J., Walther, Y., Nissling, A., Weber, P.K. and Schmitt, A.K., 2015. In search of the dead zone: use of otoliths for tracking fish exposure to hypoxia. *Journal of Marine Systems*, *141*, pp.167-178.

Limburg, K.E. and Casini, M., 2018. Effect of marine hypoxia on Baltic sea cod *Gadus morhua*: evidence from otolith chemical proxies. *Frontiers in Marine Science*, *5*, p.482.

Mackas, D.L., Strub, P.T., Thomas, A., Montecino, V., 2006. Eastern regional ocean boundaries pan-regional overview. In: Robinson, A.R., Brink, K. (Eds.), The Sea, vol. 14a. Harvard University Press, Cambridge, Massachussetts, pp. 21–60

Martino, J., Doubleday, Z.A., Woodcock, S.H. and Gillanders, B.M., 2017. Elevated carbon dioxide and temperature affects otolith development, but not chemistry, in a diadromous fish. *Journal of Experimental Marine Biology and Ecology*, *495*, pp.57-64.

McClatchie, S., Goericke, R., Cosgrove, R., Auad, G. and Vetter, R., 2010. Oxygen in the Southern California Bight: multidecadal trends and implications for demersal fisheries. *Geophysical Research Letters*, *37*(19).

Meinvielle, M. and Johnson, G.C., 2013. Decadal water-property trends in the California Undercurrent, with implications for ocean acidification. *Journal of Geophysical Research: Oceans*, *118*(12), pp.6687-6703.

Melo, Y.C. and Le Clus, F., 2005. Growth and reproduction of the pelagic goby *Sufflogobius bibarbatus* off the Orange River, southern Africa. *African Journal of Marine Science*, *27*(1), pp.265-273.

Morales-Azpeitia, R., López-Martínez, J., Herrera-Valdivia, E. and Acevedo-Cervantes, A., 2018. Population dynamics of black brotula (*Cherublemma emmelas*) in deep waters of the Gulf of California. *Latin american journal of aquatic research*, *46*(5), pp.1103-1109.

Moreau, G., Barbeau, C., Frenette, J.J., Saint-Onge, J. and Simoneau, M., 1983. Zinc, manganese, and strontium in opercula and scales of brook trout (Salvelinus fontinalis) as indicators of lake acidification. *Canadian Journal of Fisheries and Aquatic Sciences*, *40*(10), pp.1685-1691.

Morford, J.L. and Emerson, S., 1999. The geochemistry of redox sensitive trace metals in sediments. *Geochimica et Cosmochimica Acta*, *63*(11-12), pp.1735-1750.

Moser, H.G. 1974. Development and distribution of larvae and juveniles of *Sebastolobus* (Pisces: family Scorpaenidae). *Fishery Bulletin 72* (4), pp. 865–884.

Munday, P.L., Hernaman, V., Dixson, D.L. and Thorrold, S.R., 2011. Effect of ocean acidification on otolith development in larvae of a tropical marine fish. *Biogeosciences*, *8*, pp.1631-1641.

Nielsen, J.G., Cohen D.M., Markle D.F. and Robins C.R., 1999. Ophidiiform fishes of the world (Order Ophidiiformes). An annotated and illustrated catalogue of pearlfishes, cusk-eels, brotulas and other ophidiiform fishes known to date. FAO Fish. Synop. 125(18):178p. Rome: FAO.

O'Toole, M.J. 1978. Development, distribution and relative abundance of the larvae and early juveniles of the pelagic goby *Sufflogobius bibarbatus* (von Bonde) off South West Africa 1972–1974. Sea Fish Branch Invest Rep 116:1–28.

Paulmier, A. and Ruiz-Pino, D., 2009. Oxygen minimum zones (OMZs) in the modern ocean. *Progress in Oceanography*, *80*(3-4), pp.113-128.

Paulmier, A., Ruiz-Pino, D. and Garçon, V., 2011. CO_2 maximum in the oxygen minimum zone (OMZ). *Biogeosciences*, *8*(2), pp.239-252.

Pearson, K.E. and Gunderson, D.R., 2003. Reproductive biology and ecology of shortspine thornyhead rockfish, *Sebastolobus alascanus*, and longspine thornyhead rockfish, *S. altivelis*, from the northeastern Pacific Ocean. *Environmental Biology of Fishes*, *67*(2), pp.117-136.

Pörtner, H., 2001. Climate change and temperature-dependent biogeography: oxygen limitation of thermal tolerance in animals. *Naturwissenschaften*, *88*(4), pp.137-146.

Pörtner, H.O., 2021. Climate impacts on organisms, ecosystems and human societies: integrating OCLTT into a wider context. *Journal of Experimental Biology*, *224*(Suppl 1).

Ramírez-Valdez, A., Rowell, T.J., Dale, K.E., Craig, M.T., Allen. L.G., Villaseñor-Derbez, J.C., Cisneros-Montemayor, A.M., Hernández-Velasco, A., Torre, J., Hofmeister, J., Erisman, B.E. (2021) Asymmetry across international borders: research, fishery and management trends, and economic value of the giant sea bass (*Stereoleopis gigas*). Manuscript submitted for publication.

Rouault, M., Illig, S., Lübbecke, J. and Koungue, R.A.I., 2018. Origin, development and demise of the 2010–2011 Benguela Niño. *Journal of Marine Systems*, *188*, pp.39-48.

Salvanes, A.G., Utne-Palm, A.C., Currie, B. and Braithwaite, V.A., 2011. Behavioural and physiological adaptations of the bearded goby, a key fish species of the extreme environment of the northern Benguela upwelling. *Marine Ecology Progress Series*, *425*, pp.193-202.

Salvanes, A.G.V., Bartholomae, C., Yemane, D., Gibbons, M.J., Kainge, P., Krakstad, J.O., Rouault, M., Staby, A. and Sundby, S., 2015. Spatial dynamics of the bearded goby and its key fish predators off Namibia vary with climate and oxygen availability. *Fisheries oceanography*, *24*, pp.88-101.

Salvanes, A.G.V., Christiansen, H., Taha, Y., Henseler, C., Seivåg, M.L., Kjesbu, O.S., Folkvord, A., Utne-Palm, A.C., Currie, B., Ekau, W. and van der Plas, A.K., 2018. Variation in growth, morphology and reproduction of the bearded goby (*Sufflogobius bibarbatus*) in varying oxygen environments of northern Benguela. *Journal of Marine Systems*, *188*, pp.81-97.

Sarmiento, J.L., Hughes, T.M., Stouffer, R.J. and Manabe, S., 1998. Simulated response of the ocean carbon cycle to anthropogenic climate warming. *Nature*, *393*(6682), pp.245-249.

Sato, K.N., Andersson, A.J., Day, J., Taylor, J.R., Frank, M.B., Jung, J.Y., McKittrick, J. and Levin, L.A., 2018. Response of sea urchin fitness traits to environmental gradients across the Southern California oxygen minimum zone. *Frontiers in Marine Science*, *5*, p.258.

Schmidtko, S., Stramma, L. and Visbeck, M., 2017. Decline in global oceanic oxygen content during the past five decades. *Nature*, *542*(7641), pp.335-339.

Sinclair, D.J., 2005. Correlated trace element "vital effects" in tropical corals: a new geochemical tool for probing biomineralization. *Geochimica et cosmochimica acta*, *69*(13), pp.3265-3284.

Shiao, J. C., Sui, T. D., Chang, N. N., & Chang, C. W. (2017). Remarkable vertical shift in residence depth links pelagic larval and demersal adult jellynose fish. *Deep Sea Research Part I: Oceanographic Research Papers*, *121*, 160-168.

Skrypzeck, H., Salvanes, A.G.V., Currie, B. and Kotze, A., 2014. First records of reproductive behaviour and early development of the bearded goby Sufflogobius bibarbatus. *Journal of fish biology*, *84*(4), pp.1256-1261.

Solé, V.A., Papillon, E., Cotte, M., Walter, P. and Susini, J.A., 2007. A multiplatform code for the analysis of energy-dispersive X-ray fluorescence spectra. *Spectrochimica Acta Part B: Atomic Spectroscopy*, *62*(1), pp.63-68.

Staby, A. and Krakstad J.-O. 2006. Review of the state of knowledge, research (past and present) of the distribution, biology, ecology and abundance of non-exploited mesopelagic fish and the bearded goby (*Sufflogobius bibarbatus*) in the Benguela Ecosystem. Report on BCLME project LMR/CF/03/08.

Stramma, L., Johnson, G. C., Sprintall, J., and Mohrholz, V. (2008). Expanding oxygen-minimum zones in the tropical oceans. *Science*, *320*(5876), 655-658.

Stramma, L., Schmidtko, S., Levin, L. A., and Johnson, G. C. (2010). Ocean oxygen minima expansions and their biological impacts. *Deep Sea Research Part I: Oceanographic Research Papers*, *57*(4), 587-595.

Stramma, L., Prince, E.D., Schmidtko, S., Luo, J., Hoolihan, J.P., Visbeck, M., Wallace, D.W., Brandt, P. and Körtzinger, A., 2012. Expansion of oxygen minimum zones may reduce available habitat for tropical pelagic fishes. *Nature Climate Change*, *2*(1), pp.33-37.

Sturrock, A.M., Trueman, C.N., Milton, J.A., Waring, C.P., Cooper, M.J., and Hunter, E. 2014 Physiological influences can outweigh environmental signals in otolith microchemistry research. *Marine Ecology Progress Series 500*: 245– 264.

Sturrock, A.M., Hunter, E., Milton, J.A., Johnson, R.C., Waring, C.P., Trueman, C.N. 2015 Quantifying physiological influences on otolith microchemistry. *Methods in Ecology and Evolution 6:* 806-816. DOI: https://doi.org/10.1111/2041-210X.12381

Sverdrup, H.U., 1938. On the process of upwelling. *Journal of Marine Research, I,* 155-164.

Sverdrup, H.U., Johnson, M.W., Fleming, R.H., 1942. The oceans, their physics, chemistry, and general biology. Prentice-Hall Inc.

United States Geological Survey (USGS), 2013. Microanalytical reference materials and accessories. U.S. Geological Survey Geochemical Reference Materials and Certificates.

Utne-Palm, A.C., Salvanes, A.G., Currie, B., Kaartvedt, S., Nilsson, G.E., Braithwaite, V.A., Stecyk, J.A., Hundt, M., Van der Bank, M., Flynn, B. and Sandvik, G.K., 2010. Trophic structure and community stability in an overfished ecosystem. *Science*, *329*(5989), pp.333-336.

Van der Bank, M.G., Utne-Palm, A.C., Pittman, K., Sweetman, A.K., Richoux, N.B., Brüchert, V. and Gibbons, M.J., 2011. Dietary success of a 'new'key fish in an overfished ecosystem: evidence from fatty acid and stable isotope signatures. *Marine Ecology Progress Series*, *428*, pp.219-233.

Vaquer-Sunyer, R. and Duarte, C.M., 2008. Thresholds of hypoxia for marine biodiversity. *Proceedings of the National Academy of Sciences*, *105*(40), pp.15452-15457.

Vogel, R.M. and Fennessey, N.M., 1994. Flow-duration curves. I: New interpretation and confidence intervals. *Journal of Water Resources Planning and Management*, *120*(4), pp.485-504.

Wakefield, W.W. 1990. Patterns in the distribution of demersal fishes on the upper continental slope off central California with studies on the role of ontogenetic vertical migration in particle flux. Ph.D. thesis, Scripps Institution of Oceanography, University of California, San Diego, Calif.

Weber, P.K., Hutcheon, I.D., McKeegan, K.D. and Ingram, B.L., 2002. Otolith sulfur isotope method to reconstruct salmon (Oncorhynchus tshawytscha) life history. *Canadian Journal of Fisheries and Aquatic Sciences*, *59*(4), pp.587-591.

Weeks, S.J., Currie, B. and Bakun, A., 2002. Massive emissions of toxic gas in the Atlantic. *Nature*, *415*(6871), pp.493-494.

Wickham, H. (2016). ggplot2: Elegant Graphics for Data Analysis. Springer-Verlag New York, 2016.

Yu, J., Elderfield, H. and Hönisch, B., 2007. B/Ca in planktonic foraminifera as a proxy for surface seawater pH. *Paleoceanography*, *22*(2).

Zamorano, P., Hendrickx, M.E. and Toledano-Granados, A., 2007. Distribution and ecology of deep-water mollusks from the continental slope, southeastern Gulf of California, Mexico. *Marine Biology*, *150*(5), pp.883-892.

Zamorano, P., Hendrickx, M.E., Méndez, N., Gómez, S., Serrano, D., Aguirre, H., Madrid, J. and Morales-Serna, F.N., 2014. La exploración de las aguas profundas del Pacífico mexicano: Proyecto Talud. *La frontera final: el océano profundo. Secretaría de Medio Ambiente y Recursos Naturales, Instituto Nacional de Ecología y Cambio Climático, México*.

Table 4.1. Fish (n = 79) used for the quantification of trace and minor elements of otoliths using LA-ICPMS and the respective environmental data (depth, temperature, oxygen and salinity) obtained from a CTD-O at the time of fish collection. Environmental data for the giant sea bass samples were obtained through the World Ocean Atlas 2018 database.

Common name	Scientific name	*n*	Year of collection	Location	Depth (m)	T (°C)	O_2 (µmol kg^{-1})	Salinity (psu)
Longspine thornyhead	*Sebastolobus altivelis*	8	2013-2015	Southern California Bight OMZ	475-1280	4.09-6.71	8.17-19.28	34.17-34.46
Shortspine thornyhead	*Sebastolobus alascanus*	10	2013-2015	Southern California Bight OMZ	339-878	4.41-8.11	7.38-44.39	34.15-34.45
Dover sole	*Microstomus pacificus*	18	2013-2015	Southern California Bight OMZ	198-1115	4.22-10.17	8.17-92	34-34.46
Rubynose brotula	*Cataetyx rubirostris*	8	2013-2015	Southern California Bight OMZ	607-705	5.39-5.43	8.29-8.43	34.39
Cusk eel	*Cherublemma emmelas*	1	2015	Gulf of California OMZ	793	6.02	1.73	34.54
Bearded goby	*Sufflogobius bibartus*	24	2012	Namibia shelf OMZ	74-280	9.73-13.56	21.75-150.96	34.76-35.32
Giant sea bass	*Stereolepis gigas*	10	2017	<30 m Off Baja California	30	13.70-20.46	65.29-255.08	33.34-33.78

Table 4.2. Maximum Mn:Ca ratios (mmol mol^{-1}) and the estimated duration of hypoxia for deep-sea fish from Southern California, Gulf of California and Namibia OMZs and the shallow-water giant sea bass off Baja California Peninsula. The duration of hypoxia is defined as the percentage of time the Mn:Ca ratios along the otolith transect exceeded a chosen hypoxia threshold.

			Duration of hypoxia	
Species	***n***	**max Mn:Ca**	**Hypoxia threshold (> 0.01 mmol mol^{-1})**	**Hypoxia threshold (> 0.0001 mmol mol^{-1})**
Longspine thornyhead	8	0.00234	0%	87.37%
Shortspine thornyhead	10	0.00185	0%	63.11%
Dover sole	18	0.00987	8.86%	100%
Rubynose brotula	8	0.0101	10.70%	100%
Cusk eel	1	0.0129	77.77%	100%
Bearded goby	24	0.0394	31.44%	100%
Giant sea bass	10	0.0000232	0%	0%

Table 4.3. Thermal history reconstruction for 10 marine fish individuals. Depth (m), temperature (°C), dissolved oxygen (μmol kg^{-1}) and salinity (psu) at the time of collection are provided for each specimen. $\delta^{18}O$ values (‰ vs. VSMOW) for seawater were estimated based on outermost spot and temperature at the time of fish collection. Lengths (L, cm) are standard length for shortspine and longspine thornyheads, Dover soles, rubynose brotula and black brotula and total length for bearded gobies and giant sea bass. Total weight (TW, g) and age in years or days are provided for each individual. Spots are the number of isotope values measured along the otolith transect. The range of $\delta^{18}O$ values (‰ vs. VSMOW) recorded in the otoliths and their respective estimated lifetime temperatures are provided.

Species	Fish ID	Depth (m)	T (°C)	O_2 (µmol kg^{-1})	Salinity	$\delta^{18}O_{sw}$	L (cm)	TW (g)	Age	Spots (*n*)	$\delta^{18}O$ otolith	Estimated T (°C)
Longspine thornyhead	#951	951	4.46	12.30	34.34	-1.06	20.2	217.69	34 yrs	31	28.4-33.3	1.5-25.0
Shortspine thornyhead	#703	703	5.59	9.76	34.36	0.89	31.10	591	40 yrs	18	32.5-35.4	1.3-14.5
Dover sole	#1116	1115	4.22	11.05	34.47	0.39	30.7	471.76	30 yrs	14	31.8-34.2	4.2-15.5
Rubynose brotula	#705	705	5.39	8.30	34.39	2.65	10.9	7.24	13 yrs	13	32.7-36.3	5.3-22.3
Black brotula	#732	793	6.023	1.7356	34.54	0.33	15.1	14.38	272 days	15	31.4-34.1	4.4-16.8
Black brotula	#737	854	5.13	4.12	34.52	0.94	20.1	52.59	330 days	13	32.1-34.8	4.0-16.4
Bearded goby	#3081	280	10.93	23.53	34.97	-0.72	8.80	5.3	2 yrs	21	28.5-32.1	8.3-26.2
Bearded goby	#3044	280	10.93	23.53	34.97	-0.01	10.2	3.8	3 yrs	14	30.9-33.2	7.0-17.5
Giant sea bass	#170506	30	16.65	239.90	33.36	-0.96	172	140000	41 yrs	41	28.0-31.8	8.7-27.6
Giant sea bass	#170606	30	13.82	224.51	33.78	-1.77	195	117000	44 yrs	37	27.9-31.2	7.7-23.4

Chapter 4 Appendix

Marine fish as mobile monitors of low oxygen, temperature and pH conditions

Supplementary Information

by

LETICIA MARIA CAVOLE[1,*], KARIN LIMBURG[2], NATALYA GALLO[1], ANNE GRO VEA SALVANES[3], ARTURO RAMÍREZ-VALDEZ[1], LISA A. LEVIN[1], OCTAVIO ABURTO OROPEZA[1], ANDREAS HERTWIG[4,5], MING-CHANG LIU[4], KEVIN D. MCKEEGAN[4]

[1]Scripps Institution of Oceanography, University of California San Diego, 9500 Gilman Drive, La Jolla, CA 92093, USA

[2]Department of Environmental Biology, State University of New York College of Environmental Science and Forestry, Syracuse, NY 13210, USA

[3] Department of Biological Sciences, University of Bergen, 5020 Bergen, Norway

[4] Department of Earth, Planetary, and Space Sciences, University of California - Los Angeles, Los Angeles, CA, 90095, USA

[5] Institute of Earth Sciences, Heidelberg University, 69120 Heidelberg, Germany

*Corresponding Author: lcavole@ucsd.edu

Table 4.S1. Environmental data at the time of fish collection (depth, temperature, oxygen and salinity), collection site position (latitude and longitude) and analytical methods used (LA-ICPMS, SIMS and SXFM) to analyze the otoliths of OMZs-dwelling fish and the shallow-water giant seas bass.

Fish ID	Common name	Site	Lat	Long	TW (g)	SL (cm)	Depth (m)	T (°C)	O (µmol/kg)	S (psu)	LA-ICPMS	SXFM	SIMS
SST703 #1	Shortspine thorn.	Southern Calif.	32.81	-117.47	402.93	26.70	703	5.59	9.76	34.36	X		
SST703 #2	Shortspine thorn.	Southern Calif.	32.81	-117.47	591.71	31.10	703	5.59	9.76	34.37	X	X	X
SST705 #1	Shortspine thorn.	Southern Calif.	32.87	-117.48	225.58	22.00	705	5.39	8.30	34.39	X		
SST705 #2	Shortspine thorn.	Southern Calif.	32.87	-117.48	142.48	19.20	705	5.39	8.30	34.39	X		
LST703 #6	Longspine thorn.	Southern Calif.	32.81	-117.47	100.16	16.40	703	5.59	9.76	34.36	X	X	
LST703 #11	Longspine thorn.	Southern Calif.	32.81	-117.47	134.70	18.20	703	5.59	9.76	34.37	X		
LST705 #1	Longspine thorn.	Southern Calif.	32.87	-117.48	118.22	17.80	705	5.39	8.30	34.39	X		
LST705 #2	Longspine thorn.	Southern Calif.	32.87	-117.48	122.09	17.90	705	5.39	8.30	34.39	X	X	
LST951#1	Longspine thorn.	Southern Calif.	32.61	-118.71	217.69	20.20	951	4.46	12.3	34.34			X
DSP703 #1	Dover sole	Southern Calif.	32.81	-117.47	289.97	27.60	703	5.59	9.76	34.36	X	X	
DSP698 #1	Dover sole	Southern Calif.	32.81	-117.47	497.20	33.60	698	5.43	8.44	34.39	X	X	
DSP NH1406 #1	Dover sole	Southern Calif.	32.70	-117.38	52.43	15.60	340	8.10	30.64	34.30	X		
DSP NH1406 #2	Dover sole	Southern Calif.	32.70	-117.38	54.11	16.10	340	8.10	30.64	34.30	X		
DSP NH1406 #3	Dover sole	Southern Calif.	32.70	-117.38	53.93	16.00	340	8.10	30.64	34.30	X		
DSP SP1609 #1	Dover sole	Southern Calif.	32.81	-117.47	50.20	15.70	338	7.67	34.55	34.25	X		
DSP SP1609 #2	Dover sole	Southern Calif.	32.81	-117.47	55.12	16.40	338	7.68	34.56	34.25	X		
DSP SP1609 #3	Dover sole	Southern Calif.	32.81	-117.47	78.42	18.60	338	7.69	34.57	34.25	X		
DSP715 #1	Dover sole	Southern Calif.	32.81	-117.47	170.17	22.30	715	5.46	9.65	34.37	X		
DSP715 #2	Dover sole	Southern Calif.	32.81	-117.47	513.64	33.50	715	5.47	9.66	34.38	X		
DSP198 #1	Dover sole	Southern Calif.	32.82	-117.47	62.98	16.90	198	10.17	92.01	34.00	X		
DSP307 #1	Dover sole	Southern Calif.	32.96	-117.32	21.12	11.60	307	8.09	50.90	34.19	X		
DSP438 #1	Dover sole	Southern Calif.	33.15	-117.50	75.79	17.20	438	7.78	25.90	34.28	X		
DSP561 #1	Dover sole	Southern Calif.	32.78	-117.44	150.09	22.30	561	6.87	15.77	34.10	X		
DSP823 #1	Dover sole	Southern Calif.	33.27	-118.00	285.61	28.80	823	5.15	8.17	34.25	X		
DSP900 #1	Dover sole	Southern Calif.	32.91	-117.84	653.05	34.50	900	4.33	12.42	34.46	X		
DSP1116 #1	Dover sole	Southern Calif.	33.22	-118.22	471.76	30.70	1115	4.22	11.05	34.47	X		X
DSP1116 #3	Dover sole	Southern Calif.	33.22	-118.22	301.11	28.90	1115	4.22	11.05	34.47	X		
RNB705 #1	Rubynose brotula	Southern Calif.	32.87	-117.48	7.24	10.90	705	5.39	8.30	34.39	X		X
RNB705 #2	Rubynose brotula	Southern Calif.	32.87	-117.48	6.71	11.30	705	5.39	8.30	34.39	X		
RNB705 #3	Rubynose brotula	Southern Calif.	32.87	-117.48	2.86	8.90	705	5.39	8.30	34.39	X		
RNB697 #2	Rubynose brotula	Southern Calif.	32.89	-117.47	4.27	9.30	697	5.43	8.44	34.39	X		
RNB697#3	Rubynose brotula	Southern Calif.	32.89	-117.47	2.93	7.30	697	5.43	8.44	34.39	X		
RNB698#1	Rubynose brotula	Southern Calif.	32.81	-117.47	3.54	9.20	698	5.43	8.44	34.39	X		
RNB698#2	Rubynose brotula	Southern Calif.	32.81	-117.47	3.60	9.10	698	5.43	8.44	34.39	X		
RNB698#3	Rubynose brotula	Southern Calif.	32.81	-117.47	2.67	8.80	698	5.43	8.44	34.39	X		
SST741#1	Shortspine thorn.	Southern Calif.	32.81	-117.47	1218.00	37.20	741	5.26	9.15	34.39	X		
SST438#3	Shortspine thorn.	Southern Calif.	33.15	-117.50	100.42	16.90	438	7.78	25.90	34.28	X		
SST SP1506#2	Shortspine thorn.	Southern Calif.	32.72	-117.38	20.72	10.10	339	8.12	44.39	34.22	X		
SST580#7	Shortspine thorn.	Southern Calif.	32.81	-117.47	145.65	19.90	580	6.53	14.60	34.31	X		
SST841#1	Shortspine thorn.	Southern Calif.	33.27	-118.04	398.26	26.80	841	5.09	7.38	34.15	X		
SST878#1	Shortspine thorn.	Southern Calif.	33.16	-117.99	494.07	28.70	878	4.42	12.76	34.46	X		
LST475#1	Longspine thorn.	Southern Calif.	32.90	-118.62	90.47	16.60	475	6.71	16.11	34.18	X		
LST1061#3	Longspine thorn.	Southern Calif.	32.46	-118.54	336.64	23.80	1061	4.10	19.29	34.47	X		
LST823#1	Longspine thorn.	Southern Calif.	33.27	-118.00	188.91	20.20	823	5.15	8.17	34.25	X		
LST1280#3	Longspine thorn.	Southern Calif.	32.92	-118.31	149.46	18.80	1280	4.21	10.74	34.36	X		
737	Black brotula	Gulf of Calif.	24.22	-109.79	52.59	20.10	854	5.12	4.12	34.52			X
732B	Black brotula	Gulf of Calif.	24.22	-109.79	14.38	15.10	793	6.02	1.74	34.54	X	X	X
2323	Benguela goby	Namibia	-27.96	15.53	2.60	71.14	86	9.73	85.69	34.76	X		
2410	Benguela goby	Namibia	-27.96	15.53	4.00	74.87	86	9.73	85.69	34.76	X	X	
3081	Benguela goby	Namibia	-20.18	12.23	5.30	88.00	280	10.93	23.53	34.97	X		X
3270	Benguela goby	Namibia	-20.18	12.23	3.20	76.00	280	10.93	23.53	34.97	X	X	

Table 4.S1. Environmental data at the time of fish collection (depth, temperature, oxygen and salinity) (continued)

Fish ID	Common name	Site	Lat	Long	TW (g)	SL (cm)	Depth (m)	T (°C)	O (µmol/kg)	S (psu)	LA-ICPMS	SXFM	SIMS
3273	Benguela goby	Namibia	-20.18	12.23	3.50	71.00	280	10.93	23.53	34.97	X	X	
2742	Benguela goby	Namibia	-19.37	12.38	10.80	104.75	128	13.56	21.76	35.32	X		
2768	Benguela goby	Namibia	-19.37	12.38	15.90	119.69	128	13.56	21.76	35.32	X		
3074	Benguela goby	Namibia	-20.18	12.23	14.10	120.00	280	10.93	23.53	34.97	X	X	
3269	Benguela goby	Namibia	-20.18	12.23	13.40	121.00	280	10.93	23.53	34.97	X	X	
3274	Benguela goby	Namibia	-20.18	12.23	14.70	113.47	280	10.93	23.53	34.97	X		
3303	Benguela goby	Namibia	-25.97	14.68	19.50	125.00	74	10.41	150.96	34.86	X		
3310	Benguela goby	Namibia	-25.97	14.68	18.30	120.00	74	10.41	150.96	34.86	X		
3311	Benguela goby	Namibia	-25.97	14.68	18.50	125.00	74	10.41	150.96	34.86	X		
3312	Benguela goby	Namibia	-25.97	14.68	15.40	120.00	74	10.41	150.96	34.86	X		
3319	Benguela goby	Namibia	-25.99	14.49	14.90	120.00	111	10.41	149.18	34.86	X	X	
2302	Benguela goby	Namibia	-27.96	15.51	4.60	81.20	86	9.73	85.69	34.76	X		
2307	Benguela goby	Namibia	-27.96	15.51	4.80	84.80	86	9.73	85.69	34.76	X		
2316	Benguela goby	Namibia	-27.96	15.51	4.30	80.00	86	9.73	85.69	34.76	X	X	
2355	Benguela goby	Namibia	-27.96	15.51	3.50	75.00	86	9.73	85.69	34.76	X		
2374	Benguela goby	Namibia	-27.96	15.51	3.10	72.00	86	9.73	85.69	34.76	X		
2848	Benguela goby	Namibia	-20.18	12.23	1.50	63.00	280	10.93	23.53	34.97	X		
3044	Benguela goby	Namibia	-20.18	12.23	3.80	102.00	280	10.93	23.53	34.97	X		X
3065	Benguela goby	Namibia	-20.18	12.23	3.60	78.00	280	10.93	23.53	34.97	X	X	
3089	Benguela goby	Namibia	-20.18	12.23	2.20	68.00	280	10.93	23.53	34.97	X		
SG-EN-170506-01	Giant sea bass	Guerrero Negro	28.03	-114.34	140000.00	172.00	50	16.65	239.90	33.36	X	X	X
SG-SD-170803-01	Giant sea bass	Carlsbad	33.16	-117.36	NA	136.00	50	13.70	245.06	33.35	X		
SG-TJ-170723-03	Giant sea bass	San Juanico	26.23	-112.46	6900.00	76.00	50	18.63	65.29	33.79	X		
SG-PA-170703-01	Giant sea bass	Punta Abreojos	26.73	-113.51	4980.00	69.00	50	18.63	65.29	33.79	X		
SG-EN-170705-01	Giant sea bass	Erendira	31.29	-116.42	2000.00	50.00	50	15.13	255.09	33.34	X		
SG-TJ-170804-04	Giant sea bass	San Ignacio	26.56	-113.08	1180.00	44.00	50	18.43	147.85	33.50	X		
SG-GN-170616-01	Giant sea bass	Guerrero Negro	28.03	-114.34	5600.00	68.00	50	13.82	224.51	33.78	X		
SG-EN-170606-01	Giant sea bass	Guerrero Negro	28.03	-114.34	117000.00	195.00	50	13.82	224.51	33.78	X		X
SG-EN-170710-01	Giant sea bass	Guerrero Negro	28.03	-114.34	168000.00	171.00	50	20.47	216.35	33.56	X		
SG-EN-170610-04	Giant sea bass	Bahia Tortugas	27.61	-114.87	43000.00	140.00	50	14.17	224.51	33.78	X		

Table 4.S2. Mean Mn:Ca ratios (ppt) for freshwater and coastal fish species (yellow perch, Baltic flounder, Atlantic croaker and giant sea bass) and for deep-sea fish (Benguela goby, black brotula, Dover soles, rubynose brotulas, and longspine and shortspine thornyheads).

Common name	Scientific name	Habitat	Mean Mn:Ca (ppt)	Reference
Yellow perch	*Perca flavescens*	Lake Erie	0.0183	Limburg et al. 2015
Baltic flounder	*Platichthys flesus*	Baltic Sea	0.0531	Limburg et al. 2015
Atlantic croaker	*Micropogonias undulatus*	Gulf of Mexico	0.0131	Limburg et al. 2015
Benguela goby	*Sufflogobius bibartus*	Namibia shelf OMZ	0.01401	This study
Cusk eel	*Cherublemma emmelas*	Gulf of California OMZ	0.01654	This study
Doversoles	*Microstomus pacificus*	Southern California Bight OMZ	0.00703	This study
Rubynosw brotula	*Cataetyx rubirostris*	Southern California Bight OMZ	0.00752	This study
Longspine thornyhead	*Sebastolobus altivelis*	Southern California Bight OMZ	0.00209	This study
Shortspine thornyhead	*Sebastolobus alascanus*	Southern California Bight OMZ	0.00164	This study
Giant sea bass	*Stereolepis gigas*	<30 m California/Baja California	0.00002	This study

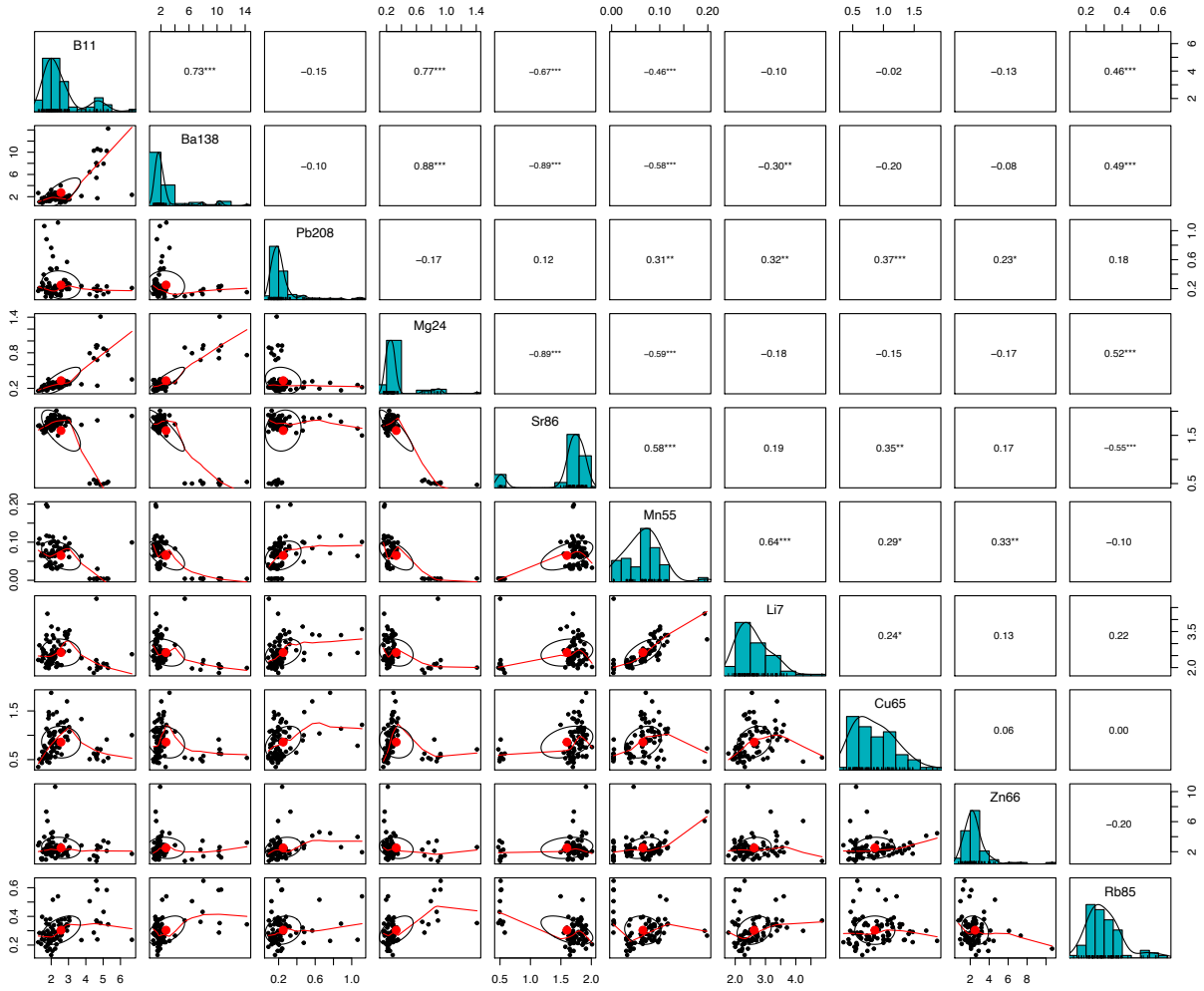

Figure 4.S1. Scatterplot matrices for all pairs of elemental ratios (Me:Ca) in otoliths of fishes off the Southern California Bight, the Gulf of California, the Namibian shelf and the Baja California Peninsula. Bivariate scatter plots are below the diagonal, histograms are on the diagonal, and the Pearson correlations with significance levels (* = 0.05, ** = 0.01, *** = 0.001) are above the diagonal. Me:Ca ratios were log-transformed prior to the analysis.

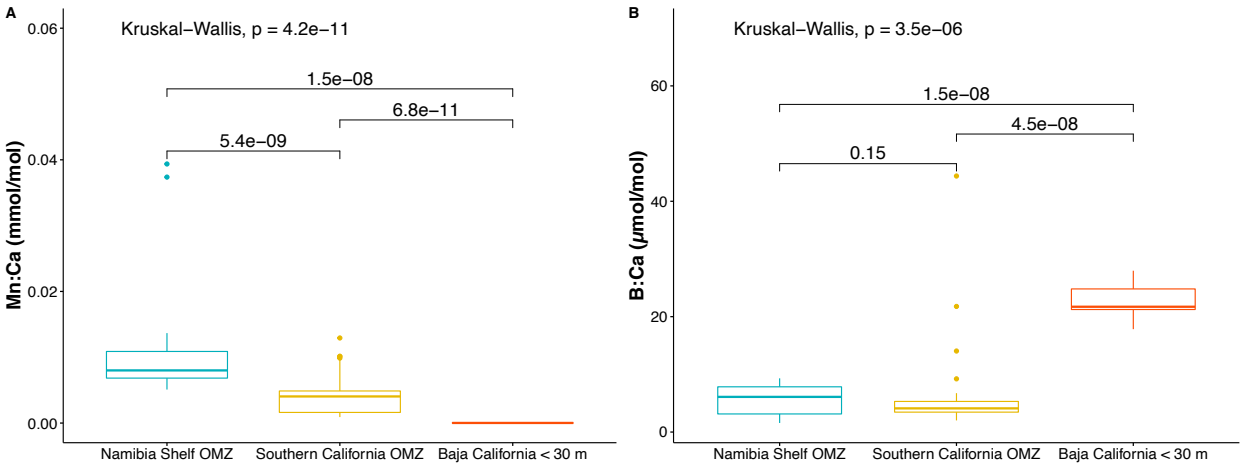

Figure 4.S2. Boxplot of a Kruskal-Wallis test of Mn:Ca (mmol/mol) (A) and B:Ca (μmol/mol) (B) otolith ratios among the bearded gobies from the Namibian shelf OMZ, demersal species from the Southern California Bight OMZ and the giant sea bass from surface waters off the peninsula of Baja California (< 30 m deep). A global Kruskal-Wallis *p*-value is provided at the top of the graphic, as well as pairwise comparisons *p*-values based on the Wilcoxon test.

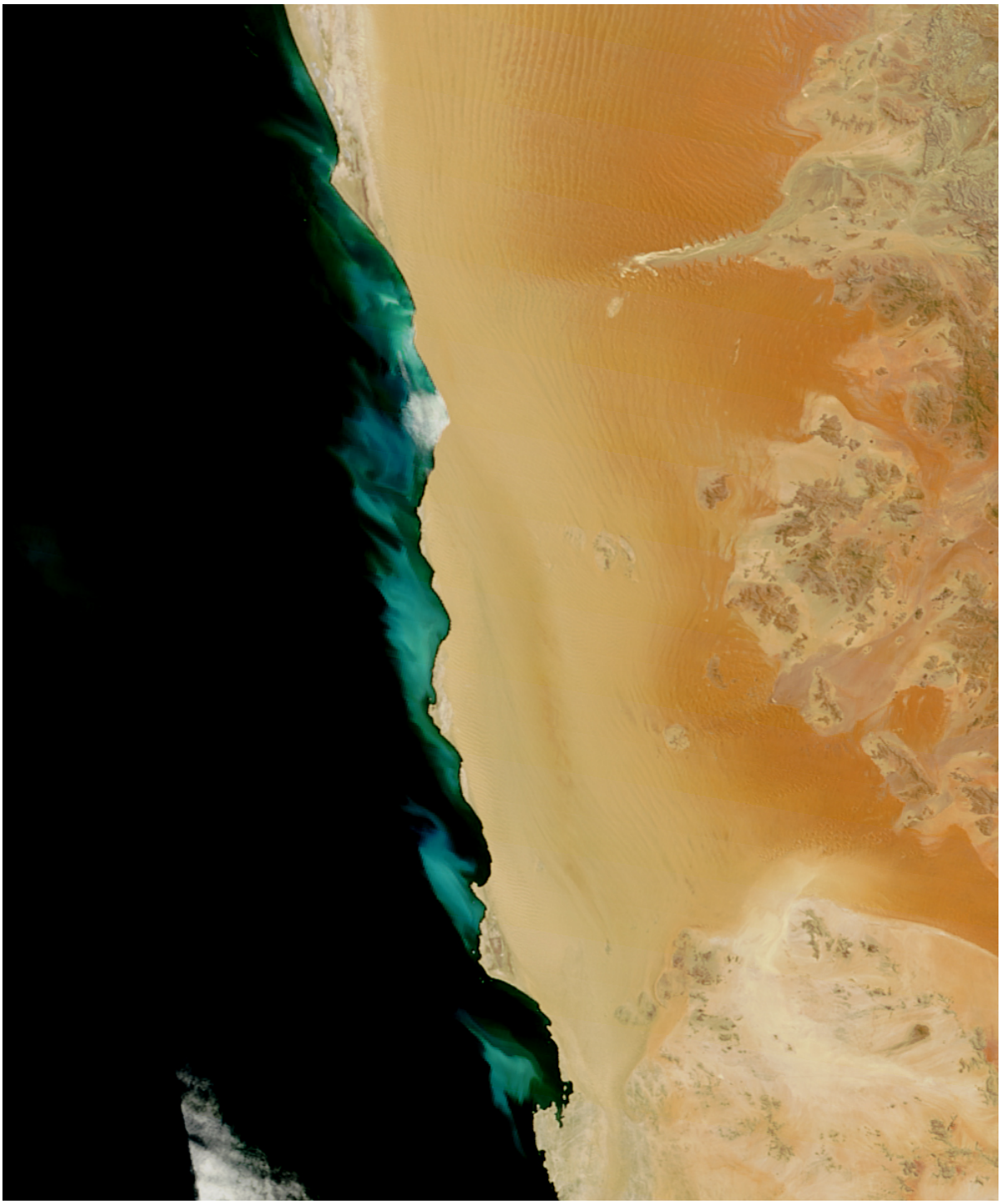

Figure 4.S3. Sulphidic water column conditions of elemental sulfur are observable from space as milky surface waters off Namibia's coast. Image captured on February 13, 2015, by the Moderate Resolution Imaging Spectroradiometer (MODIS) on NASA's Aqua satellite.

CHAPTER 5:

Using Local Ecological Knowledge of Fishers to infer the impact of climate variability in Galápagos' small-scale fisheries

LETICIA MARIA CAVOLE, SOLANGE ANDRADE-VERA, JOSÉ R MARIN JARRIN, DANIELA FAGGIANI DIAS, OCTAVIO ABURTO-OROPEZA AND MARÍA JOSÉ BARRÁGAN-PALADINES

Abstract

Galápagos has been characterized with great abundance of marine life and high levels of endemism. Due to its geographical position, this archipelago experiences tremendous climate variability during El Niño events, which disturbs the entire marine food web, and ultimately affects the artisanal fishing activity. In this study, we explored the main impacts of El Niño events on artisanal fishing and marine life using the local ecological knowledge provided by four generations of fishers on the most populated islands in Galápagos. Anecdotal information and perceptions coincided with the current scientific literature and provided novel insights about: (i) the positive and negative effects of the El Niño years on artisanal fisheries and marine animals, (ii) differences in species caught during warm and cold seasons and (iii) current interactions among artisanal fisheries, tourism and unauthorized industrial fisheries activities within the 40 nautical miles that surround the Galápagos Marine Reserve. In addition, fishers provided valuable information for governing resources under anomalously warm years, by identifying sites that function as natural refuges for fish and invertebrates during El Niño events. Data derived from these interviews highlight an urgent need for a novel, bottom-up and collaborative fisheries governance, between the artisanal fishing sector and decision and policy makers in Galápagos. Collaborative initiatives, involving one of the sectors that first inhabited the archipelago, is essential to achieve sustainable and long-term use of marine resources and to increase and anticipate human and environmental resilience under continued long-term global warming.

Introduction

The Galápagos Islands are one of the most dynamic biogeographical settings on Earth; they are a subtropical archipelago with more than 100 volcanic islands and islets, located at the intersection of major warm and cold-water currents. Galápagos' unique geographic position, right at the equator, at 906 km west of the continental coast of Ecuador and under the dynamics of different oceanographic currents, allows marine life to thrive in the archipelago, but also increases its vulnerability to climatic events of anomalous warm oceanic conditions, such as during El Niño years [1].

The main currents in Galápagos are the cold eastward Equatorial Undercurrent (EUC) or Cromwell current that upwells nutrient-rich waters on the western side of the archipelago and the westward South Equatorial Current (SEC) that reaches the eastern side of the archipelago [2] (**Figure 5.1a**). The SEC can transport warm, nutrient-poor waters from the northern Panama current (locally known as El Niño current) during the warm-wet season from December to May or June, or cool and nutrient-rich waters from the southern Peru current (Humboldt) during the cold-dry season from June to November or December [3]. Due to this natural variability, marine life and fishers have to constantly adapt to changes in the marine environment.

In addition to the local and dynamic oceanographic system in Galápagos, El Niño events further affect the marine food web in its islands. El Niño is an inter-annual phenomenon that occurs every 2-7 years in the Equatorial Pacific due to the weakening of the trade winds from the east, which leads to unusually warm waters on the west coast of the Americas and Galápagos islands [4] (**Figure 5.1b**). El Niño events are a relatively well-studied phenomenon throughout the Galápagos archipelago. For example, during those years, the EUC substantially weakens or disappears [5] or if the costal upwelling continues to occur, it upwells warmer waters with lower

nutrients [4]. These changes in the physical environment lead to dramatic consequences for the entire marine food web from phytoplanktonic organisms to pelagic fish, Galápagos penguins *Spheniscus mendiculus* [6], sea lions *Zalophus wollebaeki* [7], marine iguanas *Amblyrhynchus cristatus* [8], and seabirds, such as blue-footed boobies *Sula nebouxii* [9].

Fisheries in Galápagos have been researched quite substantially in the last decades by projects looking mainly at the isolated effects of El Niño events [1,10] or fishing exploitation on marine resources [11,12]. Yet, the social dimensions of fisheries have barely been addressed. The remarkable rise in water temperature, increase of precipitation and strong currents during El Niño events heavily affect the dynamics of fishing resources and fisheries activities around the Galápagos islands. In this regard, by exploring the strong relationship between climatic events and human systems in the archipelago, it is expected to find that climate change dramatically affects the local human population and their social relationships.

The knowledge about fisheries produced in Galápagos has predominantly adhered to the traditional Western scientific practices and has generated scientific-based results [13]. However, almost no local knowledge has been recorded nor used to inform management and policy in the Galápagos, despite it demonstrated track record of improving resource management elsewhere [14]. With this in mind, it can be claimed that fishers' testimonials on regional climate and fisheries patterns are limited within the Galápagos historical context, and thus, the Local Ecological Knowledge (LEK) from fishers is crucial to understand how the climate variability, ecological systems, and social behavior work in concert.

Artisanal fishing is an important socioeconomic activity in Galápagos Islands and represents an integral source of income and seafood for local communities on Santa Cruz, San Cristóbal, Isabela Islands and Floreana Islands (**Figure 5.2**). For more than seventy years, fishers

have dove and fished around the islands, islets and rocky protuberances found throughout the archipelago. In doing so, they have accumulated a vast knowledge about the climatic cycles that affect regional marine life. They have also established social-ecological relationships marked by climatic, socioeconomic, political and governance regimes [15,16].

In recent years, local and traditional knowledge of common users of natural resources have been used by policy makers to improve the governance of natural resources in developing and developed regions, like the Brazilian Amazon [17] and Canada [18]. Unconventional sources of information such as anecdotal, perceptions and stories have made it possible to understand the state of marine resources prior to exploitation [19]. Yet, the knowledge acquired by local and traditional users regarding their resilience and adaptations, what they have learned and observed in natural systems during unfavorable years and how this information can assist in the governance of natural resources under continuous warming scenarios, are far from being fully appreciated by the prevailing Western scientific framework.

Through the use of LEK, our main objectives are to: (1) understand how El Niño events have affected fishers and marine life in the Galápagos within a historical context, (2) illustrate the main species catches during the warm and cold season, and (3) characterize the main economic, environmental and governance interactions with the artisanal fishing sector in Galápagos, as well as the main demands by this sector. In addition, we have included fishers' testimonials to enrich the discussion analyzed in the present study, in the hope that their perceptions and opinions may be taken into account in future strategies of governance.

Material and methods

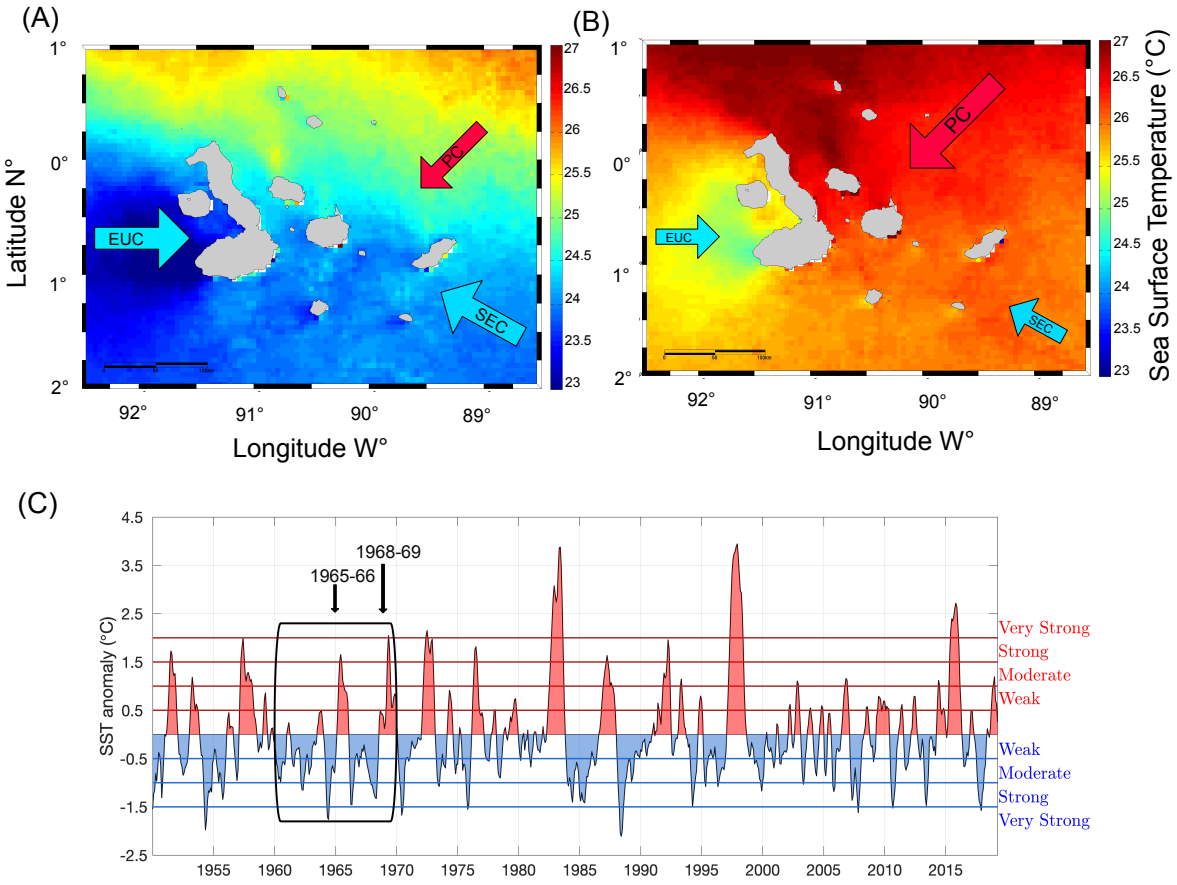

Figure 5.1. Physical oceanography characterizing the Galápagos archipelago. (A) Common year, showing the warm Panama Current (PC), South Equatorial Current (SEC) and cold Under Equatorial Current (EUC). (B) The extreme El Niño event of 2015-2016 based on weekly averages of sea surface temperature (SST). The size of arrows indicates the relative strength of the oceanographic current. (C) Niño-Galapagos index, corresponding to a 3-month running mean of SST anomalies averaged around the Galápagos Archipelago (1°N to 2°S of latitude and 93°W to 88°W of longitude). For (A) and (B) the data products are from VIIRS-SNPP sensors on NASA satellites (https://oceancolor.gsfc.nasa.gov); for (C) the index was created using the HadISST dataset [20].

Survey approach

To understand local fisheries dynamics in conjunction with climate variability throughout the Galápagos, we gathered fisher's anecdotal information, perceptions and testimonials about the changes in fisheries and marine communities during past El Niño events (i.e. back to the El Niño of 1965), and throughout annual cold and warm seasons.

We used a snowball sampling method, where key informants helped us to identify other individuals, and these in turn more, allowing a chain of information [21]. We used semi-structured, in-depth and exploratory interviews with 23 fishers from towns in three populated islands in Galápagos: Puerto Ayora in Santa Cruz Island (n= 12), Puerto Villamil in Isabela Island (n= 7) and Puerto Baquerizo Moreno in San Cristóbal Island (n= 4). Floreana Island was excluded since it lacks full-time artisanal fishers (**Figure 5.2**). Open-ended questions were adapted to each fishers' knowledge or expertise, allowing each contributor to extend on topics they considered most interesting or important. The open-ended questions also aimed at understanding the personal perceptions of fishers regarding their work and their memories regarding past water warming events. The interviews lasted between 30 and 200 minutes, summing up 31 hours of active conversations and mutual learning process with the local fishers. Verbal informed consent was asked from fishers taking part of the process. The conversations were conducted in Spanish.

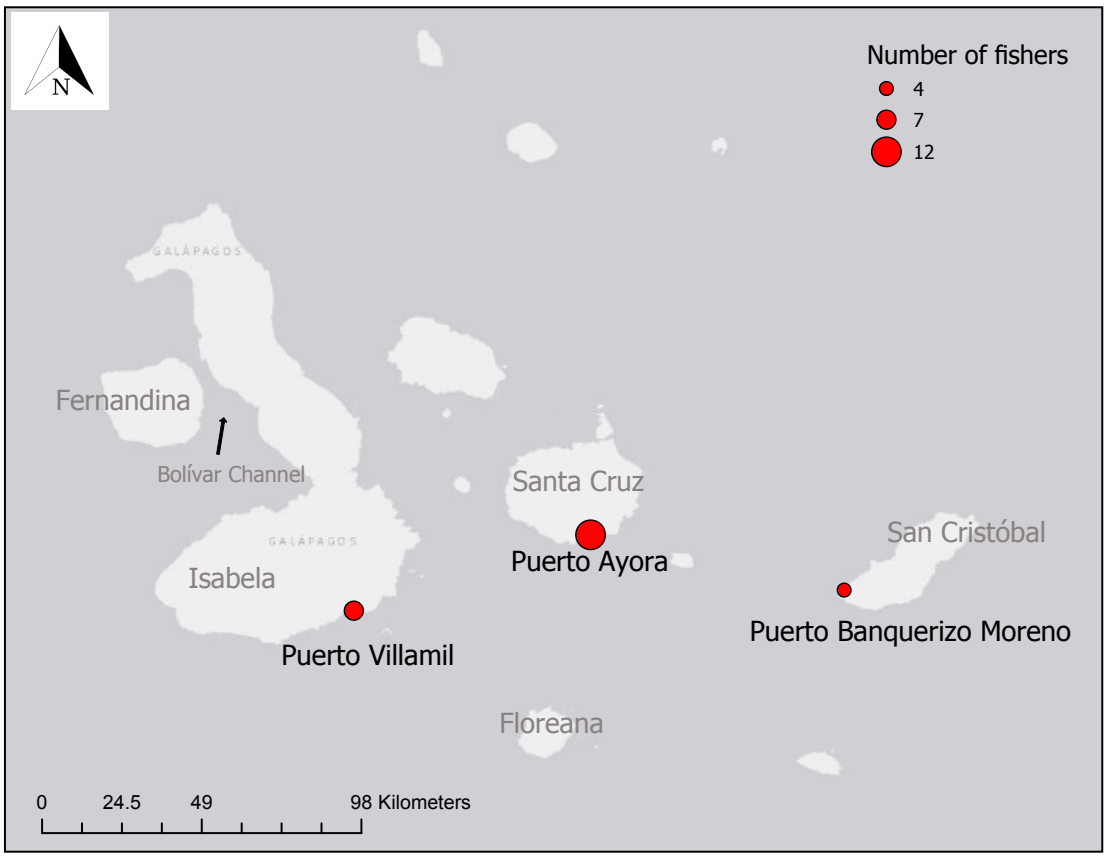

Figure 5.2. Map of the Galápagos Islands showing the port locations and number of interviewed fishers.

Data analysis

To address objective (1), we asked fishers how El Niño phenomenon affect fishing and other marine animals, later comparing these results with a literature review on the web of knowledge platform (search terms: El Niño* Galápagos* fisheries, total papers n = 19, searched on September 2019). We identified keywords as those that were cited most often among interviewees. Those key words were then organized in bubble charts to allow the visualization of the data about the main effects of El Niño on fisheries and on the marine life in Galápagos, from the local fishers' standpoint.

To address objective (2), we asked fishers what are the common fish species caught during the warm and cold seasons. These answers were then compared with the mean preferred temperature occupied by these species, available for fishes in Fishbase (www.fishbase.org) and for invertebrates in SeaLifeBase (www.sealifebase.org) online platforms. In the context of semi-structured and in-depth interviews, we adapted questions [19,22] to assess changes in fish captures across warm and cold seasons. We also compared fishers' perceptions with the available landing data for the white fin fisheries in Galápagos during the year of 2019, obtained from monitoring data of the Galápagos National Park Directorate (GNDP).

To address objective (3) we asked fishers to expand on topics they considered most interesting or relevant to their current activities.

Results

Fishing demographics and artisanal fishing methods

More than half of the fishers interviewed (52.17%) corresponded to families with three or four fisher generations living in Galápagos, extending their knowledge back to the early 60s. Most of the fishers (70%) have been fishing or diving for 20 to 74 years, for instance, by performing the traditional *hookah* diving. In Galápagos, *hookah* diving is a simple form of surface-supplied diving, wherein fresh air is channeled through a compressor left topside of a fiberglass or wooden boat, for a diver to breathe freely underwater. The duration of the dives varies and can last up to 6 h, in particular during the spiny lobster fisheries. *Hookah* diving is still a common fishing practice in Galápagos and allows fishers to observe marine life from a holistic perspective, as well as to sense ocean temperatures at different depths across the seasons. Another common fishing gear employed locally is the *empate*, which consists of a handline with

a drag named *señuelo*. The *empate* is mainly used for the white fin fishery locally known as *pesca blanca*.

Strong El Niño effects on fisheries and the marine life associated

The main effects of El Niño on artisanal fisheries in Galápagos (**Figure 5.3a**) were drawn from the fisher's perceptions of warmer seawater temperatures (very warm), of increased difficulty in fishing (less favorable), and of behavioral changes of fishes including them moving to further sites (fishes go outside), deeper sites (fishes go deeper) or simply not entering within the 40 nm of the Galápagos Marine Reserve – GMR (fishes do not enter). Moreover, half of the fishers identified rougher ocean conditions (wild sea) or abrupt changes in seawater temperature and in the ocean currents (abrupt changes) and higher precipitation levels (more precipitation) during El Niño years. Interestingly, interviewed fishers also recalled specific El Niño years and its main effects (1982/1983, 1997/1998 and 2015/2016) (**Supplementary Table 5.S1**), as exemplified by the testimonial below:

> *"I felt the **El Niño of 1982-1983 pretty strong**. At that time, I was in San Cristóbal and I observed many changes in all activities within the Galápagos, affecting both marine animals and humans. In the marine realm, I observed that **the winter season looked like the summer season**. The water was very hot, the sea lions very weak, and the marine algae was dying, which affected the marine iguanas. I also observed that all the corals in San Cristóbal bleached, and **a little less in Isabela.** Since this El Niño the corals have not fully recovered. This El Niño affected fishing as a whole, for instance: **the sailfin grouper (locally known as bacalao) went into deeper waters or it would leave the area**, so fishing*

large pelagic fishes was a better option, like tunas. On the other hand, there was more jaiba (local crab). In the human realm, there were physical losses. There was a lot of ***heavy rain*** *in San Cristóbal, destroying the Malecon (Boardwalk), and my aunt lost 3000 chickens."* (code 10, Isabela Island)

The main El Niño effects on marine animals (**Figure 5.3b**) included the fisher's perceptions of the change of marine animal sightings (change sightings), the increase in the losses and mortality of specific marine animal groups (losses and mortalities), the overall negative effects in the entire marine food web (negative effects) and the reduction of small pelagic fish (pelagic fish) and pups and adults of sea lions (sea lions).

In addition to specific El Niño effects, we also asked fishers to expand on personal observations they considered of special interest. Two *hookah* fishers, an 82-years old and a 58-years old, identified 'anomalous warm' years back in 1965 and 1968, when they were diving for the lobster fishery:

"When I arrived in Galápagos ***, in 1965****, I was diving, and I noticed that* ***all the corals in the islands I used to fish were fully bleached*** *because the water back then was very warm. I've seen the water get warm in posterior years, but in those years the corals would just partially bleach, which would allow them to recover later…"* (code 04, Santa Cruz Island)

Those years identified as anomalously warm by those two subjects correspond to the strong El Niño events of 1965/66 and 1968/69 El Niño (**Figure 5.1c**). These testimonials were

also supported by other two senior fishers (72 and 74 years old) who identified the 1960s as decades with strong El Niño years and anomalously high precipitation levels and lightnings.

Figure 5.3. Bubble chart showing the keywords associated with the main effects of the El Niño phenomenon on Galápagos. (a) The El Niño effects on artisanal fishing and the percentage (%) of fishers interviewed who mentioned each keyword. (b) The El Niño effects on marine animals and the percentage (%) of fishers interviewed who mentioned each keyword.

Figure 5.3. Bubble chart showing the keywords associated with the main effects of the El Niño phenomenon on Galápagos (continued).

In addition to the main effects of El Niño years on fisheries and marine life, three subjects have identified the Bolívar Channel (between the west of Isabela and the east of Fernandina), and the north of Isabela and Fernandina Islands as marine refuge sites for corals

(**Figure 5.2**), fish and sea cucumbers during these events (code 18 in **Supplementary Table 5.S1** and code 9 and 10 in **Supplementary Table 5.S2**).

> *"The El Niño change the amount of fish, which decreases. But it is a natural process. In some places, like in the north of Isabela and Fernandina, and in Bolívar Channel, the water is always cold, even during El Niño years."* (code 18, Santa Cruz Island)

These sites are surprisingly the same ones identified as marine refuges under climate change due to the intensification and northward expansion of the EUC in the past 33 years [23].

Catches during the warm and cold season

The fishers' perceptions of catches during the warm season (i.e., December to May or June) were mainly composed of Galápagos sailfin grouper *Mycteroperca olfax* (locally known as *bacalao*), sharks and tunas. The shark category was subdivided into two species, bigeye thresher *Alopias superciliosus* and silky shark *Carcharhinus falciformes*, following the catch composition proportion stated in [24]. The tuna category was subdivided in the three main species captured in Galápagos: skipjack tuna *Katsuwonus pelamis,* yellowfin tuna *Thunnus albacares*, and bigeye tuna *Thunnus obesus*. Longfin yellowtail *Seriola rivoliana*, wahoo *Acanthocybium solandri* and pacific dog snappers *Lutjanus novemfasciatus* were also associated to warmer water conditions. The mean preferred temperature occupied by these six most cited species vary between 19.3 °C and 27.3 °C, with the Galápagos sailfin grouper preferring the coolest waters (mean of 19.3 °C) (**Figure 5.4**).

Fishers' perceptions of catches during the cold and dry season (i.e., June to November or December) were mainly composed of red spiny lobsters *Panulirus penicillatus*, blue spiny

lobsters *Panulirus gracilis*, wahoo *Acanthocybium solandri,* and yellowfin tuna *Thunnus albacares*. The mean preferred temperature occupied by these four species vary between 24.7 °C and 27°C, with red and blue spiny lobsters preferring the warmest waters (26.7 °C - 27 °C) (**Figure 5.4**).

Fishers' perceptions for Galápagos grouper (#1) and wahoo (#8) catches agree with the seasonality of available landing data. Yellowfin tuna (#4) was also found to be fished throughout the year, especially during the transition months (June and January), as noted by fishers (**Supplementary Figure 5.S1**).

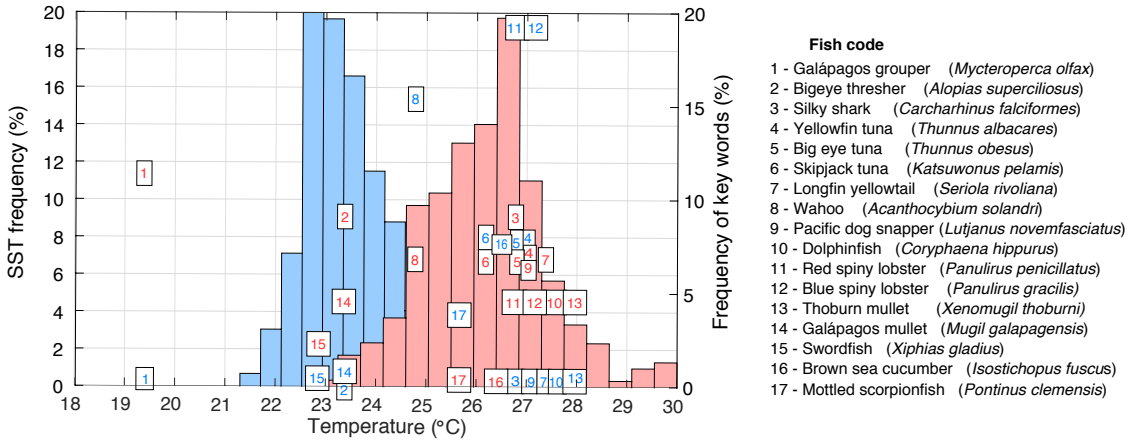

Figure 5.4. Preferred temperature for the 18 species most cited by artisanal fishers and the typical SST around Galápagos Archipelago for cold (June to November) and warm (January to May) seasons. The right y-axis shows the frequency that each fisher cited each of these 18 species as caught during the cold season (numbers depicted in blue) and/or the warm season (numbers depicted in red). The position on the x-axis of each of these numbers corresponds to the mean preferred temperature for each species, obtained from the Fishbase database. The blue and red bars correspond to the 1950 to 2018 distribution of SST around Galápagos for the cold and warm season, respectively, which frequency is shown on the left y-axis. For example, Galápagos grouper (fish number 1) has a preferred cold temperature (19.3°C), but artisanal fishers catch this specie mainly in the warm season.

Main dimensions interacting with the artisanal fishing sector in GMR

During the interviews, fishers constantly talked about the interactions between their fishing activities and tourism industry, climate shifts (mainly during El Niño years), the Galápagos National Park Directorate (GNPD) and illegal industrial fishing (**Figure 5.5, Supplementary Figure 5.S2**).

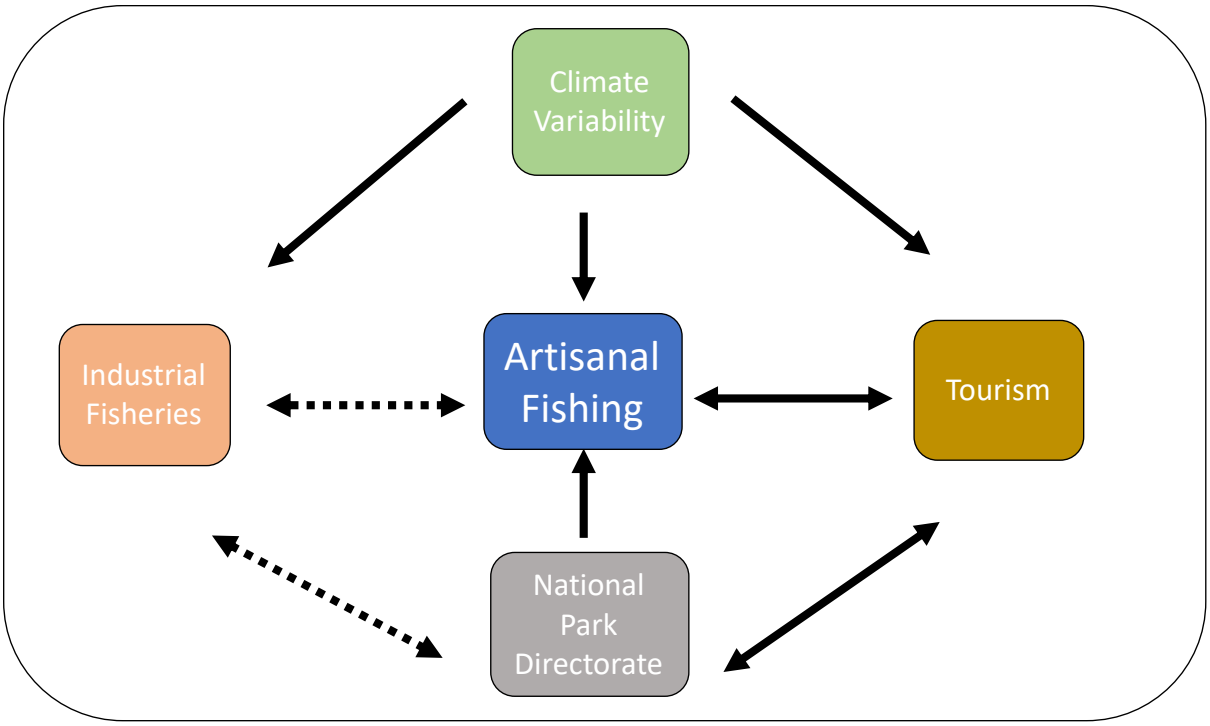

Figure 5.5. General scheme of the sectors and governing bodies interacting with artisanal fisheries in Galápagos, according to fishers interviewed: economic (tourism/ illegal industrial fisheries), environmental (climate) and governing body (Galápagos National Park Directorate). Dashed lines indicate the illegal nature of some industrial fisheries caught inside the Galápagos Marine Reserve.

Tourism interaction with artisanal fisheries

Fishers acknowledged that tourism in Galápagos boosts the local economy. Yet, they also recognized that tourism increased living costs, the demand for seafood and the competition for the use of space in a non-sustainable way. For example, fishers are currently catching the mottled scorpionfish *Pontinus clemensi* (**Figure 5.6**) in large amounts (~ 50,000 kg/year;

Supplementary Figure 5.S1), including specimens below the size at first reproduction [25], to supply the local tourist demand at restaurants in Santa Cruz Island, the most visited and populated island in Galápagos. Additionally, since in Darwin and Wolf Islands are home to intense tourism activities, especially dive operations, fishers do not recognize the current "Marine Sanctuary" status of the area. The lack of legitimacy for this protection label among artisanal fishers leads to the continuity of illegal fishing operations around these islands.

Fishers also mentioned that intense tourism activities can frighten seabirds away from their resting and breeding sites;

> *"In Española Island during the 90s, we used to see many seabirds and the amount of guano (seabird excrement) on our boats was so high, that it had to be cleaned many times along the day; now you hardly see much, the sky is clear, and fishing is prohibited near these areas. At Punta Pitt (San Cristóbal Island), in addition to fishing pressure, tourism has also been affecting resident seabirds"* (code 21, San Cristóbal)

Figure 5.6. Landings of mottled scorpionfish *Pontinus clemensi* in Puerto Ayora, Santa Cruz Island. Photo: Leticia Cavole.

Galápagos National Park Directorate (GNPD) interactions with artisanal fisheries

The history of the interaction between the GNPD and local fishers is not new. During the interviews, at least 12 fishers expressed a poor previous and current relationship with the GNPD, which are exemplified below by those comments:

> *"There has not been a good communication among the different sectors (**GNPD**, NGOs and fisher sector); but we acknowledge that everyone should work together in the process to achieve sustainable fisheries."* (code 23, San Cristóbal Island*)*

*"The **GNPD** wants certain regulations to be implemented. They speak in technical language that are not accessible by us. The Participatory Management was implemented in theory, but not in practice. There was no dialogue, only conflict. In 2009, there was a lobster strike, with no catch limit. The fishery was closed for six months due to overfishing. We admit we lost control and overfished."* (code 19, San Cristóbal Island)

*"The **GNPD** imposes many restrictions and does not provide solutions. These are nothing more than political interests. The Galápagos Marine Reserve Zoning Plan of 2000 was poorly implemented. Conservation is a negotiation process. The best Parqueño (ranger) is the one that comes from anywhere in the world and wants to take care of Galápagos."* (code 14, Isabela Island)

*"**The decisions are made just by the government and the Park**. The information that we give to them, including the best fishing sites, will be used against us. For example, these will be the fishing sites closed to the fisheries."* (code 08, Santa Cruz Island)

Fishers understand that such asymmetric relationships hamper the sustainability of their livelihoods and hinder compliance with current fisheries-management strategies among themselves. Additionally, some fishers recognized that the closed season improved the sustainability of key fisheries resources (i.e. lobsters and sea cucumbers) and encourage a rotation of fishing sites, for example by alternating no-take zones to open zones and vice versa.

Industrial fisheries interactions with artisanal fisheries

At the time of this study (September 2018), fishers were complaining that yellowfin tuna *Thunnus albacares* was not entering the marine reserve due to the heavy industrial fishing effort around the 40 nautical miles (NM) of the marine reserve. It was relatively common to hear that industrial fishers from other countries can enter the marine reserve illegally and overexploit its resources at a much higher rate than the entire artisanal fishing sector in Galápagos.

> *"The industrial fishing boats fish inside 40* NM *and are currently overexploiting our resources. Today there are around 90 large boats of around 100 meters long and with fishing storage capacity of up to 580 tons each. We, artisanal fishermen, take about 500 kg on each of our trips."* (code 08, Santa Cruz Island)

> *"The industrial boats are concentrated in the eastern side of the archipelago, at the border line of the reserve. They capture fishes that are coming from the mainland. These industrial boats are basically at the entrance of the Galápagos Marine Reserve. They catch most of the migratory fish, and we have much less fish left for us."* (code 21, San Cristóbal).

> *"The industrial boats are from Colombia, Peru, Costa Rica, Japan…they enter in the marine reserve at night and leave at the dawn at around 5-6 am."* (code 11, Isabela Island)

> *"There are industrial fisheries occurring inside the 40* NM. *The artisanal fishermen do not report it because they are afraid that their own irregularities will be punished by the*

Park. These fishing boats are from China, Costa Rica and Colombia. They will fish in a day what we would fish in about one year." (code 17, Santa Cruz Island)

Discussion

Strong El Niño effects on fisheries and the marine life associated

Fishers' perceptions about El Niño events are broadly aligned with the current literature [1,10,26–29]. During El Niño years, the local oceanography in Galápagos are deeply modified, with dramatic effects on flora and fauna [1,4,30]. As the Equatorial Undercurrent weakens or completely shuts down during El Niño events, topographically induced upwelling is suppressed [31], resulting in a general reduction in primary productivity, mainly in the western part of the archipelago [3]. The reduction in primary productivity available to the food chain leads to proportional reductions in the growth and reproductive success of the entire marine food web, from primary producers such as hermatypic corals, macroalgae and phytoplankton to top predators such as sea lions and sharks [4,32].

Keywords detected during the interviews reveal that fishers recognize the El Niño years as anomalously warmer and overall negative for fishing. During El Niño events, Galápagos waters can reach 5 °C above long-term averages, with a reduction in primary productivity of about ten times throughout the archipelago [4]. Geographically, the fishing effort in Galápagos follows high levels of chlorophyll-a concentration, so highly productive areas like Fernandina, the west coast of Isabela and southeast of Santa Cruz can withstand greater fishing intensity than impoverished regions [3] and are the areas where upwelling is suppressed the most during El Niño years.

However, it is essential to distinguish the mechanisms that weaken and shut down the Equatorial Undercurrent (EUC) during El Niño events from those that strengthen it under global climate change scenarios. As the Equatorial Undercurrent (EUC) is projected to intensify in the near future, SST will warm less rapidly and upwelling will be enhanced in the western side of Galápagos, potentially offering marine refuges in the long turn [23,33]. Interestingly, sites in the western side of Galápagos were also recognized by fishers to remain cooler and to concentrate more fish and invertebrates than the rest of the archipelago during strong El Niño years. These sites - Bolívar Channel (between Fernandina and Isabela) (black arrow in **Figure 5.2**), and the north of Isabela and Fernandina Islands - might not be exactly the same marine refuge areas under global climate change scenarios but are still of interest to policy makers as they could serve as refuge areas for marine organisms during anomalously warm years. However, such cool marine sites are also essential for maintaining fishing activities during the El Niño years, so adaptive management could, for example, allow for a rotational system of these fishing areas between El Niño and La Niña years. In agreement with fisher's testimonials of higher abundance of fish and invertebrates in those colder regions, Murillo-Posada et al. [12] found higher abundance and CPUE of lobsters during colder temperatures (< 22° C) in this region.

Regarding the effects of El Niño on other marine animals, the most common keyword identified by fishers was "change in sightings". Shifts in distribution are among the main consequences of climate changing, with tropical and subtropical species expanding their distributional ranges to higher latitudes and deeper waters [34]. Considering this, the fishers' ability to perceive shifts in the normal distribution of species confirmed their awareness of the environment and their intrinsic relationship with climatic drivers and physical-biological interactions. For example, they were able to identify shifts in the abundance of small pelagic fish

and to specify precise numbers of animal reductions, especially for sea lion *Zalophus wollebaeki* adults and pups, and coral reefs. For example, during the 1982/1983 El Niño, almost 90% of Galápagos sea lions pups died [35], which is the same estimate of 90% of decline by one fisher (code 8, **Supplementary Table 5.S2**). For corals, a total of 95-99% of reef coral cover was lost from Galápagos between 1983 and 1985 [27], similar to the estimate of 100% of reef coral mortality in San Cristóbal Island by another fisher (code 10, **Supplementary Table 5.S2**).

Fishers perceived "shifts in the behavior" of large fish and sea lions, who moved to further sites in an attempt to find new sources of prey. They also noticed reductions in seabird populations, such as pelicans, blue-footed boobies, and frigate birds, but an increase in hammerhead and blacktip sharks during these events (code 14, **Supplementary Table 5.S2**). Species such as the Galápagos penguin (*Spheniscus mendiculus*) have breeding colonies that overlap with productive areas of western Isabela, making them highly dependent on the proximity of its food source, and thus up to 77% of its population perished during the 1982/1983 El Niño [28]. Therefore, during El Niño years, low primary productivity patterns were the main cause of poor foraging and reproductive success of local seabird colonies, unlike other mobile marine species such as sharks and large pelagics, which can simply move to offshore and between feeding sites [3].

Fishers recalled some unexpected memories of large fish during El Niño events:

> *"Small pelagics, like sardines, leave the area when the water is warmer, then larger fish, like bacalao, are hungrier and grabs the bait faster, so El Niño increases the catchability of big fish"* (Code 20, **Supplementary Table 5.S1**)

The phenomenon of larger fish sizes in the landings was observed in Galápagos during the 2015/2016 El Niño [10]. These authors attributed these changes to the lower phytoplankton production that would (i) increase visibility of bait items otherwise not easily detected by fish, and (ii) decrease in prey biomass that would force starving fish to increase bait attacks. These explanations are supported by fishers' perception.

Fishers also extended on topics they found curious during their dives and fishing activities. Remarkably, the oldest fisher we interviewed (82 years old) was able to recall anomalous warm water conditions in 1965, noting a widespread coral bleaching across several Galápagos' islands at that time [36]. In the 60s, there were two major warm anomalous conditions that affected Galápagos, in 1965-66 and in 1968-69 (**Figure 5.2c**.). We believe that the testimony of this fisher indirectly validates the effects of the 1965-1966 El Niño on the Galápagos corals. Since the first ecology-based paper on Galápagos coral reefs was written in mid-70s [37], this testimonial might be one of the first direct observations on temperature-induced coral bleaching in the world.

LEK might be critical to understand the resilience of coral systems prior to the 1970s. In agreement with our findings, former authors [29] noticed anomalously high precipitation in 1965 at Santa Cruz Island, which led to a widespread desertion of eggs by waved Albatrosses due to high mosquito density. Negative effects associated with higher precipitation are common during El Niño years in Galápagos [38], and support the testimony of the 1965 coral bleaching by our interviewee. In addition, strong rainfall patterns and rougher seas during El Niño years in Galápagos were recurrent reminders during our interviews, which indicates the fear of going out to fish in such conditions. In fact, coastal winds may intensify during El Niño due to increased thermal differences between land and sea [4], potentially increasing the risk of accidents.

Catches during the warm and cold season

Bacalao was the main species caught during the warm season (i.e., December to May or June), although it occupies the coldest preferred temperature (19.3°C) among the warm species listed. Bacalao has an annual reproductive season that peaks from October through December [11], so catching this species during its reproductive peak is problematic for this extremely vulnerable species. In addition, this catch trend aims to meet a demand from the Ecuadorian mainland fish market for the traditional dish called *fanesca*, which is consumed during the Easter Holiday in April. Cultural and religious habits on the mainland have an impact on the bacalao populations of Galápagos, and suggest bacalao-specific management regulations should be applied together with the fishing sector in order to avoid the collapse of this fishery, as stated by Usseglio et al. (2016) [11].

Shark species were also reported to be frequently caught during warm seasons. Such information suggest that sharks may be still caught as bycatch in the hook and line and gillnet fisheries or as part of an illegal fishery for shark fins [39]. Fisher's motivations for continuing to catch sharks included their perception of higher biomass of sharks at the present than those observed in the 1990s. For example, in Isabela, it was common to hear that local fishers are frightened by the high numbers and large size of sharks (e.g. hammerhead sharks) and perceive this as a risk to their relatives who want to swim or surf on local beaches. As a concrete recommendation, the GNPD together with NGOs could implement a flagging system at the beaches with high biomass of sharks in order to avoid an overlap between the local communities and sharks.

Red and blue spiny lobsters were the main species caught during the cold season (i.e. June to November or December), although they have mean preferred temperatures of around

27°C. The fishing season for lobsters occurs from July 1st to December 31st of each year, explaining that such temporal patterns of capture are controlled by the fishing regulations at place and not the preferred temperature of these species. Female lobsters with eggs are illegal to catch and keep. Notwithstanding, a fisher admitted shaking ovigerous females underwater to release its eggs before coming into the vigilance at the port. A viable way to avoid these behaviors is to strengthen the social cohesion of the artisanal fisheries sector, its commitment to the resource sustainability and to improve its legitimacy among the stakeholders. For example, regulations and alternative governance for fishing resources may be interesting to explore so new motivations may emerge, and compliance with regulations and surveillance among fishers can be promoted and improved [40]. Two fishers also suggested that the open season for the lobster fisheries should be postponed to January or February, as this would allow ovigerous females to spawn at least once before being caught, thus contributing to the long-term population viability of the species. This is in agreements with Hearn and Toral-Granda (2007) [41], which observed higher presence of ovigerous females of red spiny lobster in November and January.

The overall results suggest that market demand for bacalao and fisheries regulations for the lobster fishery, were more important aspects to define captures across seasons than the mean preferred temperature by each of these species. This showcases the importance of cultural and regulation factors in driving the exploitation of such emblematic species.

Main challenges of the artisanal fishing sector in Galápagos

Tourism interactions

Most of the mottled scorpionfish *Pontinus clemensi* seems to be consumed locally by tourists who may not be aware that they are consuming a deep-sea fish with slow growth and late

maturity rates (at around 12 years for females and14 years for males) [25]. Also, fishers complained recurrently about the conservation status of Marine Sanctuary for Darwin and Wolf Islands at the time of our interviews, and the high tourism performed at these sites, especially for diving operations. Their understanding is that "Marine Sanctuary" precludes the use of these sites irrespective of its purposes and makes them feel in a disadvantaged position towards decision-making bodies. This undermines fisher's willingness to comply with environmental regulations and could motivate the ignorance of rules by this sector, preventing the full conservation of these northernmost sites. One possible spatial refinement would be to keep these marine sanctuaries open to uniquely scientific purposes. This decision may decrease the tourism income for Galápagos, but it can also potentially increase the artisanal fisher's compliance with the law – which can translate into even greater biomass of fish and invertebrates around these islands.

Galápagos National Park Directorate interactions with artisanal fisheries

The paramount goal of the GNDP is to protect and care for the biodiversity of the GMR. Naturally, negotiations and common agreements with local resource users constitute a gigantic challenge, with many intricacies, mistakes and learnings along the process. The relationship between the artisanal fishing sector and Galápagos National Park is historically complex, involving civil unrest, strikes, protests and illegal activities. These civil movements were composed of road blockades, the takeover of administrative buildings, forced apprehension of monitoring vessels, kidnapping of guards, threats to release invasive goats on islands from where they were previously eradicated [42] and the poaching of giant tortoises [43]. Until today, this relationship is misleading and prevents the compliance of artisanal fishers with no-take zones.

Fishers claim a lack of lobbying in the decision-making process with the Ecuadorian government, contrary to the multimillion-dollar, mostly foreign, tourism sector. They also consider themselves marginalized and unfairly categorized as "predators" by wealthy tourists visiting the archipelago and by conservation sectors. Fishers want to be part of the zoning and regulation plan for the GMR from the project design stage to final reporting, calling for a novel bottom-up and collaborative management approach with stronger leadership, social cohesion and organization than the past zoning experience in the late 2000s [40]. Fishers also considered themselves a "threatened/endangered" social group. This definition coincides with the downward trend in the total number of active fishers in Galápagos, from 1229 individuals in 2000 to around 400 individuals nowadays [13,44].

Industrial fisheries interactions with artisanal fisheries

There are recurring cases of large industrial boats illegally fishing within the 40 nm of the Galápagos Marine Reserve. These foreign boats have been identified as Costa Rican, Colombian, Japanese, Taiwanese and Koreans [32,45]. Most legally and illegally extracted fisheries resources from the Economic Exclusive Zone surrounding Galápagos is by industrial fishers, totalizing 744,500 tons between 1950 – 2010. This is at least fourteen times higher than the artisanal fisheries total catch of 52,500 ton for the same period, which included finfish, lobsters and sea cucumber [24]. Artisanal fishers have fiberglass and wooden boats that operate mainly inside the marine reserve, with limited storage capacity. Artisanal fishers consider Galápagos a "natural seedbed or nursery" in the middle of the Pacific Ocean, working as a big spillover area for adjacent marine areas outside the marine reserve; *"Galápagos es un semillero natural"*. This is a very precise definition in agreement with compelling evidence from models and observations

that the Galápagos plays a significant role in regional and basin-scale biogeochemistry. For example, the presence of Galápagos leads to a 500 km wide patch of elevated surface chlorophyll concentrations in the middle of the Pacific [33], which ultimately sustain entire marine food webs. In the fisher's conception, this sustained abundance of marine life is the reason why there are so much illegal industrial activities surrounding the marine reserve and the Exclusive Economic Zone (EEZ). The fishers interviewed also identified 90 industrial fishing boats operating in Galápagos in the past few years. Between 1989 and 1996, 48 vessels (both Ecuadorian and foreign) were caught illegally fishing for tuna [3] and from 1996 -1998, 119 tunas boats were either caught or observed [46]. Fishers could be the main enforcement agents against illegal industrial fisheries. They do not do so because they are aware of their own illegalities and are afraid of calling GNPD and suffering further prosecutions. As the GNPD has severe difficulties at maintaining infrastructure, and fostering technical capacity and funding to appropriately govern the Galápagos protected areas, it should work in conjunction with the artisanal fisheries to enforce GMR regulations against illegal industrial fisheries, which can have a broader impact on marine biodiversity than the artisanal sector.

Conclusions

After 485 years of human attention towards the Galápagos, since Fray Tomás de Berlanga's first descriptions of this archipelago, only 16 socioeconomic fishery-related peer-reviewed papers have been published. To the best of our knowledge, none of them include insights about the impact of climate variability on Galápagos artisanal fisheries nor do they address this sector's adaptability to climate (including social change). Here, we document testimonials from fishers, leading valuable historical context for fisheries research in the region,

including previously unstudied/undocumented El Niño events. For example, the 1965 El Niño was likely responsible for the widespread coral bleaching observed. Fishers also identified marine refuge areas during anomalous warm seawater temperature events. Anomalous events such as these are soon to become the new normal as both the atmosphere and ocean continue to warm. It is, therefore, extremely important to protect areas that are identified as marine refuge areas.

Conflict has been identified among artisanal fishers and other sectors, such as tourism and the Galápagos National Park Directorate. Fishers recognize that tourism activities boost the economy, but it also increases the demand for seafood, forcing them to look after further and deeper sites to supply the local market with new target species (e.g. mottled scorpionfish). Regarding their relationship with GNPD, the lack of legitimacy and credibility for the Galápagos Marine Reserve's zoning elaborated at the end of 2000s still affects fisher's compliance with regulations [40]. The GMR was classified as a multi-use zone, where management policies defined on paper and not in agreement with the local reality resulted in unclear zoning, leading to confusion and conflicts between users and poor compliance with the GMR zoning [47]. This animosity remains and precludes social cohesion of the artisanal fishing sector, which in turn prevents their participation in the long-term decision-making process for socio-environmental sustainability. Moreover, artisanal fishers could be strong allies to supervise the GMR against illegal industrial fisheries as they currently fish in more than 100 islands, islets and rock protuberances of the archipelago and also during night times.

All the lessons gained herein suggest that scientists should integrate the prevailing scientific "resource-focused" approach with the social-ecological systems framework (i.e. local ecological knowledge of fishers and other resource users). Furthermore, given that these fishers

have experienced the dynamic conditions of the ocean and associated marine life daily for the last 70 years, they are among the best observers of climatic changes that constantly plague this marine diversity hotspot. We should give them credit for their empirical knowledge and try to establish a bottom-up and collaborative management approach to maintain the ecological and social sustainability in this unique archipelago at the face of global climate change. We anticipate that working with local inhabitants will be the only way to secure this goal.

Acknowledgments

We are grateful to the artisanal fishers of Isabela, San Cristóbal and Santa Cruz Islands for their valuable observations and to the Charles Darwin Foundation for their institutional support. This publication is contribution number 2297 of the Charles Darwin Foundation for the Galápagos Islands.

Chapter 5 in full, is a reprint of the material as it appears in Marine Policy. Cavole L.M., Andrade-Vera S., Jarrin J.R.M., Dias D.F., Aburto-Oropeza O., Barrágan-Paladines M.J. The dissertation author was the primary investigator and author of this material.

References

[1] G.J. Edgar, S.A. Banks, M. Brandt, R.H. Bustamante, A. Chiriboga, S.A. Earle, L.E. Garske, P.W. Glynn, J.S. Grove, S. Henderson, C.P. Hickman, K.A. Miller, F. Rivera, G.M. Wellington, El Niño, grazers and fisheries interact to greatly elevate extinction risk for Galapagos marine species, Glob. Chang. Biol. 16 (2010) 2876–2890. https://doi.org/10.1111/j.1365-2486.2009.02117.x.

[2] Y. Liu, L. Xie, J.M. Morrison, D. Kamykowski, W. V. Sweet, Ocean Circulation and Water Mass Characteristics around the Galápagos Archipelago Simulated by a Multiscale Nested Ocean Circulation Model, Int. J. Oceanogr. 2014 (2014) 1–16. https://doi.org/10.1155/2014/198686.

[3] E. Danulat, G. Edgar, Reserva Marina de Galápagos, Fundación Charles Darwin/Servicio

Parque Nacional Galápagos, Santa Cruz, Galápagos, Ecuador, 2002.

[4] R.T. Barber, F.P. Chavez, Biological consequences of El Niño, Science (80-.). 222 (1983) 1203–1210. https://doi.org/10.1126/science.222.4629.1203.

[5] E. Firing, R. Lukas, J. Sadler, K. Wyrtki, Equatorial Undercurrent Disappears during 1982-1983 El Niño, Science (80-.). 222 (1983) 1121–1123. http://www.jstor.org/stable/1690908.

[6] P.D. Boersma, Population Trends of the Galápagos Penguin: Impacts of El Niño and La Niña, Condor. 100 (1998) 245–253. https://doi.org/10.2307/1370265.

[7] F. Trillmich, J.W.E. Jeglinski, K. Meise, P. Piedrahita, The Galapagos Sea Lion: Adaptation to Spatial and Temporal Diversity of Marine Resources Within the Archipelago, in: J. Denkinger, L. Vinueza (Eds.), Galapagos Mar. Reserv., Springer Science & Business Media, 2014: pp. 61–70. https://doi.org/10.1007/978-3-319-02769-2_3.

[8] W.A. Laurie, Effects of the 1982-83 el niño-southern oscillation event on marine iguana (amblyrhynchus cristatus bell, 1825) populations on galapagos, Elsevier Oceanogr. Ser. 52 (1990) 361–380. https://doi.org/10.1016/S0422-9894(08)70041-2.

[9] D. Anderson, Differential responses of boobies and other seabirds in the Galapagos to the 1986-87 El Nino-Southern Oscillation event, Mar. Ecol. Prog. Ser. 52 (2007) 209–216. https://doi.org/10.3354/meps052209.

[10] J. Marin Jarrin, P. Salinas-de-León, Effects of the 2016 El Niño on the Galapagos artisanal coastal fin-fish fishery, Galapagos Res. (2020). https://doi.org/10.7287/peerj.preprints.26773.

[11] P. Usseglio, A.M. Friedlander, H. Koike, J. Zimmerhackel, A. Schuhbauer, T. Eddy, P. Salinas-de-León, So long and thanks for all the fish: Overexploitation of the regionally endemic galapagos grouper mycteroperca olfax (Jenyns, 1840), PLoS One. 11 (2016) 1–20. https://doi.org/10.1371/journal.pone.0165167.

[12] J.C. Murillo-Posada, S. Salas, I. Velázquez-Abunader, Factors affecting relative abundance of low-mobility fishing resources: Spiny lobster in the Galapagos Marine Reserve, PeerJ. 2019 (2019) 1–31. https://doi.org/10.7717/peerj.7278.

[13] M. Castrejon, Co-Manejo Pesquero en la Reserva Marina de Galápagos: Tendencias, Retos y Perspectivas de Cambio, Fundación Charles Darwin/Kanankil/Plaza-Váldes, Mexico, 2011.

[14] M. Gadgil, P. Olsoon, F. Berkes, C. Folke, Exploring the role of local ecological knowledge in ecosystem management: three case studies, in: F. Berkes, J. Colding, F. Carl (Eds.), Navig. Soc. Syst. Build. Resil. Complex. Chang., Cambridge University Press,

Cambridge, UK, 2003: pp. 189–209.

[15] J.A. González, C. Montes, J. Rodríguez, W. Tapia, Rethinking the Galapagos Islands as a Complex Social-Ecological System: Implications for Conservation and Management, Ecol. Soc. 13 (2008). http://www.jstor.org/stable/26267990.

[16] D. V Burbano, C.F. Mena, P. Guarderas, L. Vinueza, Shifitng Baselines in the Galapagos White Fin Fishery, Using Fisher's Anecdotes to Reassess Fisheries Management: The case of the Galapagos Grouper, in: J. Denkinger, L. Vinueza (Eds.), Galapagos Mar. Reserv., Springer Science & Business Media, 2014: pp. 227–246. https://doi.org/10.1007/978-3-319-02769-2.

[17] L. Castello, J.P. Viana, G. Watkins, M. Pinedo-Vasquez, V.A. Luzadis, Lessons from integrating fishers of arapaima in small-scale fisheries management at the mamirauá reserve, amazon, Environ. Manage. 43 (2009) 197–209. https://doi.org/10.1007/s00267-008-9220-5.

[18] F. Berkes, C. Folke, M. Gadgil, Traditional Ecological Knowledge, Biodiversity, Resilience and Sustainability, in: Biodivers. Conserv., Springer, Dordrecht, 1994: pp. 269–287. https://doi.org/10.1007/978-94-011-1006-8_15.

[19] A. Sáenz-Arroyo, C.M. Roberts, J. Torre, M. Carin, Using fishers' anecdotes, naturalists' observations and grey literature to reassess marine species at risk: the case of the Gulf grouper in the Gulf of California, Mexico, Fish Fish. 6 (2005) 121–133.

[20] N.A. Rayner, D.E. Parker, E.B. Horton, C.K. Folland, L. V. Alexander, D.P. Rowell, E.C. Kent, A. Kaplan, Global analyses of sea surface temperature, sea ice, and night marine air temperature since the late nineteenth century, J. Geophys. Res. D Atmos. 108 (2003). https://doi.org/10.1029/2002jd002670.

[21] M. Statistics, Snowball Sampling Author (s): Leo A . Goodman Source : The Annals of Mathematical Statistics , Vol . 32 , No . 1 (Mar ., 1961), pp . 148-170 Published by : Institute of Mathematical Statistics Stable URL : http://www.jstor.org/stable/2237615 Accessed , Statistics (Ber). 32 (2016) 148–170. https://doi.org/10.1214/009117906000000124.

[22] M.M. Early-Capistrán, A. Sáenz-Arroyo, J.G. Cardoso-Mohedano, G. Garibay-Melo, S.H. Peckham, V. Koch, Reconstructing 290 years of a data-poor fishery through ethnographic and archival research: The East Pacific green turtle (Chelonia mydas) in Baja California, Mexico, Fish Fish. 19 (2018) 57–77. https://doi.org/10.1111/faf.12236.

[23] K.B. Karnauskas, S. Jenouvrier, C.W. Brown, R. Murtugudde, Strong sea surface cooling in the eastern equatorial Pacific and implications for Galápagos Penguin conservation, Geophys. Res. Lett. 42 (2015) 6432–6437. https://doi.org/10.1002/2015GL064456.

[24] L. Schiller, J.J. Alava, J. Grove, G. Reck, D. Pauly, The demise of Darwin's fishes: Evidence of fishing down and illegal shark finning in the Galápagos Islands, Aquat. Conserv. Mar. Freshw. Ecosyst. 25 (2015) 431–446. https://doi.org/10.1002/aqc.2458.

[25] J.R. Marin Jarrin, S. Andrade-Vera, C. Reyes-Ojedis, P. Salinas-de-León, Life History of the Mottled Scorpionfish, Pontinus clemensi , in the Galapagos Marine Reserve, Copeia. 106 (2018) 515–523. https://doi.org/10.1643/ci-17-706.

[26] F. Trillmich, J.W.E. Jeglinski, K. Meise, P. Piedrahita, The Galapagos Marine Reserve, in: J. Denkinger, L. Vinueza (Eds.), Galapagos Mar. Reserv., Springer Science & Business Media, 2014: pp. 61–70. https://doi.org/10.1007/978-3-319-02769-2.

[27] P.W. Glynn, Widespread coral mortality and the 1982-83 El-Nino warmign event, Environ. Conserv. 11 (1984) 133–146.

[28] C.A. Valle, Present Status of the Flightless Cormorant , Galapagos Penguin and Greater Flamingo Populations in the Galapagos Islands , Ecuador , after the 1982-83 El Niño Author (s): Carlos A . Valle and Malcolm C . Coulter Published by : American Ornithological So, 89 (2017) 276–281.

[29] D.J. Anderson, S. Fortner, Waved Albatross Egg Neglect and Associated Mosquito Ectoparasitism, Condor. 90 (1988) 727–729. https://www.jstor.org/stable/1368369?seq=1#metadata_info_tab_contents.

[30] F.P. Chavez, P.G. Strutton, G.E. Friederich, R.A. Feely, G.C. Feldman, D.C.G. Foley, M.J. McPhaden, C.E. Friederich, Response of the equatorial Pacific Ocean to the 1997-1998 El Nino, Science (80-.). 286 (1999) 2126–2131. http://www.ncbi.nlm.nih.gov/pubmed/10591638.

[31] J. Jakoboski, R.E. Todd, W. Brechner Owens, K.B. Karnauskas, D.L. Rudnick, Bifurcation and upwelling of the equatorial undercurrent west of the galápagos archipelago, J. Phys. Oceanogr. 50 (2020) 887–905. https://doi.org/10.1175/JPO-D-19-0110.1.

[32] G.P. Podestá, P.W. Glynn, Sea surface temperature variability in Panamá and Galápagos: Extreme temperatures causing coral bleaching, J. Geophys. Res. 102 NO. C7 (1997) 15749–15759. https://doi.org/10.1029/96JC03557.

[33] K.B. Karnauskas, R. Murtugudde, W.B. Owens, Climate and the Global Reach of the Galápagos Archipelago: State of the Knowledge, Galapagos A Nat. Lab. Earth Sci. (2014) 215–231. https://doi.org/10.1002/9781118852538.ch11.

[34] W.W.L. Cheung, R. Watson, D. Pauly, Signature of ocean warming in global fisheries catch, Nature. 497 (2013) 365–368. https://doi.org/10.1038/nature12156.

[35] F. Trillmich, D. Limberger, Drastic effects of El Niño on Galapagos pinnipeds, Oecologia.

67 (1985) 19–22. https://doi.org/10.1007/BF00378445.

[36] L.M. Cavole, T.M. Decarlo, Early observations of heat-induced coral bleaching in the Galápagos Islands, Reef Encount. 35 (2020) 68–72.

[37] P.W. Glynn, G.M. Wellington, C. Birkeland, Coral reef growth in the Galápagos: Limitation by sea urchins, Science (80-.). 203 (1979) 47–49. https://doi.org/10.1126/science.203.4375.47.

[38] H. Snell, S. Rea, The 1997–98 El Niño in Galápagos: can 34 years of data estimate 120 years of pattern?, Not. Galápagos. 60 (1999) 11–20.

[39] J. Jacquet, J.J. Alava, G. Pramod, S. Henderson, D. Zeller, In hot soup: sharks captured in Ecuador's waters, Environ. Sci. 5 (2008) 269–283. https://doi.org/10.1080/15693430802466325.

[40] M. Castrejón, A. Charles, Improving fisheries co-management through ecosystem-based spatial management: The Galapagos Marine Reserve, Mar. Policy. 38 (2013) 235–245. https://doi.org/10.1016/j.marpol.2012.05.040.

[41] Alex Hearn and M . Veronica Toral-Granda, Reproductive Biology of the Red Spiny Lobster , Panulirus penicillatus and the Galapagos Slipper Lobster , Scyllarides astori in the Galapagos Islands, Crustaceana. 80 (2007) 297–312.

[42] P.J.S. Jones, A governance analysis of the Galápagos Marine Reserve, Mar. Policy. 41 (2013) 65–71. https://doi.org/10.1016/j.marpol.2012.12.019.

[43] C. Márquez, D.A. Wiedenfeld, S. Landázuri, J. Chávez, Human-caused and natural mortality of giant tortoises in the Galapagos Islands during 1995-2004, Oryx. 41 (2007) 337–342. https://doi.org/10.1017/s0030605307000211.

[44] E. Llerena, T. Quisingo, R. Maldonado, Analysis of agreements reached in the Participatory Management Board 2010-2015, in: C. and G. GNPD, GCREG (Ed.), Galapagos Rep. 2015-2016, Puerto Ayora, Galápagos, Ecuador, 2017: pp. 105–111.

[45] M. Camhi, Industrial Fisheries Threaten Ecological Integrity of the Galapagos Islands, Conserv. Biol. 9 (2003) 715–719. https://doi.org/10.1046/j.1523-1739.1995.09040715.x.

[46] H. Reyes, C. Murillo, Efforts to control illegal fishing activities in the Marine Reserve, 2008.

[47] N. Moity, Evaluation of No-Take Zones in the Galapagos Marine Reserve , Zoning Plan 2000, 5 (2018) 1–5. https://doi.org/10.3389/fmars.2018.00244.

Chapter 5 Appendix

Using Local Ecological Knowledge of fishers to infer the impact of climate variability in Galápagos small-scale fisheries

Supplementary Information

by

LETICIA MARIA CAVOLE[1,*], SOLANGE ANDRADE-VERA[2], JOSE R MARIN JARRIN[2,3], DANIELA FAGGIANI DIAS[1], OCTAVIO ABURTO-OROPEZA[1] AND MARÍA JOSÉ BARRÁGAN-PALADINES[2,4]

[1] Scripps Institution of Oceanography at the University of California San Diego, La Jolla, CA, USA

[2] Charles Darwin Research Station, Charles Darwin Foundation, Galapagos, Ecuador

[3] Department of Fisheries Biology, Humboldt State University, Arcata, CA, USA

[4] Leibniz Centre for Tropical Marine Research, ZMT, University of Bremen, Germany

*Corresponding Author: lcavole@ucsd.edu

Table 5.S1. Fishermen' comments about the effects of El Niño events on their fisheries activities.

Fishers code	Island	*Q7. How does El Niño phenomenon affect fishing?*
2	Santa Cruz	It affects a lot. There are more rain and currents, making the sea choppier and turbid, which affects fishing. Rocks also become covered with sand because of stronger oceanic currents, which affects fishing. There are more fish migrations, with many fish moving away to further sites. But there are also winners and losers.
3	Santa Cruz	Abrupt changes in the currents, rougher sea, a lot of wind. The majority of fishers returns to the port. Depending on the location, you can fish without any problems.
4	Santa Cruz	There is more rain and the water is warmer. The El Niño also heats the water up to 5 fathoms deeper, generally.
10	Isabela	I felt the El Niño of 1982-1983 pretty strong. At that time, I was in San Cristóbal and I observed many changes in all activities within the Galápagos, affecting both marine animals and humans…This El Niño affected fishing. For instance, the sailfin grouper went into deeper waters or it would leave the area, so fishing large pelagic fishes was a better option, like tunas. On the other hand, there was more *jaiba* (local crab). In the human realm, there were physical losses. There was a lot of heavy rain in San Cristóbal, destroying the Malecón (coast boardwalk), and my aunt lost 3000 chickens.
11	Isabela	Before it was well defined, now it is very variable.
12	Isabela	It has not affected much. In 2016, the whole year was warm, and it was still possible to fish, but there was not so much trade.
14	Isabela	In 1982, fishing decreased both in coastal and open sea areas, including pelagic, epipelagic, and demersal resources. In 1997, the sea was so rough that there was almost no fish to catch. I wanted to do other economic activities such as construction, whereas other people were engaged in farming. In 2015-2016 we hardly felt any effects on our fisheries activities, but the effects were greater on agriculture and livestock.
15	Isabela	Three years ago, back in 2015, the water was warmer, so you could stay longer underwater. It was a good year for lobster fishing.
17	Santa Cruz	It affects a lot. The El Niño of 1982 decreased the lobster fishing massively. I think the water was very warm for several months, from January onwards. The lobster migrated further and deeper. The white fin fishery was also affected, but to a lesser extent. There was more abundance of small pelagic fish, like sardine and herring. I also observed that marine birds altered their behavior.
18	Santa Cruz	Change the amount of fish, which decreases. But it is a natural process. In some places, like in the north of Isabela and Fernandina, and in Bolívar Channel, the water is always cold, even during El Niño years. There are mainly changes in the depth in which the fish is normally found. I think the fish goes deeper, or it can move to other places. I recalled the El Niño of 1982, when there were many lightnings and heavy rain in Santa Cruz Island. But these are natural phenomena that can change the amount of prey, like small pelagic fish for larger fish. I believe that in the end, the reduction of fishing is driven mainly by us and our seafood consumption.
19	San Cristóbal	It is not favorable. There is a decrease in species; less pelagic fish compared to 10 years ago. Small and large pelagic fish migrate.
20	San Cristóbal	Small pelagic fish, like sardines, leave the area when the water is warmer, then larger fish, like bacalao, are hungrier and grab the bait faster, so El Niño increases the catchability of big fish. It was much rainier than it is nowadays, with torrential rains and lightnings during the El Niño between 1960s and 1970s.
23	San Cristóbal	It reduces the amount of sardine. When it rains a lot, the water gets murky, so you cannot fish because the fish do not eat, since they lost visibility.

Table 5.S2. Fishermen' comments about the effects of El Niño events on the fauna and flora of Galapagos.

Fishers code	Island	*Q9. How does El Niño phenomenon affect marine animals?*
2	Santa Cruz	In the "*bajos*", there is a lot of algae mortality and as a consequence, many iguanas die. I have also observed the appearance of many marine plagues. The sea lion pups are very skinny, and they die. It is a "Run for your lives, everybody!".
4	Santa Cruz	The sea lions will migrate farther to find their food.
6	Santa Cruz	It affects everything. A lot of big fish enters the marine reserve, but for a shorter amount of time.
7	Santa Cruz	Pelicans, boobies, marine iguanas and sea lions get skinnier. The white sea urchin is already gone, and there are dead corals because of the previous strong currents during El Niño years.
8	Santa Cruz	Up to 70% of adult sea lions die, and almost all of their pups (~90%). Many marine birds also die.
9	Santa Cruz	I have not seen. In 2015, the water temperature was still low at around 13°C in the Bolívar Channel for the sea cucumber fishery.
10	Isabela	I felt the El Niño of 1982-1983 pretty strong... In the marine realm, I observed that the winter season looked like the summer season. The water was very warm, the sea lions very weak, and the marine algae was dying, which affected the marine iguanas. I also observed that all the corals in San Cristóbal bleached, and a little less in Isabela, and since this El Niño the corals have not fully recovered.
14	Isabela	Sea lion pups died, and pelicans, frigate bird and adult sea lions were very skinny. But there were a lot of hammerhead sharks and blacktip sharks around.
16	Isabela	In 1998 and 1999, the marine iguanas were mostly dead.
17	Santa Cruz	Sea lions need to migrate farther to look for their food. There were more small pelagic fish.
21	San Cristóbal	There were pelicans and blue-footed boobies dead in the Bolívar Channel in 2004 and 2005. I also found juveniles of mottled scorpionfish smaller than 5 cm of size floating on the surface, dead. We thought this was related with some source of tectonic uplift and lava flow leakage underwater or due to a warming event.
23	San Cristóbal	Sea lions and marine birds are affected because their prey items are reduced, as they feed on sardines, and the sardines love cold water. The sea lions get skinnier and their pups die.

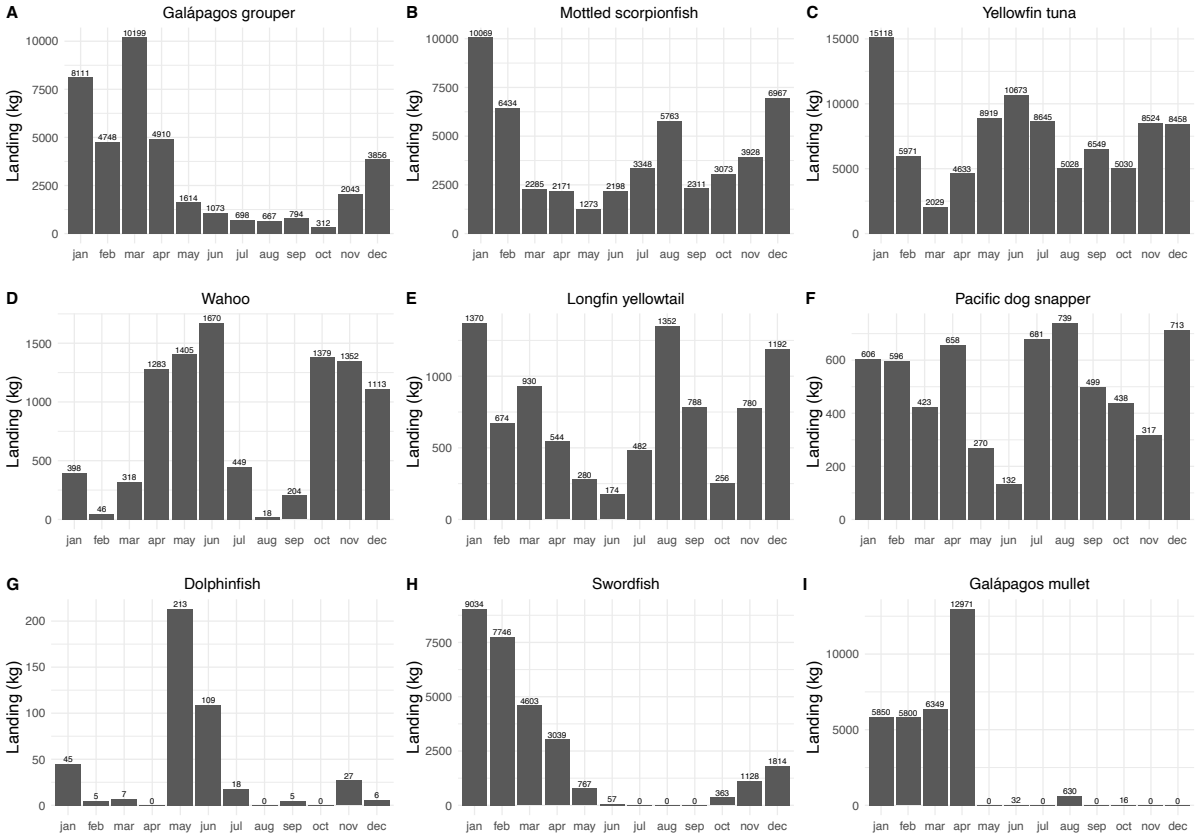

Figure 5.S1. Landing data for Galápagos white fin fishery for 2019 (GNPD, unpublished data).

Figure 5.S2. Sectors interacting with the artisanal fishing in the Galápagos Marine Reserve (GMR). The dashed line corresponds to the limit of the reserve, created in 1998, and covering an area of 138,000 km^2.

Conclusions

LETICIA MARIA CAVOLE

In my **first chapter**, we asked how the water temperature inside mangrove lagoons from the Gulf of California influences the first year of growth of yellow snapper juveniles *Lutjanus argentiventris*. To achieve this goal, we examined daily growth rings in otoliths (a proxy for daily somatic growth in fish) in conjunction with daily *in situ* water temperature recordings. Data gathered was also used to calculate an optimal thermal preference for this species. We observed that snapper juveniles grew linearly with increasing temperature until a temperature threshold is reached (~ 32 °C), beyond which growth is then reduced. Currently, days above this thermal threshold are more frequent in the coast of the Gulf of California than ten years ago, potentially exposing early life stages of fish to detrimental growth conditions. We also tested if oxygen isotope ratios ($\delta^{18}O$) in snapper otoliths allow us to accurately reconstruct variations in water temperature inside mangrove lagoons in Baja California Peninsula. The thermal history reconstruction using otolith $\delta^{18}O$ values captured the great water seasonality ($\Delta T \sim 20$ °C) observed in our mangrove sites, validating the use of this technique for fish in mangrove waters for the first time.

In my **second chapter**, we investigated the role of intrinsic (physiologically-driven) and extrinsic (environmentally-driven) factors on trace and minor element composition in otoliths. There is an ongoing debate about which elements may be suitable for use as environmental proxies for temperature, primary productivity, salinity and oxygen levels. We analyzed the otolith microchemistry of the same species (yellow snapper *Lutjanus argentiventris*) from two ecosystems (Gulf of California and Galápagos), and different species (yellow snapper *Lutjanus argentiventris* and sailfin grouper *Mycteroperca olfax*) from the same ecosystem (Galápagos), in order to test for physiological and environmental drivers on otolith chemistry. The co-occurring species exhibited similar otolith chemistry in Galápagos, whereas snappers across ecosystems

exhibited marked differences in most trace and minor elements. This study suggests that extrinsic factors (e.g., water chemistry, temperature, salinity) can be more important than intrinsic factors (e.g., physiology, growth rates, genetics) for influencing elemental incorporation in the otoliths of juvenile fishes from mangrove waters (with respect to Mn, Sr, Ba and Li).

In my **third chapter,** we asked how we can use otolith microchemistry and genetic markers (microsatellite DNA) to elucidate the metapopulation patterns for the yellow snapper *Lutjanus argentiventris*. These techniques were compared at several life stages (e.g., embryo, larval and juvenile) using snappers collected in its northern and southern distributional limits in the Eastern Tropical Pacific. In Galápagos (southern limit), both otolith microchemistry and genetic markers supported the presence of a source-sink metapopulation structure with high levels of connectivity among mangroves. The designing and placing of marine reserves in Galápagos should include most mangroves in a network of Marine Protected Areas for maintaining the long-term population viability of the snappers. For the Gulf of California, we observed a scenario of self-recruitment that is not compatible with the metapopulation structure found offshore in adults from rocky reefs. This suggests that some mangrove sites in the Gulf of California are disproportionately important to the sustainability of local yellow snapper populations.

In my **fourth chapter**, we explored the potential of using deep-sea fish as monitors of hypoxic conditions in distinct ocean basins; the Northeast Pacific and the Southeast Atlantic. We quantified the minor elements, trace elements and isotope ratios in the otoliths of six fish species from three Oxygen Minimum Zones (OMZs) off the Southern California Bight (USA), the Gulf of California (Mexico) and the Namibian shelf (Namibia). We observed that all OMZ-dwelling fish had a similar microchemistry, despite different life history traits (e.g., longevity, size and

age at maturity, growth rate, parental investment and thermal history). This result suggests that the OMZs in Eastern Boundary Upwelling Systems have a unique water biogeochemistry imprinted on the otoliths of dwelling fish. Manganese to calcium (Mn:Ca) in otoliths works as an indicator of hypoxic exposure in OMZ-dwelling fish, but thresholds chosen to detect hypoxia exposure must be reduced in comparison to those used for coastal species. Furthermore, we have identified boron to calcium (B:Ca) in otoliths as a potential tracer for fish exposure to low pH (~ 7.5) waters characteristic of OMZs, and we have reconstructed the thermal history and OMZ residence of our species using otolith $\delta^{18}O$ profiles. This study offers a benchmark for future comparison of otolith elemental composition in fishes from OMZs, which can be extremely important to track the ongoing deoxygenation trends and vertical expansion of these unique regions.

In my **fifth chapter**, we investigated how the knowledge provided by local fishers, with over 60 years of experience diving and fishing in the Galápagos, might help us to understand the consequences of climate variability common to this archipelago. Focusing on fisher's recollections of anomalous weather, animal behavior and oceanic conditions during El Niño years, we demonstrated that there is agreement between their knowledge, the scientific literature, and environmental indices since the strong El Niño of 1965 to the present. LEK can also provide insights on how to increase human and ecosystem resilience under imminent climate change. Artisanal fishers call for a bottom-up management approach along with the conservation and scientific sectors to achieve long-term marine conservation goals in Galápagos Archipelago.

In summary, this dissertation inquiries how environmental factors (mainly water temperature and dissolved oxygen levels) influence the chemistry and chronological properties of otoliths, and how we can use otolith chemistry and genetic analysis to understand fish

population patterns. I explore these ideas by using fish from coastal ecosystems with immense intra-annual temperature variability, such as the mangrove lagoons from the Gulf of California and Galápagos, and by using fish from extremely low oxygen conditions off the Southern California Bight, the Gulf of California and the Namibian shelf OMZs. Both the variability of mangrove waters as well as the constancy of OMZ conditions are imprinted on otoliths in unique ways that can help us to track fishes' natural world through time and space. In addition, the knowledge provided by artisanal fishers in Galápagos, who are at sea on almost a daily basis and have been diving in the entire archipelago since the 1960s, revealed the major impacts of past El Niño years on marine species and weather and oceanic conditions. In summary, my dissertation advances our current understanding of how past environmental conditions can affect both fish and humans in concert, and how considering both components is vital for a more holistic, inclusive and effective marine conservation.